12-2006

Development of Fatigue Predictive Models of Rubberized Asphalt Concrete (RAC) Containing Reclaimed Asphalt Pavement (RAP) Mixtures

Feipeng Xiao
Clemson University, feipenx@clemson.edu

DEVELOPMENT OF FATIGUE PREDICTIVE MODELS OF RUBBERIZED ASPHALT CONCRETE (RAC) CONTAINING RECLAIMED ASPHALT PAVEMENT (RAP) MIXTURES

A Dissertation
Presented to
the Graduate School of
Clemson University

In Partial Fulfillment
of the Requirements for the Degree
Doctor of Philosophy
Civil Engineering

---

by
Feipeng Xiao
December 2006

Accepted by:
Dr. Serji N. Amirkhanian, Committee Chair
Dr. C. Hsein Juang
Dr. Prasada R. Rangaraju
Dr. Bradley J. Putman

ABSTRACT

In recent years, some by-products such as crumb rubber has been used to save money, protect the environment, and extend the life of asphalt pavements. In addition, the utilization of reclaimed asphalt pavement (RAP) is an acceptable practice in many states around the United States and many countries all over the world. However, the use of RAP containing crumb rubber has not been investigated in great detail, so it is essential to explore whether these materials have a positive effect on the fatigue life of asphalt pavement. In general, previous experience shows that the use of RAP has proven to be cost-effective, environmentally sound, and successful in improving some of the engineering properties of asphalt mixtures. Crumb rubber has also been used successfully in improving the mechanical characteristics of hot mix asphalt (HMA) mixtures in many parts of the world.

Fatigue is considered to be one of the most significant distress modes in any flexible pavement which is subjected to repeated traffic loading or stress. Several researchers, for the last two decades, have developed some fatigue predictive models that predict the fatigue life of asphalt mixture in the laboratory and even in the field. However, there are no research studies in the area of developing prediction models for mixtures containing crumb rubber and RAP.

For this research study, A total of 39 mix designs, including two types of aggregate source, were made and tested to perform fatigue analysis and modeling. Superpave mix design procedures were used for preparation of fatigue testing specimens.

The major objective of this study was to develop a mathematical model to predict the fatigue life of rubberized asphalt concrete containing RAP and included: 1) evaluating the performance of the modified binder and mixture in the laboratory; 2) measuring the fatigue life, stiffness and dissipated energy of the fatigue specimens; 3) developing the mathematical model to predict the fatigue life of the modified composite using the conventional statistical regression analysis and artificial neural network (ANN) approaches; 4) validating the fatigue predictive models using modified mixtures made from a second aggregate source.

The following conclusions were drawn based on the laboratory investigation: 1) the use of crumb rubber is effective in improving the aging resistance of rubberized asphalt concrete, 2) the addition of RAP decreased the virgin asphalt content and increased the ITS values, 3) the developed specific regression models predicted a reasonable fatigue response of mixture, and the measured and predicted fatigue values were found to be close regardless of the crumb rubber, RAP content, and even testing conditions, 4) ANN approach has been shown to be effective in performing fatigue testing data of mixture and the established ANN model was able to predict fatigue occurrence accurately.

DEDICATION

I dedicate this dissertation to my mother, Fuyuan Chen, my wife, Boli Wu, and my sisters, Xiaoyun Xiao and Jiaoyun Xiao. Without their love and support, I would not have completed my research work and doctoral degree program.

ACKNOWLEDGEMENTS

I would like to express my deep appreciation to everyone who has dedicated time and effort to the completion of my research and dissertation. I would first like to thank Dr. Serji N. Amirkhanian, my academic advisor, for all of his untiring guidance and support during the course of my master and doctoral programs at Clemson University.

I also acknowledge other committee members, Drs. Hsein Juang, Prasada R. Rangaraju, and Bradley J. Putman, for their guidance and help in experimental testing, data analysis, and thorough review of the dissertation.

I also wish to thank all staff, including Mrs. Teri Oswald, Mary Corley, and other students, working at the Asphalt Rubber Technology Services (ATRS). Their support and help made my research easier in last four years. I would also like to thank Mr. Cheng-Liang Hsiao for his advice and help in the data analysis.

Finally, I would like to gratefully acknowledge financial support of South Carolina Department of Health and Environmental Control (SC DHEC) to conduct this research work.

TABLE OF CONTENTS

Page

TITLE PAGE i

ABSTRACT ii

DEDICATION iv

ACKNOWLEDGEMENTS v

LIST OF TABLES vi

LIST OF FIGURES xvi

CHAPTER

1. INTRODUCTION 1

    Background 4
    Research Objectives 6
    Scope of Research 7
    Organization of Dissertation 9

2. LITERATURE REVIEW 10

    Fatigue Behavior and Characteristics 10
    Fatigue Characteristics of asphalt binder 13
    Crumb Ground Rubber 15
    Reclaimed Asphalt Pavement 19
    Fatigue Analysis Method 21
    Statistical Analysis Models of Fatigue Life 26
    Artificial Neural Network Analysis Models of Fatigue Life 28

3. MATERIAL AND EXPERIMENTAL DESIGN AND TESTING 32

    Materials 32
        Asphalt Binder 32
        Crumb Rubber 33
        Reclaimed Asphalt Pavement 36
        Virgin Aggregate Property 38
    Mix design 41

Table of Contents (Continued)

Page

Method 41
Asphalt Binder 41
Aggregate Structure 42
Crumb Rubber 46
Volumetric Properties of the Mixtures 46
Sample Mixing 47
Moisture Sensitivity 50
Fatigue Test Procedure 50
Beam Fabrication 50
Fatigue Beam Testing 52

4. EXPERIMENTAL STATISTICAL METHODS 56

5. EXPERIMENTAL RESULTS AND DISCUSSIONS 66

Hypothisis and Assumptions 66
Binder Property Analysis 68
Superpave Mix Design Anlysis 75
Optimum Binder Content Analysis 75
Indirect Tensile Strength 77
Fatigue Prediction Models 81
Analysis of Fatigue Test Results 81
Statistical Regression Fatigue Prediction Models 86
Strain Dependent Models 88
Models of Using Ambient Rubber at 5ºC 88
Energy Dependent Models 97
Articial Neural Network Fatigue Prediction Models 100
Validation of Fatigue Prediction Models 103

6. SUMMARY, CONCLUSIONS, AND RECOMMENDATIONS 118

Summary 118
Conclusions 119
Recommendations 121

APPENDICES 123

A: Volumetric Properties of Superpave Mix Design 124
B: Viscosity of the Modified Binder 135
C: G*sin(δ) Values of the Modified Binder 140
D: ITS Values of Modified Mixtures 143
E: Fatigue Life and Stiffness Values of the Modified Mixtures 148

Table of Contents (Continued)

Page

F: Average Values of Independent and Dependent Variables of the modified mixture 159
G: Fatigue Life and Stiffness Values of the Modified Mixtures 163

REFERENCES 186

LIST OF TABLES

Table		Page
3.1	Engineering properties of virgin asphalt binders	32
3.2	Engineering properties of aged binders	33
3.3	Gradations of -40 mesh crumb rubber	34
3.4	Average surface area of crumb rubber (-40 mesh)	35
3.5	Component of two RAPs	38
3.6	Split sample aggregate tests	39
3.7	Engineering properties of aggregate sources L and C	40
3.8	Gradations of aggregate Sources L and C	40
3.9	Design structure of aggregate source C	43
3.10	Design structure of aggregate source L	44
3.11	SCDOT 9.5 mm Superpave Volumetric Specifications	47
4.1	Data for multiple linear regression	57
4.2	ANOVA for significance of regression in multiple regression models	60
5.1	Mixing temperatures of modified mixtures	72
5.2	Compacting temperatures of modified mixtures	72
5.3	Optimum binder content of the mixtures	76
5.4	TSR values of mixture made with aggregate L	78
5.5	Typical fatigue test results, raw data file	82
5.6	Typical analyzed fatigue test results	83

List of Tables (Continued)

Table		Page
5.7	Pearson correlation matrix for the dependent and independent variables of mixture containing ambient rubber and RAP L tested at 5ºC	89
5.8	ANOVA and GLM of log fatigue life for mixture containing ambient rubber and RAP L at 5ºC (traditional strain dependent VFA method)	90
5.9	ANOVA and GLM of log fatigue life for mixture containing ambient rubber and RAP L at 5ºC (specific strain dependent VFA method)	91
5.10	ANOVA and GLM of log fatigue life for mixture containing ambient rubber and RAP L at 5ºC (traditional strain dependent air void method)	92
5.11	ANOVA and GLM of log fatigue life for mixture containing ambient rubber and RAP L at 5ºC (specific strain dependent air void method)	93
5.12	Stress dependent prediction models of the mixture using aggregate source L.....	96
5.13	Energy dependent prediction models of the mixture using aggregate source L.....	98
5.14	Comparison of fatigue lives between predicted and measured results of regression models using soft binder (PG52-28) with 30% RAP L at 5^{o}C and 20^{o}C (ambient rubber).....	99
5.15	Connection weights and biases of ANN model defined in Equation 2-13 (specific strain dependent method for ambient rubber)	107
5.16	Connection weights and biases of ANN model defined in Equation 2-13 (specific strain dependent method for cryogenic rubber)	108
5.17	Connection weights and biases of ANN model defined in Equation 2-13 (specific energy dependent method for ambient rubber)	109
5.18	Connection weights and biases of ANN model defined in Equation 2-13 (specific energy dependent method for cryogenic rubber)	110
5.19	Comparison of fatigue lives between predicted and measured results of ANN models using soft binder (PG52-28) with 30% RAP L at 5^{o}C and 20^{o}C (ambient rubber).....	111

List of Tables (Continued)

Table		Page
A.1	Volumetric properties of Superpave mix design with 0% rubber using aggregate source L	125
A.2	Volumetric properties of Superpave mix design with 5% 40mehs ambient rubber using aggregate source L	126
A.3	Volumetric properties of Superpave mix design with 10% 40mehs ambient rubber using aggregate source L	127
A.4	Volumetric properties of Superpave mix design with 15% 40mehs ambient rubber using aggregate source L	128
A.5	Volumetric properties of Superpave mix design with 5% 40mehs cryogenic rubber using aggregate source L	129
A.6	Volumetric properties of Superpave mix design with 10% 40mehs cryogenic rubber using aggregate source L	130
A.7	Volumetric properties of Superpave mix design with 15% 40mehs cryogenic rubber using aggregate source L	131
A.8	Volumetric properties of Superpave mix design with 30%RAP (PG52-28) using aggregate source L	132
A.9	Volumetric properties of Superpave mix design with 0% rubber using aggregate source C	133
A.10	Volumetric properties of Superpave mix design with 10% 40mesh ambient Rubber using aggregate source C	134
B.1	Viscosity of modified binder containing ambient rubber with aged binder L	136
B.2	Viscosity of modified binder containing cryogenic rubber with aged binder L	137
B.3	Viscosity of modified binder containing ambient rubber with aged binder C	138
B.4	Viscosity of modified binder containing cryogenic rubber with aged binder C	139

List of Tables (Continued)

Table		Page
C.1	G* sin δ of modified binder using aged binder L	141
C.2	G* sin δ of modified binder using aged binder C	142
D.1	ITS values of mixtures using 0-5% 40 mesh ambient rubber with aggregate L	144
D.2	ITS values of mixtures using 10-15% 40 mesh ambient rubber with aggregate L	145
D.3	ITS values of mixtures using 5-15% 40 mesh cryogenic rubber with aggregate L	146
D.4	ITS values of mixtures using 0-15% 40 mesh ambient rubber with aggregate C	147
E.1	Fatigue lives and stiffness values of modified mixture containing 0-5% ambient rubber using RAP L at 5ºC	149
E.2	Fatigue lives and stiffness values of modified mixture containing 10-15% ambient rubber using RAP L at 5ºC	150
E.3	Fatigue lives and stiffness values of modified mixture containing 0-5% cryogenic rubber using RAP L at 5ºC	151
E.4	Fatigue lives and stiffness values of modified mixture containing 10-15% cryogenic rubber using RAP L at 5ºC	152
E.5	Fatigue lives and stiffness values of modified mixture containing 0-5% ambient rubber using RAP L at 20ºC	153
E.6	Fatigue lives and stiffness values of modified mixture containing 10-15% ambient rubber using RAP L at 20ºC	154
E.7	Fatigue lives and stiffness values of modified mixture containing 0-5% cryogenic rubber using RAP L at 20ºC	155
E.8	Fatigue lives and stiffness values of modified mixture containing 10-15% cryogenic rubber using RAP L at 20ºC	156

List of Tables (Continued)

Table		Page
E.9	Fatigue lives and stiffness values of modified mixture using RAP L at 5ºC	157
E.10	Fatigue lives and stiffness values of modified mixture using RAP L at 20ºC	158
F.1	Average values of independent and dependent variables of modified mixtures using RAP L at 5ºC	160
F.2	Average values of independent and dependent variables of modified mixtures using RAP L at 20ºC	161
F.3	Average values of independent and dependent variables of modified mixtures using soft binder (PG52-28) and RAP L at 5ºC and 20ºC	162
F.4	Average values of independent and dependent variables of modified mixtures using RAP C	162
G.1	Pearson correlation matrix for the dependent and independent variables of mixture containing ambient rubber and RAP L at 20ºC	164
G.2	Pearson correlation matrix for the dependent and independent variables of mixture containing cryogenic rubber and RAP L at 5ºC	164
G.3	Pearson correlation matrix for the dependent and independent variables of mixture containing cryogenic rubber and RAP L at 20ºC	164
G.4	ANOVA and GLM of log fatigue life for mixture containing ambient rubber and RAP L at 20ºC (traditional strain dependent VFA method)	165
G.5	ANOVA and GLM of log fatigue life for mixture containing ambient rubber and RAP L at 20ºC (specific strain dependent VFA method)	165
G.6	ANOVA and GLM of log fatigue life for mixture containing ambient rubber and RAP L at 20ºC (traditional strain dependent air void method)	166
G.7	ANOVA and GLM of log fatigue life for mixture containing ambient rubber and RAP L at 20ºC (specific strain dependent air void method)	166
G.8	ANOVA and GLM of log fatigue life for mixture containing cryogenic rubber and RAP L at 5ºC (traditional strain dependent VFA method)	167

List of Tables (Continued)

Table Page

G.9 ANOVA and GLM of log fatigue life for mixture containing cryogenic rubber and RAP L at 5ºC (specific strain dependent VFA method) 167

G.10 ANOVA and GLM of log fatigue life for mixture containing cryogenic rubber and RAP L at 5ºC (traditional strain dependent air void method) 168

G.11 ANOVA and GLM of log fatigue life for mixture containing cryogenic rubber and RAP L at 5ºC (specific strain dependent air void method) 168

G.12 ANOVA and GLM of log fatigue life for mixture containing cryogenic rubber and RAP L at 20ºC (traditional strain dependent VFA method) 169

G.13 ANOVA and GLM of log fatigue life for mixture containing cryogenic rubber and RAP L at 20ºC (specific strain dependent VFA method) 169

G.14 ANOVA and GLM of log fatigue life for mixture containing cryogenic rubber and RAP L at 20ºC (traditional strain dependent air void method) ... 170

G.15 ANOVA and GLM of log fatigue life for mixture containing cryogenic rubber and RAP L at 20ºC (specific strain dependent air void method) 170

G.16 ANOVA and GLM of log fatigue life for mixture containing ambient rubber and RAP L at 5ºC (traditional energy dependent VFA method) 174

G.17 ANOVA and GLM of log fatigue life for mixture containing ambient rubber and RAP L at 5ºC (specific energy dependent VFA method) 174

G.18 ANOVA and GLM of log fatigue life for mixture containing ambient rubber and RAP L at 5ºC (traditional energy dependent air void method) ... 175

G.19 ANOVA and GLM of log fatigue life for mixture containing ambient rubber and RAP L at 5ºC (specific energy dependent air void method) 175

G.20 ANOVA and GLM of log fatigue life for mixture containing ambient rubber and RAP L at 20ºC (traditional energy dependent VFA method) 176

G.21 ANOVA and GLM of log fatigue life for mixture containing ambient rubber and RAP L at 20ºC (specific energy dependent VFA method) 176

G.22 ANOVA and GLM of log fatigue life for mixture containing ambient rubber and RAP L at 20ºC (traditional energy dependent air void method). 177

List of Tables (Continued)

Table Page

G.23 ANOVA and GLM of log fatigue life for mixture containing ambient rubber and RAP L at 20ºC (specific energy dependent air void method) 177

G.24 ANOVA and GLM of log fatigue life for mixture containing cryogenic rubber and RAP L at 5ºC (traditional energy dependent VFA method) 178

G.25 ANOVA and GLM of log fatigue life for mixture containing cryogenic rubber and RAP L at 5ºC (specific energy dependent VFA method) 178

G.26 ANOVA and GLM of log fatigue life for mixture containing cryogenic rubber and RAP L at 5ºC (traditional energy dependent air void method) ... 179

G.27 ANOVA and GLM of log fatigue life for mixture containing cryogenic rubber and RAP L at 5ºC (specific energy dependent air void method) 179

G.28 ANOVA and GLM of log fatigue life for mixture containing cryogenic rubber and RAP L at 20ºC (traditional energy dependent VFA method) 180

G.29 ANOVA and GLM of log fatigue life for mixture containing cryogenic rubber and RAP L at 20ºC (specific energy dependent VFA method) 180

G.30 ANOVA and GLM of log fatigue life for mixture containing cryogenic rubber and RAP L at 20ºC (traditional energy dependent air void method) . 181

G.31 ANOVA and GLM of log fatigue life for mixture containing cryogenic rubber and RAP L at 20ºC (specific energy dependent air void method) 181

LIST OF FIGURES

Table		Page
2.1	Initiation of fatigue cracking	11
2.2	Images of fatigue cracking	12
2.3	Example of a three-layer feedforward neural network architecture	29
2.4	Schematic representation of an artificial neuron	30
2.5	Transfer Function for Neurons	30
3.1	Microstructure images of crumb rubber at 60x magnification	36
3.2	Microstructure images of crumb rubber at 2000x magnification	36
3.3	9.5 mm mixture gradations	45
3.4	Experimental design flow chart	48
3.5	Vibratory compactor	51
3.6	Fatigue beams of the mixture	51
3.7	Fatigue beam size of the mixture	52
3.8	Fatigue beam test apparatus	53
3.9	Simulation loading of fatigue beam	53
4.1	Flowchart illustrating backpropagation training algorithm	63
5.1	Viscosity comparison of the modified binder with aged binder extracted for RAPs L and C containing ambient rubber	69
5.2	Viscosity comparison of the modified binder with aged binder extracted for RAPs L and C containing cryogenic rubber	70
5.3	Viscosity comparison of the modified binder with ambient and cryogenic rubber containing aged binder extracted for RAP L	70

List of Figures (Continued)

Figure		Page
5.4	Viscosity comparison of the modified binder with ambient and cryogenic rubber containing aged binder extracted for RAP C	71
5.5	G*sin δ comparison of the modified binder with ambient and cryogenic rubber containing aged binder extracted for RAP C	74
5.6	G*sin δ comparison of the modified binder with ambient and cryogenic rubber containing aged binder extracted for RAP C	74
5.7	Optimum binder contents of the mix designs using aggregate L	76
5.8	ITS values of the mixtures containing ambient rubber using aggregate L	79
5.9	ITS values of the mixtures containing cryogenic rubber using aggregate L	80
5.10	ITS and TSR values of the mixtures using aggregate C	81
5.11	Stiffness ratio versus number of cycles, flexural beam fatigue controlled-stress and controlled-strain	84
5.12	Stress-stress hysteresis loop, flexural bema fatigue controlled-strain test	85
5.13	Dissipated energy per cycle versus number of cycles, flexural beam fatigue controlled-stress and controlled-strain tests	86
5.14	Comparison of fatigue lives between predicted and measured results using traditional strain dependent method at 5^{o}C	94
5.15	Comparison of fatigue lives between predicted and measured results using specific strain dependent method at 5^{o}C	94
5.16	Performance of ANN modes used specific strain dependent method for ambient rubber at 5^{o}C	112
5.17	Performance of ANN modes used specific strain dependent method for ambient rubber at 20^{o}C	112

List of Figures (Continued)

Figure		Page
5.18	Performance of ANN modes used specific strain dependent method for cryogenic rubber at 5°C	113
5.19	Performance of ANN modes used specific strain dependent method for cryogenic rubber at 20°C	113
5.20	Performance of ANN modes used specific energy dependent method for ambient rubber at 5°C	114
5.21	Performance of ANN modes used specific energy dependent method for ambient rubber at 20°C	114
5.22	Performance of ANN modes used specific energy dependent method for cryogenic rubber at 5°C	115
5.23	Performance of ANN modes used specific energy dependent method for cryogenic rubber at 20°C	115
5.24	Comparison of fatigue lives between predicted and measured results used second aggregate source at 5°C (regression models)	116
5.25	Comparison of fatigue lives between predicted and measured results used second aggregate source at 20°C (regression models)	116
5.26	Comparison of fatigue lives between predicted and measured results used second aggregate source at 5°C (ANN models)	117
5.27	Comparison of fatigue lives between predicted and measured results used second aggregate source at 20°C (ANN models)	117
G.1	Comparison of fatigue lives between predicted and measured results using traditional strain dependent method at 20°C (ambient rubber)	171
G.2	Comparison of fatigue lives between predicted and measured results using specific strain dependent method at 20°C (ambient rubber)	171
G.3	Comparison of fatigue lives between predicted and measured results using traditional strain dependent method at 5°C (cryogenic rubber)	172
G.4	Comparison of fatigue lives between predicted and measured results using specific strain dependent method at 5°C (cryogenic rubber)	172

List of Figures (Continued)

Figure Page

G.5 Comparison of fatigue lives between predicted and measured results using traditional strain dependent method at 20°C (cryogenic rubber)..... 173

G.6 Comparison of fatigue lives between predicted and measured results using specific strain dependent method at 20°C (cryogenic rubber)..... 173

G.7 Comparison of fatigue lives between predicted and measured results using traditional energy dependent method at 5°C (ambient rubber)..... 182

G.8 Comparison of fatigue lives between predicted and measured results using specific energy dependent method at 5°C (ambient rubber)..... 182

G.9 Comparison of fatigue lives between predicted and measured results using traditional energy dependent method at 20°C (ambient rubber)..... 183

G.10 Comparison of fatigue lives between predicted and measured results using specific energy dependent method at 20°C (ambient rubber)..... 183

G.11 Comparison of fatigue lives between predicted and measured results using traditional energy dependent method at 5°C (cryogenic rubber)..... 184

G.12 Comparison of fatigue lives between predicted and measured results using specific energy dependent method at 5°C (cryogenic rubber)..... 184

G.13 Comparison of fatigue lives between predicted and measured results using traditional energy dependent method at 20°C (cryogenic rubber)..... 185

G.14 Comparison of fatigue lives between predicted and measured results using specific energy dependent method at 20°C (cryogenic rubber)..... 185

CHAPTER I
INTRODUCTION

Fatigue, associated with repetitive traffic loading, is considered to be one of the most significant distress modes in flexible pavements. The fatigue life of an asphalt pavement is related to the various aspects of hot mix asphalt (HMA). Previous studies have been conducted to understand how fatigue life can occur and be extended under repetitive traffic loading (SHRP 1994; Daniel and Kim 2001; Benedetto et al. 1996; Anderson et al. 2001). When an asphalt mixture is subjected to a cyclic load or stress, the material response in tension and compression consists of three major strain components: elastic, viscoelastic, and plastic. The tensile plastic (permanent) strain or deformation is responsible for the fatigue damage and consequently results in fatigue failure of the pavement. A perfectly elastic material will never fail in fatigue regardless of the number of load applications (Khattak and Baladi 2001**)**.

An asphalt mixture is a composite material of graded aggregates bound with a mastic mortar. The physical properties and performance of HMA is governed by the properties of the aggregate (e.g., shape, surface texture, gradation, skeletal structure, modulus, etc.), properties of the asphalt binder (e.g., grade, complex modulus, relaxation characteristics, cohesion, etc.), and asphalt aggregate interaction (e.g., adhesion, absorption, physiochemical interactions, etc.). As a result, the properties of asphalt mixtures are very complicated (You and Buttlar 2004). However, the properties of its constituents are relatively less complicated and easier to characterize. For example, aggregate can be considered as linearly elastic; the asphalt binder can be considered as

viscoelastic/viscoplastic. Therefore, if the microstructure of asphalt mix can be obtained, its properties can be evaluated from the properties of its constituents and microstructure (Wang et al. 2004). Abbas et al. (2004) considered that the behavior of aggregate, asphalt binder, and air voids in the asphalt mixture is defined by the interaction between these three phases and the complex viscoelastic behavior of the binder, which depends on temperature, loading frequency, and strain magnitude. Studying the behavior of the composite material requires modeling the viscoelastic behavior of the binder and incorporating these models into representations of the asphalt concrete microstructure.

HMA mixture's resistance to fatigue cracking thus consists of two components, resistance to fracture (both crack initiation and propagation) and the ability to heal. These two components change over time. Healing, defined as the closure of fracture surfaces that occurs during rest periods between loading cycles, is one of the principal components of the laboratory to field shift factor used in the traditional fatigue analysis. Prediction of fatigue life or the number of cycles to failure must account for this process that affects both the number of cycles for microcracks to coalesce to macrocrack initiation and the number of cycles for macrocrack propagation through the HMA layer that add to fatigue life. Both components of mixture fatigue resistance or the ability to dissipate energy that causes primarily fracture at temperatures below 25 °C (77 °F), called dissipated pseudo strain energy, can be directly measured in simple uniaxial tensile and compression tests (Kim et al. 2003).

Accurate prediction of the fatigue life of asphalt mixtures is a difficult task due to the complex nature of fatigue phenomenon under various material, loading, and environmental conditions. For the past several decades, significant research efforts have

focused on developing reliable fatigue prediction models. There are two main approaches in the fatigue characterization of asphalt concrete: phenomenological and mechanistic. One of the most commonly used phenomenological fatigue models relates the initial response of an asphalt mixture to the fatigue life because only the mixture response at the initial stage of fatigue testing needs to be measured. In general, fracture mechanics or damage mechanics with or without viscoelsticity is adopted in the mechanistic approach to describe the fatigue damage growth in asphalt concrete mixtures (Lee et al. 2000).

Understanding the ability of an asphalt pavement to resist fracture from repeated loads is essential for the design of HMA pavement. However, reaching a better understanding of this fatigue behavior of asphalt pavements continues to challenge researchers all over the world, particularly as newer materials with more complex properties are being used in HMA pavements. For example, a very few fatigue studies of modified asphalt mixtures, including crumb rubber or reclaimed asphalt pavements, have been performed in recent years (Raad et al. 2001; Reese Ron 1997). In addition, the modified asphalt mixtures containing two materials together are not yet studied in great detail. Many rubberized asphalt pavements are in need of recycling after 15-20 years of service. Therefore, it is important to obtain the fatigue behavior of these modified mixtures in the laboratory, so that the performance can be predicted in the field. In addition, the utilization of these materials will enable the engineers to find an environmental friendly method to deal with these materials, save money, energy, and furthermore, protecting the environment.

Background

In 1960, Charles McDonald became the first engineer to use crumb rubber in asphalt mixtures to improve pavements in the United States. Since then, many experimental studies and field test sections have been constructed and tested. The mixing of crumb rubber with conventional binders results in an improvement of the asphalt mixtures in the resistance to rutting, fatigue and thermal cracking (Way 2003; Sebaaly et al. 2003). Antunes et al. (2003) pointed out; however, that the stiffness of the asphalt rubber is somewhat lower than the values generally obtained from the conventional asphalt mixture at the test temperatures (about 150 to 177°C).

Most of the rubberized asphalt projects conducted in the United States use the wet process. In this process, the crumb rubber is being reacted with the virgin binder before mixing it with the aggregate. The research conducted and reported in this paper used this process. There are many issues involved with the wet process that must be considered before the completion of the mix design including rubber size and percentage, rubber particle shape, etc. For example, the proportion of the crumb rubber changes significantly in the mixture since a rubber particle swells to 3 to 5 times its size (Mathias Leite et al. 2003).

The recycling of existing asphalt pavement materials produces new pavements with considerable savings in material, money, and energy. Aggregate and binder from old asphalt pavements are still valuable even though these pavements have reached the end of their service lives. The reclaimed materials have been used, for many years, with virgin aggregates and binders to produce new asphalt pavements, proving to be both economically feasible and effective in protecting the environment. Furthermore,

mixtures containing reclaimed asphalt pavement (RAP) have been found, for the most part, to perform as well as the virgin mixtures with respect to rutting resistance. The NCHRP (2001) report provides the basic concepts and recommendations concerning the components of mixtures, including new aggregate and RAP materials. The Superpave Mixtures Expert Task Group of the Federal Highway Administration (FHWA) developed interim guidelines for using RAP based on past experience (FHWA 1997a). In NCHRP Project 9-12 (NCHRP 2001), use of the tiered approach for RAP was considered appropriate. The recommendation conducted that the relatively low levels of RAP can be used without extensive testing of the binder, but when higher RAP contents are desirable, conventional Superpave binder tests must be used to determine how much RAP should be added or which virgin binder is recommended to be added to the mixture.

Since the mid-1970's, several million tons of RAP have been used to produce recycled HMA mixture around the country. The use of RAP has evolved into routine practice in many areas around the world. In the United States, the Federal Highway Administration reported that 73 of the 91 million metric tons of asphalt pavement removed each year during resurfacing and widening projects are reused as part of new roads, roadbeds, shoulders and embankments (FHWA 2002). Meanwhile, in 2003, there were approximately 290 million scrap tires generated in the United States, where over 233 million of which were recycled and reused (RMA 2003; Amirkhanian 2003). In recent years, more and more states have begun to ban whole tires from landfills, and most states have laws specially dealing with scrap tires. As a result, it is necessary to find safer and economical ways for disposing these tires. The civil engineering market involves a wide range of uses for scrap tires, exemplified by the fact that currently 39 states have approved

the use of tire shreds in civil engineering applications (RMA 2003). The market for crumb rubber has been growing over the past several years both in the United States and in other countries. Rubberized asphalt, the largest single Civil engineering market for crumb rubber, is being used in increasingly large amounts by several Department of Transportations (e.g., Arizona, California, Florida, Texas, and South Carolina).

Most laboratory and field experiments indicate that the rubberized asphalt concretes (RAC), in general, show an improvement in durability, crack reflection, fatigue resistance, skid resistance, and resistance to rutting not only in an overlay, but also in stress absorbing membrane (SMA) layers (Hicks et al. 1995). However, the influence of two by products (crumb rubber and RAP) mixed with virgin mixtures together is not yet identified clearly. The interaction of modified mixtures is not well understood from the stand point of binder properties to field performance. For example, pavement engineers only know the aged binder will reduce the fatigue life, but the addition of crumb rubber makes this issue more complicated. Because of the complicated relationship of these two materials in the modified mixtures, more information will be beneficial in helping obtain an optimum balance in the use of these materials. The properties of the binder should be tested in the modified mixtures, containing RAP and crumb rubber, in order to study fatigue behavior of modified mixtures.

Research Objectives

The major objective of this research was to develop a mathematical model to predict the fatigue life and stiffness of rubberized asphalt concrete (RAC) containing RAP. The specific objectives of this study included:

1. Conducting a literature review of the uses of RAC and RAP in the field and in the

laboratory.

2. Evaluating the laboratory performance of crumb rubber modified asphalt binders in the HMA mixture.
3. Evaluating the properties of the RAP in the laboratory.
4. Measuring the properties of modified mixtures for the fatigue beams.
5. Evaluating the fatigue life, stiffness and cumulative dissipated energy of the fatigue beams.
6. Developing a mathematical model to predict the fatigue life of the modified composites through using the conventional statistical analysis and artificial neural network approaches.
7. Validating the fatigue predictive model using another aggregate source.

Scope of Research

The objectives of this study were accomplished through the completion of the tasks described below.

1. A literature review of the uses of RAC and RAP in the field and in the laboratory was conducted.
2. The performance of crumb rubber modified asphalt binders including the rubber size, type, content and RAP content (aged binder) in the laboratory was evaluated. In addition, the following testing was conducted:
    a. Viscosity (modified binder) (AASHTO T 316)
    b. DSR: at intermediate temperature (AASHTO T 315)
3. The properties of the RAP in the laboratory were investigated using the following

testing procedures:

   a. Extraction of RAP binder (AASHTO T170; AASHTO TP 2)
   b. RAP aggregate gradation (AASHTO T 27; AASHTO T 30)

4. Laboratory mixtures testing used one aggregate source (L); two asphalt binder types (one used as a rejuvenator in the high RAP percentage); one type of the crumb rubber (-40 mesh); two types of rubber (ambient and cryogenic), and two types of RAP (sources L and C). Second aggregate source (C) was used to validate the developed models.
5. The optimum modified binder of modified mixtures in the laboratory was obtained using Superpave mix design procedure.
6. The fatigue strength and endurance for the modified composites at two different temperatures (5ºC, 20ºC) was evaluated using the following test procedures (AASHTO T321)
   a. Flexural Stiffness, Maximum Tensile Stress or Strain
   b. Fatigue Life
   c. Dissipated Energy
7. A mathematical model was developed to predict the fatigue life of the modified composites and a comparison of results with conventional asphalt concrete mixtures was conducted. The following concepts were used to accomplish this task:
   a. Fracture Mechanics Method (conventional statistical models)

$$N_f = a(1/\varepsilon)^b \text{ or } N_f = c(1/\sigma)^d$$

(1-1)

$$N_f = a\exp^{bMF}\exp^{cV_o}(\varepsilon_o or \sigma_o)^d (S_o)^e \quad (1\text{-}2)$$

Where,

MF = mode factor;

V_o = initial air-void content, in percentage;

ε, ε_o = test and initial flexural strain, in m/m;

σ, σ_o = test and initial flexural stress, in Newton;

N_f = number of load application or crack initiation;

S_o= initial mix stiffness, in Pa, respectively; and

a, b, c, d , e = experimentally determined coefficients

b. Artificial Neural Network Method (ANN models)

The network is trained and tested with the experimental database to approximate the following function:

$$N_f = f(VFA, \varepsilon, S, R_b, R_p) \quad (1\text{-}3)$$

Where,

R_b = the percentage of rubber in the binder, in N/N; and

R_p = the percentage of RAP in the mixture, in N/N.

VFA = voids filled with asphalt binder, and

S = mix stiffness, in Pa

Organization of the Dissertation

Chapter II includes the background information of materials (e.g., crumb rubber and reclaimed asphalt pavement) used in this study, fatigue behavior and characteristics, the previous use of conventional statistical fatigue predictive models and artificial neural network models of fatigue life. Chapter III presents the materials used in this study, experimental design including the sample preparation, testing conditions, and related binder and mixture tests. Chapter IV presents the statistical and artificial neural network

(ANN) methods used to develop the fatigue prediction models. Chapter V includes the experimental results and discussions, such as conventional statistical and ANN fatigue prediction models. Finally, Chapter VI gives a summary of analysis results, indicates conclusions of this study, and provides some recommendations for future related research projects.

CHAPTER II
LITERATURE REVIEW

Fatigue behavior and characteristics

Fatigue cracking is often called alligator cracking because this closely spaced crack pattern is similar to the pattern on an alligator's back. This type of failure generally occurs when the pavement has been stressed to the limit of its fatigue life by repetitive axle load applications. Fatigue cracking is often associated with loads which are too heavy for the pavement structure or more repetitions of a given traffic loading than provided for in design. The problem is often made worse when pavement layers become saturated and lose strength. The tensile stresses and strains develop at the bottom of the pavement structure, when tensile stresses can exceed the tensile strength of the asphalt mixture, which result in a crack at the bottom of the pavement structure (Figure 2.1). The HMA layers experience high strains when the underlying layers are weakened by excess moisture and fail prematurely in fatigue. Fatigue cracking is also often caused by repetitive loading with overweight trucks and/or inadequate pavement thickness due to poor quality control during construction.

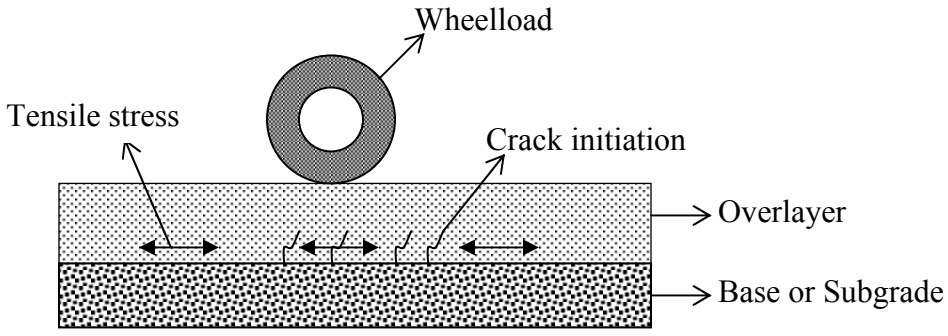

Figure 2.1 Initiation of fatigue cracking

Fatigue cracking, a significant major structure distress, is a symptom of insufficient structural strength in the pavement, weak subgrade, or overloading of the pavement. It can lead to the development of potholes when the individual pieces of HMA physically separate from the adjacent material and are dislodged from the pavement surface by the action of traffic. Potholes generally occur when fatigue cracking is in the advance stages and when relatively thin layers of HMA comprise the bound portion of the pavement (Roberts et al. 1996).

The severity of fatigue cracking can be rated in three main types (Lavin 2003):

Low severity: Fine, longitudinal cracks running parallel to each other with none or only a few interconnecting cracks. The cracks are not spalled. Initially there may only be a single crack in the wheelpath or pavement loading area (Figure 2.2a).

Medium severity: Further development of light alligator cracks into pattern or network of cracks. The cracks may also be slightly spalled (Figure 2.2b).

High severity: The pattern of cracks has progressed so that the individual pieces are well defined and the cracks are spalled at the edges. Some of the pieces may move under traffic or loading. Pieces may begin to disintegrate, forming potholes. Pumping of the pavement may also exist (Figure 2.2c).

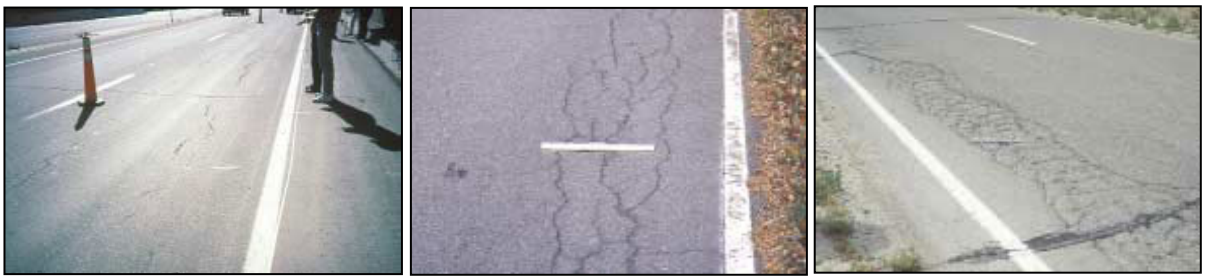

(a) (b) (c)

Figure 2.2 Images of fatigue cracking (Lavin 2003)

Fatigue cracking is measured in square meter of surface area. There are usually various degrees of severity within the same pavement section. If the different levels of severity can be easily distinguished from each other, they should be measured and recorded separately. If they cannot be easily identified, the entire area should be rated at the highest severity present (Local Road Research Board 1991; Lavin 2003)

Fatigue Characteristics of Asphalt Binder

Asphalt concrete is a mixture of asphalt binder, aggregate and air avoids. The properties of asphalt concrete are related to the properties of these constituents and the interaction among them, which is related to the spatial location of the constituents or the microstructure of the mixture. The microstructure of asphalt concrete is complicated and is related to the gradation of aggregate, the properties of aggregate-binder interface, the void size distribution, and the interconnectivity of voids (Wang et al. 2004).

Much research has indicated that some properties (e.g., $G^* \sin\delta$) of asphalt binder are related to fatigue life of an asphalt pavement. The evaluation of the binders in a controlled laboratory mix "failure" test was considered a necessary tie between the binder properties and the filed performance data (Reese 1997; Anderson et al. 2001). For example, Dynamic shear rheometer (DSR) is used to characterize both viscous and elastic behavior by measuring the complex shear modulus (G^*) and phase angle (δ) of an asphalt binder. Performing DSR measurements over a range of frequencies allows fitting mechanistic models to such binder rheological data. These models are well suited for implementation into numerical solutions of the microstructural behavior of asphalt concrete (Abbas et al. 2004). This parameter is based on the theory that as an asphalt

binder ages in a pavement, its G* and δ rise to a point where the combination of viscous and elastic components become so high that the binder can no longer relieve the stresses of repeated loading, and therefore crack (Hines et al. 1998).

However, comparing binder properties with the fatigue life of mixtures containing various binder, Reese (1997) indicated that fatigue models based on G* and sinδ from mix frequency sweeps at medium temperature are subject to the same shortcomings as the binder fatigue parameter; and the SHRP binder fatigue parameter (G*sinδ) does not correlate adequately with mix fatigue tendencies.

The viscosity of and asphalt binder is used to determine the flow characteristics of the binder to provide some assurance that it can be pumped and handled at the hot mixing facility; also to determine the mixing and compacting temperature of an asphalt mixture. This property is related to aging behavior of asphalt mixtures and even affects its fatigue life. Bending beam rheometer (BBR) is used to measure how much a binder deflects or creeps under a constant load at a constant temperature, which is related to a pavement's lowest service temperature; also related to its fatigue life (e.g., stiffness).

Furthermore, high pressure – gel permeation chromatography (HP-GPC) has also been used to test engineering properties of asphalt binders according to the ratio of different molecular sizes (e.g., large molecular size, medium molecular size, and small molecular size). It has been used to determine the molecular size distribution of an asphalt cement (Churchill et al. 1995; Shen et al. 2006). This technique has the potential of characterizing the strongly associating molecular components that play a major role in determining the rheological properties and aging characteristics of an asphalt binder related to the pavement performance (fatigue cracking) (Jennings 1980; Kim et al. 1995).

Crumb Ground Rubber

In 1960s, Charles McDonald was the first engineer, in the United States, to use scrap tires in asphalt mixtures aimed at improving pavement performance. Since then, many other experimental studies and test sections have been conducted with ground tire rubber. Several states including Florida, Arizona and California use ground tire rubber in asphalt binder with contents ranging from 5% to 25% in dense, gap and open mixes (e.g. overlays, stress absorbing membranes, and stress absorbing membrane inter-layers). The completed projects show an improvement in durability, crack reflection, fatigue resistance, skidding resistance, and resistance to rutting (Hicks 1995; Xiao et al. 2006).

In addition to rubber, tires comprise textile fibers and steel, where 50% to 60% of the weight can be recovered as rubber, corresponding to 4.5 to 5.5 kg per 9 kg of tire. Tire rubber, in general, is comprised of synthetic rubber, natural rubber, plasticizer, carbon black and mineral fillers. The natural rubber and the synthetic rubber content in tires vary depending on the type of vehicle. Truck tires, in most cases, have a greater percentage of natural rubber as compared with synthetic rubber. In general, automobile tires have around 16% natural rubber and 31% synthetic rubber, while truck tires have around 31% natural rubber and 16% synthetic rubber. In spite of these variations in the rubber composition, the composition of bulk ground rubber is quite uniform and the ground rubber industry is not based on a specific type of tire (Ruth 1997).

The particle size and the surface texture of the ground rubber vary in accordance with the type of grinding, which can be either ambient or cryogenic. Each method has the ability to produce crumb rubber of similar particle size, but the major difference between them is the particle morphology. The ambient process often uses a conventional high

powered rubber cracker mill set with a close nip where vulcanized rubber is sheared and ground into a small particle. The process produces a material with an irregular jagged particle shape. However, the cryogenic grinding usually starts with chips or a fine crumb. This is cooled using a chiller and the rubber, while frozen, is put through a mill. The cryogenic process produces fairly smooth fracture surfaces. Previous research indicated that the engineering properties of two type rubbers are significantly different. The interaction effect (IE) and particle effect (PE) are affected by the method used to produce the crumb rubber (Putman 2005). Putman (2005) pointed out that the crumb rubber modifier binders (CRM), containing ambient rubber, resulted in higher IE and PE values than the CRM binders made with cryogenic rubber. This is due to the increased surface area and irregular shape of the ambient CRM.

In general, crumb rubber-modified (CRM) asphalt can be divided into two categories, wet process and dry process. The wet process is a method that blends the crumb rubber with asphalt binder before incorporating the binder into the mix. The dry process involves any method that mixes the CRM with the aggregate before the mixture is charged with the asphalt binder. In the United States, the wet process is the one predominantly used today, where the high chromatic oil extender can either be used or not in the preparation of asphalt mixtures with tire rubber. The mixture is prepared at a temperature ranging from 150ºC to 190ºC for about one hour. However, Thompson and Xiao (2004) found that the mixing temperature at 177ºC and reaction time of 30 minutes are suited to blend CRM in the wet process for the mixtures tested in their project. Since the resulting asphalt rubber is not storage stable, the storage period is restricted to tanks provided with recirculation and agitation features. In the U.S. there are various

companies that mix ground tire rubber with asphalt in mobile units within asphalt plants or in asphalt modified industries (Hicks 1995; Ruth 1997).

Polymers, including rubbers, are known to absorb liquids and swell with the amount being dependent on the nature, temperature and viscosity of the liquid/solvent and type of polymer (Treloar 1975). The swelling of rubber in organic solvents is a diffusion process. The rubber particle undergoes a swelling of 3 to 5 times in size when incorporated into the asphalt binder. Xiao et al. (2006) investigated the dimension changes of crumb rubber after extract from reacted modified binder. The polymers existing in the rubber absorb the aromatic portion of the binder and in most cases the viscosity, at 135ºC, of the resulting binder increase up to ten times in relation to the original value. Interaction of the rubber with the asphalt cement can be affected by several factors (Mathias Leite et al. 2003).

- temperature, time, type of mixer
- rubber size, texture and content
- chemical composition of the asphalt binder

Airey et al. (2003) also found that the initial rate of bitumen absorption is directly related to the viscosity as well as the chemical composition of the binders. The report indicated that with the softer and lower asphaltene content binder have the highest rate of absorption. In addition to the traditional oxidation of bitumen at high temperatures, the residual asphalt experienced further changes in their chemical constitution as a result of the crumb rubber-asphalt interaction and the absorption.

Development of modified asphalt materials to improve the overall performance of pavement has been the focus of several research efforts over the past few decades. Several attempts were made in the past to modify asphalt mixtures using crumb rubber to

improve the performance of asphalt pavements. Many researchers found that the utilization of crumb rubber in pavement construction is effective and economical (McDonald 1966; Little 1986; Button et al. 1987; Bahia and Davies 1994; Raad and Saboundjian 1998; Hossain et al. 1999; Anderson et al. 2001; Amirkhanian 2003; Way 2003; Airey et al. 2003; Shen et al. 2006; and Xiao et al. 2006).

The results of some research projects indicated that fatigue behavior of rubberized mixtures significantly improved compared to conventional mixtures. At the same time, the crumb rubber improved the resistance to aging. The application of the fatigue results in the analysis of thin and thick pavement sections indicated that aging prolonged the fatigue life of the pavement structures (Raad et al 2001; Palit et al. 2004) and the improvement to fatigue life of rubberized asphalt mixture. At the same time, there are many other benefits. For example, it was found that the use of rubberized asphalt on highways resulted in an average 4 dB reduction in traffic noise levels as compared to the conventional asphalt overlay (Way 2003). Adding crumb rubber to asphalt binder increases the damping ratio of asphalt mixes. It has been reported that the CRM mixture is a viable material to use to achieve vibration attenuation of railway trackbeds (Zhong et al. 2002). Way (2003) and Xiao et al. (2007) indicated that the rubberized asphalt mixtures have many positive qualities including: they are highly resistance to rutting; they reduced the reflective cracking and improve durability of surface courses. However, the increase of rubber content produces a decrease in the values of resilient modulus of the mixtures, therefore, an increase of the flexibility. The incorporation of the crumb rubber with conventional binders produces a slight reduction in the indirect tensile strength of modified mixture (Xiao et al. 2007).

Reclaimed Asphalt Pavement

During the 1970's, the milling machine became an integral part of many asphalt rehabilitation programs and millions of tons of RAP were generated annually. Some of these millings were trucked to HMA plants where they were hot recycled or stockpiled for future use. However, initially much of this RAP was merely used as fill material or even wasted. In 1981, the FHWA issued its policy statement that "Recycling should be one of the options considered at the design state on all rehabilitation projects" (Kearney 1997).

Many studies concluded that the use of RAP is economical and can help to offset the increased initial costs sometimes associated with Superpave binders and mixtures and conserves natural resources, avoids disposal problem and associated costs. Recycled materials have proven to be equal or even better than new materials in quality. Over years, recycling has become one of the most attractive pavement rehabilitation alternatives, and different recycling methods are now available to address specific pavement distress and structural needs (Kandhal 1997; Kearney 1997; Terrel 1997; Decker 1997; Gardiner and Wagner 1999). For the mixing of RAP with virgin materials, the NCHRP 9-12 report has developed guidelines for incorporating RAP in the Superpave system on a scientific basis and prepared a manual for RAP usage that can be used by laboratory and field technicians (NCHRP 2001; McDaniel et al. 2002).

Recycling of RAP can produce new pavement materials resulting in considerable saving of material, money and energy. The continued use of RAP in Superpave pavements is desired due to the following specific benefits (Kandhal 1997; NCHRP 2001):

- RAP can result in substantial savings over the use of new materials, and the cost of hauling can be avoided if recycling is performed in place.
- Use of RAP is economical and can help in conservation of natural resources by reducing the need for new materials.
- Use of RAP has been proven to be equal or even better than new materials in quality and also it avoids disposal problems and costs.
- Recycling of RAP can save a considerable amount of energy compared to the conventional construction techniques.

The asphalt recycling and reclaiming association defines five different types of recycling methods (Kandhal 1997):

- Cold planning
- Hot recycling
- Hot in-place recycling
- Cold in-place recycling
- Full depth reclamation

All of the different recycling techniques offer some advantages in dealing with RAP. However, the choice of a particular recycling method should be primarily on the basis of the type of distress shown in the existing pavement. This is because all of the recycling methods are not equally suited for treating different types of distress (e.g. rutting, pothole, fatigue, etc.), and the choice must be made for the specific method which is capable of rectifying the existing distress conditions. A comprehensive evaluation of the existing pavement is necessary before attempting any recycling process (Kearney 1997).

A subgroup of the FHWA Superpave Mixtures Expert Task Group developed interim guidance for the use of RAP based on past experience. These guidelines established a tiered approach for RAP usage. The three-tier approach gives guidance in

choosing the blending method for recycled mixture with first tier dealing with low percentage of RAP (0-15%). In this case, it is assumed that the aged binder has relatively no effect on the mixture performance and the RAP can be added without making any modification to the design virgin binder. The second tier, with a percentage range of RAP of 15%-25%, involves the use of new binder that is one grade softer (on both the high and low grade) than the specification grade to be used. And the third tier is using a high percentage (25% or greater) of RAP. For this case, there is an extensive mixing of the aged RAP binder and the new virgin binder and the linear blending formulas can be used in determining performance grade of this modified binder and what softer binder is needed to be incorporated in the mixture (FHWA 1997a; FHWA 1997b).

Fatigue Analysis Method

The definition of fatigue life, especially in the controlled-strain mode, is a controversial issue. There are two approaches to develop a fatigue life prediction model: phenomenological and mechanistic. The phenomenological fatigue model is simple to use; however, it does not account for damage evolution throughout the fatigue process. On the other hand, mechanistic models are based on fracture mechanics or damage mechanics. This approach is inherently more complex than the phenomenological approach but is more widely accepted because it uses material properties based on stress-strain relationships (Kim et al. 2003).

Kim et al. (1997) described a mechanistic approach to viscoelastic constitutive modeling of asphalt concrete with damage evolution under realistic cyclic loading conditions. The most common and classical fatigue model is developed by correlating

fatigue life with initial strain or stress levels applied during tests. The limitation of this phenomenological model is that the damage evolution is not taken into consideration and hence it can only be applied to a given set of loading conditions (Kim et al. 2003). Recently, Lee et al. (2000) successfully developed a fatigue performance prediction model of asphalt concrete based on an elastic-viscoelastic correspondence principle and continuum damage mechanics.

A series of studies by Lee (1996); Kim et al. (2000) suggested a new failure criterion using 50% loss in pseudo stiffness. The pseudo stiffness can be reasonably used to represent damage accumulation due to repeated fatigue loading, as it eliminates linear viscoelastic time-dependency, which does not induce damage. A 50% loss in stiffness or modulus from the initial value was used by Hicks et al. (1993); Williams (1998); Smith and Hesp (2000); and others. In particular, Reese (1997) proposed evaluation of changes in the phase angle during fatigue testing. According to his hypothesis, a point showing the maximum phase angle is a reasonable fatigue failure point, since the phase angle versus time curve shows a rapid loss of phase angle when asphalt mixtures stop accumulating distress (Kim et al. 2003).

Schapery (1984) proposed the extended elastic-viscoelastic correspondence principle, which is applied to both linear and nonlinear viscoelastic materials. Torsional shear pseudo strain is defined as:

$$\gamma^R \equiv \frac{1}{G_R}\int_0^t G(t-\xi)\frac{\partial \gamma}{\partial \xi}d\xi \qquad (2\text{-}1)$$

Where,

$\gamma^R(t)$ = pseudo strain in the shear mode;

G_R = reference shear modulus that is an arbitrary constant;

$G_{(t)}$ = shear relaxation modulus; and

γ =time-dependent shear strain

And pseudo stiffness is expressed as:

$$S^R = \frac{\tau_m}{\gamma_m^R} \tag{2-2}$$

Where,

S^R = pseudo stiffness;

γ_m^R = peak pseudo strain in each physical stress-pseudo strain cycle; and

τ_m = physical stress corresponding to γ_m^R

The fatigue characteristics of asphalt mixtures are usually expressed as relationships between the initial stress or strain and the number of load repetitions to failure-determined by using repeated flexure, direct tension, or diametral tests performed at several stress or strain levels. The fatigue behavior of a specific mixture can be characterized by the slope and relative level of the stress or strain versus the number of load repetitions to failure and can be defined in the following form (Monismith et al. 1985).

$$N_f = a(1/\varepsilon_0)^b(1/S_0)^c \quad \text{or} \quad N_f = a(1/\sigma_0)^b(1/S_0)^c \tag{2-3}$$

Where,

N_f = number of load application or crack initiation;

ε_0, σ_0 = tensile strain and stress, respectively; and

a, b, c = experimentally determined coefficients

Several models have been proposed to predict the fatigue lives of pavement (Finn et al. 1977; Shell 1978; Asphalt Institute 1981; Tayebali et al. 1994). To develop these models, laboratory results have been calibrated by applying shift factors based on field observations to provide reasonable estimates of the in-service life cycle of a pavement based on limiting the amount of cracking due to repeated loadings.

The fatigue behavior of a specific mixture can be characterized by the slope and relative level of the stress or strain versus the number of load repetitions to failure and can be defined by a relationship of the following form (Tayebali et al. 1994):

$$N_f = a \exp^{bMF} \exp^{cV_o} (\varepsilon_o or \sigma_o)^d (S_o)^e \quad (2\text{-}4)$$

Where,

N_f = Cycles to Failure;

MF = mode factor;

V_o = initial air-void content in percentage;

ε_0 = initial flexural strain;

σ_0 = initial flexural stress;

S_o = initial mix stiffness; and

a b, c, d, e = regression constants

The fatigue models developed by Shell, the Asphalt Institute, and University of California at Berkeley (SHRP A-003A contractor) are shown in following forms:

Shell Equation (Shell 1978):

$$N_f = \left[\frac{\varepsilon_t}{(0.856V_b + 1.08)S_{mix} * 0.36} \right]^{-5} \quad (2\text{-}5)$$

Where,

N_f = fatigue life;

ε_t = tensile strain;

V_b = volume of asphalt binder; and

S_{mix} = mixture stiffness (flexural)

Asphalt Institute Equation (Asphalt Institute 1981):

$$N_f = S_f * 10^{[4.84(VFA-0.69)]} * 0.004325 * \varepsilon_t^{-3.291} * S_{mix}^{-0.845} \quad (2\text{-}6)$$

Where,

VFA = Volume of Voids filled with asphalt binder; and

S_f =shift factor to convert lab test results to field

SHRP A-003A Equation (Tayebali et al. 1994):

$$N_f = S_f * 2.738E05 * \exp^{0.077VFA} * \varepsilon_0^{-3.624} * (S_0^{"})^{-2.720} \quad (2\text{-}7)$$

Where,

$S_0^{"}$= initial loss-stiffness;

In recent years, the dissipated energy approach has been employed in predicting the fatigue lives of asphalt concrete that is based on the assumption that the number of cycles to failure is related mainly to the amount of energy dissipated during the test. A major advantage of this approach compared with the classical model is that predicting the fatigue behavior of a certain mix type over a wide range of conditions, from a few simple fatigue tests, is possible. Other criteria based on changes in dissipated energy including dissipated energy ratio or damage accumulation ratio were selected in studies by Rowe (1993) and Anderson et al. (2001).

The dissipated energy per cycle, W_i, for a linear viscoelastic material is given by the following equation:

$$W_i = \pi \sigma_i \varepsilon_i \sin(\delta_i) \quad (2\text{-}8)$$

Where,

W_i = dissipated energy at load cycle i;

σ_i = stress amplitude at load cycle i;

ε_i = strain amplitude at load cycle i; and

δ_i = phase shift between stress and strain at load cycle i

The cumulative dissipated energy (W_N) up to cycle n is defined as follows:

$$W_{\Sigma_n} = \sum_{i=1}^{n} W_i \quad (2\text{-}9)$$

Several researches (Van Dijk 1975; Van Dijk and Visser 1977; Pronk and Hopman 1990; Tayebali 1992; Read and Collop 1997; Hossain and Hoque 1999; Birgisson et al. 2004) have used the energy approach for predicting the fatigue behavior of the asphalt mixtures. Research has shown that the dissipated energy approach will make it possible to predict the fatigue behavior of mixtures in the laboratory over a wide range of conditions from the results of a few simple fatigue tests. Such a relationship can be characterized in the form of the following equation:

$$W_N = A\,(N_f)^Z \tag{2-10}$$

Where,

N_f = fatigue life;

W_N = cumulative dissipated energy to failure; and

A, Z = experimentally determined coefficients.

Statistical Analysis Models of Fatigue Life

Previous research has indicated that the main purpose of the statistical analysis of test results was to determine the sensitivity of the fatigue test methods to mix and test variables in characterizing the fatigue response of the asphalt-aggregate mixtures and then build the statistical models of fatigue life through regression analysis (Tayebali et al. 1994). They used the statistical analysis for each data set included the following sequence:

- Test for correlation among the independent variables (Pearson);
- Analysis of variance (ANOVA) of full models to determine the sensitivity of stiffness, fatigue life, and cumulative dissipated energy to mix and testing variables;
- General linear modeling (GLM) to develop models for stiffness, fatigue life, and cumulative dissipated energy; and

- Summaries of the effects of the experimental variables included in the experiment on stiffness, fatigue life, and cumulative dissipated energy based on the results of GLM.

One of the assumptions necessary for ANOVA and GLM is that the dependent and independent variables are normally distributed. Distribution for stress, strain, stiffness, cycles to failure, and cumulative dissipated energy were reviewed and found to be log-normally distributed. Therefore, log transformations were used in ANOVA and GLM through regress analysis.

The results of these research projects indicated that:

- Fatigue life as a response variable is sensitive to asphalt binder type for all test types;
- The flexural beam controlled-strain tests show an interaction between asphalt binder type and content;
- Flexural beam tests exhibit sensitivity to aggregate type;
- Asphalt binder content did not have a significant effect on fatigue life for any of the fatigue tests considered;
- Air-void contents significantly influences fatigue life for all test types in that the fatigue is higher in the mixes with low voids than for mixes with high voids; and
- Both temperature and stress or strain significantly influence fatigue life for all test types.

The summary of the regression analysis is based on calibrations in which outliers, defined as cases where the absolute values of the residuals (natural log of fatigue life) exceeded 1.1, were removed. Removal of outliers not only enhanced the accuracy of the models but, more importantly, improved their consistency and reasonableness.

Artificial Neural Network Analysis Models of Fatigue Life

The application of neural networks is to help developing the fatigue predictive models of the asphalt mixtures and reduce the influence of complicated variables and incompleteness of the available data. Neural networks are composed of simple elements operating in parallel. These elements are inspired by biological nervous systems. It has been trained to perform complex functions in various fields, including pattern recognition, identification, classification, speech, vision, and control systems. Today, neural networks can be trained to solve problems that are difficult for conventional computers or human beings. Recently, some researchers have used neural networks as a new tool in solving complicated problems in the civil engineering area. In this research project, the neural network will be used to train the target parameters of models and to support the decision process and improve the efficiency of the models (Kim et al. 2004; Tarefder et al. 2005). The objective of the network training is to map the input to the output by determining the connection weights and biases through an error reduction process.

An example of a three-layer neural network architecture used in this research is shown in Figure 2.3. This architecture consists of an input layer, a hidden layer, and an output layer. The input neurons are nodes that require no processing; the output neurons produce the output of the net; and the layer between the input and output layers is the hidden layer.

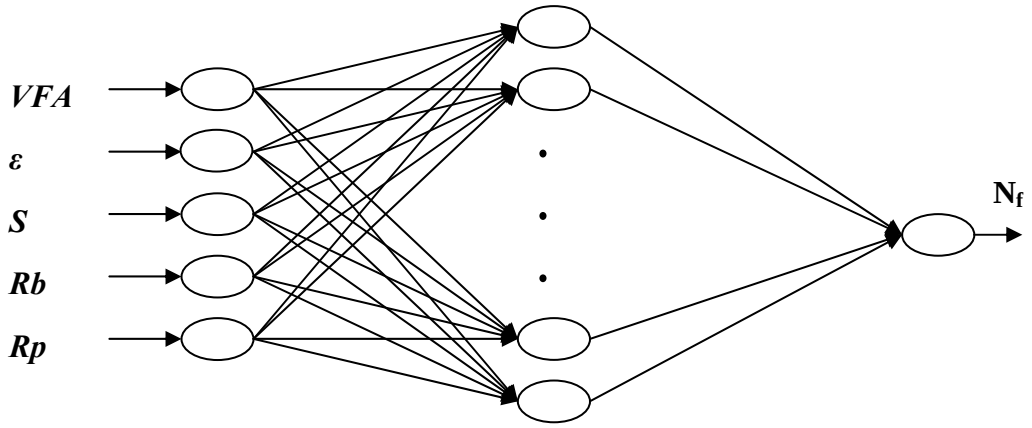

Figure 2.3 Example of a three-layer feedforward neural network architecture

Each of the neurons in the hidden and output layers consists of two parts (shown in Figure 2.4). The first part simply aggregates the weighted inputs resulting in a quantity; the second is the transfer function, through which the combined signal flows. It can be expressed as:

$$a = f(Wp + b) \tag{2-11}$$

Where,

a = output of the neuron;

W = weight vector;

b = bias;

p = input vector of the neuron; and

f = transfer function

Commonly used transfer functions include hard limit function, liner function or sigmoidal function (shown in Figure 2.5). The logistic function, one of the sigmodial functions, is the most widely used transfer function. The equation of this function is expressed as following:

$$f(t)=\frac{1}{1+e^{-t}} \tag{2-12}$$

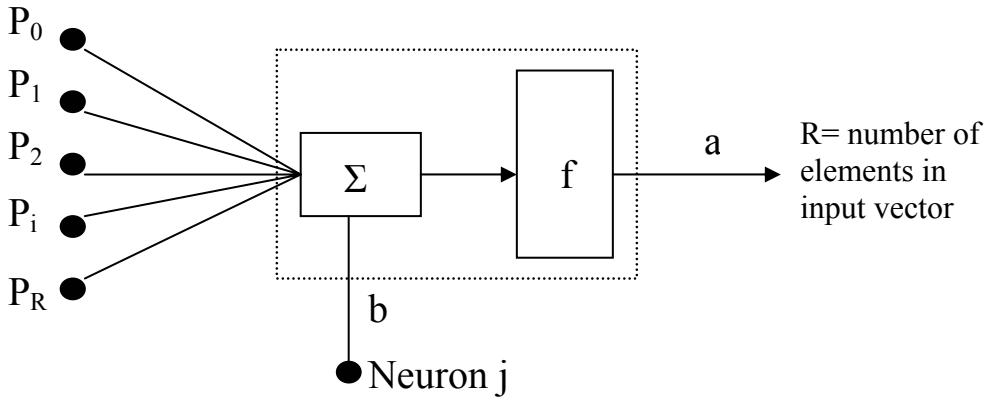

Figure 2.4 Schematic representation of an artificial neuron

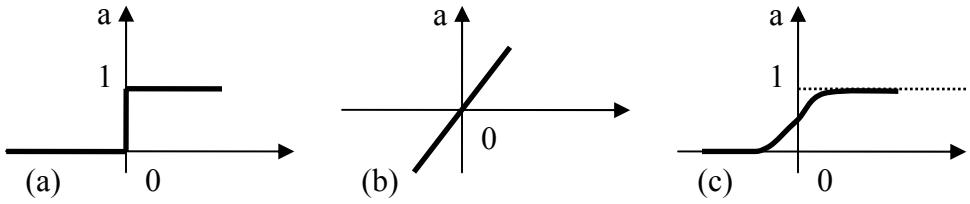

Figure 2.5 Transfer Function for Neurons: (a) Hardlimit transfer function, (b) Linear transfer function, (c) Logistic transfer function

A popular training algorithm commonly adopted for training a feed-forward neural network is backpropagation. It is a systematic method for training multiple-layer artificial neural networks. In spite of its limitations, backpropagation has dramatically expanded the application range of neural networks due to its strong mathematical foundation. So the backpropagation will be used as a training multiple-layer artificial neural networks algorithm in this research.

For the three-layer network shown in Figure 2.3, the output of the network N_f is calculated as follows:

$$N_f = f_T\left\{B_0 + \sum_{k=1}^{n}\left[W_k \bullet f_T\left(B_{HK} + \sum_{i=1}^{m} W_{ik} P_i\right)\right]\right\} \quad (2\text{-}13)$$

Where,

B_o = bias at the output layer;

W_k = weight of the connection between neuron k of the hidden layer and the single output layer neuron;

B_{HK} = bias at neuron k of the hidden layer;

W_{ik} = weight of the connection between input variable i and neuron k of the hidden layer;

P_i = input parameter i; and

f_T = transfer function

CHAPTER III
MATERIALS AND EXPERIMENTAL DESIGN AND TESTING

Materials

Asphalt Binder

Two grades of virgin asphalt binders (PG 64-22 and PG 52-28) were used in this study. In order to reduce the effects of asphalt binder source, only one source of PG 64-22 was utilized for all mix designs. The PG 52-28 was used as a softer binder in mixtures containing 30% RAP in accordance with the recommended guidelines of NCHRP subgroup expert group (NCHRP 2001). Some of the engineering properties of two binders are shown in Table 3.1.

Table 3.1 Engineering properties of virgin asphalt binders

Aging states	Test properties	PG64-22	PG52-28
No aging	Viscosity @135^{o}C (Pa-s)	0.430	0.213
	G*/sin(δ) @64 ^{o}C (kPa)	1.279	0.398
RTFO	G*/sin(δ) @64 ^{o}C (kPa)	2.810	0.825
PAV	G*sin(δ) @25 ^{o}C (kPa)	4074	821
	Stiffness @-12 ^{o}C (MPa)	217	60.4
	m-value @-12 ^{o}C	0.307	0.476

For a recycled mixture, it is important to determine the amount of aged asphalt binder present in the RAP material, so it can be accounted for in the mix design process. It is also important to know some physical properties of the RAP aggregate, such as the gradation and the angularity. These properties can be determined by extracting the asphalt binder from RAP to measure the binder content and test the aggregate properties.

Aged binders were extracted from two sources of RAP (L and C) according to ASTM D 5402 (Standard Practice for Recovery of Asphalt from Solution Using the Rotary Evaporator) and AASHTO TP 2-01 (Standard Test Method for the Quantitative Extraction and Recovery of Asphalt Binder from Asphalt Mixtures). The base properties of the extracted binders from RAP were tested using the Superpave mix design method and the results are shown in Table 3.2. Table 3.2 shows that aged binder of source L has a higher viscosity value, G*/sin(δ) value in the virgin and RTFO aging states. For PAV aging states, source C has a better fatigue resistance (G*sin(δ)) and a smaller stiffness values than that of source C.

Table 3.2 Engineering properties of aged binders

Aging states	Test properties	Source L	Source C
No aging	Viscosity @135^{o}C (Pa-s)	5.982	2.55
	G*/sin(δ) @64 ^{o}C (kPa)	58.542	45.625
RTFO	G*/sin(δ) @64 ^{o}C (kPa)	109.780	95.298
PAV	G*sin(δ) @25 ^{o}C (kPa)	8000	11000
	Stiffness @-12 ^{o}C (MPa)	294	277
	m-value @-12 ^{o}C	0.241	0.243

Crumb Rubber

Two types of crumb rubber (ambient and cryogenic) were used in this study. Ambiently produced rubber, in general, has an irregular shape and therefore a greater surface area than cryogenically produced rubber due to the different manufacturing process. At the same time, different grinding processes also results in different gradations between ambient and cryogenic rubber particles. Previous research and field projects conducted in South Carolina indicated that the -40 mesh ambient rubber is effective in

improving the engineering properties of rubberized mixtures (Amirkhanian 2003). Therefore, the -40 mesh rubber is employed in this study.

The gradations of crumb rubber are shown in Table 3.3, which shows that -40 mesh cryogenic rubber has a larger passing percentage for the 50 mesh and 80 mesh sizes, while ambient rubber has a greater amount of fine rubber (smaller than 75μm) than cryogenic. These various rubber particles absorb a various amount of aromatic and light oil from the asphalt binder and swell to different sizes due to influences of their surface shape and grinding method. This absorption process affects the performance of these modified binders in the mixture.

Table 3.3 Gradations of -40 mesh crumb rubber

	%Passing	
Sieve No.(μm)	Ambient	Cryogenic
20 (850)	0	0
30 (600)	0	0.7
40 (425)	9.0	7.7
50 (300)	31.9	45.7
80 (180)	32.9	34.4
100 (150)	7.6	4.1
-100 (75)	18.6	7.4

The surface areas of ambient and cryogenic rubbers are shown in Table 3.4, which indicates that the fine crumb rubber has greater average surface area than coarse one. At the same time, the average surface area of ambient rubber per gram at each particle size is greater than that of cryogenic. On the other hand, the fewer particles and smaller surface area exist in coarser rubber than fine at the same mass condition. Putman (2005) indicated that the surface area of the crumb rubber could be measured using a Coulter SA 3100 surface area and pore size analyzer. The SA 3100 uses the gas sorption method, in which gas molecules of known size are absorbed on sample surfaces. The

quantity of gas condensed and the resultant sample pressure are recorded at a constant temperature, which allows the construction of an isotherm (Coulter Corporation 1996). The isotherm data are then subjected to the BET (Brunauer, Emmett, and Teller) calculation for surface area of samples (Brunauer et al. 1938).

Table 3.4 Average surface area of crumb rubber (-40 mesh)

	Ambient Rubber			Cryogenic Rubber		
Sieve No.(μm)	Average (m^2/g)	Std dev.	C.V.(%)	Average (m^2/g)	Std dev.	C.V.(%)
30 (600)	0.040	0.0006	1	0.018	0.0017	10
40 (425)	0.047	0.0032	7	0.026	0.0122	47
50 (300)	0.064	0.0000	0	0.031	0.0059	19
80 (180)	0.103	0.0114	11	0.042	0.0078	19
100 (150)	0.152	0.0012	1	0.061	0.0021	3
-100 (75)	0.170	0.0053	3	0.105	0.0322	31

The microstructure analysis of crumb rubber particle is beneficial to understand the absorption and swell of the crumb binder during its reaction with a binder at a high temperature. Putman (2005) and Xiao et al. (2006) found that the surface morphology of crumb rubber particle can be evaluated using a scanning electron microscope (SEM). A Hitachi S3500N SEM was used to record images of individual crumb rubber particles at magnification levels of 60 and 2000. During the sample testing process, several crumb rubber particles were placed onto an aluminum specimen tab covered with double-sided carbon tape. These particles were not treated or coated prior to evaluation in the SEM. Then, the degree of each particle roughness of different types of crumb rubber from their micrographs was compared. The microstructure images of ambient and cryogenic are shown in Figures 3.1 and 3.2. These images also show that cryogenic crumb rubber has more smooth surface shape. Putman (2005) also indicated other crumb rubber particle sizes (e.g., 20 and 80 mesh) have similar properties as 40 mesh.

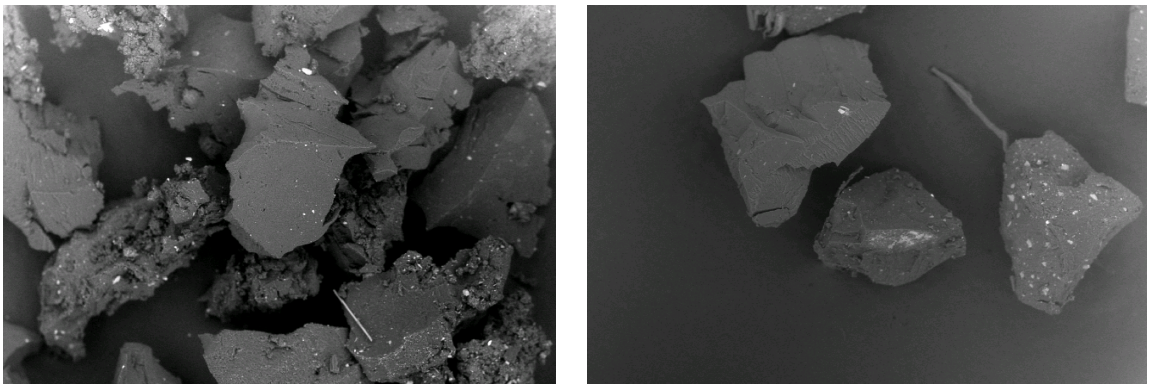

(a) (b)

Figure 3.1 Microstructure images of crumb rubber at 60x magnification (a) 40 mesh cryogenic (b) 40 mesh ambient (From Putman 2005)

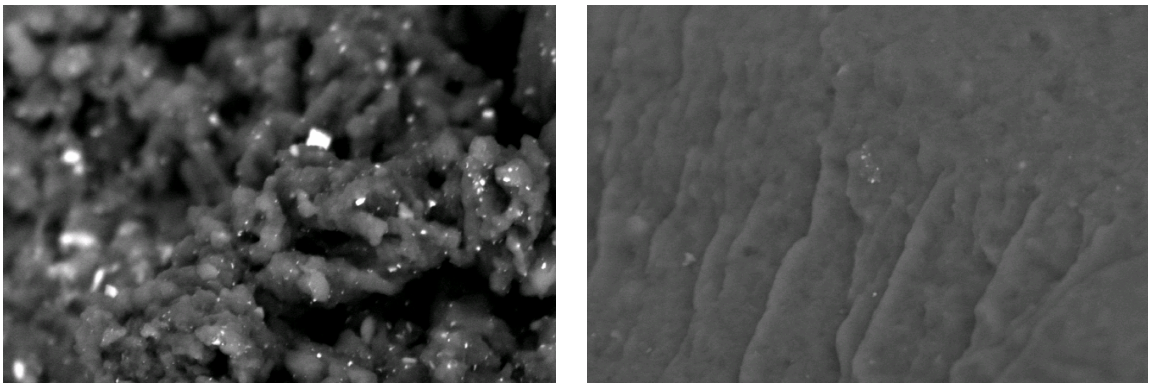

(a) (b)

Figure 3.2 Microstructure images of crumb rubber at 2000x magnification (a) 40 mesh cryogenic (b) 40 mesh ambient (From Putman 2005)

Reclaimed Asphalt Pavement

The sampling of RAP is a necessary process in order to reduce its variability that results in a loss of quality control for a recycling project. RAP can be sampled from the roadway (by coring before the pavement is milled), from a stockpile, or from the haul trucks. The process for stockpile or haul-truck sampling is similar to the sampling process used for aggregates. It is important to get samples that accurately reflect the material that is available for use. For example, in a stockpile of RAP, some segregation may have occurred, and there may be parts of the pile that are coarser than the rest of the pile.

When sampling a pile, it is important to sample from several locations to avoid taking the entire sample from a segregated area (NCHRP 2001). The size of sample needed depends on the purpose of the sampling. To test the RAP for gradation and asphalt content or to monitor variability for quality-control testing, sample sizes of about 10 kg (22 lb) are usually adequate. Superpave specimens are much larger than Marshall or Hveem specimens, so more material will be needed when doing a Superpave mix design. Typically, a sample of at least 25 kg (55 lb) is needed (NCHRP 2001).

RAP materials used in this study were taken from the same geographical area as the new aggregate sources (L and C) to ensure that the aggregate in the RAP had similar properties as the new one. Both RAP sources satisfied the requirements of the South Carolina Department of Transportation (SCDOT).

The ignition oven was used to obtain the asphalt content of the RAP and then the gradation analysis was conducted on the aggregate. The NCHRP (2001) report indicated ignition ovens may cause degradation of some aggregates, so care should be used when analyzing the gradation of aggregates after the ignition oven. Experience with local aggregate can indicate whether the ignition oven is an appropriate method to use.

The nominal maximum size of the aggregate used in this study was 9.5 mm. The RAP passed 12.5 mm (1/2 inch) sieve and retained on No. 4 sieve was referred to as +4 RAP, while the RAP passed No. 4 sieve was referred to as -4 RAP. The analysis of the binder content and aggregate gradation was performed according to these two types (+4 RAP and -4 RAP). The engineering properties of the aged binder and the gradation of the aggregate are shown in Tables 3.2 and Table 3.5; respectively.

Table 3.5 Component of two RAPs

Aggregate Source	Type of RAP	9.5 mm 3/8"	4.75 mm #4	2.36 mm #8	0.60 mm #30	0.150 mm #100	0.075 mm #200	Asphalt Binder (%)
L	+4 RAP	97	59	45	30	14	8	4.66
	-4 RAP	100	100	88	57	24	14	6.96
C	+4 RAP	84	43	33	21	9	5.4	4.46
	-4 RAP	100	100	90	56	16	8	5.66

Properties of Virgin Aggregates

Two granite aggregate sources were selected (Sources C and L) for this study. The engineering properties of two aggregate sources were tested in accordance with test designation, as shown in Table 3.6, which gives the base sampling, testing procedure, and comparison limits information for the aggregates.

The test results of base properties of aggregates are shown in Table 3.7, where the aggregate source C exhibits lower LA abrasion loss, absorption, and specific gravity values than that of source L, while the soundness percentage loss at 5 cycles is different at different sizes for two aggregate sources. At the same time, Source C shows a lower sand equivalent (clay content) and higher hardness than Source L. Obviously, when using aggregate source C, these physical properties should be beneficial in improving the workability of the asphalt mixture.

Table 3.6 Split sample aggregate tests (SC DOT Policy 2000)

Test Designation	Sampling Procedure	Testing Procedure	Comparison Limits
Aggregate Dry Gradation (No. 4 sieve and coarser)	AASHTO T2/T248	AASHTO T27	± 7.0
Aggregate Dry Gradation (Finer than No. 4 sieve)	AASHTO T2/T248	AASHTO T27	± 3.0
Los Angeles Abrasion	AASHTO T2/T248	AASHTO T96	± 12.7% of average
Percent Absorption	AASHTO T2/T248	AASHTO T85	± 0.41
Bulk (Dry) Specific Gravity	AASHTO T2/T248	AASHTO T85	± 0.038
Bulk (SSD) Specific Gravity	AASHTO T2/T248	AASHTO T85	± 0.032
Apparent Specific Gravity	AASHTO T2/T248	AASHTO T85	± 0.032
Sand Equivalency (Unwashed screenings only)	AASHTO T2/T248	AASHTO T176	± 12.0

One main reason for selecting these particular aggregate sources was based on past experience. These quarries have been found to exhibit very consistent physical properties with regard to specific gravity, gradation and particle shape. Aggregate sampled from the quarry's main stockpiles was designated as #789, Regular Screenings (RS), and Washed Screenings (WS), which coincide with the standard aggregate type designations as specified by AASHTO M43-88. The sampled aggregate was brought back to the laboratory where it was washed and oven dried, then sieved into the individual size fractions according to specification of AASHTO T96. The sieved gradations of two aggregate sources L and C are shown in Table 3.8, where aggregate source C exhibits a greater passing percentage of 0.75 mm material than source L. The distributions of two aggregate particle sizes are helpful in determining further blending of various aggregate types and achieve suitable gradation curves for the Superpave mix design.

Table 3.7 Engineering properties of aggregate sources L and C

Aggregate Source	LA Abrasion Loss (%)	Absorption (%)	Specific Gravity			Soundness % Loss at 5 Cycles			Sand Equivalen	Hardness
			Dry (bulk)	SSD (bulk)	Apparent	37.5 mm to 19.0 mm 1 1/2" to 3/4"	19.0 mm to 9.5 mm 3/4" to 3/8"	9.5 mm to 4.75 3/8" to #4"		
L	51	0.70	2.650	2.660	2.690	0.3	0.2	0.3	76	5
C	23	0.50	2.610	2.620	2.640	0.2	2.4	1.0	60	6

Table 3.8 Gradations of aggregate Sources L and C

Type of Aggregate	Aggregate Source	37.5 mm 1 1/2"	25.0 mm 1"	19.0 mm 3/4"	12.5 mm 1/2"	9.5 mm 3/8"	4.75 mm #4	2.36 mm #8	0.60 mm #30	0.150 mm #100	0.075 mm #200
#789 stone	L	100	100	100	100	90	35	6.3	1.4	0.7	0.44
Reg. Screenings		100	100	100	100	100	99.8	96	60.5	22.3	12
Man. Sand		100	100	100	100	100	99.4	82.5	47.2	7.6	2.3
#789 stone	C	100	100	100	100	87.5	22.9	4.3	1.5	0.9	0.6
Reg. Screenings		100	100	100	100	100	100	81.4	45.47	24.17	16.35
Man. Sand		100	100	100	100	100	99.73	75.7	31.7	8.3	3.2

Mixture Design

Method

A vital component in the process of constructing an asphalt pavement is the design of the asphalt mixture that will be used for the pavement. Asphalt mixtures are different from most engineering materials in that the highest strength mixture design is not necessarily the best choice for the particular asphalt pavement application. The equivalent single axle loading (ESAL), desired surface texture, environmental conditions, and other factors are all considered in the designing of an asphalt mixture. The stability (resistance to deformation caused by traffic loading) and durability (resistance to weathering, cracking, and traffic abrasion) of the asphalt mixtures are also the two primary characteristics that are considered at the mix design stage. The workability of the mixture needs to be balanced with the stability and durability requirements of the particular pavement. It is important that the asphalt mixture is designed as an economical and practical mixture as possible (Lavin 2003).

Asphalt Binder

PG64-22 asphalt binder, most widely used in SC and many states all over the country, was used in this study. The base physical properties of the asphalt binder are shown in Table 3.1. The mix design was based on 0.3 to less than 3 million design ESALs,, where the average traffic speed ranges from 20 to 70 km/h. However, it should be emphasized that proper or conservative binder selection does not guarantee total pavement performance.

Fatigue cracking performance is greatly affected by the pavement structure and traffic. Permanent deformation or rutting is directly a function of the shear strength of the mixture, which is greatly influenced by aggregate properties. Low temperature cracking of a pavement correlates most significantly to the binder properties. So it is important for engineers to try to achieve a balance among the many factors affecting the the selection process of binders (Superpave mix design 2001). The use of RAP in this study should improve the performance of mixture at the high temperature but might reduce the cracking resistance at the low temperatures. However, a softer binder can decrease the ratios of these large molecular particles, increase the low temperature and fatigue resistance, and reduce the effect of the aged binder. Four RAP contents (0%, 15%, 25%, and 30% by weight of the modified mixture) were used in this study.

Aggregate Structure

In general, in Superpave mix design, the aggregate properties play a major role in overcoming permanent deformation. Fatigue and low-temperature cracking are less affected by aggregate characteristics. However, the effect of aggregate gradation is significant in determining the physical properties of the asphalt mixture. Selection of the design aggregate structure is accomplished by comparing the properties of a series of trial mixtures. Three trial blends are normally employed for this purpose. A trial blend is considered acceptable if it possesses suitable volumetric properties (based on traffic and environment conditions) at an appropriate design binder content. The 0.45-power gradation chart is used to define a permissible gradation that follows the requirement of

control points and restricted zone with respect to nominal maximum size of aggregate used in this study. The gradation curve is a combination of virgin and RAP aggregate.

The distribution percentages of various aggregate sizes are determined in accordance with the aggregate specification of SC DOT. These combinations of the aggregate sources C and L are shown in Tables 3.9 and 3.10, respectively. The passing percentage values of particle sizes of aggregate source C are close at various RAP percentages, as shown in Table 3.9. Table 3.10 shows that the design aggregate structures of the aggregate source L are the same when using different rubber types (ambient and cryogenic) at the same percentages of RAP, while these passing percentage values of aggregate structures are similar at different particle sizes regardless of the RAP percentages.

Table 3.9 Design structure of aggregate source C

Aggregate Size	Specification	Type of Superpave mixture		
		0% RAP	15% RAP	30% RAP
Sieve	Limits	Ambient	Ambient	Ambient
12.5mm	98-100	100	100	100
9.5mm	90-100	94	93	92
4.75mm	54-70	61	59	56
2.36mm	32-48	41	41	40
0.6mm	14-26	20	21	22
0.15mm	5 --13	8.4	8.7	8.2
0.075mm	3 --9	5.04	5.20	4.77
Aggregate Blend				
Stone 789	-	50	49	48
Regular Screenings	-	18	15	7
Manufactured Screenings	-	31	20	14
Lime	-	1	1	1
-4RAP	-	0	6	12
+4RAP	-	0	9	18

Table 3.10 Design structure of aggregate source L

Aggregate Size	Specification	Type of Superpave mixture							
		0% RAP		15% RAP		25% RAP		30% RAP	
Sieve	Limits	Ambient	Cryogenic	Ambient	Cryogenic	Ambient	Cryogenic	Ambient	Cryogenic
12.5mm	98-100	100	100	100	100	100	100	100	100
9.5mm	90-100	94	94	94.2	94.2	94.1	94.1	94	94
4.75mm	54-70	61	61	62.7	62.7	59.4	59.4	61	61
2.36mm	32-48	41	41	42	42	38.2	38.2	40	40
0.6mm	14-26	24	24	24.7	24.7	22.9	22.9	24	24
0.15mm	5 --13	7.7	7.7	8.3	8.3	8.9	8.9	9.8	9.8
0.075mm	3 --9	4.11	4.11	4.5	4.5	5.14	5.14	5.66	5.66
Aggregate Blend									
Stone 789	–	59	59	53	53	56	56	53	53
Regular Screenings	–	22	22	12	12	8	8	8	8
Manufactured Screenings	–	18	18	19	19	10	10	8	8
Lime	–	1	1	1	1	1	1	1	1
-4RAP	–	0	0	9	9	15	15	18	18
+4RAP	–	0	0	6	6	10	10	12	12

At the same time, the rubber percentage of the mixture did not change the aggregate gradation trends. On the other word, the mixture used the same gradation curve at different rubber percentages when using one type of RAP percentage (e.g., 0%, 15%, 25% or 30% RAP). These similar gradation curves reduced the variability of mixture properties caused by the aggregate source. The 0.45-power gradation curves of the mixtures used in this study are shown in Figure 3.3. In order to achieve the Superpave volumetric requirements of the mixtures, these gradation curves were adjusted several times prior to selecting them as the design aggregate structures.

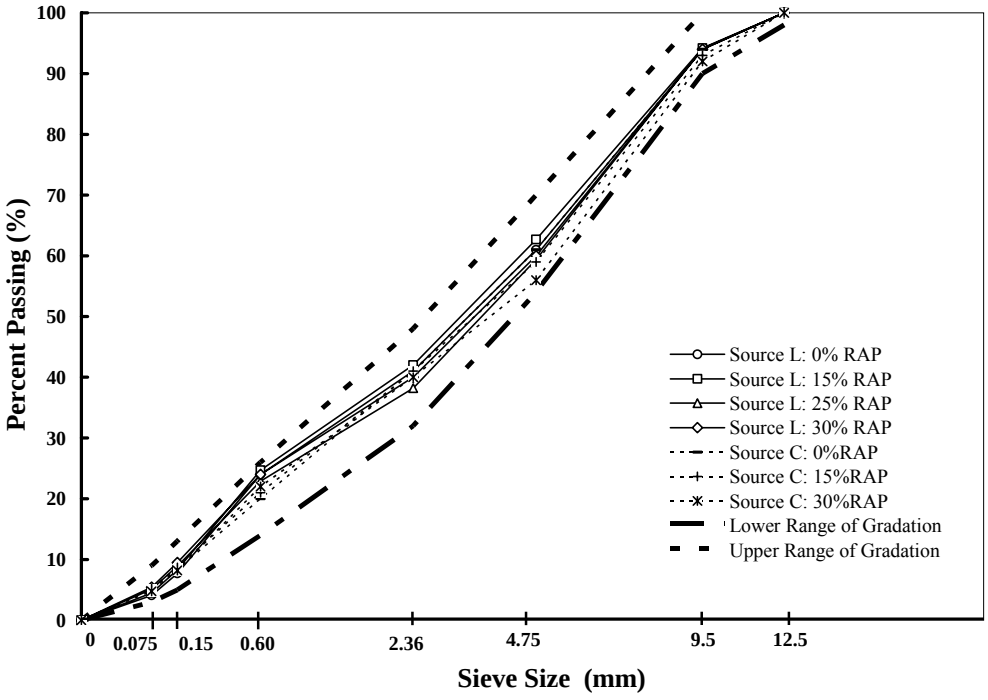

Figure 3.3 Gradations of 9.5 mm of all mixtures

Crumb Rubber

The experimental design detailed in this study included the use of two rubber types (ambient and cryogenic), four rubber contents (0%, 5%, 10%, and 15% by weight of virgin binder), and one crumb rubber size (-40 mesh [-0.425 mm]). The wet process was used to make the modified binders, where the rubber was blended with the virgin asphalt binder at a high temperature (approximate 177^{o}C) for 30 minutes.

Volumetric Properties of the Mixture

The volumetric proportion of asphalt mixture, playing a key role in Superpave mix design procedure, is an important factor that must be taken into account when considering asphalt mixture behavior. The volumetric properties of a paving mixture provide some indication of pavement service performance. However, these volumetric properties are only accompanied by the virgin binder and aggregate. The original Superpave mix design system did not address the volumetric analysis of RAP and crumb rubber materials and no guidelines on such analysis are available at this time. Recently, some researchers have conducted several studies to give some recommendation and guidelines for these materials (FHWA 1997b; NCHRP 2001; Xiao et al. 2006).

A nominal maximum size 9.5mm Superpave mixture was used for the mix design in this experiment. This particular mix design is used as a primary route surface course mix in many states including South Carolina. The SCDOT 9.5 mm Superpave volumetric and compaction specifications, as shown in Table 3.11, were used.

Table 3.11 SCDOT 9.5 mm Superpave volumetric specifications

Superpave 9.5 mm Mix Specifications	
% Max. Density at N_{des}	96
% VMA	>15.5
%Voids Filled	70 - 80
% Max. Density at N_i	< 89
% Max. Density at N_m	< 98
Dust to Asphalt Ratio	0.6-1.2

The procedures described in AASHTO PP 19 (Volumetric Analysis of Compacted Hot Mix Asphalt) and AASHTO T312 (Preparing and Determining the Density of Hot Mix Asphalt Specimens by Means of the Superpave Gyratory Compactor) regarding the preparation of HMA specimens were followed.

Sample Mixing

A mechanical mixer was used to blend the rubber and the virgin binder, which were reacted in one quart cans. Each can was filled with 600 grams of virgin binder and sealed until it was blended with crumb rubber. The crumb rubber was added to the asphalt binder and reacted for 30 minutes at a reaction temperature of 177 °C (350 °F) and a reaction speed of 700 rpm. The reaction time of 30 minutes was considered suitable based on a preliminary study indicating that the mixing time did not significantly influence the binder properties (Thompson and Xiao 2004). The reacted modified binders were allowed to cool at the room temperature and sealed prior to Superpave mix design. Previous research conducted by Asphalt Rubber Technology Services (ARTS) staff, Clemson University, has developed some detailed information regarding the behavior of asphalt binder reacting with crumb rubber (Xiao et al. 2006; Putman 2005).

The aggregate was brought from the quarry and dried in the oven at a temperature of 110 °C. The dried aggregate was sieved to desired size prior to mixing. At the same time, the RAP materials were also oven-dried and sieved to obtain particles with target sizes. Each aggregate was weighed into a pan with the proper weights, a total weight of 4500 grams, while the RAP material was separated into other pans. Hydrated lime, which is used as an anti-strip additive, was added at a rate of 1% by dry mass of virgin aggregate. The lime was blended uniformly to cover the dry aggregate surface, and then 5% water by weight of the aggregate was added and mixed thoroughly before placing the sample in the oven. The experimental design flow chart, shown in Figure 3.4, will be used for this study.

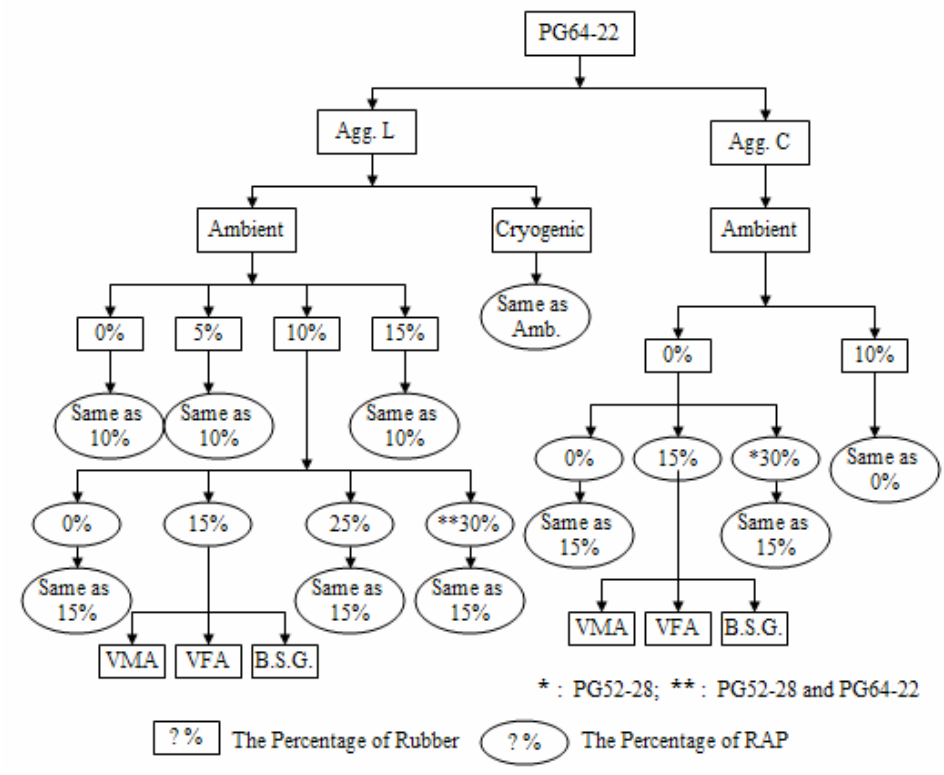

Figure 3.4 Experimental design flow chart

Superpave mix design defines that the laboratory mixing and compaction temperatures can be determined by using a plot of viscosity versus temperature. The selection of mixing and compaction temperatures is corresponding with binder viscosity values of 0.17±0.02 Pa•s and 0.28±0.02 Pa•s; respectively. However, Superpave mix design does not mention that these viscosity ranges are valid for modified asphalt binders. It is necessary for the researchers to consider the manufacture's recommendations. Especially, in this study, due to the complexity of the mixtures (crumb rubber and RAP in the mixture), it is difficult to determine the appropriate mixing and compaction temperatures. Previous research has given the guidelines of the mixing containing crumb rubber or RAP to select the temperatures (FHWA 1997a, 1997b; NCHRP 2001; Xiao et al. 2006).

The Superpave gyratory compactor (SGC) was used to compact the specimens, which has a diameter of 150 mm. The 0.3 to < 3 millions ESALs was selected as the design number of ESALs for all mixtures. The N_{ini}, N_{des}, and N_{max} values used for this study were 7, 75, and 115; respectively.

The oven-dried RAP materials, at the room temperature, were blended with the virgin aggregate at the specified (target) mixing temperatures. The blended mixture was heated for about one hour in order to maintain the target mixing temperature before the modified binder (rubber and virgin binder) was added to the mixtures, and then the component was blended until the aggregate was thoroughly coated by the binder. Finally, the mixed mixture was heated for two hours as short term aging prior to compaction. The detailed information and volumetric result data set of the Superpave mix design for each mixture are given in Appendix A.

Moisture Sensitivity

The AASHTO T283 (Resistance of a Compacted Bituminous Mixture to Moisture Induced Damage) was used to test the moisture susceptibility of mixture. Six specimens from each mixture were made at the optimum asphalt binder contents, and then compacted to 7 ± 1 percentage air voids. One subset, consisting of three specimens, is considered the control set (dry samples). Other subset of three specimens is wet conditioned, where the specimens are subjected to a partial vacuum with water to 70-80 percent of the air void volume, followed by a 24-hour moisture curing at 60^{o}C. The wet subset specimens are then placed in a 25^{o}C bath for 2 hours prior to determining their indirect tensile strength (ITS). Then, tensile strength ratio (TSR) of each mixture is determined as a ratio of the average tensile strengths of the conditioned subset divided by the average tensile strengths of the control subset. SCDOT requires that the TSR values should be greater than 85% and minimum wet ITS value to be 65 psi (449 kPa).

Fatigue Test Procedures

Beam Fabrication

Fatigue beams were made in the laboratory. The total aggregate weight of 10,800 grams was used for making one big beam. The mix was placed in an oven for two hours to simulate the short term aging. The vibratory compactor equipment, as shown in Figure 3.5, was used to compact the flexural bending fatigue beams used in this study. The compaction time was dependent on the types of the mixture (i. e., the percentage of rubber and RAP). The compacted beam was sawn into two small test fatigue beams after bulk specific gravity testing. A compacted beam and a sawed small beam are shown in

Figure 3.6. Test specimens were sawn to a 380 mm (15 inches) length by 63 mm (2.5 inches) width and 50 mm (2 inches) thickness. Figure 3.7 gives the dimensions of the final test specimens.

Figure 3.5 Vibratory compactor

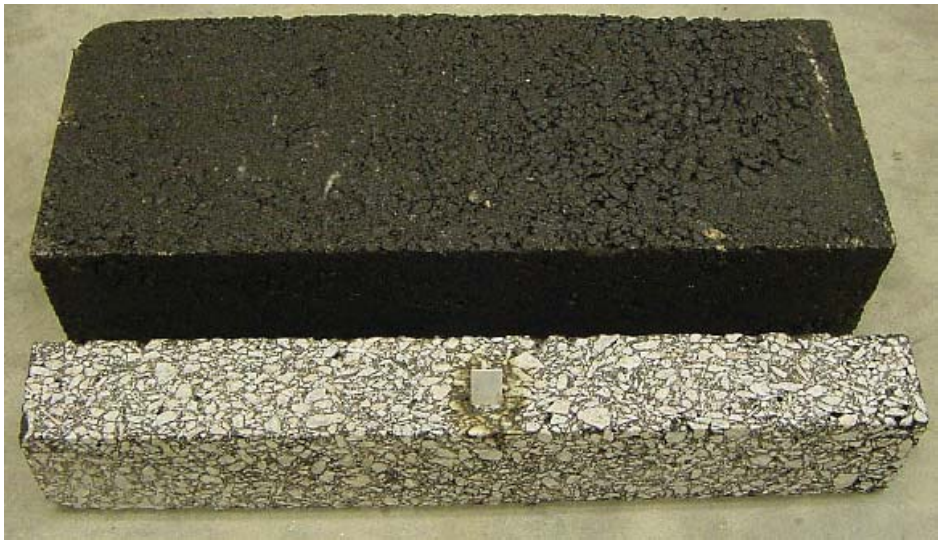

Figure 3.6 Fatigue beams of the mixture

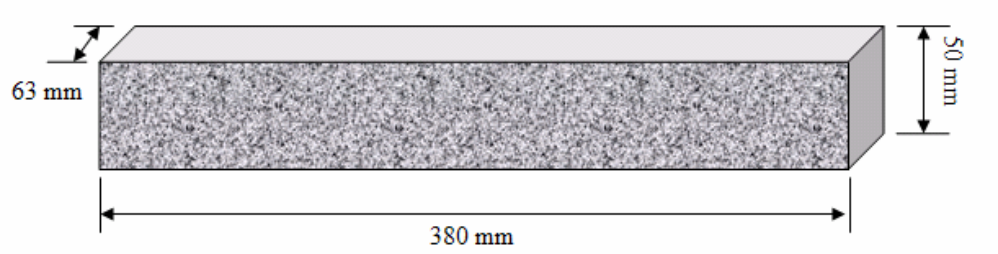

Figure 3.7 Fatigue beam size of the mixture

After the specimens were sawn, volumetric analysis was conducted on various mixtures. The beams were placed in a temperature-controlled room at approximately 25 °C (77 °F) for a week before obtaining their specific gravities and air voids.

Fatigue Beam Testing

Beam specimens ready for testing were stored at the room temperature. All tests were performed in two controlled-temperature rooms at 20.0 ± 0.5°C (68 ± 32.9°F) and 5.0 ± 0.5°C (41 ± 32.9°F). In order to maintain the testing temperature, each beam specimen was placed in the environmental chamber of the fatigue testing equipment for two hours prior to beginning the test. The test apparatus, as shown in Figure 3.8, developed as part of SHRP A-003A and described in SHRP Report A-404 and other references (Tayebali et al., 1994a and 1994b), subjects beam specimens to four-point bending with free rotation and horizontal translation at all load and reaction points and forces the specimen back to its original position at the end of each load pulse, as shown in Figure 3.9.

In this study, a repeated sinusoidal loading at a frequency of 5 Hz was used. The control and data acquisition software measured the deflection of the beam specimen, computed the strain in the specimen and adjusted the load applied by the loading device

such that the specimen experienced a constant level of strain on each load cycle.

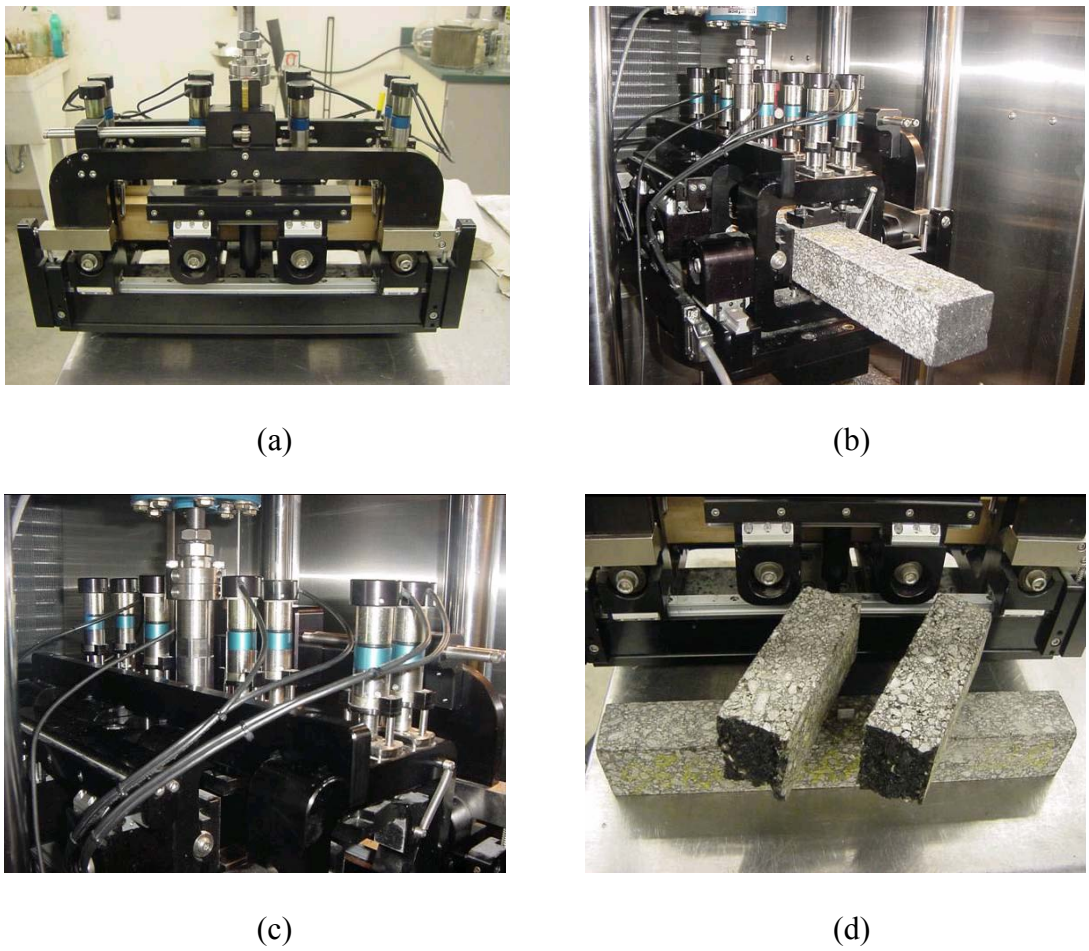

(a) (b)

(c) (d)

Figure 3.8 Fatigue beam test apparatus (a) test head, (b) beam installation, (c) beam testing, (d) tested beam

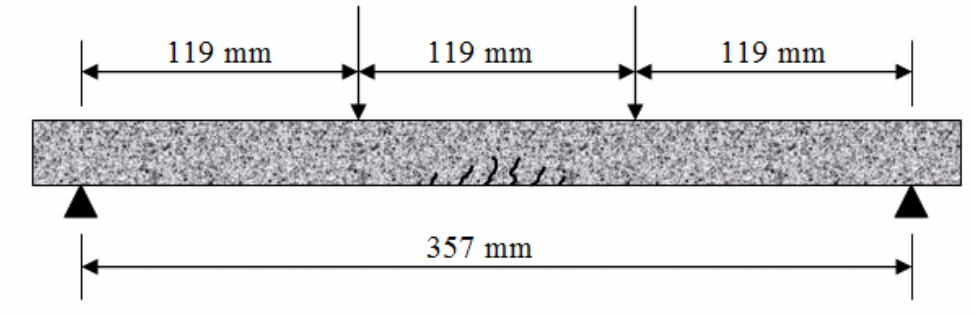

Figure 3.9 Simulation loading of fatigue beam

In addition, test apparatus recorded load cycles, applied load, and beam deflections. Failure is assumed to occur when the stiffness reaches half of its initial value, which is determined from the load at approximately 50 repetitions; the test is terminated automatically when this load has diminished by 50 percent. Maximum stress, strain, and other variables are determined as follows:

1. Maximum tensile stress (Pa):

$$\sigma = \frac{3aP}{bh^2} \tag{3-1}$$

where,

P = applied peak-to-peak load, in Newton;

b = average beam width, in meters;

h = average beam height, in meters; and

a = space between inside clamps, in meters

2. Maximum tensile strain (m/m):

$$\varepsilon = \frac{12hd}{3l^2 - 4a^2} \tag{3-2}$$

where,

δ = beam deflection at neutral axis, in meters; and

l = length of beam between outside clamps, in meters

3. Flexural stiffness (Pa):

$$S = \sigma / \varepsilon \tag{3-3}$$

4. Phase angle (deg.):

$$\varphi = 360 f\theta \tag{3-4}$$

where,

f = load frequency, in Hz; and

θ = time lag between $P_{\max}$ and $\delta_{\max}$, in second

5. Dissipated energy (J/m^3) per cycle:

$$D = \pi\sigma\varepsilon\sin(\varphi) \tag{3-5}$$

6. Cumulative dissipated energy, J/m^3

$$\sum_{i=1}^{i=n} D_i \tag{3-6}$$

where,

D_i = D for the i^{th} load cycle

A detailed description of the test method is described as AASHTO Designation T 321-03.

CHAPTER IV
EXPERIMENTAL STATISTICAL METHODS

Previous research indicated that the stiffness, fatigue life, and cumulative dissipated energy are associated with various variables (Tayebali et al. 1994). The statistical analysis for stiffness shows that asphalt and aggregate types, temperature, and air void content significantly influence the stiffness for all test types, while the asphalt content and stress/strain do not appear to be a big influence on the stiffness for flexural beam tests. In general, the ranking observed for the cumulative dissipated energy is similar to that observed for fatigue life. Previous research also showed that the mode of loading for fatigue life is related to various variables that involve air void content, stress or strain, and stiffness (Tayebali et al. 1994).

In this study, on the basis of the effects of crumb rubber and RAP, two additional variables, percentages of rubber and RAP, were employed in creating a group of the fatigue predictive models. The generalized linear modeling (GLM) and artificial neural network (ANN) were used for development of models predicting fatigue life of asphalt mixture.

Generalized Linear Model

Regression analysis is a collection of statistical techniques for modeling and investigating the relationship between a response variable and a set of regressor or predictor variables. Applications of regression are numerous and occur in almost every

applied field including engineering, the chemical/physical, and other sciences (Myers et al. 2001). In this study, the software Microsoft Excel and Statistical Analysis System (SAS) were used to perform statistical regression analysis of the fatigue prediction models on the research data. The multiple linear regression analysis plays a key role in constructing fatigue predictive models of the mixture. The air void content or VFA, stiffness, dissipated energy per cycles, and strain or stress were considered independent variables and the fatigue life was considered the dependent variable. The use of the general linear models was accomplished in accordance with the following process.

The following regression model was used in this study (Mendenhall and Sincich 1994):

$$y = \beta_0 + \beta_1 x_1 + \beta_2 x_2 + ... + \beta_k x_k + \varepsilon \quad (4\text{-}1)$$

where,

y = response or dependent variable;

$x_1, x_2, ...x_k$ = regressor or independent variables; and

$\beta_0, \beta_1, \beta_2, ...\beta_k$ = regression coefficients or model parameters

Typically, the method of least squares is used to estimate the regression coefficient in a multiple linear regression model, which is presented in Table 4.1.

Table 4.1 Data for multiple linear regression

Y	X_1	X_2	…	X_k
Y_1	X_{11}	X_{12}	…	X_{1k}
Y_1	X_{21}	X_{22}	…	X_{2k}
⋮	⋮	⋮		⋮
Y_n	X_{n1}	X_{n2}	…	X_{nk}

The equation 4-1 can be rewritten in terms of the observation in Table 4.1 as

$$y = \beta_0 + \beta_1 x_{i1} + \beta_2 x_{i2} + ... + \beta_k x_{ik} + \varepsilon_i$$

or

$$y = \beta_0 + \sum_{j=1}^{k} \beta_J x_{ij} + \varepsilon_i, \qquad i = 1, 2, ..., n \tag{4-2}$$

The least square function is shown as

$$S = \sum_{i=1}^{n} \varepsilon_i^2 = \sum_{i=1}^{n} (y_i - \beta_0 - \sum_{j=1}^{k} \beta_j x_{ij})^2 \tag{4-3}$$

The function S is to be minimized with respect to $\beta_0, \beta_1, \beta_2, ...\beta_k$. The least square estimators, say $b_0, b_1, b_2, ...b_k$ must satisfy

$$\left.\frac{\partial S}{\partial \beta_0}\right|_{b_0, b_1 ..., b_k} = -2\sum_{i=1}^{n} (y_i - b_0 - \sum_{j=1}^{k} b_j x_{ij}) = 0 \tag{4-4a}$$

$$\left.\frac{\partial S}{\partial \beta_j}\right|_{b_0, b_1 ..., b_k} = -2\sum_{i=1}^{n} (y_i - b_0 - \sum_{j=1}^{k} b_j x_{ij}) x_{ij} = 0 \qquad j = 1, 2, ..., k \tag{4-4b}$$

Simplifying Equation 4-4, it is easy to obtain the following equations:

$$\begin{aligned}
&nb_0 + b_1 \sum_{i=1}^{n} x_{i1} + b_2 \sum_{i=1}^{n} x_{i2} + ... + b_k \sum_{i=1}^{n} x_{ik} = \sum_{i=1}^{n} y_i \\
&b_0 \sum_{i=1}^{n} x_{i1} + b_1 \sum_{i=1}^{n} x_{i1}^2 + b_2 \sum_{i=1}^{n} x_{i1} x_{i2} ... + b_k \sum_{i=1}^{n} x_{i1} x_{ik} = \sum_{i=1}^{n} x_{i1} y_i \\
&\vdots \qquad\qquad \vdots \qquad\qquad\qquad \vdots \\
&b_0 \sum_{i=1}^{n} x_{ik} + b_1 \sum_{i=1}^{n} x_{ik} x_{i1} + b_2 \sum_{i=1}^{n} x_{ik} x_{i2} ... + b_k \sum_{i=1}^{n} x_{ik} x_{ik} = \sum_{i=1}^{n} x_{ik} y_i
\end{aligned} \tag{4-5}$$

These equations are called the least squares normal equations. The solution to the normal equations will be the least squares estimators of the regression coefficients $b_0, b_1, b_2, ...b_k$. It is simpler to solve the normal equations if they are expressed in a matrix notation. The model in terms of the observation, Equation 4-2, may be written in matrix notation as

$$y = X\beta + \varepsilon$$

$$y = \begin{bmatrix} y_1 \\ y_2 \\ \vdots \\ y_n \end{bmatrix}, \quad X = \begin{bmatrix} 1 & x_{11} & x_{12} & \cdots & x_{1k} \\ 1 & x_{21} & x_{22} & \cdots & x_{2k} \\ \vdots & \vdots & \vdots & & \vdots \\ 1 & x_{n1} & x_{n2} & \cdots & x_{nk} \end{bmatrix}, \quad \beta = \begin{bmatrix} \beta_0 \\ \beta_1 \\ \vdots \\ \beta_k \end{bmatrix}, \quad and \quad \varepsilon = \begin{bmatrix} \varepsilon_1 \\ \varepsilon_2 \\ \vdots \\ \varepsilon_n \end{bmatrix}$$

In general, y is an $(n \times 1)$ vector of the observations, X is an $(n \times p)$ matrix of the level of the independent variables, β is a $(p \times 1)$ vector of the regression coefficients, the ε is an $(n \times 1)$ vector of random errors. The least squares estimator of β is

$$X'Xb = X'y \quad or \quad b = (X'X)^{-1}X'y \tag{4-6}$$

where b is the ordinary least squares estimator of β to distinguish it from other estimators based on the least squares idea. It is easy to see that the matrix form of the normal equation is identical to the scalar form. The equation (4-6) can be written as following matrix equation:

$$\begin{bmatrix} n & \sum_{i=1}^{n} x_{i1} & \sum_{i=1}^{n} x_{i2} & \cdots & \sum_{i=1}^{n} x_{ik} \\ \sum_{i=1}^{n} x_{i1} & \sum_{i=1}^{n} x_{i1}^2 & \sum_{i=1}^{n} x_{i1}x_{i2} & \cdots & \sum_{i=1}^{n} x_{ik} \\ \vdots & \vdots & \vdots & & \\ \sum_{i=1}^{n} x_{ik} & \sum_{i=1}^{n} x_{ik}x_{i1} & \sum_{i=1}^{n} x_{ik}x_{i2} & \cdots & \sum_{i=1}^{n} x_{ik}^2 \end{bmatrix} \begin{bmatrix} y_1 \\ y_2 \\ \vdots \\ y_n \end{bmatrix} = \begin{bmatrix} \sum_{i=1}^{n} y_i \\ \sum_{i=1}^{n} y_i \\ \vdots \\ \sum_{i=1}^{n} x_{ik}y_i \end{bmatrix}$$

The fitted regression model is

$$\hat{y} = Xb \tag{4-7}$$

In scalar notion, the fitted model is

$$\hat{y}_i = b_0 + \sum_{i=1}^{k} b_j x_{ij} \qquad i = 1, 2, \cdots, n$$

In multiple linear regression problems, certain tests of hypotheses about the model parameters are helpful in measuring the usefulness of the model. The test for significance of regression is a test to determine if there is a linear relationship between the response variables and subset of the regressor variables. The analysis of variance (ANOVA) for significance of regression model is shown in Table 4.2.

Table 4.2 ANOVA for significance of regression in multiple regression models

Source of Variation	Sum of Squares	Degrees of Freedom	Mean Square	F_0
Regression	SS_R	k	MS_R	MS_R/MS_E
Error or residual	SS_E	$n-k-1$	MS_E	
Total	SS_T	$n-1$		

$$SS_R = \sum_{i=1}^{n}(y_i - \bar{y})^2,\ SS_E = \sum_{i=1}^{n}(y_i - \hat{y}_i)^2,\ SS_T = SS_R + SS_E$$

Where,

$\hat{y}_i$ = the predicted value of y_i

$\bar{y}$ = mean value of y_i

Moreover, in order to find a measure of how well a multiple regression model fits a set of data, it is necessary to use the multiple regression equivalent of R^2, the coefficient of determination for the straight line model. It is defined as following:

$$R^2 = 1 - \frac{\sum_{i=1}^{n}(y_i - \hat{y}_i)^2}{\sum_{i=1}^{n}(y_i - \bar{y})^2} = 1 - \frac{SS_E}{SS_R} \tag{4-8}$$

R^2 is a sample statistic that represents the fraction of the sample variation of the y values that is attributed to the regression model. Thus, R^2=0 implies a complete lack of fit of the model to the data, where R^2=1 exhibits a perfect fit, with the model passing through every data point. In general, the lager the value of R^2, the better the model fits the data.

Previous research indicated that one of the assumptions necessary for ANOVA and GLM is that the dependent and independent variables are normally distributed. Distribution for stress, strain, stiffness, cycles to failure, and cumulative dissipated energy were reviewed and found to be log-normally distributed. Therefore, log transformations (using natural logarithm, base e) were used in ANOVA and GLM through the regression analysis (Tayebali et al. 1994). This analysis method was also employed in this study. Since some replicates (2-6) were included in the experimental design, it was possible to estimate the variance associated with specimen preparation and testing. The coefficient of variation for log-normally distributed data may be computed using the following relationship:

$$CV = 100 * (e^{VAR} - 1)^{0.5} \tag{4-9}$$

where,

CV = coefficient of variation in percentage;
VAR = variance of log-transformed data or MSE from GLM;
e = base of natural logarithms; and
MSE = mean square error

Artificial Neural Network

Chapters I and II have given some basic concepts for an artificial neural network (ANN), while the detailed analysis process will be discussed here. Artificial neural networks are adaptive model-free estimators. An artificial neural network can be presented by the following properties in mathematical terms (Müller and Reinhardt 1990; Rumelhart et al. 1986; Juang and Chen 1999; Chen 1999):

1. Each neuron or node consists of a simple processing unit
2. A state variable is associated with each node

3. A real-valued weight w_{ij} is associated with each link between nodes i and j
4. A real-valued bias b_i is associated with each node i
5. A transfer function, f_i, is defined for each node, i, which determines the state of the node as a function of its bias, the weights of its incoming links, and the states of the nodes connected to it by the links
6. A pattern of connectivity among the nodes is defined
7. A propagation rule is defined
8. A learning rule is defined

Backpropagation, a popular training algorithm, is commonly adopted for training a feed-forward neural network and is a systematic method for training multiple-layer artificial neural networks. It played a critically important role in the resurgence of the neural network field in the mid-1980s (Chen 1999). Backpropagation algorithm, used in this study, was created by generalizing the Widrow-Hoff learning rule (Tsoukalas and Uhrig 1996) to multiple-layer networks and using nonlinear differentiable transfer functions. Properly trained backpropagation networks tend to give reasonable answers when presented with input they have never seen. This generalization property makes it possible to train a network on a representative set of input/target pairs and obtain good results without training the network with all possible input/output pairs (Chen 1999).

Backpropagation is a supervised learning algorithm because the network is trained and adjusted by comparing the network output and the targeted output. The neural network training starts with the initiation of all of the weights and biases with random numbers. The input vector is presented to the network and intermediate results propagate forward to yield the output vector. The difference between the target output and the network output represents the error. The error is then propagated backward through the network, and the weights and biases are adjusted to minimize the error in the next round

of prediction. The iteration continues until the error goal is reached. The iterative process is shown in Figure 4.1.

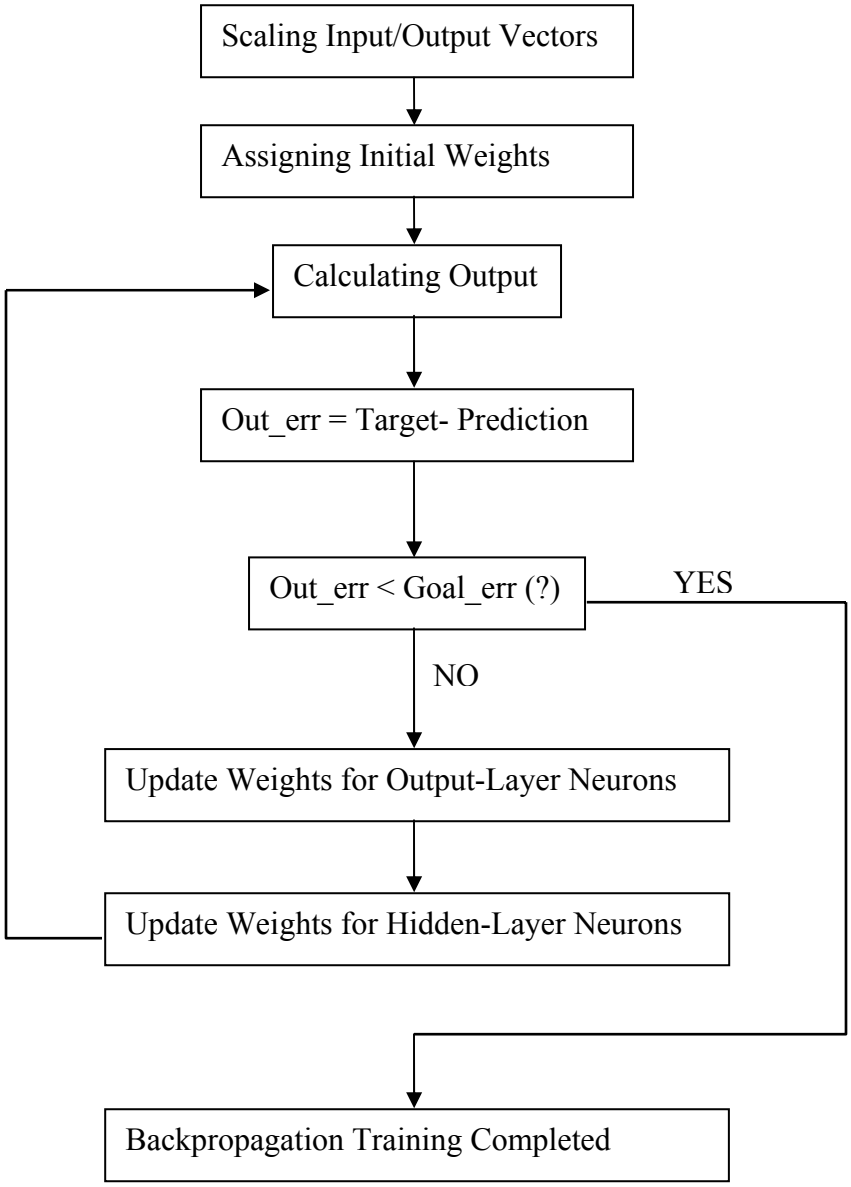

Figure 4.1 Flowchart illustrating backpropagation training algorithm (Chen 1999)

Backpropagation training involves two passes. In the forward pass, the input propagates through the network to produce an output. In the reverse pass, the calculated

network errors propagate backward through the network where they are used to adjust the weights. The weights from a node i to a node j at iteration k is updated using the following equation:

$$w_{ij}(k+1) = w_{ij}(k) + \Delta w_{ij}(k+1) \tag{4-10}$$

$$\Delta w_{ij}(k+1) = \eta \sum o_{ip}(k)\delta_{jp}(k) \tag{4-11}$$

where,

η = learning rate;

P = training set;

o_{ip} = output of node i in a previous layer; and

δ_{jp} =an associated error for node j

δ_{jp} is defined as follows:

$$\delta_j = o_j(1-o_j)(t_j - o_j) \text{ for output layer nodes}$$

$$\delta_j = o_j(1-o_j)\sum w_{jm}\delta_m \text{ for hidden layer nodes} \tag{4-12}$$

where,

t_j = target value for node j if is in the output layer; and

m = nodes in the layer following the layer where node j resides.

The bias term is updated in a similar way as follows:

$$b_{ij}(k+1) = b_{ij}(k) + \eta \sum \delta_{jp} \tag{4-13}$$

Several techniques such as adding a momentum term, adjusting learning rate, and adjusting the exponential decay constant in the sigmoid function, are often used to improve the effectiveness and efficiency of backpropagation training. To prevent the network from taking steps that are too large in the weight space, choosing an appropriate learning rate is particularly important in backpropagation.

Backpropagation training algorithm may be implemented in a program written in C/C++, and the neural network toolbox of MATLAB. The source codes of the ANN toolbox of MATLAB are available and can be modified easily to adapt to different situations. Another incentive to use the ANN toolbox of MATLAB is that is can be used with data sets formatted on popular spreadsheet software such as Excel through a macro called ExcelLink (Math Works Inc. 1999). The ExcelLink macro allows MATLAB commands to be issued from within Excel. This feature greatly simplifies data manipulation and sharing between programs (Juang and Chen 1999; Chen 1999).

CHAPTER V
EXPERIMENTAL RESULTS AND DISCUSSIONS

In this study, the experimental tests were performed in accordance with the requirements and specifications of related AASHTO and/or ASTM specifications. The data were analyzed using statistical and artificial neural network (ANN) methods. The results and discussions included in this chapter are as follows:

1. Hypothesis and assumptions
2. Binder property analysis
3. Superpave result analysis
4. Fatigue predictive models

Hypothesis and Assumptions

In general, experimental process and data will be influenced by a series of assumptions. Previous researchers had presented some hypothesis for the fatigue behavior of asphalt-aggregate mixes both as tested in the laboratory and as reflected within analytical pavement models. Some of hypothesis became targets for detailed investigation because of their strong links to fatigue performance testing and mix analysis (Tayebali et al. 1994). Further insights regarding this hypothesis, developed as the investigation progressed, are shown blow.

1. Fatigue cracking is caused by the repetitive application of traffic loads. For a typical heavy-duty pavement, fatigue results from tensile stresses or strains at the underside

of the asphalt aggregate layers. The maximum principal tensile strain is considered the primary reason of fatigue cracking.

2. For the purpose of fatigue analysis, the critical stress or strain state in the pavement structure can be estimated with reasonable accuracy by the theory of linear elasticity.
3. In the laboratory fatigue testing, pulsed loading is preferred to sinusoidal loading because the rest period permits stress relaxation similar to that happening under in-service traffic loading.
4. Although pavements become fatigued in response to repeated flexure, fatigue is basically a tensile phenomenon, and test specimens can be evaluated equally well under either tensile or flexural loading.
5. Fatigue tests accelerated by the application of large stress or strain levels are satisfactory for mix analysis and design.
6. Under simple loading, cracking initiation in a given mix is related to strain or stress level as follows:

$$N_f = a(1/\varepsilon)^b \text{ or } N_f = c(1/\sigma)^d \tag{5-1}$$

Where,

N_f = number of load application or crack initiation;

ε, σ = tensile strain and stress, respectively;

a, b, c, d = experimentally determined coefficients

7. During mixing and compacting procedures, the virgin aggregate would be combined with RAP uniformly in the modified mixtures.
8. The air void of fatigue beams will be considered to be consistent. In addition, it is assumed that every part of fatigue beam under the pulse loadings uniform.
9. The percentage level of RAP (R_p) and crumb rubber (R_b) will be assumed the

following relationships with fatigue life (N_f) and initial stiffness of asphalt pavement (S_o), respectively.

$$N_f = a(1/R_p)^b, S_o = c(R_p)^d \quad (5\text{-}2)$$

$$N_f = e(R_b)^f, S_o = g(R_b)^h \quad (5\text{-}3)$$

a, b, c, d, e, f, g, h = experimentally determined coefficients

10. The aged binder in RAP and virgin binder will surround a uniform film outside of the aggregate during and after high temperature mixing process and reach a consistency, which will make the aged and virgin binder work homogeneously in the asphalt mixtures.

Binder Property Analysis

The rheological properties and Superpave performance grade of the reclaimed and virgin asphalt binders were tested and discussed in accordance with AASHTO standards in previous chapters. However, the related fatigue rheological properties (e.g., viscosity and G*sinδ) of the binders were not presented and are discussed in the following sections.

Viscosity values of various modified binders are shown in Figures 5.1 to 5.4 and Appendix B. Figure 5.1 shows that the viscosity of the modified binder, composed of two type of aged binders (L and C) and ambient crumb rubber, increases as the percentage of crumb rubber increases regardless of the RAP types (L and C). For the modified binder containing the same percentage of crumb rubber, as expected, increasing the percentage of aged binder also results in an increase in viscosity of modified binder. The same trends were observed for all mixtures regardless of the aged binders of sources L and C. However, the statistical analysis shows that, in most cases, the modified binder used with RAP C has a significantly lower viscosity value than one used with RAP L at the 95%

level of confidence. Moreover, the viscosity of the binder blended with a binder graded as PG 64-22 shows a higher value than the binder blended with the soft binder (PG 52-28). From Figure 5.2, the same trends were evident when using cryogenic rubber. Figures 5.3 and 5.4 exhibit the effects of two types of crumb rubber (ambient and cryogenic) using RAP L and C, respectively. In most cases, statistical analysis of viscosity values, as shown in these figures, indicates that there are no significant differences in the viscosity values between the ambient and cryogenic rubber produced binder.

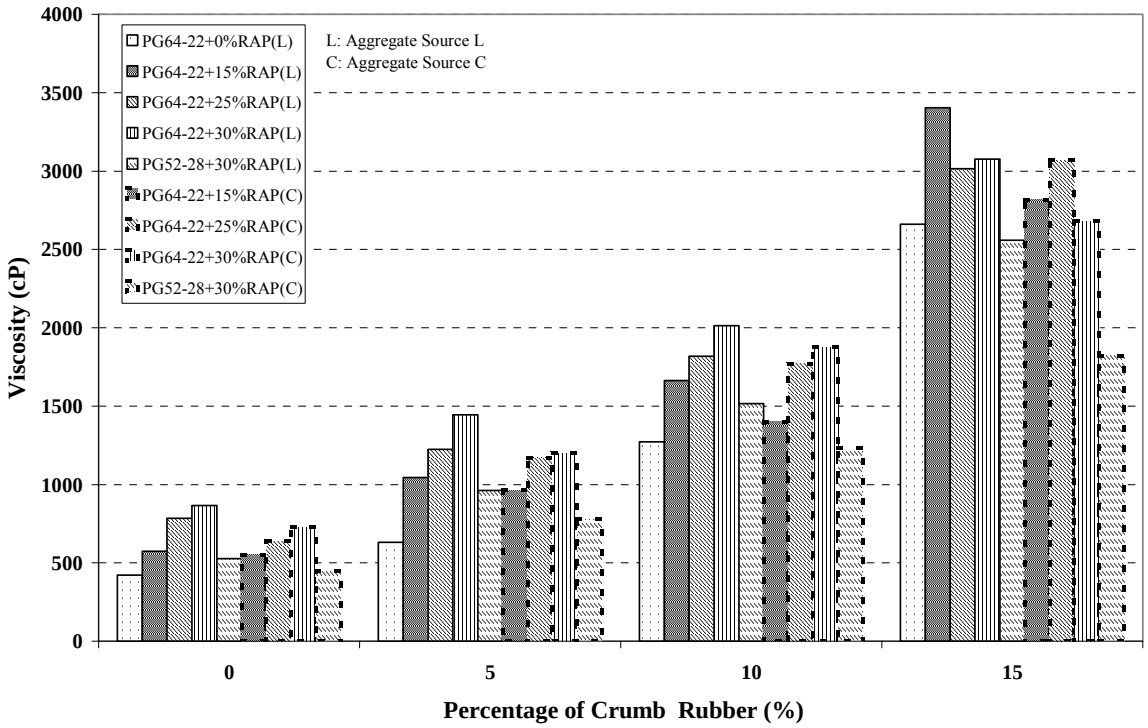

Figure 5.1 Viscosity comparison of the modified binder with aged binder extracted from RAPs L and C containing ambient rubber

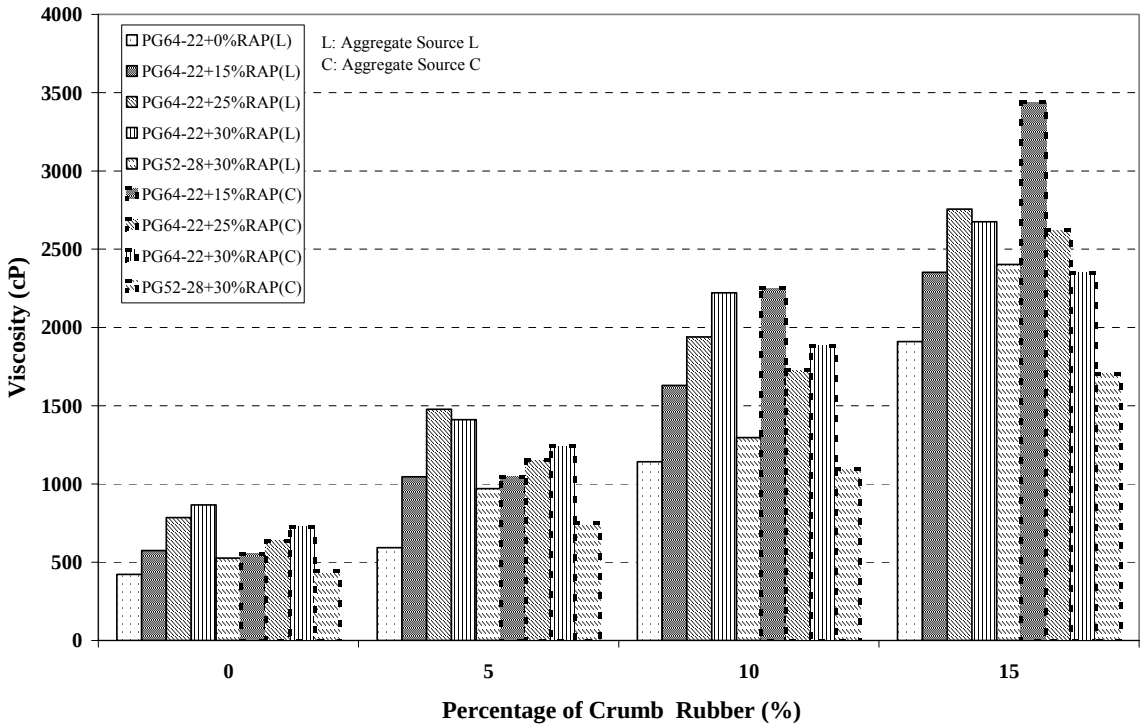

Figure 5.2 Viscosity comparison of the modified binder with aged binder extracted from RAPs L and C containing cryogenic rubber

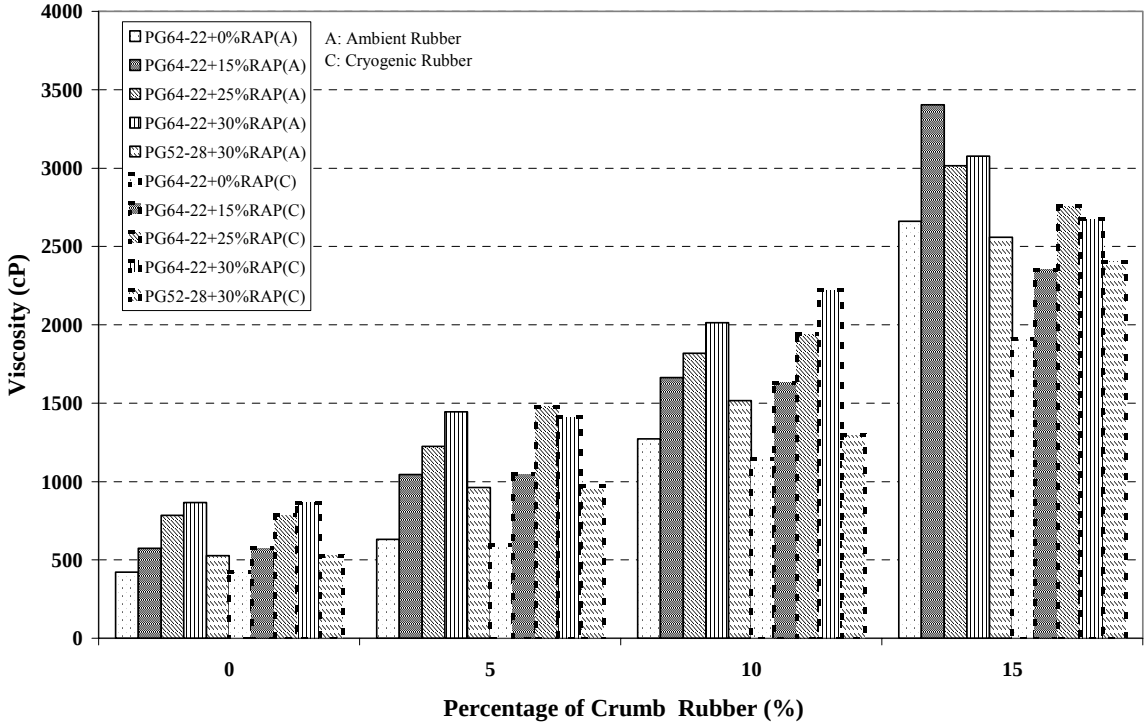

Figure 5.3 Viscosity comparison of the modified binder with ambient and cryogenic rubber containing aged binder extracted from RAP L

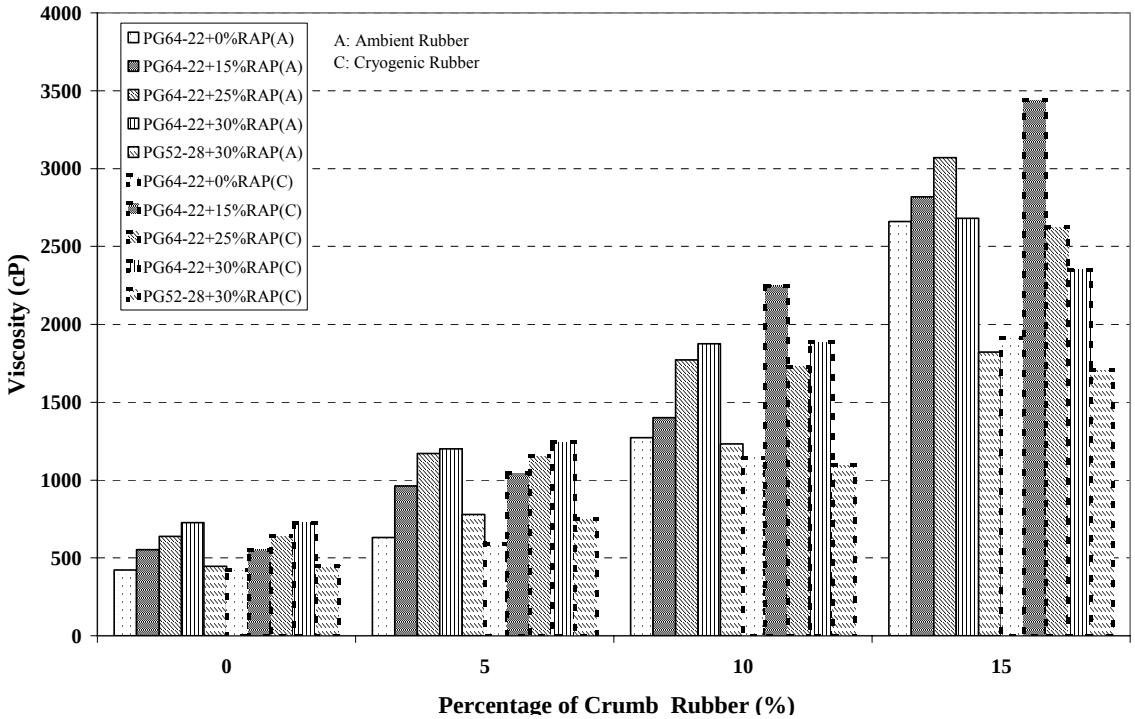

Figure 5.4 Viscosity comparison of the modified binder with ambient and cryogenic rubber containing aged binder extracted for RAP C

There are no previous specifications available for specific components in Superpave mix design regarding the mixing and compaction temperatures of modified binders. However, some researchers have developed some guidelines for mixing and compaction temperatures when using RAP or rubber (Raad et al. 2001; Way 2003). The temperature study, shown in Tables 5.1 and 5.2, were determined in accordance with previous research projects. These temperatures, which were provided by the asphalt producers, correspond to the temperature at which the binder viscosity is 0.17 ± 0.02 Pa.s for mixing and 0.28 ± 0.03 Pa.s for compacting as required by AASHTO TP4 (Lavin 2003).

Table 5.1 Mixing temperatures of modified mixtures

Temperature (°C)		Rubber (%)			
		0	**5**	**10**	**15**
Binder (PG52-28)		148	150	152	155
Binder (PG64-22)		155	160	165	172
Virgin Aggregate		173	175	177	177
RAP	15%	175	176	177	177
	25%	176	177	178	179
	30%	176	177	178	179

Table 5.2 Compacting temperatures of modified mixtures

Temperature (°C)		RAP (%)				
		0	**15**	**25**	**30**	**30 (52-28)**
Rubber (%)	**0**	150	155	160	162	140
	5	153	158	163	165	143
	10	156	161	165	167	146
	15	159	164	165	167	150

Both mixing and compacting temperatures increase as the percentages of RAP or crumb rubber increase regardless of the types of RAP and rubber. The increase in temperature, coming from the increase of viscosity values, is caused by aged binder and the addition of crumb rubber in order to produce modified binders.

Previous research indicated that, for a given aggregate source and air-void content, it could be seen that mix fatigue life correlates quite well with the loss stiffness ($G^* \sin\delta$) value of the aged binder. Increases in loss stiffness were accompanied by rather significant decrease in fatigue resistance. The binder loss stiffness seemed to be a logical candidate for inclusion in binder specification. However, it was generally not a sufficient indicator of the relative fatigue resistance of the mixtures (Tayebali et al. 1994).

Figure 5.5 and Table C.1 (Appendix C) present $G^*\sin\delta$ values of the modified binder with ambient and cryogenic rubber containing aged binder L. The loss strength

values were attained at a temperature of 25 ºC using specimens that were aged using a long term aging (RTFO+PAV). The aging process simulates the performance of asphalt mixture in the field for 15 to 20 years. G*sinδ is strongly associated with fatigue life of the mixture and has become a basic parameter to describe fatigue characteristics of asphalt binder, so the study of loss strength is beneficial for researchers and engineers to analyze fatigue behavior of asphalt pavements. Superpave mix design has a specification requirement for G*sinδ which indicated that this value must be less than 5000 kPa, which is depicted on the charts as a bold dash horizontal line. If the loss strength value is greater than 5000 kPa, the fatigue life of the asphalt pavement cannot meet the requirements of Superpave mix design. Figure 5.5 shows that the G*sinδ value increases as the RAP content increases, while the increase of rubber content decreases this value. The results indicate that the mixtures with a high percentage RAP have the higher loss strength, while the rubber is helpful in improving the fatigue resistance of the binder.

The G*sinδ value of modified binder, containing PG64-22 virgin binder with 30% RAP, is greater than 5000 kPa in a low percentage rubber (0 and 5%), while this value is less than 3000 kPa when using a softer binder (PG52-28). Obviously, the softer binder plays a key role in improving the fatigue resistance of asphalt binder and extending the aging performance of the binder. There were no statistical differences between G*sinδ values of the modified binders made with either ambient or cryogenic rubber.

Figure 5.6 and Table C.2 (Appendix C) show G*sinδ values of the modified binder made with ambient and cryogenic rubber and containing aged binder C. The results indicated that, in general, the same trends existed for RAP source C as source L.

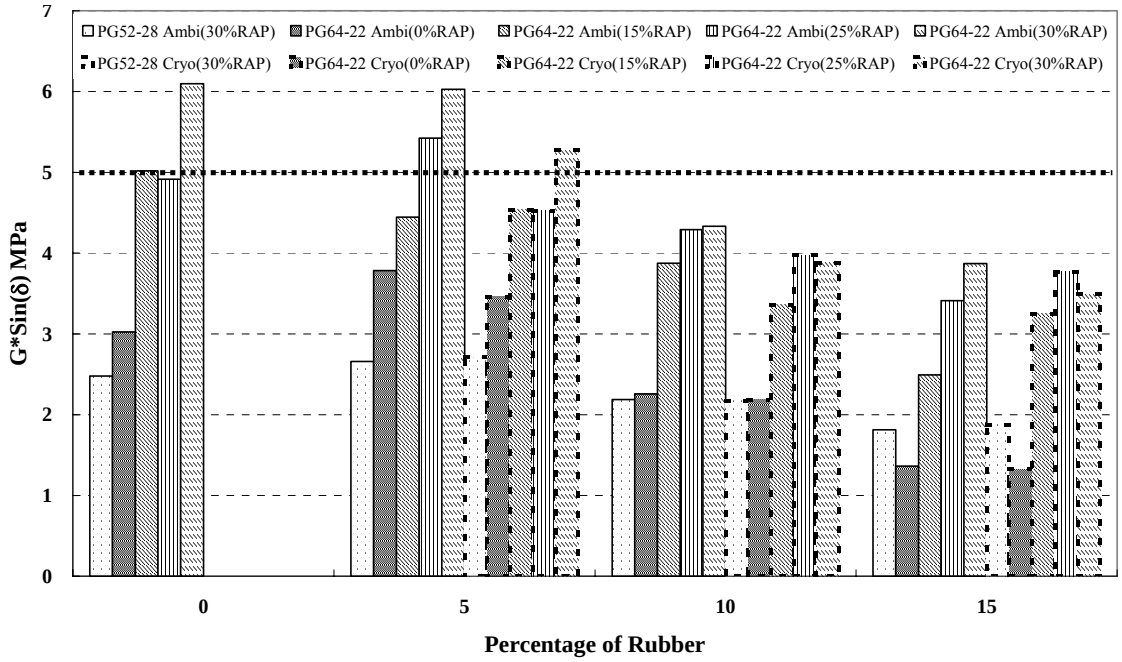

Figure 5.5 G*sin δ comparison of the modified binder with ambient and cryogenic rubber containing aged binder extracted from RAP L

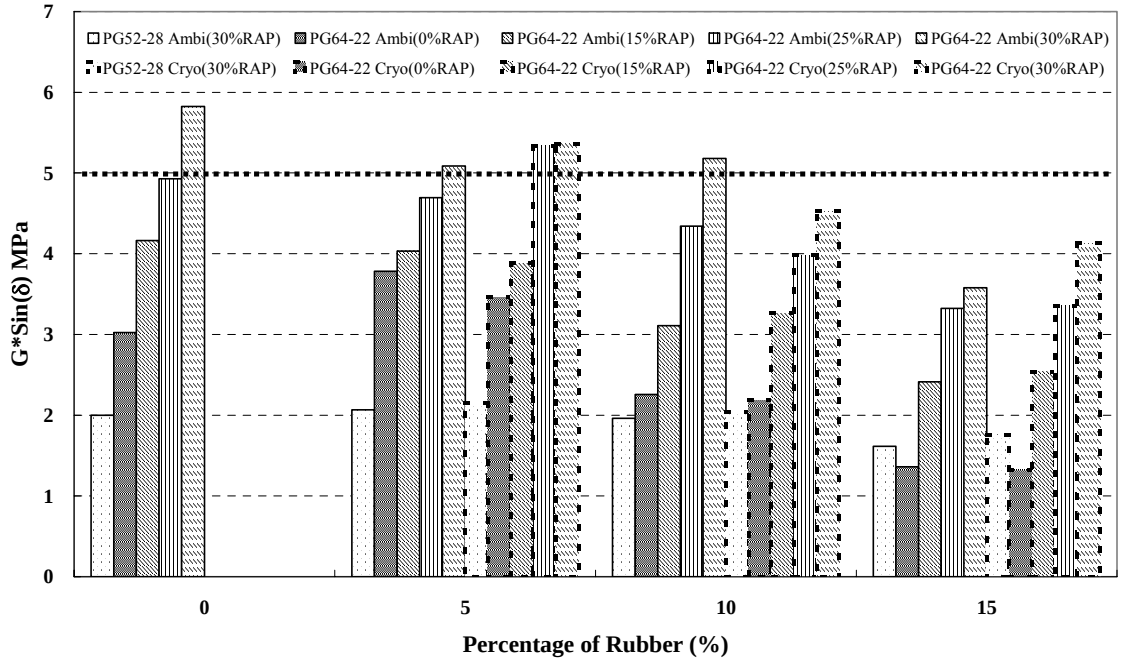

Figure 5.6 G*sin δ comparison of the modified binder with ambient and cryogenic rubber containing aged binder extracted from RAP C

Superpave Mix Design Analysis

Optimum Binder Content Analysis

In this study, the optimum asphalt binder content (OBC) was defined as the amount required to achieve 4.0% air voids at a given number of design gyrations (N_{design}= 75). Table 5.3 and Figure 5.7 show the OBC for mixtures with various percentages of RAP, rubber, and rubber types. Table 5.3 shows that the OBCs of the mixtures decrease slightly as the percentage of RAP increases for both rubber types (cryogenic and ambient) and source of RAP. The OBCs of the cryogenic modified binder were found to be slightly higher than those of the ambient binder at the same percentage of RAP when using aggregate L.

As the percentage of crumb rubber increases, the OBCs in the mixtures also slightly increase. There was not a trend between OBC values of mixtures containing 30%RAP and made with PG64-22 asphalt binder compared to mixtures used the softer binder (PG52-28). The OBC values of mixture using aggregate L are slightly higher that those of mixtures made with aggregate C. At the same time, previous research indicated that a high amount of rubber particles swell in the asphalt due to greater absorption of some of the lighter fraction (aromatic oils) from the binder. These crumb rubber particles form a viscous gel with an increase in the overall viscosity of the modified binder. Due to the increased viscosity, more modified binder is needed to achieve the target air void of the mixture at the specified mixing and compacting temperatures (Airey et al. 2003; Green and Tonlonen 1997; Heitzman 1992; Bahia and Davis 1994; Zanzotto and Kennepohl 1996; Kim et al. 2001).

Table 5.3 Optimum binder content of the mixtures

	Aggregate L							Aggregate C	
	Ambient Rubber (%)				Cryogenic Rubber (%)			Ambient Rubber (%)	
RAP	0%	5%	10%	15%	5%	10%	15%	0%	10%
0% (64)	5.40	5.60	5.85	6.35	5.25	6.08	6.11	5.00	5.75
15% (64)	5.25	5.45	5.75	5.90	5.25	5.85	5.30	5.10	5.53
25% (64)	4.70	5.02	5.08	5.65	5.02	5.18	5.10	N/A	N/A
30% (64)	4.82	4.59	5.12	5.25	4.80	5.30	5.08	N/A	5.10
30% (52)	4.65	4.95	4.90	5.05	N/A	N/A	N/A	4.85	5.00

Note:

(64): PG 64-22 asphalt binder; (52): PG52-28 asphalt binder

N/A: Not be tested in this study

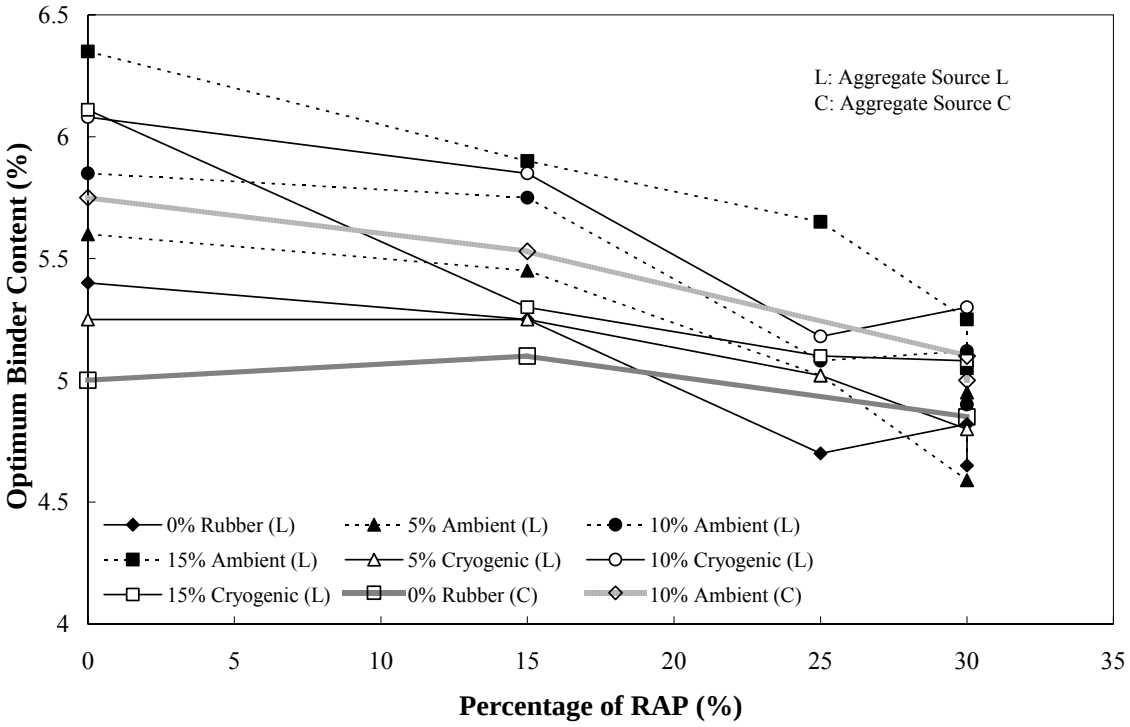

Figure 5.7 Optimum binder contents of the mix designs using aggregate L

Indirect Tensile Strength

The ITS test is often used to evaluate the moisture susceptibility of an asphalt mixture in Superpave mix design process. A high wet ITS value typically indicates that the mixture will perform well with a good resistance to moisture damage. At the same time, mixtures that are able to tolerate high strain prior to failure are more likely to resist cracking than those unable to tolerate high strains. The detrimental influences of moisture are called stripping, which produces a loss of strength through weakening the bond between the asphalt binder and the aggregate. The loss of strength can be sudden and catastrophic where the asphalt peels off the aggregate, the cohesion of the mixture is lost, and distresses develop rapidly. The more typical issue is that there is a gradual loss of strength over a period of years which contribute to the development of many distresses including rutting and shoving in the wheel paths. The use of the anti-stripping additive is inevitable and helpful to reduce the moisture damage during a long term performance of the asphalt pavement if the mixtures are susceptible to moisture damage.

In this study, AASHTO T283 test procedures were performed to determine the moisture susceptibility of the mixture. Three dry and wet specimen subsets were tested. The mean and standard deviation of ITS values are shown in Appendix D. The ITS and TSR values of specimens, containing different percentages of ambient rubber and RAP L, are shown in Figure 5.8 and Table 5.4. SCDOT's requirement are that all mixture must have at least 448 kPa (65 psi) wet ITS value and a minimum of 85% TSR values. With respect to the effect of rubber percentage, it can be seen that the increase of rubber content results in the decrease of ITS values at same percentage of RAP regardless of specimen types (dry or wet). The mixture containing 15% ambient

rubber used 0% and 15% RAP have the TSR values less than 85%. The ITS values of all wet specimens are higher than 448 kPa (65 psi). With respect to the effect of RAP percentage, Figure 5.8 and Table 5.4 shows that, in general, the increase of RAP content, from 0 to 30%, leads to an increase of ITS values at the same percentage rubber.

Table 5.4 TSR values of mixture made with aggregate L

TSR	Ambient Rubber (%)				Cryogenic Rubber (%)		
RAP	0%	5%	10%	15%	5%	10%	15%
0% (64)	86	97	85	78	90	93	61
15% (64)	86	102	96	76	86	94	69
25% (64)	88	92	93	90	85	113	80
30% (64)	94	100	100	90	94	97	97
30% (52)	86	86	89	90	N/A	N/A	N/A

Note:

(64): PG 64-22 asphalt binder; (52): PG52-28 asphalt binder

N/A: Not be tested in this study

The statistical analysis show that the ITS values of specimens made with 30%RAP and the softer binder (PG52-28) are significantly less than those of specimens using PG64-22 binder. Similar to PG64-22 binder, the increase of rubber content results in a decrease of ITS values of mixtures made with PG52-28 binder, in addition, TSR values of these mixtures are higher than 85%. Figure 5.8, Tables D.1 and D.2 also indicate that, in most cases, the standard deviations of ITS values are relatively high. The variability of test results of specimens containing RAP and crumb rubber may be a potential cause in contributing to the high standard deviation.

The ITS values of specimens containing cryogenic rubber can be seen in Figure 5.9 and Table D.3. Similar to results obtained with the ambient rubber, the ITS values of

specimens containing cryogenic rubber were decreased as the rubber contents increased. When using 15% rubber, the TSR values were less than 85% except for the specimens using 30%RAP. During ITS testing, cryogenic rubber shows similar moisture susceptibility with ambient rubber at the same percentage (15%) of rubber. The increase of RAP content not only increased the ITS values but also improved the potential moisture resistance of the mixture. In order to reduce the effect of rubber content in ITS, previous research also gave some recommendations that some additional anti-stripping additives were used to increase the cohesion of rubberized mixture (Hicks et al. 1995).

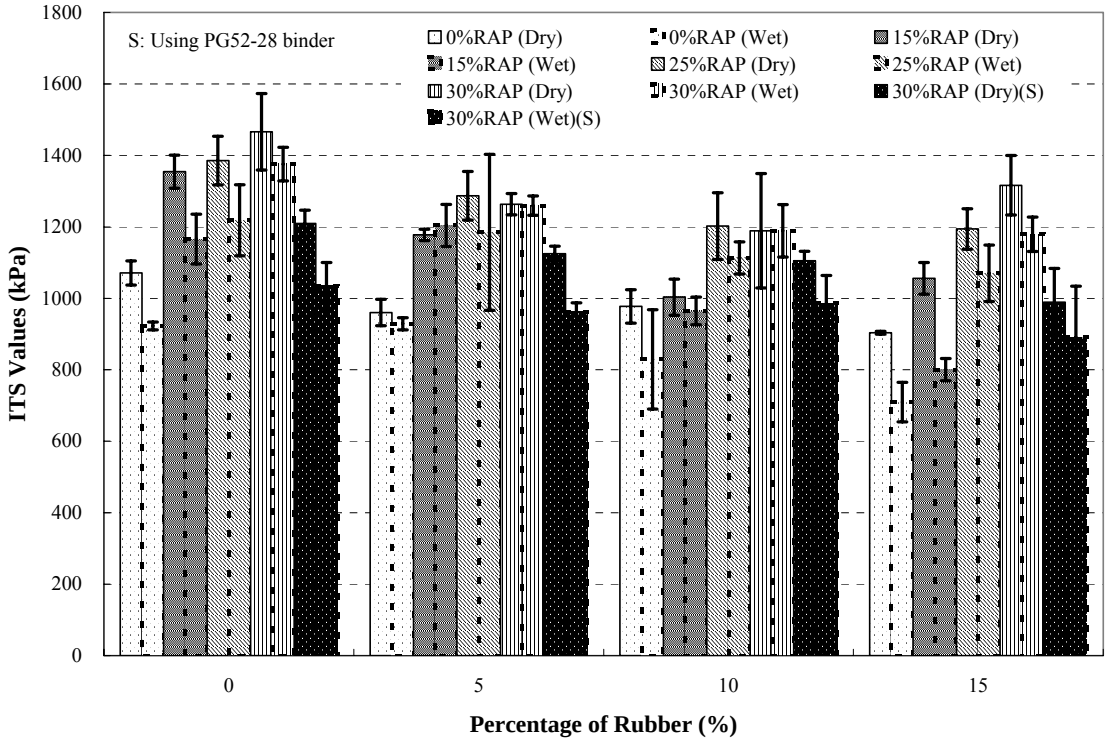

Figure 5.8 ITS values of the mixtures containing ambient rubber using aggregate L

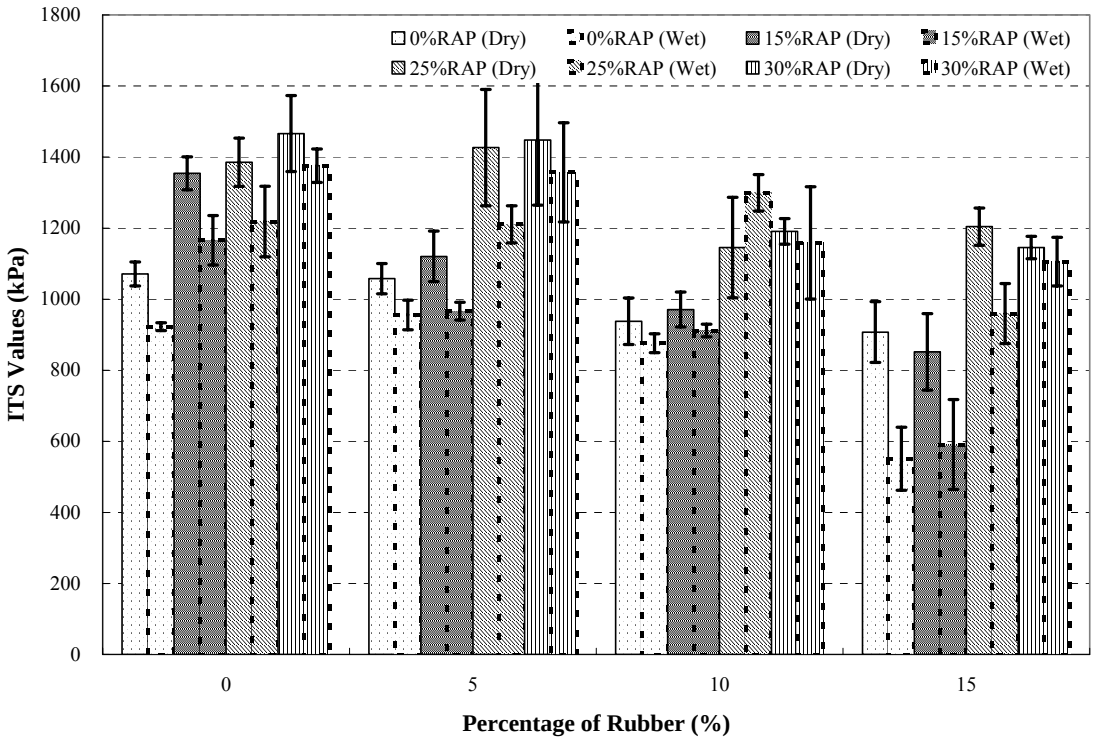

Figure 5.9 ITS values of the mixtures containing cryogenic rubber using aggregate L

The results shown in Figure 5.10 and Table D.4 indicate that the ITS values of specimens used aggregate C have similar trend to those of specimens used aggregate L. The differences in ITS values of specimens made with a softer binder (PG52-28) and PG64-22 were found to be statistically significant. Moreover, the wet and dry ITS values of specimens made with the softer binders had a significant decrease.

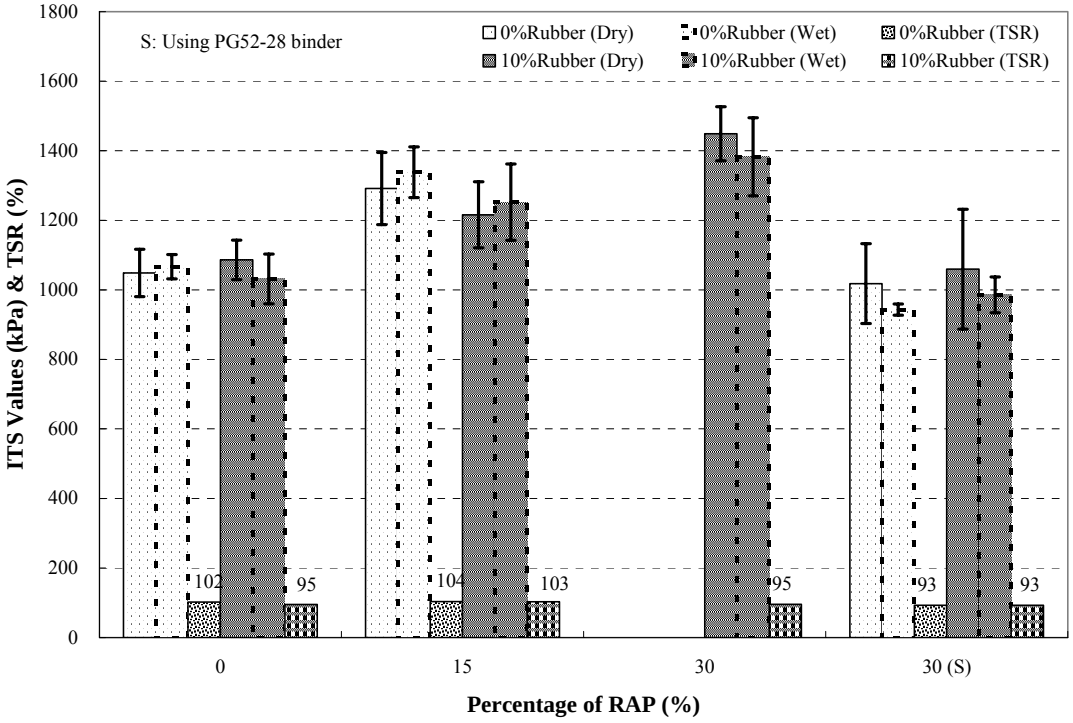

Figure 5.10 ITS and TSR values of the mixtures using aggregate C

Fatigue Prediction Models

Analysis of Fatigue Test Results

Testing data were analyzed using the equations presented in Chapter III to compute the stress, strain, stiffness, phase angle, and dissipated energy per cycle as the function of the number of load cycles, and the cumulative dissipated energy to a given load cycle. In this study, fatigue life was defined as the number of repeated cycles corresponding to a 50 percent reduction in initial stiffness, which was measured at the 50^{th} load cycle. Several fatigue beam specimens were utilized to characterize the fatigue behavior of a mixture in order to avoid too fast or slow loss in stiffness during a period of 24 hours. This procedure involved testing control specimen (0% rubber and 0%RAP) and the highest percent of rubber and RAP specimen (15% rubber and 30%RAP) at a 500

micro strain level with the controlled strain mode of loading at 5 Hz frequency. The additional RAP and rubber increased the complex level of fatigue life. The test results indicated that the 5 Hz was suitable to use at a 500 micro strain level, where the repeated cycles of mixture was generally more than 10,000 cycles. An example of some of the raw data is shown in Table 5.5. The Loads 1 and 2 are the peak to peak forces and LVDT 1 is the beam deflection at the neutral axis. The stress and strain values of specimens then be computed from these data.

Table 5.5 Typical raw data file fatigue test results (only some data shown)

Type of Collection Schedule	Logarithmic		
Cycle	Vert Load 1	Vert Load 2	Vert LVDT1
4.00	-1.9239314	-3.6115668	-0.2440772
4.01	-1.9163122	-3.6269119	-0.2457249
4.02	-1.9163122	-3.6283069	-0.2465488
4.03	-1.9086931	-3.6122644	-0.2466732
4.04	-1.9086931	-3.5990117	-0.246953
4.05	-1.9125026	-3.5794816	-0.2475748
4.06	-1.9163122	-3.5515811	-0.2482588
4.07	-1.9239314	-3.5104277	-0.24815
4.08	-1.9239314	-3.4134719	-0.2452275
4.09	-1.9239314	-3.3193042	-0.2418389
4.10	-1.9353601	-3.2021155	-0.2379531
4.11	-1.9125026	-3.065392	-0.234052

Table 5.6 presents a typical analyzed fatigue test results which are computed in various periods from the raw data. Some of these variables will be directly used as the independent variables as they are associated with fatigue prediction models. As shown in Table 5.6, the stress value and dissipated energy per cycle decrease as the number of cycle increases. That is, at the same strain level, a lager stress level is needed to reach the desired strain values at the beginning of fatigue test than at the end of the test. At the

same time, the dissipated energy per cycle at the first 50 cycles is remarkably greater than those at the final cycles (50% loss of initial stiffness).

Table 5.6 Typical analyzed fatigue test results

Period Number	Stress	Strain	Dynamic Stiffness	Phase Angle	Dissipated Energy	Cumulative Engergy
Cycles	Pa	m/m	Pa	Degree	J/m^3	J/m^3
50	4542.32	2.50E-04	6.04E+07	54	1046.65	1046.65
100	4308.69	2.45E-04	1.13E+09	90	352.78	1399.43
250	4244.48	2.43E-04	2.95E+08	72	732.06	2131.49
500	4209.59	2.45E-04	3.37E+08	72	447.51	2579.00
1000	4165.67	2.44E-04	4.23E+08	90	335.99	2914.99
1600	4186.22	2.44E-04	7.07E+08	54	526.29	3441.27
2000	4131.99	2.42E-04	1.59E+08	72	425.99	3867.26
4000	4086.26	2.46E-04	5.19E+08	72	323.98	4191.24
8000	3963.91	2.44E-04	1.37E+08	72	430.71	4621.94
10000	3945.67	2.46E-04	1.99E+08	72	137.80	4759.74
15850	3839.18	2.46E-04	1.22E+08	72	275.40	5035.14
19954	3808.18	2.44E-04	1.33E+08	90	163.15	5198.29
25120	3598.19	2.44E-04	1.13E+08	72	131.30	5329.58
31624	3346.60	2.42E-04	5.47E+08	72	112.95	5442.54
39812	3009.54	2.45E-04	1.77E+08	72	104.26	5546.80
50120	2490.61	2.44E-04	1.56E+08	72	84.85	5631.64

Previous research indicated that the stiffness at any number of load repetitions is computed from the tensile stress and strain at that specific value (Monismith et al. 1985; Hicks et al. 1993; Tayebali et al. 1994; Kim et al. 2003; Williams 1998). Figure 5.11 shows a typical plot of stiffness ratio (defined as quotient of stiffness at the i^{th} load repetition to the initial stiffness) versus the number of load repetitions for flexural beam fatigue tests in both controlled-stress and controlled-strain modes of loading. The fatigue life to failure is dependent on the mode of loading condition. The use of modes will influence the test results. For controlled-stress tests, failure is well defined since specimens are cracked through at the end of the test. However, in controlled-strain testing,

failure is not readily apparent and the specimen is considered to have failed when its initial stiffness is reduced by 50 percent (Tayebali et al. 1994).

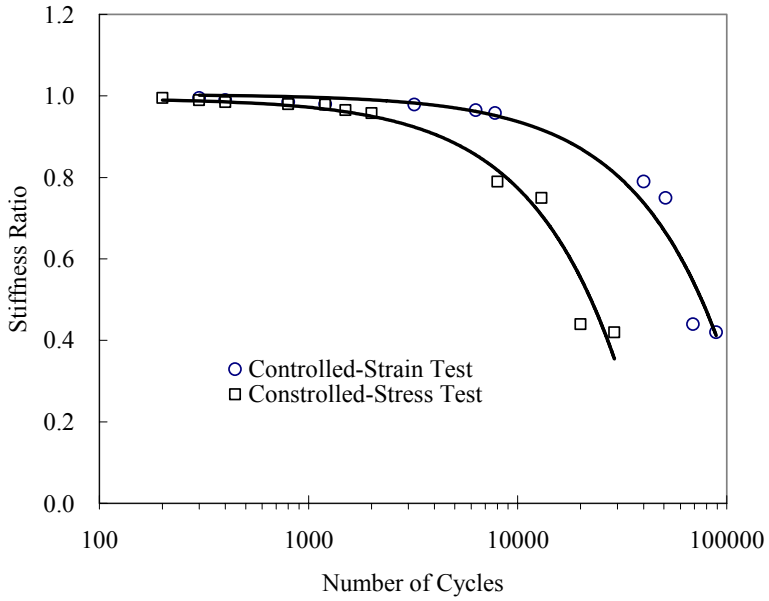

Figure 5.11 Stiffness ratio versus number of cycles, flexural beam fatigue controlled-stress and controlled-strain (after Tayebali et al. 1994)

Dissipated energy per cycle for a beam specimen tested under pulsed loading is computed as the area with the stress-strain hysteresis loop and detailed energy equations which were discussed in Chapter III. Figure 5.12 shows a typical stress-strain hysteresis loop for the controlled-strain mode of loading.

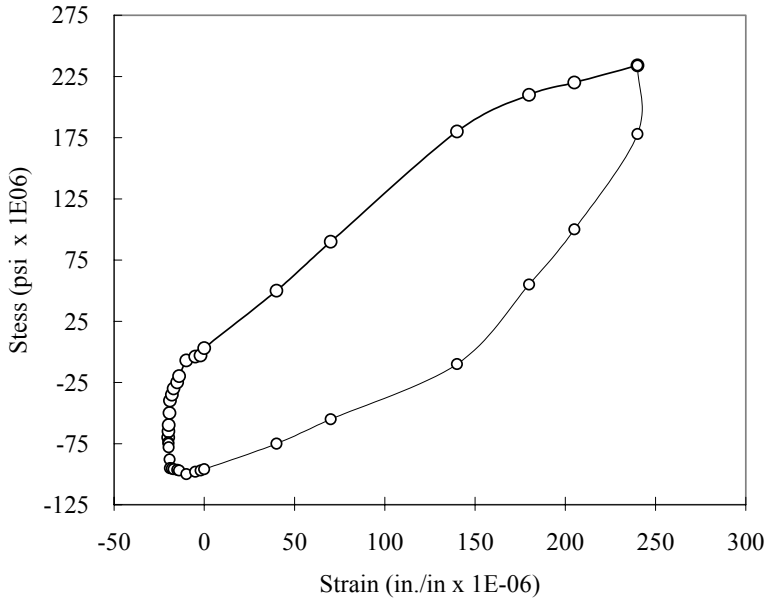

Figure 5.12 Stress-stress hysteresis loop, flexural bema fatigue controlled-strain test (after Tayebali et al. 1994)

The variation of dissipated energy per cycle with number of load repetitions is shown in Figure 5.13. The dissipated energy per cycle decreases with an increasing number of load repetition in the controlled-strain fatigue test; whereas, for the controlled-stress tests, the dissipated energy per cycle increases as the number of load repetitions increases. The cumulative dissipated energy to failure for a flexural beam fatigue test is the area under the curve between dissipated energy and number of cycles. In this study, since the flexural beam fatigue test used the controlled-strain test, the number of cycles has a greater increase than the controlled-stress test.

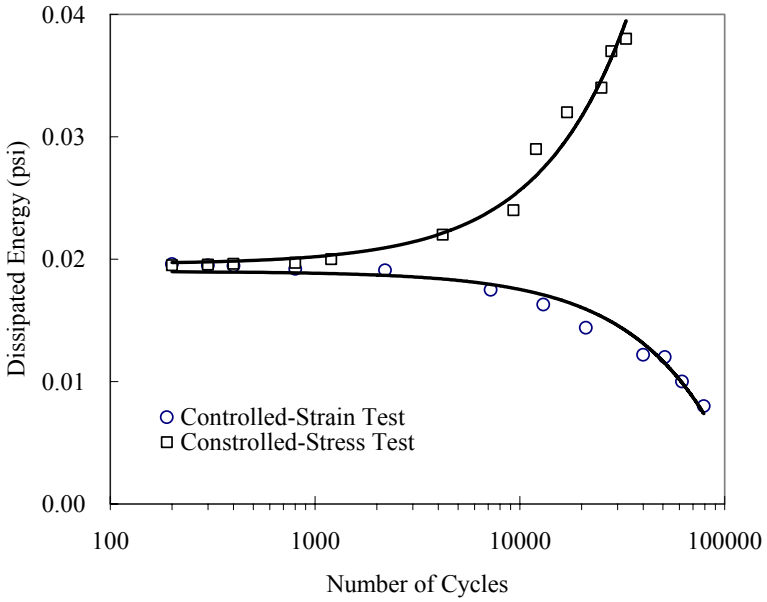

Figure 5.13 Dissipated energy per cycle versus number of cycles, flexural beam fatigue controlled-stress and controlled-strain tests (after Tayebali et al. 1994)

Statistical Regression Fatigue Prediction Models

Modeling the laboratory fatigue response was of great interest not only because of insights developed during the model-building process and in interpreting its results but also because of the possibility that a sufficiently accurate model, one that captured the essential effects of mix properties on fatigue behavior, would lessen the requirements for laboratory fatigue testing in the mix design process and even help estimate the pavement performance in the field (Tayebali et al. 1994). In order to simplify the fatigue models, previous research found that: 1) the effects of initial mix stiffness and phase angle on cycles to failure can be expressed with equal accuracy by an initial mix loss modulus; 2) the effect of mix voids on cycles to failure can be expressed with equal accuracy by either the air-void content or the VFA; 3) the effects of initial strain level, mix stiffness, and phase angle can be expressed with equal accuracy by the initial dissipated energy per

cycle (Tayebali et al. 1994). The typical fatigue prediction models, being used by many researchers, have been presented in Chapter II. The Equations 2-4 and 2-7 have addressed the strain-based and energy-based approaches, respectively. All the surrogate fatigue models were developed on the basis of these equations.

The test results of fatigue life and stiffness value of modified mixture, containing ambient rubber used RAP L at a testing temperature of 5^{o}C are shown Tables E.1 to E.2. The mean values of test results, adjusted statistically without affecting the model coefficients, can be seen in Table F.1 to F.3. Distributions for fatigue life (N_f), initial stiffness (S_0), dissipated energy (w_0) and initial strain (ε_0) were reviewed and found to be lognormally distributed. Therefore, log transformations (using natural logarithm) were used in ANOVA and GLM through regression analysis.

The experimental design selected in this study includes two types of methods, one is traditional prediction models which use the main experimental independent variables as shown in Equations 5-4 and 5-5, and the other one is specific models which permit the estimation of the main effects of the experimental factors and some of two-factor interactions, as shown in Equations 5-6 and 5-7.

According to the traditional mixture models, for ANOVA and GLM, the log-linear models of the following type were utilized.

$$Ln\,(N_f) = a + b * Ln\,(\varepsilon_0) + c * VFA\ or\ V_0 + d * Ln\,(S_0) \tag{5-4}$$

$$Ln\,(N_f) = e + f * Ln\,(w_0) + g * VFA\ or\ V_0 \tag{5-5}$$

Where,

N_f = number of load application or crack initiation;

S_0 = initial stiffness, in Pa;

ε_0 = initial tensile strain, in m/m;

VFA = volume of voids filled with asphalt, in m^3/m^3;

V_0 = initial air-void content in percentage, in m^3/m^3;

w_0 = initial energy dissipated per cycle, in J/m^3;

a, b, c, d, e, f, g = experimentally determined coefficients

With respect to specific mixtures in this study, some additional independent variables were used for the log-linear models.

$$Ln(N_f) = a + b*R_b + c*R_p + d*R_b*R_p + e*R_b^2 + f*R_b^3 + g*Ln(\varepsilon_0) + h*(VFA \text{ or } V_0) + i*R_b*(VFA \text{ or } V_0) + j*R_p*(VFA \text{ or } V_0) + k*Ln(S_0) \quad (5\text{-}6)$$

$$Ln(N_f) = a + b*R_b + c*R_p + d*R_b*R_p + e*R_b^2 + f*R_b^3 + g*(VFA \text{ or } V_0) + h*R_b*(VFA \text{ or } V_0) + i*R_p*(VFA \text{ or } V_0) + j*Ln(w_0) \quad (5\text{-}7)$$

Where,

R_b = percentage of rubber, in kg/kg;

R_p = percentage of RAP, in kg/kg;

h, I, j, k = experimentally determined coefficients

Strain Dependent Models

Models of Using Ambient Rubber at 5ºC

The Pearson correlation of dependent and independent variables of mixture is presented in Table 5.7. Considering the correlation values in Table 5.7, it can be seen that VFA and percentage of RAP have the higher values than the other variables. That is VFA and percentage of RAP play a key role in determining the fatigue life and establishing

strain dependent predictive models of mixture which is containing ambient rubber and RAP L and tested at 5ºC.

Table 5.7 Pearson correlation matrix for the dependent and independent variables of mixture containing ambient rubber and RAP L at 5ºC

	$Ln(N_f)$	$Ln(S_0)$	$Ln(w_0)$	$Ln(\varepsilon_0)$	VFA	V_0	R_b	R_P
$Ln(N_f)$	1.000							
$Ln(S_0)$	0.176	1.000						
$Ln(w_0)$	-0.091	-0.006	1.000					
$Ln(\varepsilon_0)$	-0.122	-0.231	0.444	1.000				
VFA	0.471	-0.268	-0.217	-0.412	1.000			
V_0	-0.264	-0.131	-0.266	0.235	-0.631	1.000		
R_b	0.473	-0.600	-0.123	-0.086	0.554	-0.073	1.000	
R_P	-0.067	-0.078	0.252	0.521	-0.601	0.661	0.000	1.000

Tables 5.8 and 5.9 show typical results of ANOVA and GLM for the traditional and specific VFA models, respectively. The results are derived from using regression analysis technique. The Microsoft Excel software package and SAS were used to analyze the data. The statistical results show a poor fit for the fatigue life of traditional VFA models with an R^2 less than 0.4. The coefficient of variation based on the actual data is 60 percent. However, the statistical results of specific VFA models show a R^2 value of 0.95 which exhibits a good fit for the fatigue life prediction. The coefficient of variation of this GLM is 53 percent.

The traditional strain dependent VFA fatigue prediction model of the modified mixture, drawn from Table 5.8, is shown in Equation 5-8.

$$Ln(N_f) = -29.9 + 1.6 * Ln(\varepsilon_0) + 20.2 * VFA + 2.2 * Ln(S_0) \quad (5\text{-}8)$$

The Equation 5-8 can be rewritten into

$$N_f = 1.0E(-13) * \varepsilon_0^{1.6} * e^{20.2*VFA} * S_0^{2.2} \qquad R^2 = 0.37 \qquad C.V. = 61\% \tag{5-9}$$

As using the specific strain dependent VFA fatigue prediction model, GLM model can be drawn from Table 5.9, as shown in Equation 5-10.

$$Ln(N_f) = -57.3 - 426.8 * R_b + 187.4 * R_p + 98.6 * R_b * R_p + 470.5 * R_b^2 - 2382.5 * R_b^3 + 2.3 * Ln(\varepsilon_0) + 48.5 * VFA + 519 * R_b * VFA - 255.3 * R_p * VFA + 2.9 * Ln(S_0) \tag{5-10}$$

The Equation 5-10 can be rewritten into

$$N_f = 1.3E(-25) * e^{-426.8*R_b + 187.4*R_p + 98.6*R_b*R_p + 470.5*R_b^2 - 2382.5*R_b^3} * \varepsilon_0^{2.3} * e^{48.5*VFA + 519*R_b*VFA - 255.3*R_p*VFA} * S_0^{2.9}$$
$$R^2 = 0.95 \qquad C.V. = 52\% \tag{5-11}$$

Table 5.8 ANOVA and GLM of log fatigue life for mixture containing ambient rubber and RAP L tested at 5ºC (traditional strain dependent VFA method)

Dep. Variable	Multiple R	R Square	Adjusted R Square	Standard Error	Number of Samples	
Ln (N_f)	0.607	0.368	0.210	0.368	16*(4 repetition)	
Analysis of Varance (ANOVA)						
	df	Sum of Square	Mean Square	F Ratio	Significance F	C.V.
Regression	3	0.945	0.315	2.328	0.126	60.848
Residual	12	1.624	0.135			
Total	15	2.569				
	Coefficients	Standard Error	t Stat	P-value	Lower 95%	Upper 95%
Intercept	-29.853	22.701	-1.315	0.213	-79.314	19.608
Ln (ε_0)	1.558	1.637	0.952	0.360	-2.008	5.124
VFA	20.173	8.062	2.502	0.028	2.607	37.739
Ln (S_0)	2.180	1.337	1.630	0.129	-0.733	5.094

Table 5.9 ANOVA and GLM of log fatigue life for mixture containing ambient rubber and RAP L tested at 5ºC (specific strain dependent VFA method)

Dep. Variable	Multiple R	R Square	Adjusted R Square	Standard Error	Number of Samples	
Ln (N_f)	0.976	0.952	0.857	0.156	16*(4 repetition)	
Analysis of Varance (ANOVA)						
	df	Sum of Square	Mean Square	F Ratio	Significance F	C.V.
Regression	10	2.447	0.245	10.006	0.010	52.649
Residual	5	0.122	0.024			
Total	15	2.569				
	Coefficients	Standard Error	t Stat	P-value	Lower 95%	Upper 95%
Intercept	-57.325	18.539	-3.092	0.027	-104.981	-9.669
R_b	-426.836	102.382	-4.169	0.009	-690.017	-163.655
R_p	187.429	74.453	2.517	0.053	-3.957	378.815
R_b*R_p	98.648	25.884	3.811	0.012	32.111	165.186
R_b^2	470.535	130.612	3.603	0.016	134.786	806.284
R_b^3	-2382.455	606.366	-3.929	0.011	-3941.167	-823.744
Ln (ε_0)	2.323	0.961	2.416	0.060	-0.148	4.795
VFA	48.509	22.545	2.152	0.084	-9.446	106.463
R_b*VFA	518.987	130.015	3.992	0.010	184.774	853.199
R_p*VFA	-255.336	100.801	-2.533	0.052	-514.453	3.782
Ln (S_0)	2.917	0.750	3.888	0.012	0.989	4.846

As using air voids to establish the fatigue prediction models of the modified mixtures, this predictive model is similar to the VFA model. The ANOVA and GLM analysis of log fatigue life for air voids are shown in Tables 5.10 and 5.11. It can be seen that a value of R^2 using traditional air void model is less than 0.1. This value shows a very poor fit for fatigue predictive model, which would not be suitable to predict the fatigue life of the specimen. However, when using specific air void model, the R^2 of GLM is approximate 0.8. This value shows a reasonable fit for fatigue life. When analyzing the coefficient of variation values of two types of model, they are 28% and 47%, respectively.

Similarly, the traditional strain dependent air void model derived from Table 5.10 is summarized in Equation 5-12:

$$N_f = 0.048 * \varepsilon_0^{-0.2} * e^{-0.1*V_0} * S_0^{0.7} \qquad R^2 = 0.09 \qquad C.V. = 28\% \tag{5-12}$$

When using the specific strain dependent air void fatigue predictive model of the modified mixture, GLM model can be drawn from Table 5.11, as shown in Equation 5-13.

$$N_f = 1.9E(-18) * e^{7.3*R_b - 7.5*R_p + 30.1*R_b*R_p + 204.4*R_b^2 - 831.3*R_b^3} * \varepsilon_0^{1.2} * e^{0.2*V_0 - 4.0*R_b*V_0 + 1.0*R_p*V_0} * S_0^{3.5}$$
$$R^2 = 0.77 \qquad C.V. = 47\% \tag{5-13}$$

Table 5.10 ANOVA and GLM of log fatigue life for mixture containing ambient rubber and RAP L tested at 5ºC (traditional strain dependent air void method)

Dep. Variable	Multiple R	R Square	Adjusted R Square	Standard Error	Number of Samples	
Ln (N_f)	0.302	0.091	-0.136	0.441	16*(4 repetition)	
Analysis of Varance (ANOVA)						
	df	Sum of Square	Mean Square	F Ratio	Significance F	C.V.
Regression	3	0.234	0.078	0.401	0.755	28.491
Residual	12	2.335	0.195			
Total	15	2.569				
	Coefficients	Standard Error	t Stat	P-value	Lower 95%	Upper 95%
Intercept	-3.035	25.576	-0.119	0.907	-58.761	52.690
Ln (ε_0)	-0.205	1.733	-0.118	0.908	-3.980	3.570
V_0	-0.090	0.108	-0.837	0.419	-0.325	0.144
Ln (S_0)	0.711	1.468	0.484	0.637	-2.487	3.909

Table 5.11 ANOVA and GLM of log fatigue life for mixture containing ambient rubber and RAP L tested at 5ºC (specific strain dependent air void method)

Dep. Variable	Multiple R	R Square	Adjusted R Square	Standard Error	Number of Samples	
Ln (N_f)	0.877	0.770	0.310	0.344	16*(4 repetition)	
Analysis of Varance (ANOVA)						
	df	Sum of Square	Mean Square	F Ratio	Significance F	C.V.
Regression	10	1.978	0.198	1.672	0.297	46.762
Residual	5	0.591	0.118			
Total	15	2.569				
	Coefficients	Standard Error	t Stat	P-value	Lower 95%	Upper 95%
Intercept	-40.767	31.529	-1.293	0.253	-121.814	40.280
R_b	7.254	17.700	0.410	0.699	-38.244	52.753
R_p	-7.452	8.661	-0.860	0.429	-29.715	14.810
$R_{b*}R_p$	30.087	20.930	1.437	0.210	-23.716	83.890
R_b^2	204.405	259.754	0.787	0.467	-463.312	872.122
R_b^3	-831.345	1139.153	-0.730	0.498	-3759.626	2096.936
Ln (ε_0)	1.208	1.948	0.620	0.563	-3.801	6.216
V_0	0.158	0.607	0.260	0.805	-1.403	1.719
R_b*V_0	-4.020	2.774	-1.449	0.207	-11.150	3.111
R_p*V_0	1.001	1.914	0.523	0.623	-3.919	5.922
Ln (S_0)	3.526	1.790	1.970	0.106	-1.075	8.126

The measured and predicted results of fatigue life, derived from traditional and specific predictive model, are shown in Figures 5.14 and 5.15, respectively. As discussed earlier in this section, the specific predictive model; where the measured and predicted results are close to a perfect-match line, in most cases, as shown in Figure 5.15, model shows a more reasonable relationship between measured and predicted results than the traditional model. The VFA model has a greater R^2 value than air void model in predicting fatigue life. Similarly, the predicted results from VFA model are closer to perfect-match line than air void model.

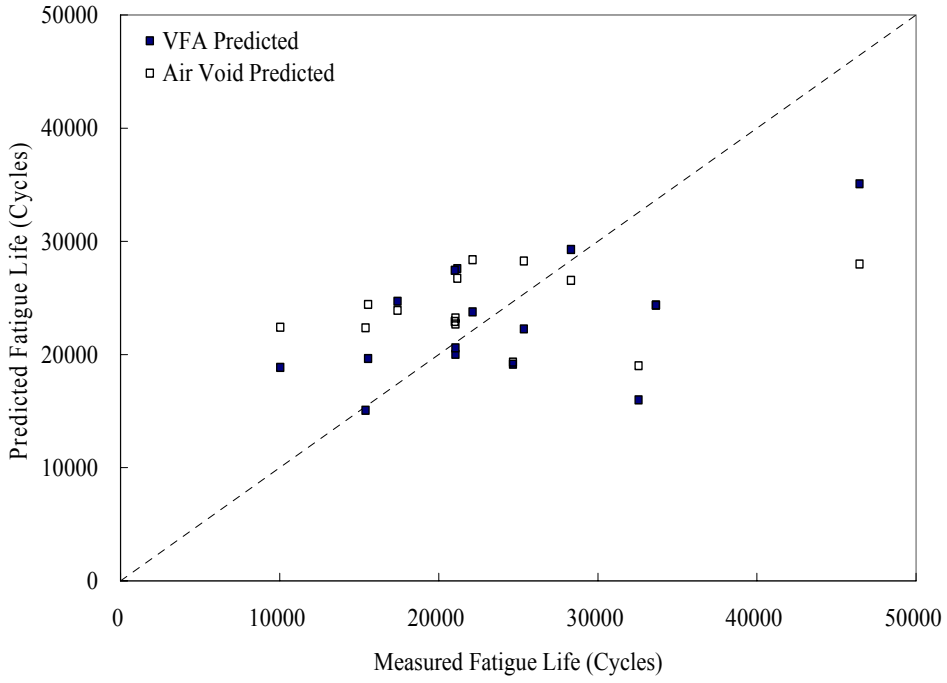

Figure 5.14 Comparison of fatigue lives between predicted and measured results using traditional strain dependent method at 5°C (containing ambient rubber and RAP L)

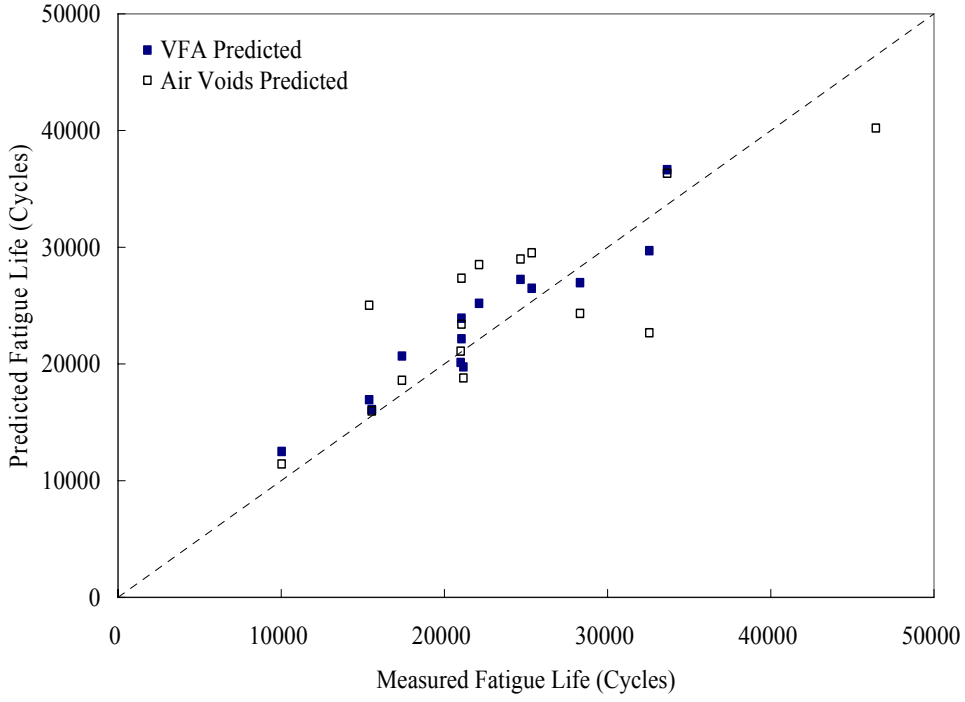

Figure 5.15 Comparison of fatigue lives between predicted and measured results using specific strain dependent method at 5°C (containing ambient rubber and RAP L)

Tables G.1 to G.3 show the Pearson correlation of dependent and independent variables of various mixtures at the different testing temperatures. The established traditional and specific models have been shown in Table 5.12, where, obviously, the specific prediction models have the higher R^2 values than the traditional models, thus, this also indicates that the additional independent variables are beneficial in improving the precision of prediction model.

Table 5.12 also shows that R^2 values of the mixtures containing ambient rubber are higher than those of cryogenic rubber. A probably potential cause is that four repeated specimens for each mixture containing ambient rubber had been accomplished while only two or four repeated specimens for each cryogenic rubber mixture.

The typically statistical results of ANOVA and GLM for two models are shown in Tables G.4 to G.15. The summary statistics show a poor fit for the fatigue life of traditional models, in most cases, the coefficient of determination values are less than 0.5, however, when using specific models to predict the fatigue life, R^2 values are higher than 0.65, the specific models exhibits a good fit for the fatigue life prediction. The predicted and measured fatigue lives of the modified mixture are shown in Figures G.1 to G.6. These measured and predicted results are closer to perfect-match line when using specific models.

Table 5.12 Stress dependent prediction models of the mixtures using aggregate source L

Ambient	Traditional Predicted Model	R^2	C.V.
VFA (20°C)	$N_f = 3.3E(5) * \varepsilon_0^{6.5} * e^{20.9*VFA} * S_0^{1.9}$	0.36	82
A.V. (20°C)	$N_f = 1.9E(26) * \varepsilon_0^{6.8} * e^{-0.4*V_0} * S_0^{0.2}$	0.53	106
Cryogenic			
VFA (5°C)	$N_f = 1.3E(5) * \varepsilon_0^{6.7} * e^{-0.1*VFA} * S_0^{2.9}$	0.13	47
A.V. (5°C)	$N_f = 3.6E(11) * \varepsilon_0^{7.2} * e^{-0.2*V_0} * S_0^{2.3}$	0.32	78
VFA (20°C)	$N_f = 1.7E(34) * \varepsilon_0^{9.1} * e^{-0.5*VFA} * S_0^{0.02}$	0.27	51
A.V. (20°C)	$N_f = 3.9E(20) * \varepsilon_0^{3.4} * e^{-0.2*V_0} * S_0^{0.6}$	0.36	61
Ambient	Specific Predicted Model	R^2	C.V.
VFA (20°C)	$N_f = 7.2E(-27) * e^{-77.3*R_b+327.1*R_p+70.7*R_b*R_p+37.8*R_b^2+58.1*R_b^3} * \varepsilon_0^{6.2} * e^{104.5*VFA+69*R_b*VFA-443.9*R_p*VFA} * S_0^{2.4}$	0.84	66
A.V. (20°C)	$N_f = 2.7E(3) * e^{32.3*R_b-0.5*R_p-19.1*R_b*R_p-135.2*R_b^2 862.9*R_b^3} * \varepsilon_0^{8.2} * e^{0.3*V_0-4.2*R_b*V_0-0.3*R_p*V_0} * S_0^{3.9}$	0.91	69
Cryogenic			
VFA (5°C)	$N_f = 1.4E(16) * e^{312.5*R_b-16.4*R_p+69.5*R_b*R_p+114.5*R_b^2-671.3*R_b^3} * \varepsilon_0^{9.2} * e^{7.5*VFA-471*R_b*VFA+19.2*R_p*VFA} * S_0^{2.2}$	0.65	58
A.V. (5°C)	$N_f = 2.0E(-32) * e^{-71.2*R_b+0.1*R_p-83.4*R_b*R_p+853.7*R_b^2-3545.1*R_b^3} * \varepsilon_0^{4.2} * e^{-0.4*V_0+6.9*R_b*V_0-0.4*R_p*V_0} * S_0^{6.9}$	0.65	58
VFA (20°C)	$N_f = 1.1E(15) * e^{-178*R_b+47*R_p-43.4*R_b*R_p+510.1*R_b^2 1982.1*R_b^3} * \varepsilon_0^{2.9} * e^{-6.2*VFA+213.3*R_b*VFA-66.2*R_p*VFA} * S_0^{0.2}$	0.73	46
A.V. (20°C)	$N_f = 11 * e^{-25.7*R_b+7.2*R_p-22.6*R_b*R_p+364.5*R_b^2-1553.2*R_b^3} * \varepsilon_0^{-1.3} * e^{-0.1*V_0+1.3*R_b*V_0-1.4*R_p*V_0} * S_0^{0.2}$	0.73	46

Energy Dependent Models

Similar to the strain dependent model analysis method, the Pearson correlation of dependent and independent variables of energy dependent models have been presented in Tables 5.7 and G.1 to G.3. The summary statistical results of ANOVA and GLM for the traditional and specific VFA models are shown in Tables G.16 through G.31. The traditional and specific fatigue predictive models of the modified mixture, drawn from these tables, are shown in Table 5.13. In general, the energy dependent prediction models show similar trends with strain dependent models although there are several different independent variables.

The measured and predicted results of fatigue lives, derived from traditional and specific energy dependent predictive model, are shown in Figures G.7 through G.14. As discussed earlier in this chapter, the measured and predicted results of specific prediction models are close to a perfect-match line.

When using the softer binder, the predicted fatigue lives of various mixtures are shown in Table 5. 14. It can be seen that the predicted results are lower than the measured results in most cases, and thus the fatigue prediction model of mixture is not suitable to predict the fatigue lives of mixtures, used in this project, made with the softer binder prior to modification. As shown in Appendix E, the measured results of mixtures containing softer binder do not show higher values than those of mixtures made with PG 64-22 binder. This also shows that the softer binder does not improve fatigue resistance of rubberized mixtures used in this research study as using a high percentage of RAP (i.e., 30%).

Table 5.13 Energy dependent prediction models of the mixtures using aggregate source L

Ambient	Traditional Predicted Model	R^2	C.V.
VFA (5°C)	$N_f = 0.74 * e^{13.8*VFA} * \varepsilon_0^{0.01}$	0.22	57
A.V. (5°C)	$N_f = 4.9E(4) * e^{-0.1*V_0} * \varepsilon_0^{-0.2}$	0.09	37
VFA (20°C)	$N_f = 4.1E(-4) * e^{21.6*VFA} * \varepsilon_0^{2.6}$	0.49	135
A.V. (20°C)	$N_f = 1.1E(5) * e^{-0.3*V_0} * \varepsilon_0^{1.0}$	0.42	121
Cryogenic			
VFA (5°C)	$N_f = 1.1E(4) * e^{-0.2*VFA} * \varepsilon_0^{0.5}$	0.04	31
A.V. (5°C)	$N_f = 2.4E(4) * e^{0.2*V_0} * \varepsilon_0^{0.4}$	0.21	78
VFA (20°C)	$N_f = 4.0E(4) * e^{-0.2*VFA} * \varepsilon_0^{0.9}$	0.40	84
A.V. (20°C)	$N_f = 8.1E(4) * e^{-2.5*V_0} * \varepsilon_0^{1.0}$	0.27	66
Ambient	Specific Predicted Model		
VFA (5°C)	$N_f = 5.6E(-6) * e^{-533.9*R_b+164.6*R_p+106.4*R_b*R_p+374.6*R_b^2-2039.9*R_b^3} * e^{30.1*VFA+665.9*R_b*VFA-224.9*R_p*VFA} * \varepsilon_0^{0.02}$	0.79	50
A.V. (5°C)	$N_f = 4.4E(4) * e^{-7.9*R_b-4.1*R_p+47*R_b*R_p+365*R_b^2-1576.8*R_b^3} * e^{0.02*V_0-3.8*R_b*V_0+0.5*R_p*V_0} * \varepsilon_0^{-0.6}$	0.66	46
VFA (20°C)	$N_f = 1.1E(-41) * e^{-382.5*R_b+500.8*R_p+155.6*R_b*R_p+403.8*R_b^2-1974.4*R_b^3} * e^{141.8*VFA+433.2*R_b*VFA-680.1*R_p*VFA} * \varepsilon_0^{0.23}$	0.81	68
A.V. (20°C)	$N_f = 602 * e^{-4.5*R_b+9.3*R_p-5*R_b*R_p+287.7*R_b^2-1183*R_b^3} * e^{0.4*V_0-1.5*R_b*V_0-2.0*R_p*V_0} * \varepsilon_0^{2.53}$	0.78	67
Cryogenic			
VFA (5°C)	$N_f = 1.84 * e^{284*R_b-20.6*R_p+48.3*R_b*R_p+163.9*R_b^2-1104.1*R_b^3} * e^{12.9*VFA-420.7*R_b*VFA+26.2*R_p*VFA} * \varepsilon_0^{-0.09}$	0.52	54
A.V. (5°C)	$N_f = 7.3E(6) * e^{-38*R_b-1.7*R_p-52.3*R_b*R_p+244.9*R_b^2-1370.9*R_b^3} * e^{-1.46*V_0+7.5*R_b*V_0+1.7*R_p*V_0} * \varepsilon_0^{-0.22}$	0.56	57
VFA (20°C)	$N_f = 2.0E(7) * e^{-180.7*R_b+44.7*R_p-39.3*R_b*R_p+606.9*R_b^2-2381.8*R_b^3} * e^{-7.9*VFA+204.7*R_b*VFA-63.4*R_p*VFA} * \varepsilon_0^{-0.01}$	0.73	49
A.V. (20°C)	$N_f = 2.7E(4) * e^{-20.7*R_b+6.5*R_p-19*R_b*R_p+261.5*R_b^2-1067.7*R_b^3} * e^{0.1*V_0+1.2*R_b*V_0-1.3*R_p*V_0} * \varepsilon_0^{0.18}$	0.73	49

Table 5.14 Comparison of fatigue lives between predicted and measured results of regression models using softer binder (PG52-28) with 30% RAP L at 5°C and 20°C (ambient rubber)

			Measured	Strain Dependent Predictive Model				Energy Dependent Predictive Model			
			Fatigue life	Traditional		Specific		Traditional		Specific	
5ºC	R_b (%)	R_P (%)	N_f	VFA	Air Void	VFA	Air Void	VFA	Air Void	VFA	Air Void
Ambient	0.00	0.30	23785	10601	20271	21349	18003	14888	19838	34756	21284
	0.05	0.30	29144	8319	20472	15197	12738	12858	20049	21938	14327
	0.10	0.30	20436	7044	19415	11322	17358	12681	19677	12460	25481
	0.15	0.30	40299	4138	15770	1321	10076	11699	21030	1546	31832
20ºC											
Ambient	0.00	0.30	22518	16469	14937	45749	38075	8380	14873	89694	8368
	0.05	0.30	20159	13061	22872	45029	18503	6554	18254	87136	7043
	0.10	0.30	21383	6935	14435	21624	3295	9682	17780	77405	11385
	0.15	0.30	24335	8916	21664	45945	8786	6736	20182	23893	10568

Artificial Neural Network Fatigue Prediction Model

Training an artificial neural network to approximate a highly-nonlinear relationship for predicting the occurrence of pavement fatigue is a new method that has not be broadly used in asphalt pavement technology. Although this analysis method is generally used for predicting the liquefaction/non-liquefaction by various researchers (Agrawal et al. 1995; Goh 1994; Juang and Chen 1999), it is still likely to be used in predicting the fatigue life of asphalt pavements. In this study, a three-layer, feed-forward network topology is used, as shown in Figure 2.3. This network is trained and tested with the database of 16 case records, including 2 to 4 replicated samples of each case, to approximate the following function:

$$N_f = f(R_b, R_p, p_1, p_2, p_3, VFA \text{ or } V_0, p_4, p_5, S_0, \varepsilon_0)$$
$$or \quad N_f = f(R_b, R_p, p_1, p_2, p_3, VFA \text{ or } V_0, p_4, p_5, w_0) \tag{5-14}$$

Where,

N_f = fatigue life (strain dependent or dissipated energy method);
VFA = the voids filled with the asphalt binder;
V_0 = the percentage of air void;
ε = tensile strain;
S = flexural stiffness;
R_b = the percentage of rubber in the binder;
R_p = the percentage of RAP in the mixture; and
$P_1 = R_b * R_p$; $P_2 = R_b^2$; $P_3 = R_b^3$; $P_4 = R_b *$ VFA or V_0; $P_5 = R_p *$ VFA or V_0

The ten variables in Equation 5-14 are simplified in a rearrangement of the ten basic input variables of each record in the database. Among the 16 case records in the database, 11 records were used as the training data set, and other 5 cases were used as the

testing set. Roughly two thirds of the entire database was selected for training and the other one third was selected for testing (Chen 1999). The network is first trained using the training data subset. The objective of the network training is to map the input to the output by determining the connection weights and biases through an error reduction process. For the three-layer network shown in Figure 2.3, the output of the network is calculated using Equation 2-13.

The number of hidden neurons is determined through a trial-and-error process; normally, the smallest number of neurons that yields satisfactory results (judged by the network performance) should be used. Note that all input variables are scaled into values in the range of 0.1 to 0.9, as is normally done in neural network training. Scaling of a variable X is carried out with the following equation (Juang and Chen 1999):

$$X_s = (X + a)/b \tag{5-15}$$

Where,

X_s = Scaled variables;

$a = (X_{max}\text{-}9X_{min})/8$;

$b = (X_{max}\text{-}X_{min})/0.8$; and

X_{max} and X_{min} are the maximum and minimum valuesof X in the database, respectively.

This scaling Equation 5-15 is employed to scale all ten variables. The transfer function adopted in this study is a sigmoidal logistic function shown in Equation 2-12. The Levenberg-Marquart algorithm (Demuth and Beale 1998) is adopted for its efficiency in training networks. The connection weights and biases are determined by

gradually reducing the root mean square of errors in the predictions to within an error goal of 0.005.

The weights and biases of the trained network for strain dependent method are shown in Tables 5.15 and 5.16. Sixteen case records, each one including four repeated testing data, are used to develop the ANN models, 11 case records of them are employed for the training data set, and the other 5 case records are tested against the data in the testing subset. The overall success rate of the developed network in predicting the occurrence of fatigue behavior for mixtures containing ambient rubberized tested at 5^{o}C are 97% and 95% for specific VFA and air void strain dependent methods, respectively. At 20^{o}C, these values of success rate are the same as those at 5^{o}C, as shown in Table 5.15. However, when using cryogenic rubber at 5^{o}C, the overall success rate of the ANN models were 91% and 84% for two types of methods, respectively, and at 20^{o}C these values increased to 92% and 97%, as shown in Table 5.16. The measured and predicted fatigue lives using ANN models and strain dependent method are presented in Figures 5.16 to 5.19.

Tables 5.17 and 5.18 show the weights and biases of the trained network for energy dependent method. Only 9 input variables are used to develop the ANN model. As shown in Tables 5.17 and 5.18, the overall success rate of fatigue predictive ANN models are greater than 86% regardless of the rubber types, analysis method (VFA or air void) and testing temperature. Figures 5.20 and 5.23 provide the measured and predicted fatigue values. Similar to the conventional regression model, the fatigue lives of mixtures used softer binder from ANN model are shown in Table 5.19.

These results, either from strain dependent or dissipated energy method, show that the developed ANN models, represented by Equation 2-13 and the associated coefficients presented in Tables 5.15 through 5.18, serve the intended purpose well. That is, the model is able to predict accurately fatigue life of the modified mixture.

Validation of Fatigue Predictive Models

The basic mathematic fatigue predictive models, obtained from the laboratory testing data through conventional regression and ANN analysis method with traditionally empirical strain dependent and energy dependent models, are presented in previous paragraphs. The calibration of these models is required to utilize the developed system with other type of sources to perform fatigue testing when the coefficients of the equation for different sources are not widely known. So it is necessary to calibrate these predictive models through analyzing the other available fatigue data.

In this study, a second aggregate source L is utilized to calibrate these fatigue predictive models. In order to simplify the fatigue testing, only seven mixtures were tested with the second aggregate source. Ambient rubber in 0% and 10% were used in fabricating the four repeated fatigue beams. The measured and predicted results drawn from the regression models at 5^{o}C and 20^{o}C are shown in Figures 5.24 and 5.25, respectively, while Figures 5.26 and 5.27 present the measured and predicted results draw from ANN models at 5^{o}C and 20^{o}C, respectively. From Figures 5.24 to 5.27, it can be seen that the measured and predicted values are significantly different. In other words, the predictive models could not be directly utilized to predict fatigue life of the mixture where a second aggregate source was used prior to modification.

Past research indicated that the addition of RAP increase the variability of the test results regardless of at low or intermediate temperatures (Sondag et al. 2002; FHWA1997a). Solaimanian and Tahmoressi (1996) also found that as RAP content increased, the variability in asphalt content, gradation, and air voids also increased. This was also observed in this study. The increase in variability with the addition of RAP is most likely due to the variability of the RAP itself. Because RAP is removed from an old roadway, it may include the original pavement materials, plus patches, chip seals, and other maintenance treatments. Base, intermediate, and surface courses from the old roadway may all be mixed together in the RAP. In addition, RAP from several projects may be mixed in a single stockpile. Mixed stockpiles may also include materials from private work that may not have been built to the same standards. Furthermore, the collection process of RAP from different locations leads inevitably to more variability. It is worth mentioning that it was very difficult to obtain consistent engineering properties using the RAP as the virgin material, even when the asphalt content was held constant during the compaction of the test samples. Especially, as using the second RAP, the variability of modified mixture shows a more significant increase.

The presence of crumb rubber also increases the complicated level of the variability of mixture, which makes the fatigue life prediction difficult specially when testing only limited numbers of repeated specimens are used for testing. A large number of repeated samples from each mixture should be compacted and tested. This should help to reduce the variability and make the data more reliable, especially in establishing the effectiveness of the predictive models.

N_f is the expected pavement fatigue life, which is representative of the actual applied traffic loading. It is a function of the total traffic ESALs summed over the entire pavement design life. However, with respect to the effect of variability during calibrating process, fatigue life prediction can be expressed by Equation 5-16.

$$N_f(final) = M * N_f(initial) \quad (5\text{-}16)$$

Where,

$N_f(final)$ = calibrated fatigue lives of models;

$N_f(initial)$ = calculated fatigue lives of models; and

M = reliability multiplier (for RAP and rubber variability)

During laboratory fatigue data analysis process, M value is dependent on RAP and rubber variability and also associated with aggregate sources.

N_f is the design HMA mixture fatigue resistance that was statistically determined as a function of the design and the laboratory determined empirical fatigue equations. While N_f represents laboratory fatigue life, the final field fatigue life for this approach in this study was obtained as expressed by Equation 5-17.

$$N_f(field) = \frac{SF * N_f(final)}{TF} \quad (5\text{-}17)$$

Where,

$N_f(field)$ = fatigue life in the field;

$N_f(final)$ = calibrated fatigue life of all models;

SF = shift factor; and

TF = temperature conversion factor

Previous research indicated that the shift factor is a result of such factors as traffic wander, crack propagation rate, construction variability, different frequencies of loading, etc., highway pavements have been found to sustain from less than 10 to perhaps as many

as 100 times the number of load applications that are estimated by procedures similar to those used herein before pavements become seriously distressed (Deacon et al. 1994; Kim et al. 2003). As a result, laboratory estimates of fatigue life can be compared with service estimates of ESALs only after applying a suitable shift factor. Using AASHTO design guidelines as a basis, SHRP A-003A studies led to the recommendation of shift factors ranging from 10 to 14 depending on the amount of surface cracking considered to be tolerable (Deacon et al. 1994). The most accurate way to develop shift factors is probably by observing the fatigue performance of full-scale pavements in test tracks or in accelerated pavement loading experiments. Determination of these parameters generally requires local calibration to field conditions, which was beyond the scope of this study.

Table 5.15 Connection weights and biases of ANN model defined in Equation 2-13

(specific strain dependent method for ambient rubber)

	Hidden	Weight											Bias	
		W_{ik} (Input Variables)										W_k	B_k	B_o
5^oC	neuron	1	2	3	4	5	6	7	8	9	10	Output	Hidden Layer	Output Layer
VFA R^2=0.97	1	-2.925	-5.434	-2.059	2.048	2.177	-1.078	-7.008	0.783	0.250	0.350	-3.837	8.508	4.067
	2	3.778	2.238	3.934	3.400	3.496	3.166	-0.516	-1.497	2.099	3.671	2.812	-9.714	
	3	0.218	1.568	3.622	-0.129	-5.613	1.707	2.257	2.871	3.637	-3.836	-4.379	-2.960	
	4	-2.584	-4.476	0.229	2.490	4.026	-1.501	-1.663	2.337	-3.444	-0.368	-4.172	-1.944	
Air Voids R^2=0.95	1	-1.801	3.769	2.434	-4.074	-1.826	-5.441	3.483	1.801	2.218	-0.364	-1.826	3.118	1.559
	2	3.337	-1.398	-2.451	-2.010	1.020	-0.805	-2.913	-3.831	-3.104	0.368	1.923	5.457	
	3	0.489	-0.363	-2.371	-0.304	-1.431	-0.221	-1.107	-4.007	-1.070	-6.857	-3.856	7.442	
	4	-0.084	4.239	2.377	1.640	-4.917	-2.808	2.189	-2.146	1.886	-2.124	3.063	-3.418	
20^oC														
VFA R^2=0.97	1	-2.258	-3.126	-1.167	2.527	-1.756	3.087	-2.511	-2.950	-1.002	1.431	-0.710	10.678	-6.557
	2	-2.430	2.601	-3.342	2.095	4.340	-1.673	3.735	-1.105	1.891	3.324	3.235	-3.537	
	3	0.071	-5.937	1.762	0.729	3.116	0.045	-5.613	4.698	-3.091	6.293	7.194	-3.598	
	4	-1.420	-1.817	-4.479	0.334	-5.405	3.237	2.215	3.909	0.228	4.600	5.253	-0.688	
Air Voids R^2=0.95	1	-1.632	-2.254	-0.309	3.164	-1.111	3.096	-1.193	-2.113	0.258	1.774	1.333	11.364	-0.947
	2	0.293	3.440	-0.850	4.365	5.552	2.655	-0.104	-0.881	0.913	-1.023	0.088	-2.512	
	3	-3.292	-1.799	3.786	-4.159	-2.565	5.789	2.957	3.776	3.263	0.774	-3.911	-2.328	
	4	-3.207	-2.890	-3.432	1.267	-2.977	6.080	0.964	3.231	0.801	4.472	4.060	-2.433	

Table 5.16 Connection weights and biases of ANN model defined in Equation 2-13

(specific strain dependent method for cryogenic rubber)

	Hidden	Weight											Bias	
		W_{ik} (Input Variables)										W_k	B_k	B_o
5^oC	neuron	1	2	3	4	5	6	7	8	9	10	Output	Hidden Layer	Output Layer
VFA R^2=0.91	1	-2.151	-1.827	-4.803	3.076	2.370	-4.542	-3.402	3.822	-2.305	3.652	5.478	8.389	-3.225
	2	1.647	4.363	1.029	3.361	4.178	-1.261	5.715	2.574	-1.068	-0.499	-6.597	-11.996	
	3	3.346	-2.808	-0.673	-1.393	-3.318	-3.495	-3.240	0.547	-4.716	-0.839	-5.081	9.703	
	4	3.972	-2.726	1.065	-2.965	4.864	-0.165	3.665	-0.900	-2.072	-0.945	5.506	-0.329	
Air Voids R^2=0.84	1	-6.997	-0.085	1.903	-3.036	-10.068	-2.496	8.947	5.690	13.290	-5.861	3.995	7.011	-3.325
	2	-3.313	-5.394	-4.678	4.724	2.154	5.525	-3.528	-4.450	-6.734	-2.037	6.607	0.250	
	3	-0.937	3.652	1.118	-1.696	5.275	-0.240	-4.450	0.579	-1.441	5.367	3.425	-1.521	
	4	6.487	-4.834	4.218	1.115	7.208	0.786	5.931	4.703	-0.306	-6.258	-3.586	1.221	
20^oC														
VFA R^2=0.92	1	-2.510	-2.950	-6.189	0.740	-1.177	-2.953	-4.031	3.862	-3.112	8.852	4.395	4.980	-4.103
	2	2.458	2.851	0.314	3.773	4.292	-3.109	-0.182	2.729	-2.974	1.017	-2.608	-9.984	
	3	2.399	-0.266	0.092	-1.902	-3.471	-2.444	-2.823	-0.548	-2.449	-0.771	-0.636	12.078	
	4	3.525	0.656	1.154	-4.094	3.874	0.858	2.691	-1.155	0.883	-3.300	4.620	-1.520	
Air Voids R^2=0.97	1	-6.472	0.968	-5.004	-5.665	1.058	-0.531	-1.429	-1.685	4.149	5.205	4.829	-2.126	3.618
	2	0.589	-1.694	-2.875	1.870	-0.794	-0.310	0.731	-2.301	6.448	2.075	-7.221	-2.044	
	3	6.053	-0.885	4.383	3.027	-1.060	0.413	-1.170	-2.670	2.019	2.817	-0.296	1.642	
	4	-1.915	-0.431	-4.447	0.261	-2.920	-1.874	2.509	1.103	-5.156	-1.091	1.716	-1.718	

Table 5.17 Connection weights and biases of ANN model defined in Equation 2-13

(specific energy dependent method for ambient rubber)

	Hidden	Weight										Bias	
		W_{ik} (Input Variables)									W_k	B_k	B_o
5^oC	neuron	1	2	3	4	5	6	7	8	9	Output	Hidden Layer	Output Layer
VFA R^2=0.94	1	0.068	3.508	0.132	-0.951	3.570	2.851	-2.947	-0.719	-4.606	2.268	7.281	4.169
	2	-5.848	1.720	-0.279	5.714	4.846	-9.356	-7.355	-2.472	-1.138	-6.569	10.061	
	3	8.197	10.585	-2.768	3.523	-0.058	-5.432	5.782	5.612	-13.904	-5.387	-0.674	
	4	-3.154	6.450	2.190	-2.066	1.865	-0.281	2.427	-0.584	-5.017	5.555	-1.275	
Air Voids R^2=0.93	1	-2.051	-5.147	-1.833	0.858	-1.261	-1.553	-1.232	-3.238	-7.273	3.456	12.499	-10.714
	2	-4.374	0.946	4.944	4.133	-0.260	3.034	-0.064	2.215	5.764	3.675	-4.531	
	3	-2.356	2.109	-5.007	-0.717	2.393	-3.327	-0.413	0.181	3.861	0.082	1.186	
	4	-2.621	-5.684	0.051	3.265	8.573	2.296	2.990	1.416	-2.215	6.853	2.266	
20^oC													
VFA R^2=0.92	1	1.887	0.933	-3.835	1.874	-4.457	-1.811	1.050	2.825	3.212	-2.804	-6.361	-5.662
	2	-3.940	-3.388	-3.429	4.313	1.403	3.505	-3.078	-6.339	-0.284	2.707	3.366	
	3	-3.038	-1.166	-1.738	3.996	3.911	-1.294	-2.411	-5.519	1.882	-3.786	0.336	
	4	4.729	-1.807	-2.613	0.812	0.219	-0.421	0.862	0.253	12.605	6.384	-3.548	
Air Voids R^2=0.90	1	4.847	0.288	5.511	2.016	-0.779	-1.335	-1.904	2.530	-4.656	-4.596	-2.404	2.058
	2	4.115	-1.403	-2.781	3.122	-0.584	-9.131	2.874	-0.369	7.176	2.562	-2.042	
	3	1.206	-8.253	-0.951	-1.170	1.950	-4.973	-0.702	-7.083	5.400	3.764	6.547	
	4	-2.028	-2.466	0.118	2.909	1.022	-2.146	-5.372	-3.190	4.001	-6.894	2.607	

Table 5.18 Connection weights and biases of ANN model defined in Equation 2-13

(specific energy dependent method for cryogenic rubber)

	Hidden	Weight										Bias	
		W_{ik} (Input Variables)									W_k	B_k	B_o
5^oC	neuron	1	2	3	4	5	6	7	8	9	Output	Hidden Layer	Output Layer
VFA R^2=0.89	1	0.812	5.905	-0.071	-6.454	-5.752	-4.463	3.299	3.032	-3.633	-6.873	0.905	10.507
	2	3.022	-8.723	-3.422	2.053	-3.600	3.491	-4.031	-4.296	3.615	-7.798	8.462	
	3	-1.860	1.511	4.975	2.830	3.968	4.843	2.693	3.547	-2.762	-9.756	-12.852	
	4	-0.411	-3.088	2.953	4.245	3.070	-3.823	-2.974	-0.448	1.855	-5.144	-4.399	
Air Voids R^2=0.86	1	0.211	-9.264	1.544	-4.969	-2.286	-0.373	-5.083	-1.613	7.374	2.800	1.013	-3.897
	2	-0.386	-2.068	3.096	-2.957	7.948	0.707	1.644	5.591	8.321	-7.334	-11.068	
	3	0.221	8.820	-6.001	3.546	7.521	-4.471	-1.099	1.589	6.841	5.044	-3.042	
	4	0.217	1.630	3.917	4.562	-1.368	0.569	6.255	-0.307	2.554	6.609	-12.556	
20^oC													
VFA R^2=0.92	1	-5.506	-4.995	-7.335	-0.917	8.519	3.088	-2.504	-6.913	7.308	4.549	9.472	-7.034
	2	-7.447	3.083	1.339	-1.221	-1.198	9.298	-3.573	-0.094	0.866	5.515	-5.595	
	3	-4.918	-4.865	2.455	-4.158	2.272	7.851	-4.540	-1.855	-2.216	-5.244	2.017	
	4	7.741	-7.647	9.945	0.493	-13.721	9.359	6.571	-2.840	-5.873	4.830	1.071	
Air Voids R^2=0.93	1	-0.102	3.182	0.223	1.609	6.234	-0.191	-3.348	0.999	-9.850	11.005	3.870	0.640
	2	1.621	2.372	4.035	5.901	0.023	-2.770	-0.015	-0.091	-8.231	-11.534	0.211	
	3	-2.325	8.846	-4.159	-2.652	-3.609	7.476	-3.101	4.776	-4.354	-7.407	-5.076	
	4	-4.906	2.480	0.969	-1.205	3.590	1.052	0.783	-4.406	-0.734	1.239	-2.971	

Table 5.19 Comparison of fatigue lives between predicted and measured results of ANN model using soft binder (PG52-28) with 30% RAP L at 5°C and 20°C (ambient rubber)

			Measured	Predicted			
			Fatigue life	Strain Dependent		Energy Dependent	
5ºC	R_b (%)	R_P (%)	N_f	VFA	Air Void	VFA	Air Void
Ambient	0.00	0.30	23785	10022	12279	18623	18910
	0.05	0.30	29144	11203	10817	14047	8914
	0.10	0.30	20436	12719	11584	14971	18096
	0.15	0.30	40299	12241	9959	22692	29887
20ºC Ambient	0.00	0.30	22518	24531	28393	8805	22584
	0.05	0.30	20159	9085	18819	8812	11078
	0.10	0.30	21383	8754	9604	12023	10650
	0.15	0.30	24335	27776	10298	10105	10660

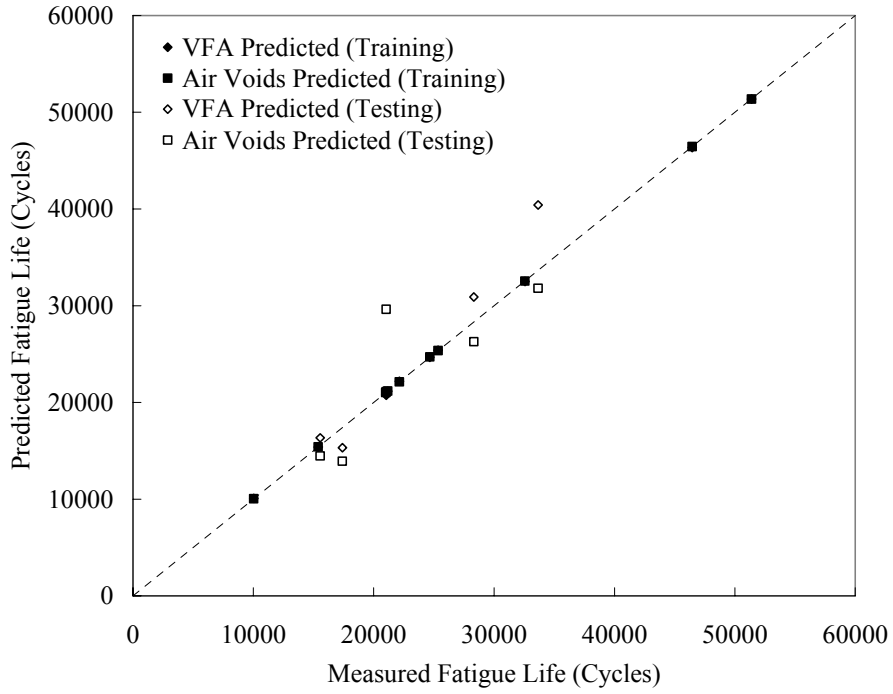

Figure 5.16 Performance of ANN modes used specific strain dependent method for ambient rubber at 5^{o}C

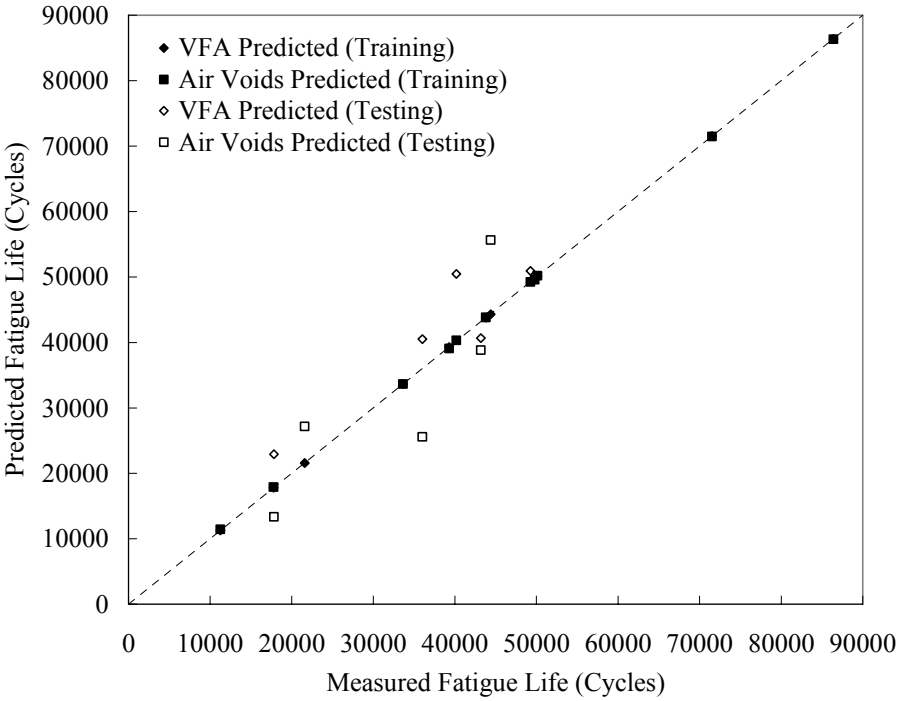

Figure 5.17 Performance of ANN modes used specific strain dependent method for ambient rubber at 20^{o}C

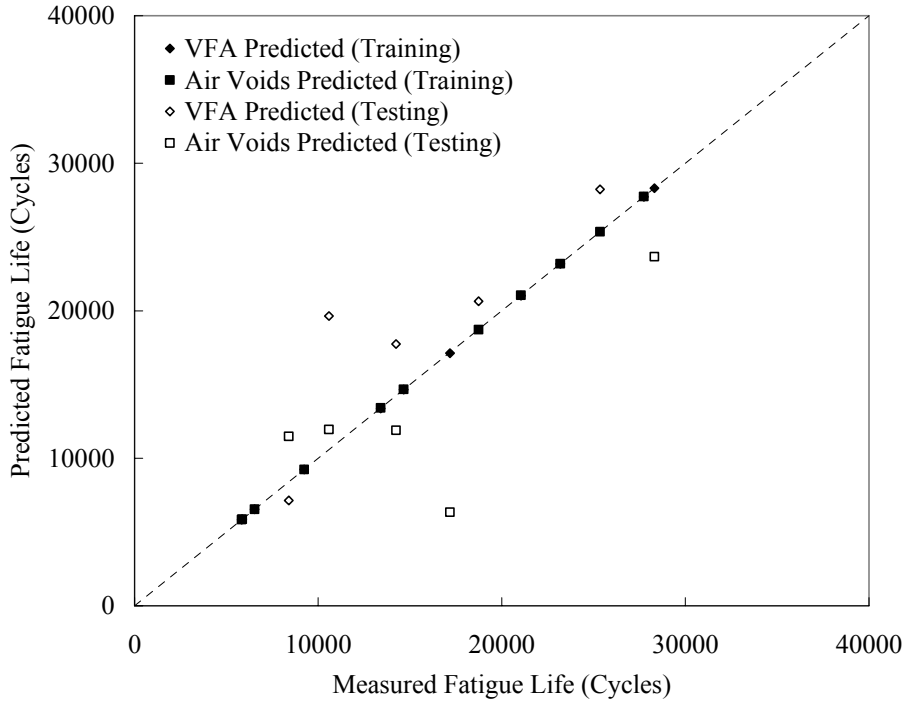

Figure 5.18 Performance of ANN modes used specific strain dependent method for cryogenic rubber at 5^{o}C

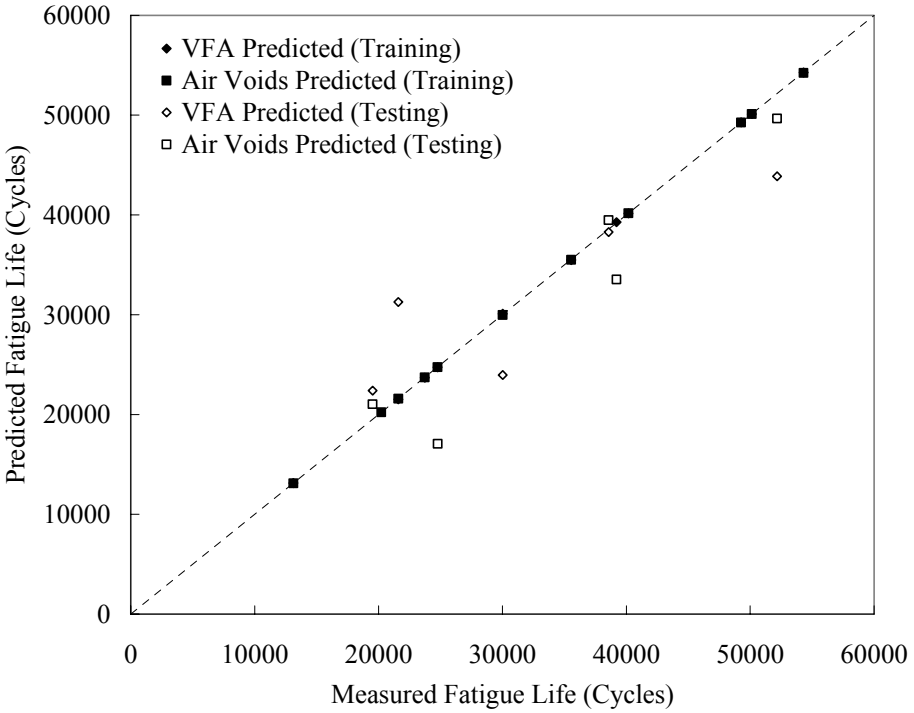

Figure 5.19 Performance of ANN modes used specific strain dependent method for cryogenic rubber at 20^{o}C

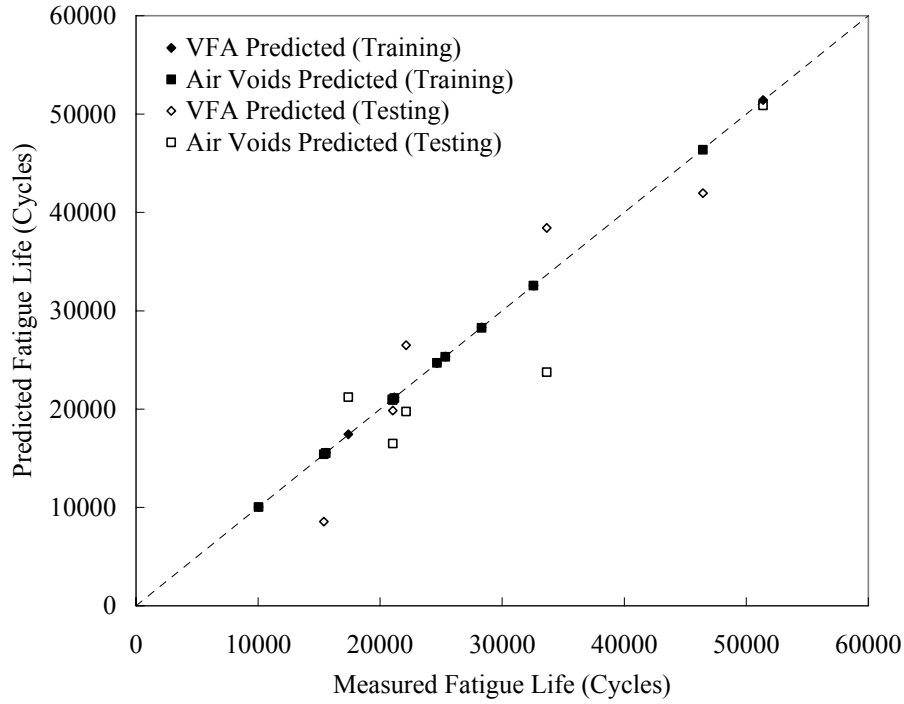

Figure 5.20 Performance of ANN modes used specific energy dependent method for ambient rubber at 5^{o}C

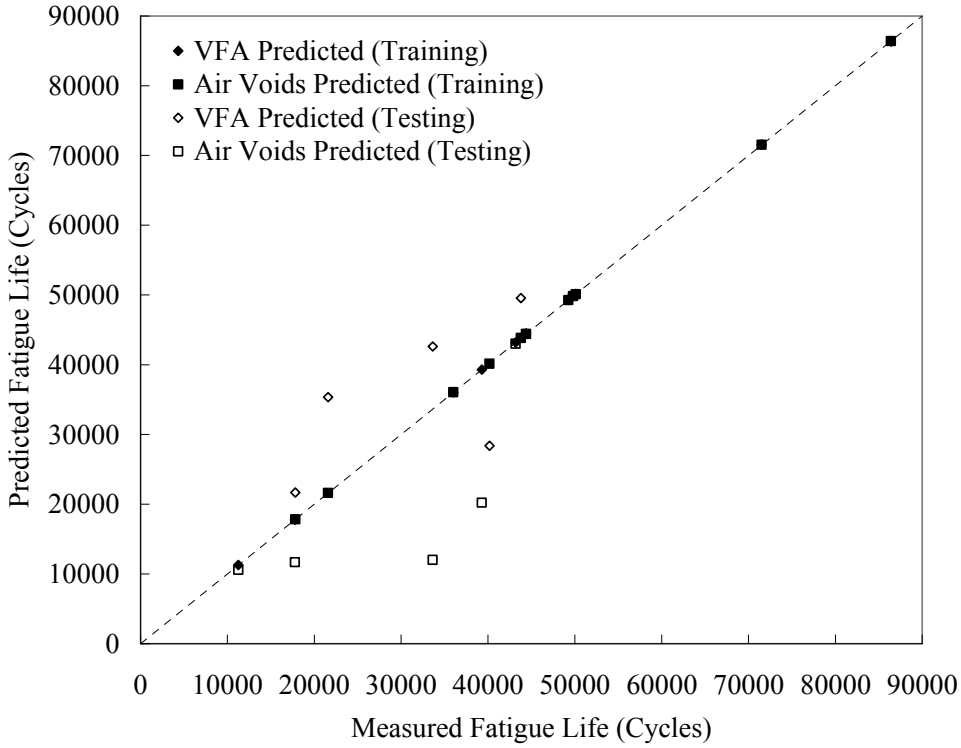

Figure 5.21 Performance of ANN modes used specific energy dependent method for ambient rubber at 20^{o}C

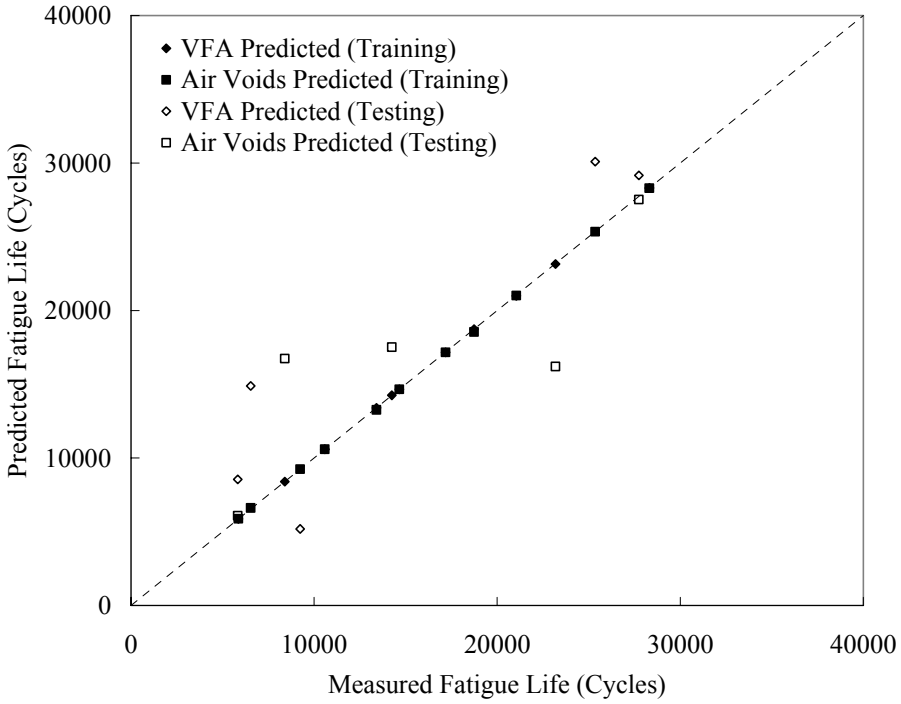

Figure 5.22 Performance of ANN modes used specific energy dependent method for cryogenic rubber at 5^{o}C

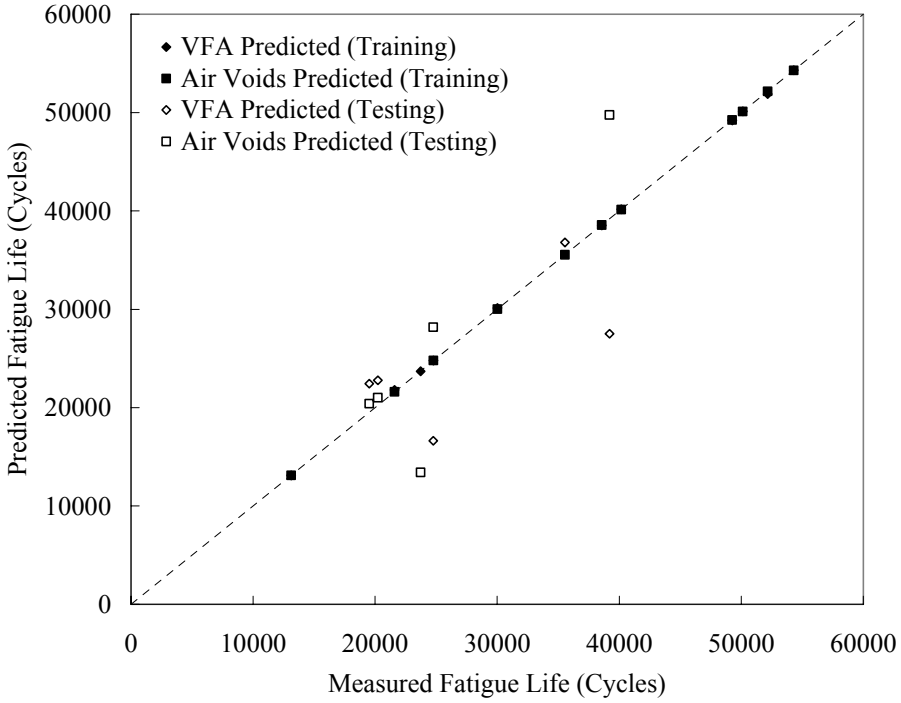

Figure 5.23 Performance of ANN modes used specific energy dependent method for cryogenic rubber at 20^{o}C

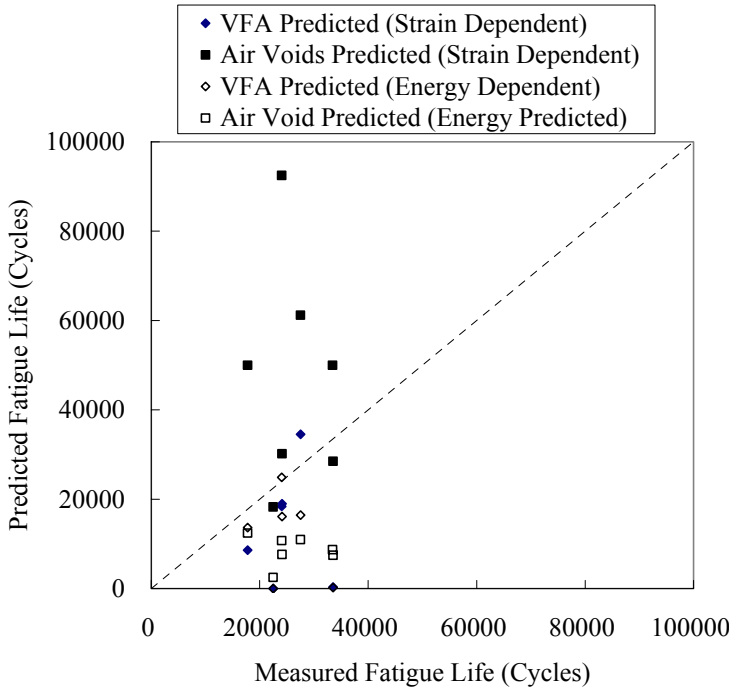

Figure 5.24 Comparison of fatigue lives between predicted and measured results used second aggregate source at 5°C (regression models)

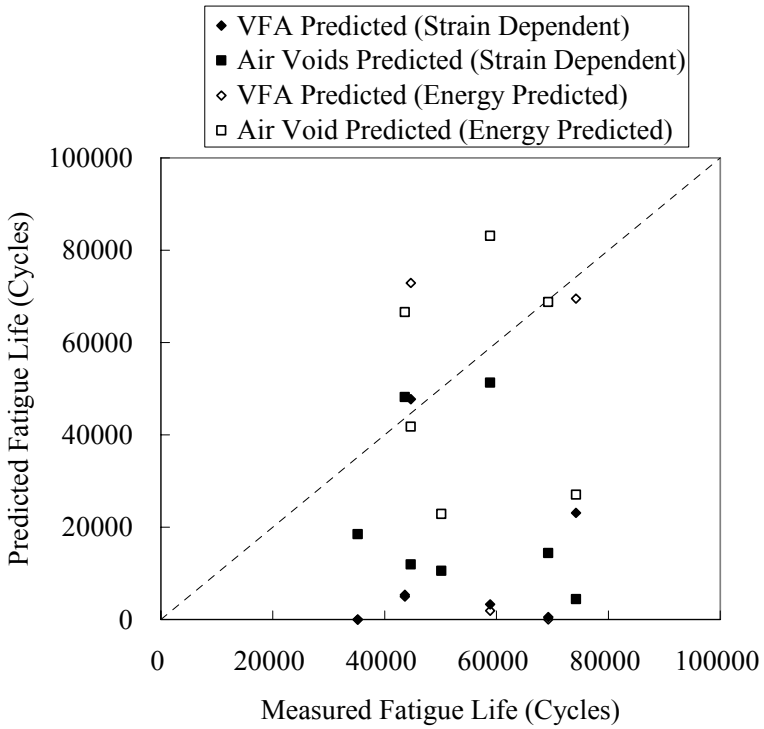

Figure 5.25 Comparison of fatigue lives between predicted and measured results used second aggregate source at 20°C (regression models)

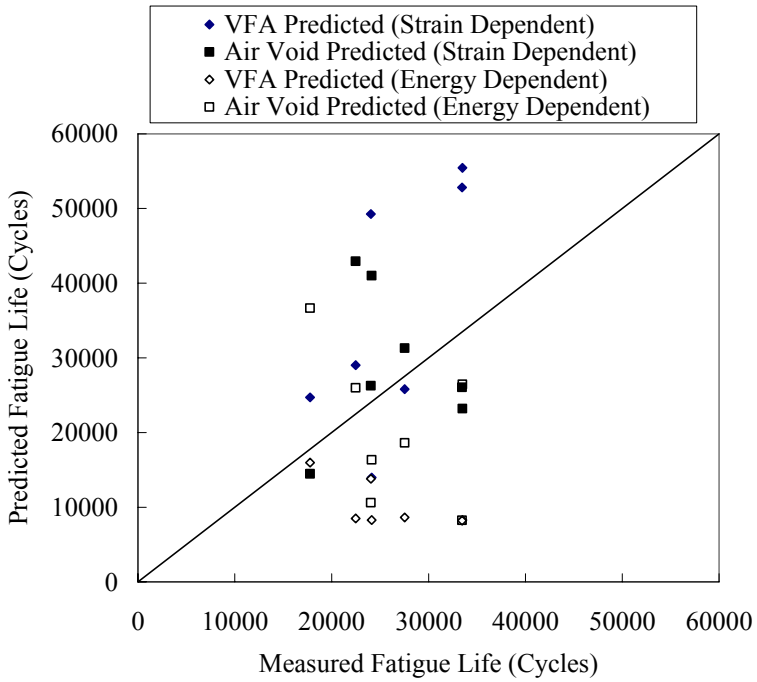

Figure 5.26 Comparison of fatigue lives between predicted and measured results used second aggregate source at 5°C (ANN models)

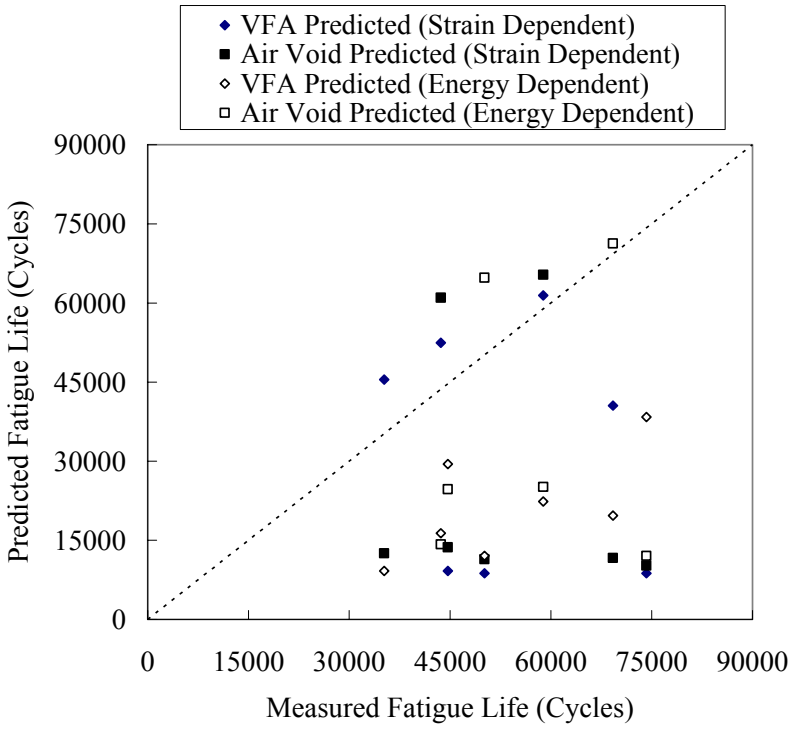

Figure 5.27 Comparison of fatigue lives between predicted and measured results used second aggregate source at 20°C (ANN models)

CHAPTER VI
SUMMARY, CONCLUSIONS, AND RECOMMEDATIONS

Summary

Fatigue behavior of asphalt mixtures is considered to be one of the most significant distress modes in a pavement that is subjected to repeated traffic loading or stress. With respect to the complexity of an asphalt mixture, fatigue is related to the properties of aggregate, asphalt, and asphalt aggregate interaction. For the last two decades, some fatigue predictive models have been developed to predict the fatigue life of asphalt mixtures in the laboratory and even in the field. They are broadly being employed in research and industry area.

The recycled material, such as crumb rubber and reclaimed asphalt pavement, are used in new HMA mixtures in order to protect the environment, save energy and money. The fatigue study of the modified HMA is helpful in understanding many factors affecting the new mixtures. Although modeling the modified HMA fatigue life has not previously been accomplished, the past fatigue predictive models and sophisticated analysis methods were utilized to make this fatigue study possible.

For this study, one aggregate source, two asphalt grades, one rubber size, two types of rubber, and one type of RAP were used to develop the predictive models. A second aggregate source was utilized to validate the model of modified mixtures. A total of 39 mix designs were accomplished to perform fatigue testing and modeling.

Superpave mix design was used for preparation of fatigue testing specimens. The related property testing of modified asphalt binders and mixtures such as, viscosity,

dynamic shear rheometer (DSR), and indirect tensile strength (ITS) were accomplished prior to beam fabrication, which includes two or four repeated beam specimens at each testing temperature (5^{o}C or 20^{o}C).

The conventional GLM analysis method used in previous fatigue predictive models was also employed in predicting the fatigue life of mixtures in this study. The regression analysis were performed in accordance with strain dependent or dissipated energy dependent method based on traditional or specific variables for various mixture types. Conventional statistical analysis was utilized to verify the effectiveness of the models.

Artificial Neural Network (ANN) modeling is the second analysis method that was used to develop the fatigue predictive model in this study. Although, in most cases, the ANN model is only employed in geotechnical data analysis in Civil Engineering field, it is still likely to become an important tool to predict fatigue life of asphalt mixtures.

Additionally, validation and calibration of models are necessary and helpful in expanding the use range, in the laboratory or the field, of fatigue model in various areas. The model modification was performed by using a second aggregate source.

Conclusions

The following conclusions were reached based on the experimental data and in accordance with the related fatigue life properties of the mixtures, including asphalt modified binders and mixtures:

- Viscosity of modified binder increases as the percentage of crumb rubber and RAP content increase regardless of the types of rubber and RAP. The use of

softer binder significantly decreases the viscosity value when using a high percentage RAP.

- The G*sinδ value increases as the RAP increases, and the occurrence of crumb rubber is helpful in reducing G*sinδ value during a long term aging regardless of the types of rubber and RAP.
- The mixing and compacting temperatures increase due to the occurrence of crumb rubber and RAP, and the lager percentage of crumb rubber and RAP content result in a higher temperature.
- According to Superpave mix design, the use of RAP benefits in decreasing the virgin asphalt binder content, while the use of crumb rubber would be able to increase the optimum binder content. Although the crumb rubber is able to reduce the bond of binder and aggregate and result in a decrease of ITS value, the additional use of RAP in the mixture is beneficial in improving this bond.

The fatigue predictive model of mixture, including strain and energy dependent method used conventional regression and ANN model, is summarized as follows:

- The traditional regression model is not able to predict the fatigue life of modified mixture accurately, and additional independent variables are indispensably employed in developing fatigue predictive models.
- Specific regression model can predict the reasonable fatigue response of mixture, and measured and predicted fatigue values are close regardless of the crumb rubber, RAP content, and even testing conditions. In additional, statistical analysis shows that coefficient of determination value of model is large in strain dependent and dissipated energy dependent methods.

- ANN approach, as a new fatigue modeling method in this study, has been shown to be effective in performing fatigue testing data of mixture. The established ANN model is able to predicting fatigue occurrence accurately. Moreover, it produces an overall success rate of larger than 84%, and, in most cases, this values is larger than 90% in predicting fatigue life. It is more effective than the conventional regression model.
- The validation and calibration are proved possible after the reliability multiple and shift factor are employed in modifying the fatigue models due to the use of a second aggregate source.

Recommendations

The methodology for fatigue life evaluation developed in the present study may be applied to the study of other similar conditions. On the other hand, the methods established in this study need further validation, calibration, and improvement. The recommendations for further study are summarized below:

- Evaluating a larger number of repeated testing specimens for each mixture and increasing the designed number of crumb rubber and RAP contents are effective in order to improve the precision of fatigue predictive models.
- Increasing the types of aggregate and RAP source and diminishing the variability of RAP will warrant for further validation of the established models.
- Collecting the field data and building the experimental pavement in the field are very beneficial in accurately calibrating the shift factor of fatigue models from the laboratory to the field.

- Developing simplified models for predicting fatigue life of mixture is attractive for most practicing engineers. Whereas these fatigue predictive models provide an accurate estimate of fatigue life, they are by no means simply models.
- Comparing the cost of these recycled materials with virgin ones used in asphalt pavement associated with fatigue life will be a very interesting issue for engineers.

APPENDICES

Appendix A

Volumetric Properties of Superpave Mix Design

Table A.1 Volumetric properties of Superpave mix design with 0% rubber using aggregate source L

0%Rubber		Specific Gravity		% AC by Vol.	Air Voids	VMA	% VFM
		Bulk	Rice				
0%RAP	4.5	2.342	2.483	10.2	5.7	15.9	64.3
	5.0	2.327	2.465	11.3	5.6	16.8	66.9
	5.5	2.349	2.447	12.5	4.0	16.5	75.8
	6.0	2.373	2.429	13.8	2.3	16.1	85.6
	O.A.C. (5.40)	**2.352**	**2.450**	**12.2**	**4.1**	**16.7**	**73.5**
15%RAP	4.5	2.323	2.487	10.1	6.6	16.7	60.5
	5.0	2.347	2.469	11.4	4.9	16.3	69.7
	5.5	2.375	2.451	12.6	3.1	15.7	80.3
	6.0	2.393	2.434	13.9	1.7	15.6	89.2
	O.A.C. (5.25)	**2.362**	**2.460**	**11.8**	**4.0**	**17.4**	**68.0**
25%RAP	4.5	2.362	2.460	10.3	4.0	14.3	72.0
	5.0	2.367	2.443	11.5	3.1	14.6	78.9
	5.5	2.393	2.425	12.7	1.3	14.1	90.5
	6.0	2.393	2.408	13.9	0.6	14.5	95.8
	O.A.C. (4.70)	**2.368**	**2.453**	**10.7**	**3.9**	**14.5**	**74.3**
30%RAP	4.5	2.360	2.485	10.3	5.0	15.3	67.1
	5.0	2.380	2.467	11.5	3.5	15.1	76.5
	5.5	2.402	2.449	12.8	1.9	14.7	87.0
	6.0	2.423	2.432	14.1	0.4	14.4	97.6
	O.A.C. (4.82)	**2.373**	**2.474**	**11.0**	**4.1**	**15.6**	**70.6**

Table A.2 Volumetric properties of Superpave mix design with 5% ambient rubber (-40mesh) using aggregate source L

5%40m Ambient		Specific Gravity		% AC by Vol.	Air Voids	VMA	% VFM
		Bulk	Rice				
0%RAP	4.5	2.294	2.473	10.0	7.3	17.2	57.9
	5.0	2.302	2.455	11.1	6.3	17.4	64.0
	5.5	2.331	2.438	12.4	4.4	16.8	73.9
	6.0	2.356	2.420	13.7	2.7	16.3	83.7
	O.A.C. (5.60)	**2.337**	**2.434**	**12.4**	**4.0**	**18.2**	**68.3**
15%RAP	4.5	2.318	2.487	10.1	6.8	16.9	59.8
	5.0	2.332	2.469	11.3	5.6	16.8	67.0
	5.5	2.354	2.451	12.5	3.9	16.5	76.1
	6.0	2.380	2.433	13.8	2.2	16.0	86.3
	O.A.C. (5.45)	**2.355**	**2.453**	**12.2**	**4.0**	**17.7**	**69.0**
25%RAP	4.5	2.344	2.468	10.2	5.0	15.2	67.1
	5.0	2.350	2.450	11.4	4.1	15.5	73.7
	5.5	2.350	2.432	12.5	3.4	15.9	78.7
	6.0	2.377	2.415	13.8	1.6	15.4	89.9
	O.A.C. (5.02)	**2.351**	**2.449**	**11.4**	**4.0**	**15.7**	**72.7**
30%RAP	4.5	2.352	2.491	10.2	5.6	15.8	64.7
	5.0	2.377	2.473	11.5	3.9	15.4	74.9
	5.5	2.397	2.455	12.8	2.4	15.1	84.4
	6.0	2.408	2.437	14.0	1.2	15.2	92.1
	O.A.C. (4.99)	**2.377**	**2.473**	**11.5**	**4.0**	**15.4**	**74.9**

Table A.3 Volumetric properties of Superpave mix design with 10% ambient rubber (-40mesh) using aggregate source L

10%40m Ambient		Specific Gravity		% AC by Vol.	Air Voids	VMA	% VFM
		Bulk	Rice				
0%RAP	4.5	2.256	2.467	9.8	8.5	18.4	53.5
	5.0	2.276	2.449	11.0	7.0	18.1	61.0
	5.5	2.311	2.431	12.3	4.9	17.2	71.4
	6.0	2.326	2.414	13.5	3.6	17.2	78.8
	O.A.C. (5.85)	**2.323**	**2.419**	**12.8**	**4.0**	**19.5**	**65.5**
15%RAP	4.5	2.300	2.473	10.0	7.0	17.0	59.0
	5.0	2.320	2.455	11.2	5.5	16.7	67.1
	5.5	2.325	2.437	12.4	4.6	17.0	73.0
	6.0	2.334	2.420	13.6	3.5	17.1	79.4
	O.A.C. (5.75)	**2.343**	**2.428**	**12.8**	**4.0**	**18.1**	**70.8**
25%RAP	4.5	2.323	2.449	10.1	5.1	15.2	66.4
	5.0	2.320	2.432	11.2	4.6	15.8	71.1
	5.5	2.345	2.414	12.5	2.9	15.3	81.4
	6.0	2.353	2.397	13.7	1.9	15.5	88.1
	O.A.C. (5.08)	**2.332**	**2.429**	**11.4**	**4.0**	**15.8**	**72.5**
30%RAP	4.5	2.333	2.484	10.2	6.1	16.2	62.6
	5.0	2.358	2.466	11.4	4.4	15.8	72.3
	5.5	2.379	2.448	12.7	2.8	15.5	81.8
	6.0	2.399	2.430	13.9	1.3	15.2	91.5
	O.A.C. (5.12)	**2.367**	**2.461**	**11.6**	**4.0**	**16.8**	**68.9**

Table A.4 Volumetric properties of Superpave mix design with 15% ambient rubber (-40mesh)using aggregate source L

15%40m Ambient		Specific Gravity		% AC by Vol.	Air Voids	VMA	% VFM
		Bulk	Rice				
0%RAP	4.5	2.216	2.463	9.7	10.0	19.7	49.2
	5.0	2.241	2.445	10.8	8.4	19.2	56.6
	5.5	2.277	2.428	12.1	6.2	18.3	66.2
	6.0	2.300	2.410	13.4	4.6	18.0	74.4
	O.A.C. (6.35)	**2.299**	**2.393**	**14.5**	**4.0**	**18.4**	**78.6**
15%RAP	4.5	2.253	2.471	9.8	8.8	18.6	52.8
	5.0	2.265	2.453	11.0	7.7	18.6	58.9
	5.5	2.298	2.436	12.2	5.6	17.9	68.5
	6.0	2.334	2.418	13.6	3.5	17.0	79.6
	O.A.C. (5.90)	**2.325**	**2.422**	**12.9**	**4.0**	**19.8**	**65.0**
25%RAP	4.5	2.302	2.462	10.0	6.5	16.5	60.9
	5.0	2.303	2.444	11.1	5.8	16.9	66.2
	5.5	2.309	2.427	12.3	4.8	17.1	71.8
	6.0	2.341	2.409	13.6	2.8	16.4	82.8
	O.A.C. (5.65)	**2.324**	**2.421**	**12.6**	**4.0**	**17.5**	**72.1**
30%RAP	4.5	2.328	2.482	10.1	6.2	16.3	62.1
	5.0	2.339	2.464	11.3	5.1	16.4	69.2
	5.5	2.369	2.446	12.6	3.2	15.8	80.0
	6.0	2.387	2.429	13.9	1.7	15.6	89.0
	O.A.C. (5.25)	**2.357**	**2.455**	**11.8**	**4.0**	**17.0**	**69.6**

Table A.5 Volumetric properties of Superpave mix design with 5% cryogenic rubber (-40mesh) using aggregate source L

5%40 m cryogenic		Specific Gravity		% AC by Vol.	Air Voids	VMA	% VFM
		Bulk	Rice				
0%RAP	4.5	2.294	2.462	10.0	6.8	16.8	59.4
	5.0	2.330	2.444	11.3	4.7	16.0	70.7
	5.5	2.353	2.427	12.5	3.1	15.6	80.4
	6.0	2.378	2.410	13.8	1.3	15.1	91.4
	O.A.C. (5.25)	**2.339**	**2.436**	**11.7**	**4.0**	**17.5**	**66.7**
15%RAP	4.5	2.312	2.469	10.1	6.4	16.5	61.2
	5.0	2.334	2.451	11.3	4.8	16.1	70.3
	5.5	2.352	2.434	12.5	3.4	15.9	78.7
	6.0	2.372	2.417	13.8	1.8	15.6	88.2
	O.A.C. (5.25)	**2.344**	**2.443**	**11.7**	**4.0**	**17.1**	**68.7**
25%RAP	4.5	2.344	2.484	10.2	5.6	15.8	64.5
	5.0	2.366	2.466	11.5	4.1	15.5	73.8
	5.5	2.386	2.448	12.7	2.5	15.2	83.3
	6.0	2.397	2.431	13.9	1.4	15.3	91.1
	O.A.C. (5.02)	**2.365**	**2.465**	**11.4**	**4.0**	**16.3**	**69.9**
30%RAP	4.5	2.363	2.484	10.3	4.9	15.2	67.9
	5.0	2.379	2.466	11.5	3.5	15.0	76.6
	5.5	2.398	2.448	12.8	2.0	14.8	86.3
	6.0	2.410	2.430	14.0	0.8	14.8	94.4
	O.A.C. (4.80)	**2.374**	**2.473**	**11.0**	**4.0**	**15.4**	**71.1**

Table A.6 Volumetric properties of Superpave mix design with 10% cryogenic rubber (-40mesh) using aggregate source L

10%40 m cryogenic		Specific Gravity		% AC by Vol.	Air Voids	VMA	% VFM
		Bulk	Rice				
0%RAP	4.5	2.247	2.452	9.8	8.4	18.2	53.9
	5.0	2.260	2.434	10.9	7.2	18.1	60.4
	5.5	2.261	2.417	12.0	6.4	18.5	65.1
	6.0	2.291	2.400	13.3	4.6	17.9	74.5
	O.A.C. (6.08)	**2.301**	**2.398**	**13.2**	**4.0**	**19.5**	**67.5**
15%RAP	4.5	2.268	2.461	9.9	7.9	17.7	55.7
	5.0	2.264	2.443	11.0	7.3	18.3	59.9
	5.5	2.284	2.426	12.2	5.8	18.0	67.5
	6.0	2.333	2.408	13.5	3.2	16.7	81.1
	O.A.C. (5.90)	**2.314**	**2.412**	**13.0**	**4.0**	**18.9**	**68.4**
25%RAP	4.5	2.319	2.456	10.1	5.6	15.7	64.3
	5.0	2.329	2.439	11.3	4.5	15.8	71.4
	5.5	2.339	2.421	12.5	3.4	15.9	78.5
	6.0	2.355	2.404	13.7	2.1	15.7	87.0
	O.A.C. (5.18)	**2.336**	**2.433**	**11.6**	**4.0**	**16.3**	**71.3**
30%RAP	4.5	2.336	2.472	10.2	5.5	15.7	64.9
	5.0	2.341	2.455	11.3	4.6	16.0	71.0
	5.5	2.358	2.437	12.6	3.2	15.8	79.4
	6.0	2.343	2.420	13.6	3.1	16.8	81.3
	O.A.C. (5.30)	**2.346**	**2.443**	**12.0**	**4.0**	**16.4**	**73.3**

Table A.7 Volumetric properties of Superpave mix design with 15% cryogenic rubber (-40mesh) using aggregate source L

15%40 m cryogenic		Specific Gravity		% AC by Vol.	Air Voids	VMA	% VFM
		Bulk	Rice				
0%RAP	5.0	2.260	2.442	10.9	7.5	18.4	59.6
	5.5	2.243	2.424	11.9	7.5	19.4	61.4
	6.0	2.292	2.407	13.3	4.8	18.1	73.8
	6.5	2.353	2.390	14.8	1.6	16.4	90.4
	O.A.C. (6.10)	**2.308**	**2.405**	**13.2**	**4.0**	**19.9**	**66.2**
15%RAP	4.5	2.288	2.437	10.0	6.1	16.1	62.1
	5.0	2.302	2.420	11.1	4.9	16.0	69.8
	5.5	2.304	2.403	12.3	4.1	16.4	75.0
	6.0	2.348	2.386	13.6	1.6	15.2	89.5
	O.A.C. (5.30)	**2.313**	**2.409**	**11.7**	**4.0**	**16.8**	**70.0**
25%RAP	4.5	2.330	2.472	10.2	5.7	15.9	64.0
	5.0	2.348	2.454	11.4	4.3	15.7	72.4
	5.5	2.366	2.437	12.6	2.9	15.5	81.3
	6.0	2.391	2.419	13.9	1.1	15.0	92.4
	O.A.C. (5.10)	**2.353**	**2.451**	**11.5**	**4.0**	**16.4**	**70.1**
30%RAP	4.5	2.347	2.482	10.2	5.4	15.7	65.3
	5.0	2.367	2.464	11.5	3.9	15.4	74.4
	5.5	2.364	2.446	12.6	3.3	15.9	79.0
	6.0	2.386	2.428	13.9	1.7	15.6	88.9
	O.A.C. (5.08)	**2.364**	**2.462**	**11.5**	**4.0**	**16.2**	**71.1**

Table A.8 Volumetric properties of Superpave mix design with 30%RAP (PG52-28) using aggregate source L

PG52-28 30%RAP		Specific Gravity		% AC by Vol.	Air Voids	VMA	% VFM
		Bulk	Rice				
0%Rubber	4.5	2.384	2.494	10.4	4.4	14.8	70.1
	5.0	2.396	2.476	11.6	3.2	14.8	78.2
	5.5	2.419	2.458	12.9	1.6	14.5	88.9
	6.0	2.424	2.440	14.1	0.7	14.7	95.5
	O.A.C. (6.35)	**2.389**	**2.489**	**10.7**	**4.0**	**15.0**	**71.8**
5% ambient	4.5	2.355	2.489	10.3	5.4	15.6	65.7
	5.0	2.373	2.471	11.5	4.0	15.4	74.4
	5.5	2.395	2.453	12.8	2.4	15.1	84.4
	6.0	2.406	2.435	14.0	1.2	15.2	92.0
	O.A.C. (5.90)	**2.373**	**2.472**	**11.4**	**4.0**	**16.1**	**70.7**
10% ambient	4.5	2.356	2.485	10.3	5.2	15.5	66.3
	5.0	2.375	2.467	11.5	3.7	15.2	75.5
	5.5	2.394	2.449	12.7	2.2	15.0	85.0
	6.0	2.404	2.432	14.0	1.1	15.1	92.5
	O.A.C. (5.65)	**2.372**	**2.471**	**11.2**	**4.0**	**15.8**	**70.6**
15% ambient	4.5	2.348	2.489	10.2	5.7	15.9	64.4
	5.0	2.367	2.471	11.5	4.2	15.7	73.2
	5.5	2.396	2.453	12.8	2.3	15.1	84.5
	6.0	2.404	2.435	14.0	1.3	15.3	91.5
	O.A.C. (5.25)	**2.371**	**2.469**	**11.5**	**4.0**	**16.4**	**70.1**

Table A.9 Volumetric properties of Superpave mix design with 0% rubber using aggregate source C

0%rubber		Specific Gravity		% AC by Vol.	Air Voids	VMA	% VFM
		Bulk	Rice				
0%RAP	4.5	2.324	2.448	10.1	5.1	15.2	66.6
	5.0	2.323	2.430	11.2	4.4	15.7	71.7
	5.5	2.357	2.413	12.6	2.3	14.9	84.4
	6.0	2.357	2.396	13.7	1.6	15.3	89.4
	O.A.C. (5.00)	**2.324**	**2.431**	**11.2**	**4.0**	**15.6**	**71.7**
15%RAP	4.5	2.312	2.455	10.1	5.8	15.9	63.3
	5.0	2.348	2.438	11.4	3.7	15.1	75.4
	5.5	2.345	2.421	12.5	3.1	15.6	80.1
	6.0	2.381	2.403	13.8	1.0	14.8	93.6
	O.A.C. (5.10)	**2.339**	**2.436**	**11.3**	**4.0**	**16.4**	**69.0**
(PG52-28) 30%RAP	4.0	2.302	2.477	8.9	7.0	16.0	55.9
	4.5	2.333	2.459	10.2	5.1	15.3	66.6
	5.0	2.349	2.441	11.4	3.8	15.1	75.1
	5.5	2.381	2.424	12.7	1.8	14.4	87.8
	O.A.C. (4.85)	**2.348**	**2.446**	**10.8**	**4.0**	**16.7**	**64.7**

Table A.10 Volumetric properties of Superpave mix design with 10% ambient rubber (-40mesh) using aggregate source C

10%40 m ambient		Specific Gravity		% AC by Vol.	Air Voids	VMA	% VFM
		Bulk	Rice				
0%RAP	4.5	2.242	2.443	9.8	8.2	18.0	54.3
	5.0	2.267	2.425	11.0	6.6	17.5	62.6
	5.5	2.302	2.408	12.3	4.4	16.7	73.4
	6.0	2.305	2.391	13.4	3.6	17.0	78.7
	O.A.C. (5.75)	**2.304**	**2.400**	**12.5**	**4.0**	**19.1**	**65.5**
15%RAP	4.5	2.278	2.452	9.9	7.1	17.0	58.4
	5.0	2.323	2.434	11.2	4.6	15.8	71.1
	5.5	2.314	2.417	12.3	4.3	16.6	74.2
	6.0	2.329	2.400	13.5	3.0	16.5	82.0
	O.A.C. (5.53)	**2.318**	**2.416**	**12.2**	**4.0**	**17.9**	**68.1**
30%RAP	4.5	2.325	2.456	10.1	5.3	15.5	65.5
	5.0	2.336	2.438	11.3	4.2	15.5	72.9
	5.5	2.350	2.421	12.5	2.9	15.4	81.0
	6.0	2.358	2.404	13.7	1.9	15.6	87.8
	O.A.C. (5.10)	**2.338**	**2.436**	**11.4**	**4.0**	**16.0**	**71.5**
(PG52-28) 30%RAP	4.5	2.326	2.456	10.1	5.3	15.4	65.7
	5.0	2.338	2.438	11.3	4.1	15.4	73.5
	5.5	2.348	2.421	12.5	3.0	15.5	80.6
	6.0	2.369	2.404	13.8	1.5	15.2	90.4
	O.A.C. (5.00)	**2.339**	**2.436**	**11.4**	**4.0**	**15.9**	**71.4**

Appendix B

Viscosity of the Modified Binder

Table B.1 Viscosity of modified binders containing ambient rubber (-40mesh) with aged binder L

PG64-22										Mean	Stdv.
0% Rubber 0%RAP	425	425	425	422.5	422.5	422.5	420	420	420	**423**	**2**
5% Ambi 0%RAP	662.5	662.5	650	625	625	612.5	612.5	612.5	625	**632**	**20**
10% Ambi 0%RAP	1275	1270	1270	1260	1255	1250	1295	1285	1285	**1272**	**14**
15% Ambi 0%RAP	2630	2625	2615	2700	2690	2680	2670	2665	2665	**2660**	**28**
0% Rubber 15%RAP	575	575	575	575	575	575	575	575	575	**575**	**0**
5% Ambi 15%RAP	1038	1050	1050	1040	1040	1050	1045	1040	1050	**1045**	**5**
10% Ambi 15%RAP	1650	1650	1650	1612	1612	1625	1725	1725	1725	**1664**	**46**
15% Ambi 15%RAP	3200	3200	3200	3513	3513	3513	3500	3500	3500	**3404**	**145**
0% Rubber 25%RAP	750	750	740	825	800	800	825	800	775	**785**	**31**
5% Ambi 25%RAP	1300	1300	1300	1200	1200	1200	1175	1175	1175	**1225**	**54**
10% Ambi 25%RAP	1850	1850	1837	1788	1788	1788	1825	1813	1825	**1818**	**24**
15% Ambi 25%RAP	3060	3060	3050	3013	3013	3000	2987	2975	2975	**3015**	**32**
0% Rubber 30%RAP	875	875	875	862.5	875	875	850	850	850	**865**	**11**
5% Ambi 30%RAP	1438	1438	1438	1450	1450	1450	1450	1450	1450	**1446**	**6**
10% Ambi 30%RAP	2088	2075	2075	2050	2050	2050	1900	1913	1913	**2013**	**75**
15% Ambi 30%RAP	3037	3025	3025	3150	3150	3150	3050	3050	3050	**3076**	**53**
PG52-28										Mean	Stdv.
0% Rubber 0%RAP	212.5	212.5	212.5	212.5	212.5	212.5	212.5	212.5	212.5	**213**	**0**
0% Rubber 30%RAP	537	537	537	513	513	525	525	525	525	**526**	**9**
5% Ambi 30%RAP	962	962	962	975	975	975	950	950	950	**962**	**10**
10% Ambi 30%RAP	1525	1525	1525	1500	1500	1500	1525	1525	1525	**1517**	**12**
15% Ambi 30%RAP	2475	2475	2475	2625	2625	2612	2575	2588	2575	**2558**	**61**
Aged binder (Source L)	5738	5750	5738	6375	6387	6375	5825	5825	5825	**5982**	**283**

Table B.2 Viscosity of modified binder containing cryogenic rubber with aged binder L

PG64-22										Mean	Stdv.
0% Rubber 0%RAP	425	425	425	422.5	422.5	422.5	420	420	420	**423**	**2**
5% Cryo 0%RAP	587.5	600	587.5	600	600	600	587.5	587.5	587.5	**593**	**6**
10% Cryo 0%RAP	1145	1145	1145	1140	1135	1135	1145	1145	1145	**1142**	**4**
15% Cryo 0%RAP	1910	1900	1900	1930	1925	1920	1910	1905	1895	**1911**	**11**
0% Rubber 15%RAP	575	575	575	575	575	575	575	575	575	**575**	**0**
5% Cryo 15%RAP	1075	1075	1075	987.5	987.5	987.5	1075	1075	1075	**1046**	**41**
10% Cryo 15%RAP	1600	1600	1612	1638	1638	1638	1638	1650	1650	**1629**	**19**
15% Cryo 15%RAP	2475	2463	2463	2313	2313	2300	2275	2275	2287	**2352**	**83**
0% Rubber 25%RAP	750	750	740	825	800	800	825	800	775	**785**	**31**
5% Cryo 25%RAP	1487	1487	1487	1462	1462	1462	1483	1483	1483	**1477**	**11**
10% Cryo 25%RAP	1925	1925	1925	1950	1950	1938	1945	1945	1945	**1939**	**10**
15% Cryo 25%RAP	2737	2737	2725	2775	2775	2775	2760	2760	2760	**2756**	**18**
0% Rubber 30%RAP	875	875	875	862.5	875	875	850	850	850	**865**	**11**
5% Cryo 30%RAP	1413	1413	1413	1388	1400	1400	1425	1425	1425	**1411**	**12**
10% Cryo 30%RAP	2200	2200	2200	2237	2237	2237	2225	2225	2225	**2221**	**15**
15% Cryo 30%RAP	2650	2650	2650	2700	2700	2700	2675	2675	2675	**2675**	**20**
PG52-28										Mean	Stdv.
0% Rubber 0%RAP	212.5	212.5	212.5	212.5	212.5	212.5	212.5	212.5	212.5	**213**	**0**
0% Rubber 30%RAP	537	537	537	513	513	525	525	525	525	**526**	**9**
5% Cryo 30%RAP	1000	1000	1000	962.5	962.5	962.5	950	950	950	**971**	**21**
10% Cryo 30%RAP	1325	1325	1325	1300	1300	1300	1263	1263	1263	**1296**	**25**
15% Cryo 30%RAP	2388	2388	2388	2388	2388	2388	2438	2425	2425	**2402**	**20**
Aged binder (Source L)	5738	5750	5738	6375	6387	6375	5825	5825	5825	**5982**	**283**

Table B.3 Viscosity of modified binder containing ambient rubber with aged binder C

PG64-22										Mean	Stdv.
0% Rubber 0%RAP	425	425	425	422.5	422.5	422.5	420	420	420	**423**	**2**
5% Ambi 0%RAP	662.5	662.5	650	625	625	612.5	612.5	612.5	625	**632**	**20**
10% Ambi 0%RAP	1275	1270	1270	1260	1255	1250	1295	1285	1285	**1272**	**14**
15% Ambi 0%RAP	2630	2625	2615	2700	2690	2680	2670	2665	2665	**2660**	**28**
0% Rubber 15%RAP	550	550	550	550	550	550	560	560	560	**553**	**5**
5% Ambi 15%RAP	987.5	987.5	987.5	950	950	950	950	950	950	**963**	**18**
10% Ambi 15%RAP	1400	1400	1400	1425	1425	1425	1375	1375	1375	**1400**	**20**
15% Ambi 15%RAP	2780	2780	2780	2825	2825	2825	2850	2850	2850	**2818**	**29**
0% Rubber 25%RAP	637.5	637.5	637.5	637.5	637.5	637.5	637.5	637.5	637.5	**638**	**0**
5% Ambi 25%RAP	1175	1175	1175	1175	1175	1175	1163	1163	1150	**1170**	**8**
10% Ambi 25%RAP	1788	1788	1788	1750	1750	1750	1775	1775	1775	**1771**	**16**
15% Ambi 25%RAP	3075	3075	3075	3088	3088	3075	3050	3050	3050	**3070**	**15**
0% Rubber 30%RAP	712.5	712.5	712.5	750	737.5	737.5	725	725	725	**726**	**12**
5% Ambi 30%RAP	1225	1225	1225	1175	1175	1175	1200	1200	1200	**1200**	**20**
10% Ambi 30%RAP	1888	1888	1888	1862	1862	1862	1875	1875	1875	**1875**	**11**
15% Ambi 30%RAP	2675	2675	2675	2688	2688	2688	2680	2680	2680	**2681**	**5**
PG52-28										Mean	Stdv.
0% Rubber 0%RAP	212.5	212.5	212.5	212.5	212.5	212.5	212.5	212.5	212.5	**213**	**0**
0% Rubber 30%RAP	425	425	425	437.5	437.5	437.5	475	475	475	**446**	**21**
5% Ambi 30%RAP	775	775	775	787.5	787.5	787.5	775	775	775	**779**	**6**
10% Ambi 30%RAP	1263	1263	1263	1200	1212	1212	1225	1225	1225	**1232**	**23**
15% Ambi 30%RAP	1813	1813	1813	1825	1825	1825	1825	1825	1825	**1821**	**6**
Aged binder (Source C)	2475	2475	2475	2563	2563	2563	2612	2612	2612	**2550**	**57**

Table B.4 Viscosity of modified binder containing cryogenic rubber with aged binder C

PG64-22										Mean	Stdv.
0% Rubber 0%RAP	425	425	425	422.5	422.5	422.5	420	420	420	**423**	**2**
5% Cryo 0%RAP	587.5	600	587.5	600	600	600	587.5	587.5	587.5	**593**	**6**
10% Cryo 0%RAP	1145	1145	1145	1140	1135	1135	1145	1145	1145	**1142**	**4**
15% Cryo 0%RAP	1910	1900	1900	1930	1925	1920	1910	1905	1895	**1911**	**11**
0% Rubber 15%RAP	550	550	550	550	550	550	560	560	560	**553**	**5**
5% Cryo 15%RAP	1025	1025	1025	1112	1112	1100	1000	1000	1000	**1044**	**46**
10% Cryo 15%RAP	2088	2088	2325	2325	2313	2362	2338	2325	2075	**2249**	**117**
15% Cryo 15%RAP	3263	3250	3237	3550	3537	3525	3525	3525	3525	**3437**	**133**
0% Rubber 25%RAP	637.5	637.5	637.5	637.5	637.5	637.5	637.5	637.5	637.5	**638**	**0**
5% Cryo 25%RAP	1200	1200	1200	1125	1138	1125	1125	1138	1125	**1153**	**34**
10% Cryo 25%RAP	1712	1712	1712	1750	1735	1750	1725	1725	1725	**1727**	**14**
15% Cryo 25%RAP	2550	2550	2550	2662	2662	2675	2650	2650	2650	**2622**	**52**
0% Rubber 30%RAP	712.5	712.5	712.5	750	737.5	737.5	725	725	725	**726**	**12**
5% Cryo 30%RAP	1250	1250	1250	1250	1250	1250	1225	1225	1225	**1242**	**12**
10% Cryo 30%RAP	1825	1825	1825	1925	1925	1938	1900	1900	1900	**1885**	**44**
15% Cryo 30%RAP	2338	2338	2338	2325	2325	2325	2388	2388	2388	**2350**	**27**
PG52-28										Mean	Stdv.
0% Rubber 0%RAP	212.5	212.5	212.5	212.5	212.5	212.5	212.5	212.5	212.5	**213**	**0**
0% Rubber 30%RAP	425	425	425	437.5	437.5	437.5	475	475	475	**446**	**21**
5% Cryo 30%RAP	750	750	750	750	750	750	750	750	750	**750**	**0**
10% Cryo 30%RAP	1100	1100	1100	1087	1087	1087	1100	1100	1100	**1096**	**6**
15% Cryo 30%RAP	1663	1663	1663	1750	1750	1750	1700	1700	1700	**1704**	**36**
Aged binder (Source C)	2475	2475	2475	2563	2563	2563	2612	2612	2612	**2550**	**57**

Appedix C

G* sin δ values of the modified binder

Table C.1 G* sin δ of modified binder containing ambient rubber (-40mesh) using aged binder L

PG64-22			Mean	Stdv.	PG64-22			Mean	Stdv.
0% Rubber 0%RAP	2.57	3.48	3.02	0.64	0% Rubber 0%RAP	2.57	3.48	3.02	0.64
5% Ambi 0%RAP	3.92	3.65	3.78	0.19	5% 40Cryo 0%RAP	3.92	3.00	3.46	0.65
10% Ambi 0%RAP	2.31	2.21	2.26	0.07	10% 40Cryo 0%RAP	2.02	2.36	2.19	0.24
15% Ambi 0%RAP	1.51	1.21	1.36	0.21	15% 40Cryo 0%RAP	1.07	1.58	1.33	0.37
0% Rubber 15%RAP	5.07	4.96	5.02	0.08	0% Rubber 15%RAP	5.07	4.96	5.02	0.08
5% Ambi 15%RAP	4.61	4.28	4.45	0.23	5% 40Cryo 15%RAP	4.30	4.77	4.54	0.34
10% Ambi 15%RAP	4.02	3.74	3.88	0.20	10% 40Cryo 15%RAP	3.12	3.61	3.36	0.35
15% Ambi 15%RAP	2.78	2.21	2.49	0.40	15% 40Cryo 15%RAP	3.20	3.30	3.25	0.07
0% Rubber 25%RAP	4.69	5.14	4.92	0.31	0% Rubber 25%RAP	4.69	5.14	4.92	0.31
5% Ambi 25%RAP	5.38	5.46	5.42	0.06	5% 40Cryo 25%RAP	4.04	5.00	4.52	0.68
10% Ambi 25%RAP	4.25	4.34	4.29	0.06	10% 40Cryo 25%RAP	4.07	3.88	3.98	0.14
15% Ambi 25%RAP	3.46	3.37	3.41	0.06	15% 40Cryo 25%RAP	3.63	3.90	3.77	0.19
0% Rubber 30%RAP	6.21	5.99	6.10	0.15	0% Rubber 30%RAP	6.21	5.99	6.10	0.15
5% Ambi 30%RAP	6.04	6.01	6.03	0.02	5% 40Cryo 30%RAP	5.20	5.36	5.28	0.12
10% Ambi 30%RAP	4.06	4.60	4.33	0.38	10% 40Cryo 30%RAP	3.88	3.88	3.88	0.00
15% Ambi 30%RAP	3.98	3.76	3.87	0.16	15% 40Cryo 30%RAP	3.73	3.25	3.49	0.34
PG52-28			Mean	Stdv.	PG52-28			Mean	Stdv.
0% Rubber 30%RAP	2.70	2.26	2.48	0.31	0% Rubber 30%RAP	2.70	2.26	2.48	0.31
5% Ambi 30%RAP	2.51	2.81	2.66	0.21	5% 40Cryo 30%RAP	2.68	2.74	2.71	0.05
10% Ambi 30%RAP	2.23	2.15	2.19	0.06	10% 40Cryo 30%RAP	2.22	2.13	2.17	0.06
15% Ambi 30%RAP	1.89	1.73	1.81	0.11	15% 40Cryo 30%RAP	2.00	1.75	1.88	0.18

Table C.2 G* sin δ of modified binder containing ambient rubber (-40mesh) using aged binder C

PG64-22			Mean	Stdv.	PG64-22			Mean	Stdv.
0% Rubber 0%RAP	2.57	3.48	3.02	0.64	0% Rubber 0%RAP	2.57	3.48	3.02	0.64
5% Ambi 0%RAP	3.92	3.65	3.78	0.19	5% 40Cryo 0%RAP	3.92	3.00	3.46	0.65
10% Ambi 0%RAP	2.31	2.21	2.26	0.07	10% 40Cryo 0%RAP	2.02	2.36	2.19	0.24
15% Ambi 0%RAP	1.51	1.21	1.36	0.21	15% 40Cryo 0%RAP	1.07	1.58	1.33	0.37
0% Rubber 15%RAP	4.04	4.28	4.16	0.17	0% Rubber 15%RAP	4.04	4.28	4.16	0.17
5% Ambi 15%RAP	3.93	4.14	4.03	0.15	5% 40Cryo 15%RAP	4.07	3.69	3.88	0.27
10% Ambi 15%RAP	3.20	3.02	3.11	0.13	10% 40Cryo 15%RAP	3.19	3.34	3.26	0.11
15% Ambi 15%RAP	2.47	2.35	2.41	0.08	15% 40Cryo 15%RAP	2.68	2.40	2.54	0.19
0% Rubber 25%RAP	4.78	5.08	4.93	0.22	0% Rubber 25%RAP	4.78	5.08	4.93	0.22
5% Ambi 25%RAP	5.17	4.22	4.70	0.67	5% 40Cryo 25%RAP	5.41	5.26	5.33	0.10
10% Ambi 25%RAP	4.43	4.26	4.34	0.12	10% 40Cryo 25%RAP	3.89	4.08	3.98	0.13
15% Ambi 25%RAP	3.30	3.35	3.32	0.04	15% 40Cryo 25%RAP	3.21	3.51	3.36	0.21
0% Rubber 30%RAP	5.94	5.71	5.82	0.16	0% Rubber 30%RAP	5.94	5.71	5.82	0.16
5% Ambi 30%RAP	4.82	5.36	5.09	0.38	5% 40Cryo 30%RAP	5.59	5.13	5.36	0.32
10% Ambi 30%RAP	4.98	5.37	5.18	0.28	10% 40Cryo 30%RAP	4.25	4.80	4.52	0.39
15% Ambi 30%RAP	3.84	3.32	3.58	0.36	15% 40Cryo 30%RAP	3.96	4.29	4.13	0.23
PG52-28			Mean	Stdv.	PG52-28			Mean	Stdv.
0% Rubber 30%RAP	2.09	1.90	2.00	0.14	0% Rubber 30%RAP	2.09	1.90	2.00	0.14
5% Ambi 30%RAP	2.10	2.03	2.07	0.05	5% 40Cryo 30%RAP	2.10	2.20	2.15	0.07
10% Ambi 30%RAP	1.95	1.98	1.96	0.02	10% 40Cryo 30%RAP	2.10	1.99	2.04	0.08
15% Ambi 30%RAP	1.67	1.55	1.61	0.09	15% 40Cryo 30%RAP	1.70	1.82	1.76	0.09

Appendix D

ITS Values of Mixtures

Table D.1 ITS values of mixtures using 0-5% ambient rubber (-40mesh) with aggregate L

PG64-22 (0% Rub)	Dry	Wet	PG64-22 (5%Ambi)	Dry	Wet
0%RAP	1100.59	933.86	0%RAP	1002.88	916.50
	1078.25	922.52		937.57	921.77
	1034.17	912.20		939.68	948.10
Mean (kPa)	**1071.00**	**922.86**	Mean (kPa)	**960.04**	**928.79**
Stdv. (kPa)	**33.80**	**10.83**	Stdv. (kPa)	**37.12**	**16.93**
TSR (%)	**86**		TSR (%)	**97**	
15%RAP	1394.15	1115.45	15%RAP	1188.29	1135.62
	1365.75	1136.24		1185.13	1237.80
	1303.64	1245.50		1158.79	1237.80
Mean (kPa)	**1354.51**	**1165.73**	Mean (kPa)	**1177.40**	**1203.74**
Stdv. (kPa)	**46.29**	**69.86**	Stdv. (kPa)	**16.19**	**59.00**
TSR (%)	**86**		TSR (%)	**102**	
25%RAP	1331.95	1321.08	25%RAP	1295.86	1192.32
	1461.96	1122.99		1349.75	962.30
	1361.49	1210.84		1214.47	1399.45
Mean (kPa)	**1385.13**	**1218.30**	Mean (kPa)	**1286.69**	**1184.69**
Stdv. (kPa)	**68.16**	**99.26**	Stdv. (kPa)	**68.10**	**218.67**
TSR (%)	**88**		TSR (%)	**92**	
30%RAP	1533.89	1408.92	30%RAP	1235.69	1284.94
	1521.39	1342.27		1259.20	1262.56
	1342.65			1295.02	1231.22
Mean (kPa)	**1465.98**	**1375.60**	Mean (kPa)	**1263.30**	**1259.57**
Stdv. (kPa)	**106.99**	**47.13**	Stdv. (kPa)	**29.87**	**26.99**
TSR (%)	**94**		TSR (%)	**100**	
PG52-28 (0% Rub)	Dry	Wet	PG52-28 (5%Ambi)	Dry	Wet
30%RAP	1180.37	961.49	30%RAP	1139.68	939.88
	1197.23	1059.98		1134.24	957.86
	1251.49	1084.15		1100.45	989.56
Mean (kPa)	**1209.70**	**1035.21**	Mean (kPa)	**1124.79**	**962.43**
Stdv. (kPa)	**37.17**	**64.98**	Stdv. (kPa)	**21.25**	**25.15**
TSR (%)	**86**		TSR (%)	**86**	

Table D.2 ITS values of mixtures using 10-15% ambient rubber (-40mesh) with aggregate L

PG64-22 (10%Ambi)	Dry	Wet	PG64-22 (15%Ambi)	Dry	Wet
0%RAP	928.14	733.96	0%RAP	900.74	645.71
	1021.14	764.77		902.22	736.76
	982.86	988.13		908.45	745.78
Mean (kPa)	**977.38**	**828.95**	Mean (kPa)	**903.80**	**709.42**
Stdv. (kPa)	**46.74**	**138.71**	Stdv. (kPa)	**4.09**	**55.36**
TSR (%)	**85**		TSR (%)	**78**	
15%RAP	1033.93	962.36	15%RAP	1005.11	764.91
	944.86	1004.21		1075.43	812.65
	1030.78	927.13		1087.32	823.76
Mean (kPa)	**1003.19**	**964.57**	Mean (kPa)	**1055.95**	**800.44**
Stdv. (kPa)	**50.54**	**38.59**	Stdv. (kPa)	**44.43**	**31.27**
TSR (%)	**96**		TSR (%)	**76**	
25%RAP	1264.48	1125.67	25%RAP	1154.18	1158.29
	1247.32	1063.23		1233.97	1005.38
	1094.90	1150.06			1045.67
Mean (kPa)	**1202.23**	**1112.99**	Mean (kPa)	**1194.08**	**1069.78**
Stdv. (kPa)	**93.35**	**44.79**	Stdv. (kPa)	**56.42**	**79.25**
TSR (%)	**93**		TSR (%)	**90**	
30%RAP	1227.14	1132.97	30%RAP	1412.36	1145.44
	1326.98	1271.93		1269.61	1213.47
	1013.33	1161.62		1266.45	
Mean (kPa)	**1189.15**	**1188.84**	Mean (kPa)	**1316.14**	**1179.46**
Stdv. (kPa)	**160.24**	**73.37**	Stdv. (kPa)	**83.34**	**48.10**
TSR (%)	**100**		TSR (%)	**90**	
PG52-28 (10%Ambi)	Dry	Wet	PG52-28 (15%Ambi)	Dry	Wet
30%RAP	1129.67	1070.58	30%RAP	1073.36	882.83
	1076.89	971.77		887.74	752.08
	1109.36	916.78		1006.88	1037.22
Mean (kPa)	**1105.31**	**986.38**	Mean (kPa)	**989.33**	**890.71**
Stdv. (kPa)	**26.62**	**77.94**	Stdv. (kPa)	**94.05**	**142.74**
TSR (%)	**89**		TSR (%)	**90**	

Table D.3 ITS values of mixtures using 5-15% cryogenic rubber (-40mesh) with aggregate L

PG64-22 (5%Cryo)	Dry	Wet	PG64-22 (10%Cryo)	Dry	Wet	PG64-22 (15%Cryo)	Dry	Wet
0%RAP	1044.57	928.04	0%RAP	914.93	870.20	0%RAP	846.70	488.00
	1105.18	1003.56		1011.74	852.34		968.10	613.50
	1023.45	935.67		886.61	905.05			
Mean (kPa)	**1057.73**	**955.76**	Mean (kPa)	**937.76**	**875.86**	Mean (kPa)	**907.40**	**550.75**
Stdv. (kPa)	**42.43**	**41.57**	Stdv. (kPa)	**65.61**	**26.81**	Stdv. (kPa)	**85.84**	**88.74**
TSR (%)	**90**		TSR (%)	**93**		TSR (%)	**61**	
15%RAP	1061.24	993.81	15%RAP	1000.57	931.32	15%RAP	837.81	558.71
	1199.87	959.72		914.39	897.23		751.94	483.56
	1100.34	945.56		997.53	906.90		965.87	730.84
Mean (kPa)	**1120.48**	**966.36**	Mean (kPa)	**970.83**	**911.81**	Mean (kPa)	**851.87**	**591.04**
Stdv. (kPa)	**71.48**	**24.80**	Stdv. (kPa)	**48.90**	**17.57**	Stdv. (kPa)	**107.66**	**126.77**
TSR (%)	**86**		TSR (%)	**94**		TSR (%)	**69**	
25%RAP	1329.01	1208.96	25%RAP	1297.70	1352.94	25%RAP	1258.22	1056.47
	1334.69	1159.34		1018.17	1292.89		1200.85	903.93
	1615.68	1263.49		1120.05	1251.21		1153.51	918.11
Mean (kPa)	**1426.46**	**1210.60**	Mean (kPa)	**1145.31**	**1299.02**	Mean (kPa)	**1204.19**	**959.50**
Stdv. (kPa)	**163.89**	**52.09**	Stdv. (kPa)	**141.47**	**51.14**	Stdv. (kPa)	**52.44**	**84.27**
TSR (%)	**85**		TSR (%)	**113**		TSR (%)	**80**	
30%RAP	1375.59	1424.83	30%RAP	1227.14	1326.99	30%RAP	1118.38	1184.39
	1655.82	1449.82		1155.31	1013.34		1137.78	1071.39
	1311.59	1196.46		1189.47	1135.88		1179.91	1061.32
Mean (kPa)	**1447.67**	**1357.04**	Mean (kPa)	**1190.64**	**1158.74**	Mean (kPa)	**1145.36**	**1105.70**
Stdv. (kPa)	**183.08**	**139.62**	Stdv. (kPa)	**35.93**	**158.07**	Stdv. (kPa)	**31.46**	**68.33**
TSR (%)	**94**		TSR (%)	**97**		TSR (%)	**97**	

Table D.4 ITS values of mixtures using 0-15% ambient rubber (-40mesh) with aggregate C

PG64-22 (0%Rub)	Dry	Wet	PG64-22 (10%Ambi)	Dry	Wet
0%RAP	1110.48	1096.85	0%RAP	1151.86	1101.50
	1059.73	1074.50		1056.77	958.32
	975.26	1028.29		1050.01	1034.60
Mean (kPa)	**1048.49**	**1066.55**	Mean (kPa)	**1086.21**	**1031.47**
Stdv. (kPa)	**68.31**	**34.97**	Stdv. (kPa)	**56.95**	**71.64**
TSR (%)	**102**		TSR (%)	**95**	
15%RAP	1377.87	1275.63	15%RAP	1304.80	1334.12
	1176.76	1319.93		1227.20	1294.67
	1319.93	1418.77		1115.78	1127.43
Mean (kPa)	**1291.52**	**1338.11**	Mean (kPa)	**1215.93**	**1252.07**
Stdv. (kPa)	**103.52**	**73.28**	Stdv. (kPa)	**95.01**	**109.73**
TSR (%)	**104**		TSR (%)	**103**	
			30%RAP	1413.41	1256.71
				1538.16	1418.29
				1394.99	1472.77
			Mean (kPa)	**1448.85**	**1382.59**
			Stdv. (kPa)	**77.89**	**112.37**
			TSR (%)	**95**	
PG52-28 (0%Rub)	Dry	Wet	PG52-28 (10%Ambi)	Dry	Wet
30%RAP	1150.25	961.65	30%RAP	1100.63	949.22
	957.83	934.89		1207.44	1021.98
	945.33	933.38		870.04	
Mean (kPa)	**1017.80**	**943.31**	Mean (kPa)	**1059.37**	**985.60**
Stdv. (kPa)	**114.87**	**15.90**	Stdv. (kPa)	**172.44**	**51.45**
TSR (%)	**93**		TSR (%)	**93**	

Appendix E

Fatigue Lives and Stiffness Values

Table E.1 Fatigue life and stiffness values of modified mixtures containing 0-5% ambient rubber using RAP L at 5ºC

PG64-22 (0%Rub)	Sample No.	Size (mmxmm)	Fatigue Life Cycles	Air Voids (%)	Initial Stiffness (Pa)	PG64-22 (5%Ambi)	Sample No.	Size (mmxmm)	Fatigue Life Cycles	Air Voids (%)	Initial Stiffness (Pa)
0%RAP	1A	52.19x64.64	58590	3.70	2.39E+07	0%RAP	1A	51.29x63.59	8005	5.55	1.82E+07
	1B	51.82x63.11	61495	3.08	2.25E+07		1B	52.81x64.15	24130	4.33	2.02E+07
	2A	52.21x62.93	9320	4.21	2.10E+07		2A	51.67x63.95	14640	4.86	1.98E+07
	2B	51.71x63.24	12295	3.92	2.15E+07		2B	51.36x64.99	14930	3.83	1.89E+07
Mean			**35425**	**3.73**	**2.22E+07**	Mean			**15426**	**4.64**	**1.93E+07**
Stdv.			**28476**	**0.48**	**1.27E+06**	Stdv.			**6626**	**0.74**	**8.90E+05**
15%RAP	1A	51.12x63.78	17190	4.57	2.34E+07	15%RAP	1A	51.37x63.83	15865	4.46	2.10E+07
	1B	50.48x62.38	25120	3.39	2.44E+07		1B	50.78x63.55	82720	5.14	1.86E+07
	2A	51.37x63.98	36025	4.76	2.22E+07		2A	50.56x63.73	33995	2.99	2.10E+07
	2B	50.54x61.82	41310	5.57	2.10E+07		2B	50.16x62.96	17575	4.10	2.22E+07
Mean			**29911**	**4.57**	**2.28E+07**	Mean			**37539**	**4.17**	**2.07E+07**
Stdv.			**10834**	**0.90**	**1.48E+06**	Stdv.			**31210**	**0.90**	**1.51E+06**
25%RAP	1A	50.67x63.05	10680	4.78	1.97E+07	25%RAP	1A	51.76x64.48	22125	4.36	2.09E+07
	1B	51.11x62.19	-	3.56	2.17E+07		1B	50.32x62.76	17020	3.12	2.13E+07
	2A	50.00x62.60	9430	6.47	1.81E+07		2A	50.39x63.01	7090	6.05	2.08E+07
	2B	51.57x63.27	-	4.87	2.30E+07		2B	50.43x61.77	-	4.44	1.87E+07
Mean			**10055**	**4.92**	**2.06E+07**	Mean			**15412**	**4.49**	**2.04E+07**
Stdv.			**5828**	**1.19**	**2.15E+06**	Stdv.			**9917**	**1.20**	**1.20E+06**
30%RAP	1A	50.21x62.74	23270	5.82	2.10E+07	0%RAP	1A	50.11x63.49	33800	6.49	2.01E+07
	1B	50.28x62.99	26495	4.36	2.42E+07		1B	50.82x62.56	19490	4.94	1.86E+07
	2A	50.31x63.61	29510	7.05	2.15E+07		2A	50.61x63.5	3430	6.75	1.96E+07
	2B	50.53x63.07	10785	5.52	2.08E+07		2B	51.49x63.34	20440	5.47	1.70E+07
Mean			**22515**	**5.69**	**2.19E+07**	Mean			**19290**	**5.91**	**1.88E+07**
Stdv.			**8225**	**1.11**	**1.56E+06**	Stdv.			**12429**	**0.85**	**1.39E+06**
30%RAP	1A	51.65x64.37	12610	6.54	1.81E+07	30%RAP	1A	51.43x63.57	44215	4.47	1.99E+07
PG52-28 (0%Rub)	1B	51.83x62.72	19690	5.28	1.94E+07	PG52-28 (5%Ambi)	1B	51.61x63.86	20360	5.95	1.68E+07
	2A	52.43x64.05	27315	6.22	1.78E+07		2A	50.09x63.42	14065	6.02	1.79E+07
	2B	51.93x63.73	35525	6.82	2.12E+07		2B	50.89x63.22	37935	5.49	1.74E+07
Mean			**23785**	**6.22**	**1.91E+07**	Mean			**29144**	**5.48**	**1.80E+07**
Stdv.			**9865**	**0.67**	**1.56E+06**	Stdv.			**14247**	**0.71**	**1.35E+06**

Table E.2 Fatigue life and stiffness values of modified mixtures containing 10-15% ambient rubber using RAP L at 5ºC

PG64-22 (10%Ambi)	Sample No.	Size (mmxmm)	Fatigue Life Cycles	Air Voids (%)	Initial Stiffness (Pa)	PG64-22 (15%Ambi)	Sample No.	Size (mmxmm)	Fatigue Life Cycles	Air Voids (%)	Initial Stiffness (Pa)
0%RAP	1A	51.70x63.43	26830	4.23	1.92E+07	0%RAP	1A	51.62x64.2	18410	4.90	1.71E+07
	1B	51.11x63.40	12800	3.97	2.26E+07		1B	51.77x62.66	12690	3.64	1.63E+07
	2A	50.97x63.47	22050	3.72	2.11E+07		2A	51.43x64.50	21690	3.49	1.89E+07
	2B	51.28x63.13	31660	3.36	2.17E+07		2B	53.43x64.50	38440	4.24	1.74E+07
Mean			**23335**	**3.82**	**2.12E+07**	Mean			**22808**	**4.07**	**1.74E+07**
Stdv.			**8045**	**0.37**	**1.43E+06**	Stdv.			**11065**	**0.64**	**1.11E+06**
15%RAP	1A	52.53x64.32	49265	3.71	2.15E+07	15%RAP	1A	52.76x64.10	66750	4.16	1.94E+07
	1B	52.91x63.38	66540	2.73	2.29E+07		1B	52.80x62.87	35910	2.88	2.02E+07
	2A	52.93x64.92	30570	4.85	2.16E+07		2A	51.33x62.26	78360	3.42	2.00E+07
	2B	53.09x64.06	101110	3.63	2.19E+07		2B	51.54x63.74	56580	2.38	2.02E+07
Mean			**61871**	**3.73**	**2.20E+07**	Mean			**59400**	**3.21**	**2.00E+07**
Stdv.			**30001**	**0.87**	**6.48E+05**	Stdv.			**18011**	**0.76**	**3.91E+05**
25%RAP	1A	53.03x64.32	11795	5.28	1.98E+07	25%RAP	1A	51.68x63.96	33980	3.68	1.76E+07
	1B	52.87x62.85	-	3.77	1.37E+07		1B	53.38x63.30	28060	4.84	1.74E+07
	2A	51.94x63.46	30875	4.85	1.90E+07		2A	51.58x64.37	35400	2.83	1.98E+07
	2B	52.83x63.33	10015	6.24	1.88E+07		2B	51.17x63.94	38000	3.74	1.87E+07
Mean			**17562**	**5.04**	**1.78E+07**	Mean			**33860**	**3.77**	**1.84E+07**
Stdv.			**12894**	**1.02**	**2.79E+06**	Stdv.			**4210**	**0.82**	**1.09E+06**
30%RAP	1A	51.75x64.81	8010	6.39	2.14E+07	0%RAP	1A	52.91x65.29	12500	8.19	1.70E+07
	1B	52.72x63.93	23010	5.51	2.05E+07		1B	52.01x64.05	28935	6.50	2.16E+07
	2A	54.79x64.25	44510	7.34	1.79E+07		2A	52.60x64.67	23055	7.06	1.73E+07
	2B	52.67x63.11	33715	7.49	1.72E+07		2B	52.63x64.63	-	5.88	1.99E+07
Mean			**27311**	**6.68**	**1.92E+07**	Mean			**21497**	**6.91**	**1.90E+07**
Stdv.			**15576**	**0.92**	**2.03E+06**	Stdv.			**12718**	**0.98**	**2.18E+06**
30%RAP	1A	51.69x64.52	17260	3.82	1.93E+07	30%RAP	1A	51.52x63.88	40830	6.05	1.63E+07
PG52-28 (10%Ambi)	1B	51.67x64.01	23520	5.46	1.62E+07	PG52-28 (15%Ambi)	1B	52.55x63.56	71915	5.26	1.57E+06
	2A	52.07x63.57	15610	6.97	1.66E+07		2A	51.90x63.51	31635	8.06	1.42E+07
	2B	51.33x63.71	25355	6.36	1.60E+07		2B	51.44x63.62	16815	6.69	1.35E+07
Mean			**20436**	**5.65**	**1.70E+07**	Mean			**40299**	**6.52**	**1.14E+07**
Stdv.			**4729**	**1.37**	**1.54E+06**	Stdv.			**23284**	**1.18**	**6.65E+06**

Table E.3 Fatigue life and stiffness values of modified mixtures containing 0-5% cryogenic rubber using RAP L at 5ºC

PG64-22 (0%Rub)	Sample No.	Size (mmxmm)	Fatigue Life Cycles	Air Voids (%)	Initial Stiffness (Pa)	PG64-22 (5%Cryo)	Sample No.	Size (mmxmm)	Fatigue Life Cycles	Air Voids (%)	Initial Stiffness (Pa)
0%RAP	1A	52.19x64.64	58590	3.70	2.39E+07	0%RAP	1A	52.00x63.5	14620	4.10	2.38E+07
	1B	51.82x63.11	61495	3.08	2.25E+07		1B	51.78x63.73	14705	3.71	2.63E+07
	2A	52.21x62.93	9320	4.21	2.10E+07						
	2B	51.71x63.24	12295	3.92	2.15E+07						
Mean			**35425**	**3.73**	**2.22E+07**	Mean			**14663**	**3.91**	**2.51E+07**
Stdv.			**28476**	**0.48**	**1.27E+06**	Stdv.			**60**	**0.28**	**1.75E+06**
15%RAP	1A	51.12x63.78	17190	4.57	2.34E+07	15%RAP	1A	51.48x64.36	26530	5.59	2.25E+07
	1B	50.48x62.38	25120	3.39	2.44E+07		1B	52.68x63.53	3215	4.73	2.20E+07
	2A	51.37x63.98	36025	4.76	2.22E+07						
	2B	50.54x61.82	41310	5.57	2.10E+07						
Mean			**29911**	**4.57**	**2.28E+07**	Mean			**14873**	**5.16**	**2.22E+07**
Stdv.			**10834**	**0.90**	**1.48E+06**	Stdv.			**16486**	**0.61**	**3.52E+05**
25%RAP	1A	50.67x63.05	10680	4.78	1.97E+07	25%RAP	1A	53.13x63.70	9345	7.58	1.99E+07
	1B	51.11x62.19	-	3.56	2.17E+07		1B	51.82x64.18	7555	5.03	2.74E+07
	2A	50.00x62.60	9430	6.47	1.81E+07						
	2B	51.57x63.27	-	4.87	2.30E+07						
Mean			**10055**	**4.92**	**2.06E+07**	Mean			**8450**	**6.31**	**2.36E+07**
Stdv.			**5828**	**1.19**	**2.15E+06**	Stdv.			**1266**	**1.80**	**5.32E+06**
30%RAP	1A	50.21x62.74	23270	5.82	2.10E+07	30%RAP	1A	52.53x63.28	7820	5.29	2.58E+07
	1B	50.28x62.99	26495	4.36	2.42E+07		1B	52.30x64.63	68745	5.51	2.59E+07
	2A	50.31x63.61	29510	7.05	2.15E+07						
	2B	50.53x63.07	10785	5.52	2.08E+07						
Mean			**22515**	**5.69**	**2.19E+07**	Mean			**38283**	**5.40**	**2.58E+07**
Stdv.			**8225**	**1.11**	**1.56E+06**	Stdv.			**43080**	**0.16**	**9.76E+04**

Table E.4 Fatigue life and stiffness values of modified mixtures containing 10-15% cryogenic rubber using RAP L at 5ºC

PG64-22 (5%Cryo)	Sample No.	Size (mmxmm)	Fatigue Life Cycles	Air Voids (%)	Initial Stiffness (Pa)	PG64-22 (15%Cryo)	Sample No.	Size (mmxmm)	Fatigue Life Cycles	Air Voids (%)	Initial Stiffness (Pa)
0%RAP	1A	51.64x62.06	63290	3.56	1.87E+07	0%RAP	1A	51.89x64.51	157060	2.42	2.36E+07
	1B	51.70x62.89	12155	4.69	2.02E+07		1B	54.14x64.32	100015	3.72	1.97E+07
Mean			**37723**	**4.13**	**1.94E+07**	Mean			**128538**	**3.07**	**2.16E+07**
Stdv.			**36158**	**0.80**	**1.08E+06**	Stdv.			**40337**	**0.92**	**2.72E+06**
15%RAP	1A	51.51x62.24	7890	4.27	2.25E+07	15%RAP	1A	51.85x63.72	7745	4.63	2.05E+07
	1B	51.94x60.94	25695	5.07	2.15E+07		1B	52.64x63.56	4400	5.40	1.94E+07
Mean			**16793**	**4.67**	**2.20E+07**	Mean			**6073**	**5.02**	**1.99E+07**
Stdv.			**12590**	**0.57**	**7.47E+05**	Stdv.			**2365**	**0.54**	**7.22E+05**
25%RAP	1A	51.02x63.48	21615	6.20	2.08E+07	25%RAP	1A	51.73x64.03	15130	4.28	2.53E+07
	1B	51.53x62.83	13665	6.84	1.91E+07		1B	51.16x64.06	2830	5.40	2.33E+07
Mean			**17640**	**6.52**	**2.00E+07**	Mean			**8980**	**4.84**	**2.43E+07**
Stdv.			**5621**	**0.45**	**1.23E+06**	Stdv.			**8697**	**0.79**	**1.42E+06**
30%RAP	1A	51.30x64.00	10015	8.11	1.95E+07	30%RAP	1A	52.09x63.81	7845	6.73	2.07E+07
	1B	50.87x63.20	3430	7.05	2.04E+07		1B	51.90x64.04	22895	7.84	2.05E+07
Mean			**6723**	**7.58**	**2.00E+07**	Mean			**15370**	**7.29**	**2.06E+07**
Stdv.			**4656**	**0.75**	**5.85E+05**	Stdv.			**10642**	**0.78**	**1.65E+05**

Table E.5 Fatigue life and stiffness values of modified mixtures containing 0-5% ambient rubber using RAP L at 20ºC

PG64-22 (0%Rub)	Sample No.	Size (mmxmm)	Fatigue Life Cycles	Air Voids (%)	Initial Stiffness (Pa)	PG64-22 (5%Ambi)	Sample No.	Size (mmxmm)	Fatigue Life Cycles	Air Voids (%)	Initial Stiffness (Pa)
0%RAP	1A	50.75x63.83	31840	7.54	1.10E+07	0%RAP	1A	51.51x62.58	71645	4.81	1.40E+07
	1B	51.49x63.76	64975	6.32	1.29E+07		1B	50.60x62.70	215240	3.67	1.43E+07
	2A	50.91x62.60	79220	4.43	1.32E+07		2A	50.89x63.37	63325	6.50	1.13E+07
	2B	50.36x63.10	35920	3.45	1.42E+07		2B	51.19x62.69	26800	5.37	1.37E+07
Mean			**52989**	**5.44**	**1.28E+07**	Mean			**94253**	**5.09**	**1.33E+07**
Stdv.			**22879**	**1.84**	**1.35E+06**	Stdv.			**82977**	**1.18**	**1.38E+06**
15%RAP	1A	51.73x64.21	28065	6.07	1.28E+07	15%RAP	1A	51.13x63.11	51530	7.40	1.28E+07
	1B	51.84x63.70	38680	4.90	1.43E+07		1B	50.25x62.66	32590	6.37	1.37E+07
	2A	51.56x63.75	110195	5.63	1.33E+07		2A	50.98x63.94	45970	8.47	1.20E+07
	2B	50.98x63.08	52755	4.16	1.43E+07		2B	50.49x63.20	45110	6.88	1.33E+07
Mean			**57424**	**5.19**	**1.37E+07**	Mean			**43800**	**7.28**	**1.30E+07**
Stdv.			**36605**	**0.84**	**7.50E+05**	Stdv.			**7997**	**0.90**	**7.33E+05**
25%RAP	1A	52.44x64.74	26570	5.98	1.04E+07	25%RAP	1A	50.11x64.22	8000	6.48	1.31E+07
	1B	51.91x64.08	11415	6.78	1.04E+07		1B	50.93x63.61	12600	5.16	1.39E+07
	2A	52.04x64.70	21335	6.34	1.02E+07		2A	51.84x64.42	39825	7.23	1.32E+07
	2B	51.77x64.88	33565	6.16	1.10E+07		2B	51.82x64.34	25120	7.15	1.34E+07
Mean			**23221**	**6.32**	**1.05E+07**	Mean			**21386**	**6.51**	**1.34E+07**
Stdv.			**9330**	**0.34**	**3.46E+05**	Stdv.			**14263**	**0.96**	**3.56E+05**
30%RAP	1A	51.10x63.72	35085	6.72	1.37E+07	0%RAP	1A	51.51X64.20	26685	4.54	1.44E+07
	1B	49.91x62.60	19960(*)	6.50	1.44E+07		1B	50.45X62.86	51130	5.64	1.43E+07
	2A	50.60x64.08	46255	7.27	1.38E+07		2A	51.29X64.54	54345	4.87	1.52E+07
	2B	51.29x63.74	80375	5.53	1.39E+07		2B	51.90X64.07	22685	6.10	1.44E+07
Mean			**53905**	**6.51**	**1.40E+07**	Mean			**38711**	**5.29**	**1.46E+07**
Stdv.			**33129**	**0.73**	**3.11E+05**	Stdv.			**16331**	**0.71**	**4.19E+05**
30%RAP	1A	51.13x62.39	40850	7.13	1.09E+07	30%RAP	1A	52.31x63.85	24540	6.67	1.28E+07
PG52-28 (0%Rub)	1B	51.80x63.39	30980	8.89	9.93E+06	PG52-28 (5%Ambi)	1B	52.23x64.60	16540	8.14	1.29E+07
	2A	51.06x64.18	8680	7.30	1.64E+07		2A	51.15x64.43	11665	6.78	1.07E+07
	2B	51.35x62.23	9560	8.55	1.58E+07		2B	50.78x63.03	27890	7.67	1.17E+07
Mean			**22518**	**7.97**	**1.33E+07**	Mean			**20159**	**7.32**	**1.20E+07**
Stdv.			**15990**	**0.88**	**3.32E+06**	Stdv.			**7398**	**0.71**	**1.04E+06**

Table E.6 Fatigue life and stiffness values of modified mixtures containing 10-15% ambient rubber using RAP L at 20ºC

PG64-22 (10%Ambi)	Sample No.	Size (mmxmm)	Fatigue Life Cycles	Air Voids (%)	Initial Stiffness (Pa)	PG64-22 (15%Ambi)	Sample No.	Size (mmxmm)	Fatigue Life Cycles	Air Voids (%)	Initial Stiffness (Pa)
0%RAP	1A	51.00x63.22	239885	5.88	1.17E+07	0%RAP	1A	51.71x64.4	102550	6.57	8.86E+06
	1B	50.93x62.7	125110	6.55	1.22E+07		1B	52.02x64.33	21235	4.95	9.47E+06
	2A	52.16x63.56	81275	4.96	1.27E+07		2A	51.86x63.68	40185	5.52	1.09E+07
	2B	52.30x63.39	91850	5.49	1.22E+07		2B				
Mean			**134530**	**5.72**	**1.22E+07**	Mean			**54657**	**5.68**	**9.74E+06**
Stdv.			**72678**	**0.67**	**4.12E+05**	Stdv.			**42545**	**0.82**	**1.05E+06**
15%RAP	1A	50.44x62.92	69825	7.32	1.18E+07	15%RAP	1A	52.05x64.18	110975	5.67	1.25E+07
	1B	50.93x63.79	23595	7.20	1.23E+07		1B	52.35x60.93	66760	4.94	1.28E+07
	2A	50.49x62.74	42200	6.19	1.49E+07		2A	51.75x64.25	41635	6.91	1.17E+07
	2B	52.17x64.57	52950	6.72	1.22E+07		2B	51.57x63.51	19955	5.44	1.23E+07
Mean			**47143**	**6.86**	**1.28E+07**	Mean			**59831**	**5.74**	**1.23E+07**
Stdv.			**19383**	**0.52**	**1.43E+06**	Stdv.			**39094**	**0.84**	**4.57E+05**
25%RAP	1A	51.62x61.77	6325	6.14	1.28E+07	25%RAP	1A	52.17x63.17	12590	6.67	1.28E+07
	1B	50.39x62.21	39815	5.92	1.26E+07		1B	51.29x62.11	10015	5.77	1.30E+07
	2A	50.47x63.01	25125	6.59	1.32E+07		2A	50.89x61.74	8050	9.52	1.23E+07
	2B	52.64x62.01	15800	6.15	1.34E+07		2B	51.25x63.01	15865	10.06	1.25E+07
Mean			**21766**	**6.20**	**1.30E+07**	Mean			**11630**	**8.01**	**1.26E+07**
Stdv.			**14272**	**0.28**	**3.98E+05**	Stdv.			**3380**	**2.11**	**3.02E+05**
30%RAP	1A	51.48x63.99	28680	7.04	1.30E+07	0%RAP	1A	51.31x63.49	49220	5.57	1.43E+07
	1B	50.86x63.56	23655	7.50	1.36E+07		1B	50.05x63.63	-	4.80	-
	2A	50.91x61.48	42290	6.86	1.42E+07		2A	52.43x63.65	34365	4.44	1.32E+07
	2B	50.52x63.50	44650	6.51	1.49E+07		2B	50.19x64.06	35870	5.98	1.37E+07
Mean			**34819**	**6.98**	**1.39E+07**	Mean			**39818**	**5.20**	**1.37E+07**
Stdv.			**10243**	**0.41**	**8.03E+05**	Stdv.			**20999**	**0.70**	**6.88E+06**
30%RAP	1A	52.04x63.42	31635	6.73	9.92E+06	30%RAP	1A	51.65X62.74	31565	6.65	1.11E+07
PG52-28 (10%Ambi)	1B	51.34x63.5	20690	7.60	9.47E+06	PG52-28 (15%Ambi)	1B	49.28x62.61	35150	7.56	1.14E+07
	2A	50.96x63.28	13700	8.65	9.34E+06		2A	50.88x63.83	17970	7.71	1.03E+07
	2B	51.46x62.57	19505	8.65	9.37E+06		2B	52.07x62.7	12655	6.87	1.09E+07
Mean			**21383**	**7.91**	**9.53E+06**	Mean			**24335**	**7.20**	**1.09E+07**
Stdv.			**7486**	**0.93**	**2.69E+05**	Stdv.			**10742**	**0.52**	**4.51E+05**

Table E.7 Fatigue life and stiffness values of modified mixtures containing 0-5% cryogenic rubber using RAP L at 20ºC

PG64-22 (0%Rub)	Sample No.	Size (mmxmm)	Fatigue Life Cycles	Air Voids (%)	Initial Stiffness (Pa)	PG64-22 (5%Cryo)	Sample No.	Size (mmxmm)	Fatigue Life Cycles	Air Voids (%)	Initial Stiffness (Pa)
0%RAP	1A	50.75x63.83	31840	7.54	1.10E+07	0%RAP	1A	52.10x64.50	28270	5.08	1.30E+07
	1B	51.49x63.76	64975	6.32	1.29E+07		1B	52.51x63.74	52600	5.31	1.35E+07
	2A	50.91x62.60	79220	4.43	1.32E+07						
	2B	50.36x63.10	35920	3.45	1.42E+07						
Mean			**52989**	**5.44**	**1.28E+07**	Mean			**40435**	**5.20**	**1.32E+07**
Stdv.			**22879**	**1.84**	**1.35E+06**	Stdv.			**17204**	**0.16**	**3.84E+05**
15%RAP	1A	51.73x64.21	28065	6.07	1.28E+07	15%RAP	1A	52.30x63.14	39890	4.31	1.35E+07
	1B	51.84x63.70	38680	4.90	1.43E+07		1B	52.94x64.37	38545	3.77	1.46E+07
	2A	51.56x63.75	110195	5.63	1.33E+07						
	2B	50.98x63.08	52755	4.16	1.43E+07						
Mean			**57424**	**5.19**	**1.37E+07**	Mean			**39218**	**4.04**	**1.40E+07**
Stdv.			**36605**	**0.84**	**7.50E+05**	Stdv.			**951**	**0.38**	**7.15E+05**
25%RAP	1A	52.44x64.74	26570	5.98	1.04E+07	25%RAP	1A	53.19x64.26	12130	6.37	1.58E+07
	1B	51.91x64.08	11415	6.78	1.04E+07		1B	52.13x64.61	33690	4.43	1.51E+07
	2A	52.04x64.70	21335	6.34	1.02E+07						
	2B	51.77x64.88	33565	6.16	1.10E+07						
Mean			**23221**	**6.32**	**1.05E+07**	Mean			**22910**	**5.40**	**1.55E+07**
Stdv.			**9330**	**0.34**	**3.46E+05**	Stdv.			**15245**	**1.37**	**4.95E+05**
30%RAP	1A	51.10x63.72	35085	6.72	1.37E+07	30%RAP	1A	51.85x64.27	15735	6.65	1.41E+07
	1B	49.91x62.60	19960(*)	6.50	1.44E+07		1B	51.97x62.24	39000	6.16	1.63E+07
	2A	50.60x64.08	46255	7.27	1.38E+07						
	2B	51.29x63.74	80375	5.53	1.39E+07						
Mean			**53905**	**6.51**	**1.40E+07**	Mean			**27368**	**6.41**	**1.52E+07**
Stdv.			**33129**	**0.73**	**3.11E+05**	Stdv.			**16451**	**0.35**	**1.54E+06**

Table E.8 Fatigue life and stiffness values of modified mixtures containing 10-15% cryogenic rubber using RAP L at 20ºC

PG64-22 (5%Cryo)	Sample No.	Size (mmxmm)	Fatigue Life Cycles	Air Voids (%)	Initial Stiffness (Pa)	PG64-22 (15%Cryo)	Sample No.	Size (mmxmm)	Fatigue Life Cycles	Air Voids (%)	Initial Stiffness (Pa)
0%RAP	1A	51.90x64.32	37680	6.19	9.96E+06	0%RAP	1A	52.45x63.05	279365	3.46	1.24E+07
	1B	63.80x50.65	43270	5.38	9.94E+06		1B	52.41x64.01	3225	3.27	1.36E+07
	2A	51.17x63.81	91520	4.91	9.74E+06						
	2B	52.17x63.60	58255	5.06	9.64E+06						
Mean			**57681**	**5.39**	**9.82E+06**	Mean			**141295**	**3.37**	**1.30E+07**
Stdv.			**24174**	**0.57**	**1.56E+05**	Stdv.			**195260**	**0.13**	**8.44E+05**
15%RAP	1A	50.16x62.92	60925	6.31	9.56E+06	15%RAP	1A	52.72x64.90	36465	5.00	1.28E+07
	1B	50.11x63.16	90230	4.65	9.60E+06		1B	51.49x63.65	34645	5.60	1.25E+07
	2A	63.88x50.14	82290	4.76	1.96E+07						
	2B	50.64x62.40	84195	4.35	1.99E+07						
Mean			**79410**	**5.02**	**1.47E+07**	Mean			**35555**	**5.30**	**1.27E+07**
Stdv.			**12780**	**0.88**	**5.87E+06**	Stdv.			**1287**	**0.42**	**2.18E+05**
25%RAP	1A	50.04x63.40	21150	5.68	1.33E+07	25%RAP	1A	52.00x64.15	32995	5.67	1.42E+07
	1B	50.95x63.83	24965	6.64	1.37E+07		1B	52.60x63.80	18590	4.49	1.67E+07
	2A	51.75x64.11	10015	5.57	1.19E+07						
	2B	52.25x63.32	27450	5.39	1.19E+07						
Mean			**20895**	**5.82**	**1.27E+07**	Mean			**25793**	**5.08**	**1.55E+07**
Stdv.			**7702**	**0.56**	**9.38E+05**	Stdv.			**10186**	**0.83**	**1.76E+06**
30%RAP	1A	51.63x63.55	32660	6.39	1.04E+07	30%RAP	1A	51.25x64.31	-	6.69	-
	1B	51.75x64.04	9670	6.87	1.08E+07		1B	51.51x63.18	4115	8.63	1.41E+07
	2A	50.81x64.43	41455	5.97	1.04E+07						
	2B	50.78x63.40	24215	6.25	1.01E+07						
Mean			**27000**	**6.37**	**1.04E+07**	Mean			**4115**	**7.66**	**1.41E+07**
Stdv.			**13529**	**0.38**	**2.87E+05**	Stdv.			**-**	**1.37**	**-**

Table E.9 Fatigue life and stiffness values of modified mixtures using RAP C at 5ºC

PG64-22 (0%Rub)	Sample No.	Size (mmxmm)	Fatigue Life Cycles	Air Voids (%)	Initial Stiffness (Pa)	PG64-22 (10%Ambi)	Sample No.	Size (mmxmm)	Fatigue Life Cycles	Air Voids (%)	Initial Stiffness (Pa)
0%RAP	1A	52.36x63.93	29005	6.64	2.50E+07	0%RAP	1A	51.59x62.46	19235	6.20	2.41E+07
	1B	50.70x62.84		8.27	1.87E+07		1B	51.72x63.21	39825	5.06	2.28E+07
	2A	52.32x62.29	6890	7.38	2.08E+07		2A	51.53x60.60	11735	8.65	1.99E+07
	2B	51.55x61.54	28060	8.73	2.10E+07		2B	52.00x62.02	28375	9.77	1.98E+07
Mean			**21318**	**7.76**	**2.14E+07**	Mean			**24793**	**7.42**	**2.17E+07**
Stdv.			**12504**	**0.93**	**2.63E+06**	Stdv.			**12113**	**2.17**	**2.14E+06**
15%RAP	1A	50.76x63.88	32710	8.15	2.40E+07	15%RAP	1A	51.46x62.45	32190	7.72	2.24E+07
	1B	51.36x62.22	37090	7.93	2.52E+07		1B	51.40x61.84	22865	7.87	2.20E+07
	2A	51.36x62.76	16150	8.22	2.37E+07		2A	51.81x62.29	27650	7.06	2.34E+07
	2B	50.56x63.44	17075	8.14	2.39E+07		2B	51.00x63.85	61910	8.11	2.25E+07
Mean			**25756**	**8.11**	**2.42E+07**	Mean			**36154**	**7.69**	**2.26E+07**
Stdv.			**10715**	**0.13**	**6.71E+05**	Stdv.			**17588**	**0.45**	**5.70E+05**
						30%RAP	1A	51.50x64.00	27380	8.94	2.18E+07
							1B	51.82x63.27	34345	5.79	2.68E+07
							2A	50.44x63.32	18480	7.12	2.49E+07
							2B	51.22x62.91	33045	7.98	2.25E+07
						Mean			**28313**	**7.46**	**2.40E+07**
						Stdv.			**7219**	**1.34**	**2.29E+06**
30%RAP	1A	51.73x61.60	43175	6.79	2.19E+07	30%RAP	1A	51.74x61.95	15750	7.92	1.97E+07
PG52-28 (0%Rub)	1B	50.98x61.60	13470	6.96	2.42E+07	PG52-28 (10%Ambi)	1B	50.98x61.60	62935	7.44	1.97E+07
	2A	51.56x62.87	50440	8.85	1.78E+07		2A	51.65x62.87	11780	6.80	1.96E+07
	2B	51.40x61.51	42730	7.01	2.21E+07		2B	51.40x61.50	28965	7.57	1.92E+07
Mean			**37454**	**7.40**	**2.15E+07**	Mean			**29858**	**7.43**	**1.96E+07**
Stdv.			**16375**	**0.97**	**2.66E+06**	Stdv.			**23243**	**0.47**	**2.21E+05**

Table E.10 Fatigue life and stiffness values of modified mixtures using RAP C at 20ºC

PG64-22 (0%Rub)	Sample No.	Size (mmxmm)	Fatigue Life Cycles	Air Voids (%)	Initial Stiffness (Pa)	PG64-22 (10%Ambi)	Sample No.	Size (mmxmm)	Fatigue Life Cycles	Air Voids (%)	Initial Stiffness (Pa)
0%RAP	1A	53.53x60.79	91140	7.32	1.11E+07	0%RAP	1A	51.02x60.43	4700	7.20	9.64E+06
	1B	51.93x61.90	78720	7.45	1.23E+07		1B	52.02x61.00	52240	7.22	9.83E+06
	2A	52.36x60.84	23585	6.44	1.04E+07		2A	50.88x61.29	113610	7.75	8.77E+06
	2B	51.55x61.84	70960	7.15	1.17E+07		2B	50.69x62.20	55035	8.51	8.48E+06
Mean			**66101**	**7.09**	**1.14E+07**	Mean			**56396**	**7.67**	**9.18E+06**
Stdv.			**29538**	**0.45**	**8.05E+05**	Stdv.			**44591**	**0.62**	**6.58E+05**
15%RAP	1A	52.10x60.66	64800	7.21	1.19E+07	15%RAP	1A	51.56x62.38	52460	6.81	1.08E+07
	1B	51.36x62.00	45420	7.88	1.20E+07		1B	51.72x62.08	36255	6.81	1.06E+07
	2A	51.16x62.76	28855	7.35	1.22E+07		2A	51.03x60.75	146225	6.05	1.06E+07
	2B	50.56x63.44	42650	6.65	1.27E+07		2B	52.28x60.92	82630	9.29	1.07E+07
Mean			**45431**	**7.27**	**1.22E+07**	Mean			**79393**	**7.24**	**1.07E+07**
Stdv.			**14806**	**0.51**	**3.61E+05**	Stdv.			**48522**	**1.41**	**1.01E+05**
						30%RAP	1A	52.32x61.68	47320	8.09	1.20E+07
							1B	51.44x60.44	59150	7.13	1.21E+07
							2A	51.92x61.05	34275	8.09	1.14E+07
							2B	51.55x61.98	41495	7.16	1.33E+07
						Mean			**45560**	**7.62**	**1.22E+07**
						Stdv.			**10514**	**0.55**	**7.74E+05**
30%RAP	1A	50.33x61.94	42520	7.21	9.85E+06	30%RAP	1A	50.33x61.94	56890	7.13	8.46E+06
PG52-28 (0%Rub)	1B	51.56x61.27	68860	8.57	8.55E+06	PG52-28 (10%Ambi)	1B	51.56x61.27	79710	6.69	8.42E+06
	2A	50.72x62.28	50440	7.52	8.06E+06		2A	50.71x62.28	95860	6.00	9.82E+06
	2B	53.00x62.28	42730	8.58	7.27E+06		2B	52.99x62.28	69765	7.19	8.01E+06
Mean			**51138**	**7.97**	**8.43E+06**	Mean			**75556**	**6.75**	**8.68E+06**
Stdv.			**12376**	**0.71**	**1.08E+06**	Stdv.			**16447**	**0.55**	**7.89E+05**

Appendix F

Average Values of Independent and Dependent Variables of Modified Mixture

Table F.1 Average values of independent and dependent variables of modified mixtures using RAP L tested at 5ºC

	Specific Independent			Traditional Independent				Dependent
5ºC	R_b (%)	R_P (%)	Ln(ε_0)	VFA	V_0	Ln(w_0)	Ln(S_0)	Ln(N_f)
Ambient rubber	0.00	0.00	-7.642	0.739	3.73	0.790	16.916	**10.140**
	0.00	0.15	-7.625	0.749	4.57	1.200	16.939	**10.251**
	0.00	0.25	-7.591	0.744	4.92	1.246	16.755	**9.214**
	0.00	0.30	-7.607	0.733	5.69	0.458	16.899	**9.955**
	0.05	0.00	-7.647	0.758	4.62	0.547	16.791	**9.765**
	0.05	0.15	-7.690	0.757	4.17	0.676	16.879	**9.960**
	0.05	0.25	-7.576	0.738	4.49	0.797	16.825	**9.652**
	0.05	0.30	-7.589	0.733	5.91	0.744	16.899	**9.955**
	0.10	0.00	-7.869	0.765	3.82	0.393	16.866	**10.005**
	0.10	0.15	-7.631	0.762	3.73	0.974	16.906	**10.746**
	0.10	0.25	-7.579	0.731	5.04	1.613	16.771	**9.642**
	0.10	0.30	-7.646	0.743	6.68	0.499	16.730	**10.391**
	0.15	0.00	-7.609	0.773	4.07	0.388	16.673	**9.953**
	0.15	0.15	-7.628	0.773	3.21	0.881	16.809	**10.847**
	0.15	0.25	-7.595	0.760	3.77	1.276	16.725	**10.424**
	0.15	0.30	-7.628	0.744	6.91	0.382	16.788	**10.113**
Cryogenic rubber	0.00	0.00	-7.642	0.739	3.73	0.790	16.916	**10.140**
	0.00	0.15	-7.626	0.749	4.57	1.200	16.939	**10.251**
	0.00	0.25	-7.592	0.744	4.92	1.246	16.838	**9.268**
	0.00	0.30	-7.607	0.733	5.69	0.458	16.899	**9.955**
	0.05	0.00	-7.681	0.667	3.91	0.692	17.036	**9.593**
	0.05	0.15	-7.620	0.687	5.16	0.446	16.917	**9.131**
	0.05	0.25	-7.699	0.699	6.31	0.849	16.965	**9.036**
	0.05	0.30	-7.608	0.711	5.40	0.899	17.067	**10.051**
	0.10	0.00	-7.556	0.675	4.13	0.997	16.782	**10.230**
	0.10	0.15	-7.619	0.684	4.67	0.887	16.907	**9.564**
	0.10	0.25	-7.590	0.713	6.52	0.661	16.809	**9.752**
	0.10	0.30	-7.577	0.733	7.58	0.784	16.809	**8.676**
	0.15	0.00	-7.651	0.662	3.07	0.662	16.886	**9.838**
	0.15	0.15	-7.599	0.700	5.02	0.752	16.808	**8.672**
	0.15	0.25	-7.678	0.701	4.84	0.716	17.004	**8.786**
	0.15	0.30	-7.627	0.711	7.29	0.909	16.841	**9.503**

Table F.2 Average values of independent and dependent variables of modified mixtures using RAP L tested at 20ºC

	Specific Independent			Traditional Independent				Dependent
20ºC	R_b (%)	R_P (%)	Ln(ε_0)	VFA	V_0	Ln(w_0)	Ln(S_0)	Ln(N_f)
Ambient rubber	0.00	0.00	-7.508	0.739	5.44	0.899	16.364	**10.805**
	0.00	0.15	-7.521	0.749	5.19	0.863	16.430	**10.822**
	0.00	0.25	-7.509	0.744	6.32	0.913	16.166	**9.980**
	0.00	0.30	-7.532	0.733	6.51	0.906	16.451	**10.601**
	0.05	0.00	-7.532	0.758	5.09	1.127	16.402	**11.178**
	0.05	0.15	-7.533	0.757	7.28	0.819	16.375	**10.674**
	0.05	0.25	-7.592	0.738	6.51	0.787	16.411	**9.788**
	0.05	0.30	-7.546	0.733	5.29	0.944	16.495	**10.492**
	0.10	0.00	-7.517	0.765	5.72	0.752	16.315	**11.367**
	0.10	0.15	-7.481	0.762	6.86	0.872	16.361	**10.687**
	0.10	0.25	-7.525	0.731	6.20	0.702	16.381	**9.786**
	0.10	0.30	-7.496	0.743	6.98	0.899	16.448	**10.424**
	0.15	0.00	-7.547	0.773	5.68	0.651	16.088	**10.701**
	0.15	0.15	-7.536	0.773	5.74	0.729	16.324	**10.816**
	0.15	0.25	-7.575	0.760	8.01	0.590	16.351	**9.329**
	0.15	0.30	-7.595	0.744	5.20	0.762	16.435	**10.579**
Cryogenic rubber	0.00	0.00	-7.508	0.739	5.435	0.899	16.364	**10.805**
	0.00	0.15	-7.521	0.749	5.190	0.863	16.430	**10.822**
	0.00	0.25	-7.509	0.744	6.315	0.913	16.166	**9.980**
	0.00	0.30	-7.532	0.733	6.505	0.906	16.451	**10.601**
	0.05	0.00	-7.509	0.667	5.195	0.994	16.399	**10.560**
	0.05	0.15	-7.519	0.687	4.040	0.978	16.457	**10.577**
	0.05	0.25	-7.559	0.699	5.400	0.931	16.553	**9.914**
	0.05	0.30	-7.573	0.711	6.405	0.794	16.535	**10.117**
	0.10	0.00	-7.491	0.675	5.385	0.875	16.100	**10.902**
	0.10	0.15	-7.493	0.684	5.623	0.947	16.086	**10.862**
	0.10	0.25	-7.510	0.713	5.820	0.776	16.355	**9.879**
	0.10	0.30	-7.513	0.733	6.370	0.952	16.159	**10.074**
	0.15	0.00	-7.505	0.662	3.365	0.649	16.380	**10.309**
	0.15	0.15	-7.537	0.700	5.300	1.069	16.355	**10.479**
	0.15	0.25	-7.507	0.701	5.080	0.250	16.551	**10.117**
	0.15	0.30	-7.554	0.711	7.660	0.412	16.459	**9.482**

Table F.3 Average values of independent and dependent variables of modified mixtures using soft binder (PG52-28) and RAP L tested at 5ºC and 20ºC

	Specific Independent			Traditional Independent				Dependent
5ºC	R_b (%)	R_P (%)	Ln(ε_0)	VFA	V_0	Ln(w_0)	Ln(S_0)	Ln(N_f)
Ambient	0.00	0.30	-7.636	0.718	6.22	0.751	16.765	**10.077**
	0.05	0.30	-7.566	0.707	5.48	1.148	16.706	**10.280**
	0.10	0.30	-7.580	0.706	5.65	1.142	16.649	**9.925**
	0.15	0.30	-7.595	0.701	6.52	0.265	16.462	**10.604**
20ºC								
Ambient	0.00	0.30	-7.562	0.718	7.97	0.522	16.403	**10.022**
	0.05	0.30	-7.532	0.707	7.32	0.519	16.300	**9.911**
	0.10	0.30	-7.558	0.706	7.91	0.680	16.070	**9.970**
	0.15	0.30	-7.543	0.701	7.20	0.581	16.204	**10.100**

Table F.4 Average values of independent and dependent variables of modified mixtures using RAP C

	Specific Independent			Traditional Independent				Dependent
5ºC	R_b (%)	R_P (%)	Ln(ε_0)	VFA	V_0	Ln(w_0)	Ln(S_0)	Ln(N_f)
PG64	0.00	0.00	-7.612	0.717	7.76	2.255	16.872	**9.785**
	0.00	0.15	-7.609	0.690	8.11	2.399	17.002	**10.088**
	0.10	0.00	-7.578	0.655	7.42	2.289	16.887	**10.020**
	0.10	0.15	-7.692	0.681	7.69	1.371	16.932	**10.419**
	0.10	0.30	-7.621	0.715	7.46	1.823	16.990	**10.223**
PG52	0.00	0.30	-7.569	0.647	7.40	2.464	16.877	**10.418**
	0.10	0.30	-7.615	0.714	7.43	2.408	16.788	**10.091**
20ºC								
PG64	0.00	0.00	-7.509	0.717	7.09	0.798	16.245	**10.983**
	0.00	0.15	-7.507	0.690	7.27	0.986	16.317	**10.683**
	0.10	0.00	-7.486	0.655	7.67	1.036	16.031	**10.469**
	0.10	0.15	-7.513	0.681	7.24	0.971	16.183	**11.145**
	0.10	0.30	-7.503	0.715	7.62	1.155	16.315	**10.707**
PG52	0.00	0.30	-7.481	0.647	7.97	0.920	15.942	**10.822**
	0.10	0.30	-7.488	0.714	6.75	0.870	15.973	**11.215**

Appendix G

Fatigue Model Analysis of the Modified Mixtures

Table G.1 Pearson correlation matrix for the dependent and independent variables of mixture containing ambient rubber and RAP L tested at 20ºC

	$Ln(N_f)$	$Ln(S_0)$	$Ln(w_0)$	$Ln(\varepsilon_0)$	VFA	V_0	R_b	R_P
$Ln(N_f)$	1.000							
$Ln(S_0)$	0.021	1.000						
$Ln(w_0)$	0.439	0.368	1.000					
$Ln(\varepsilon_0)$	0.383	-0.116	0.405	1.000				
VFA	0.372	-0.557	-0.322	0.071	1.000			
V_0	-0.606	-0.034	-0.374	0.030	0.065	1.000		
R_b	-0.120	-0.225	-0.665	-0.333	0.554	0.173	1.000	
R_P	-0.638	0.457	-0.081	-0.289	-0.601	0.369	0.000	1.000

Table G.2 Pearson correlation matrix for the dependent and independent variables of mixture containing cryogenic rubber and RAP L tested at 5ºC

	$Ln(N_f)$	$Ln(S_0)$	$Ln(w_0)$	$Ln(\varepsilon_0)$	VFA	V_0	R_b	R_P
$Ln(N_f)$	1.000							
$Ln(S_0)$	0.119	1.000						
$Ln(w_0)$	0.202	-0.106	1.000					
$Ln(\varepsilon_0)$	0.165	-0.694	0.202	1.000				
VFA	0.066	-0.131	0.371	0.271	1.000			
V_0	-0.425	-0.264	-0.052	0.229	0.378	1.000		
R_b	-0.425	-0.282	-0.200	0.001	-0.559	0.139	1.000	
R_P	-0.381	0.005	0.025	0.145	0.507	0.833	0.000	1.000

Table G.3 Pearson correlation matrix for the dependent and independent variables of mixture containing cryogenic rubber and RAP L tested at 20ºC

	$Ln(N_f)$	$Ln(S_0)$	$Ln(w_0)$	$Ln(\varepsilon_0)$	VFA	V_0	R_b	R_P
$Ln(N_f)$	1.000							
$Ln(S_0)$	-0.331	1.000						
$Ln(w_0)$	0.494	-0.390	1.000					
$Ln(\varepsilon_0)$	0.514	-0.660	0.068	1.000				
VFA	-0.136	0.025	0.058	-0.203	1.000			
V_0	-0.456	-0.083	-0.121	-0.420	0.536	1.000		
R_b	-0.337	-0.045	-0.497	0.063	-0.559	-0.114	1.000	
R_P	-0.660	0.262	-0.248	-0.570	0.507	0.656	0.000	1.000

Table G.4 ANOVA and GLM of log fatigue life for mixture containing ambient rubber and RAP L tested at 20ºC (traditional strain dependent VFA method)

Dep. Variable	Multiple R	R Square	Adjusted R Square	Standard Error	Number of Samples	
Ln (N_f)	0.601	0.362	0.202	0.478	16*(4 repetition)	
Analysis of Varance (ANOVA)						
	df	Sum of Square	Mean Square	F Ratio	Significance F	C.V.
Regression	3	1.553	0.518	2.267	0.133	82.336
Residual	12	2.740	0.228			
Total	15	4.293				
	Coefficients	Standard Error	t Stat	P-value	Lower 95%	Upper 95%
Intercept	12.711	39.412	0.323	0.753	-73.161	98.584
Ln (ε_0)	6.520	3.909	1.668	0.121	-1.997	15.036
VFA	20.854	10.483	1.989	0.070	-1.986	43.694
Ln (S_0)	1.911	1.426	1.340	0.205	-1.196	5.018

Table G.5 ANOVA and GLM of log fatigue life for mixture containing ambient rubber and RAP L tested at 20ºC (specific strain dependent VFA method)

Dep. Variable	Multiple R	R Square	Adjusted R Square	Standard Error	Number of Samples	
Ln (N_f)	0.918	0.843	0.530	0.367	16*(4 repetition)	
Analysis of Varance (ANOVA)						
	df	Sum of Square	Mean Square	F Ratio	Significance F	C.V.
Regression	10	3.620	0.362	2.692	0.143	66.047
Residual	5	0.672	0.134			
Total	15	4.293				
	Coefficients	Standard Error	t Stat	P-value	Lower 95%	Upper 95%
Intercept	-60.237	66.009	-0.913	0.403	-229.918	109.445
R_b	-77.258	368.276	-0.210	0.842	-1023.939	869.424
R_p	327.099	243.613	1.343	0.237	-299.126	953.324
$R_{b*}R_p$	70.662	102.661	0.688	0.522	-193.236	334.560
R_b^2	37.751	502.622	0.075	0.943	-1254.278	1329.781
R_b^3	58.086	2516.602	0.023	0.982	-6411.035	6527.206
Ln (ε_0)	6.156	7.284	0.845	0.437	-12.567	24.880
VFA	104.538	60.837	1.718	0.146	-51.849	260.925
R_b*VFA	68.971	452.400	0.152	0.885	-1093.958	1231.899
R_p*VFA	-443.894	330.341	-1.344	0.237	-1293.061	405.273
Ln (S_0)	2.437	2.397	1.017	0.356	-3.725	8.599

Table G.6 ANOVA and GLM of log fatigue life for mixture containing ambient rubber and RAP L tested at 20ºC (traditional strain dependent air void method)

Dep. Variable	Multiple R	R Square	Adjusted R Square	Standard Error	Number of Samples	
Ln (N_f)	0.728	0.530	0.413	0.410	16*(4 repetition)	
Analysis of Varance (ANOVA)						
	df	Sum of Square	Mean Square	F Ratio	Significance F	C.V.
Regression	3	2.277	0.759	4.517	0.024	106.577
Residual	12	2.016	0.168			
Total	15	4.293				
	Coefficients	Standard Error	t Stat	P-value	Lower 95%	Upper 95%
Intercept	60.501	28.663	2.111	0.056	-1.950	122.952
Ln (ε_0)	6.851	3.354	2.043	0.064	-0.456	14.159
V_0	-0.386	0.124	-3.113	0.009	-0.656	-0.116
Ln (S_0)	0.243	1.019	0.239	0.815	-1.977	2.463

Table G.7 ANOVA and GLM of log fatigue life for mixture containing ambient rubber and RAP L tested at 20ºC (specific strain dependent air void method)

Dep. Variable	Multiple R	R Square	Adjusted R Square	Standard Error	Number of Samples	
Ln (N_f)	0.954	0.911	0.733	0.276	16*(4 repetition)	
Analysis of Varance (ANOVA)						
	df	Sum of Square	Mean Square	F Ratio	Significance F	C.V.
Regression	10	3.911	0.391	5.122	0.043	69.180
Residual	5	0.382	0.076			
Total	15	4.293				
	Coefficients	Standard Error	t Stat	P-value	Lower 95%	Upper 95%
Intercept	7.857	35.787	0.220	0.835	-84.135	99.849
R_b	32.289	19.434	1.662	0.158	-17.667	82.245
R_p	-0.497	7.690	-0.065	0.951	-20.264	19.270
$R_{b*}R_p$	-19.136	14.297	-1.338	0.238	-55.887	17.615
R_b^2	-135.185	287.404	-0.470	0.658	-873.980	603.609
R_b^3	862.910	1297.467	0.665	0.535	-2472.331	4198.151
Ln (ε_0)	8.228	4.106	2.004	0.101	-2.326	18.782
V_0	0.275	0.299	0.917	0.401	-0.495	1.044
R_b*V_0	-4.221	2.008	-2.102	0.089	-9.381	0.940
R_p*V_0	-0.299	1.326	-0.225	0.831	-3.708	3.111
Ln (S_0)	3.874	1.194	3.243	0.023	0.803	6.944

Table G.8 ANOVA and GLM of log fatigue life for mixture containing cryogenic rubber and RAP L tested at 5ºC (traditional strain dependent VFA method)

Dep. Variable	Multiple R	R Square	Adjusted R Square	Standard Error	Number of Samples	
Ln (N_f)	0.365	0.133	-0.084	0.569	16*(2 or 4 repetition)	
Analysis of Varance (ANOVA)						
	df	Sum of Square	Mean Square	F Ratio	Significance F	C.V.
Regression	3	0.595	0.198	0.614	0.619	46.858
Residual	12	3.880	0.323			
Total	15	4.475				
	Coefficients	Standard Error	t Stat	P-value	Lower 95%	Upper 95%
Intercept	11.828	33.115	0.357	0.727	-60.324	83.980
Ln (ε_0)	6.693	5.375	1.245	0.237	-5.017	18.403
VFA	-0.095	5.587	-0.017	0.987	-12.267	12.077
Ln (S_0)	2.887	2.392	1.207	0.251	-2.326	8.099

Table G.9 ANOVA and GLM of log fatigue life for mixture containing cryogenic rubber and RAP L tested at 5ºC (specific strain dependent VFA method)

Dep. Variable	Multiple R	R Square	Adjusted R Square	Standard Error	Number of Samples	
Ln (N_f)	0.805	0.648	-0.056	0.561	16*(2 or 4 repetition)	
Analysis of Varance (ANOVA)						
	df	Sum of Square	Mean Square	F Ratio	Significance F	C.V.
Regression	10	2.900	0.290	0.920	0.576	58.003
Residual	5	1.575	0.315			
Total	15	4.475				
	Coefficients	Standard Error	t Stat	P-value	Lower 95%	Upper 95%
Intercept	37.210	62.432	0.596	0.577	-123.276	197.697
R_b	312.472	297.234	1.051	0.341	-451.591	1076.535
R_p	-16.408	53.343	-0.308	0.771	-153.531	120.715
R_b*R_p	69.539	64.538	1.077	0.330	-96.362	235.440
R_b^2	114.458	844.960	0.135	0.898	-2057.577	2286.493
R_b^3	-671.276	3337.113	-0.201	0.849	-9249.584	7907.032
Ln (ε_0)	9.202	6.768	1.360	0.232	-8.195	26.598
VFA	7.478	24.377	0.307	0.771	-55.186	70.141
R_b*VFA	-471.001	377.966	-1.246	0.268	-1442.593	500.590
R_p*VFA	19.222	73.030	0.263	0.803	-168.507	206.952
Ln (S_0)	2.226	3.242	0.687	0.523	-6.107	10.559

Table G.10 ANOVA and GLM of log fatigue life for mixture containing cryogenic rubber and RAP L tested at 5ºC (traditional strain dependent air void method)

Dep. Variable	Multiple R	R Square	Adjusted R Square	Standard Error	Number of Samples	
Ln (N_f)	0.565	0.319	0.149	0.504	16*(2 or 4 repetition)	
Analysis of Varance (ANOVA)						
	df	Sum of Square	Mean Square	F Ratio	Significance F	C.V.
Regression	3	1.428	0.476	1.874	0.188	78.069
Residual	12	3.048	0.254			
Total	15	4.475				
	Coefficients	Standard Error	t Stat	P-value	Lower 95%	Upper 95%
Intercept	26.626	28.907	0.921	0.375	-36.357	89.608
Ln (ε_0)	7.215	4.618	1.562	0.144	-2.847	17.278
V_0	-0.195	0.108	-1.810	0.095	-0.429	0.040
Ln (S_0)	2.302	2.137	1.077	0.303	-2.354	6.959

Table G.11 ANOVA and GLM of log fatigue life for mixture containing cryogenic rubber and RAP L tested at 5ºC (specific strain dependent air void method)

Dep. Variable	Multiple R	R Square	Adjusted R Square	Standard Error	Number of Samples	
Ln (N_f)	0.804	0.647	-0.060	0.562	16*(2 or 4 repetition)	
Analysis of Varance (ANOVA)						
	df	Sum of Square	Mean Square	F Ratio	Significance F	C.V.
Regression	10	2.894	0.289	0.915	0.579	57.930
Residual	5	1.582	0.316			
Total	15	4.475				
	Coefficients	Standard Error	t Stat	P-value	Lower 95%	Upper 95%
Intercept	-73.065	92.876	-0.787	0.467	-311.809	165.680
R_b	-71.290	51.934	-1.373	0.228	-204.790	62.211
R_p	0.119	10.131	0.012	0.991	-25.922	26.161
$R_{b*}R_p$	-83.436	78.208	-1.067	0.335	-284.476	117.604
R_b^2	853.669	765.270	1.116	0.315	-1113.517	2820.856
R_b^3	-3545.121	3132.554	-1.132	0.309	-11597.593	4507.351
Ln (ε_0)	4.179	8.374	0.499	0.639	-17.347	25.704
V_0	-0.414	1.282	-0.323	0.760	-3.711	2.882
R_b*V_0	6.870	7.867	0.873	0.422	-13.353	27.093
R_p*V_0	0.367	2.068	0.178	0.866	-4.949	5.684
Ln (S_0)	6.888	6.173	1.116	0.315	-8.980	22.757

Table G.12 ANOVA and GLM of log fatigue life for mixture containing cryogenic rubber and RAP L tested at 20ºC (traditional strain dependent VFA method)

Dep. Variable	Multiple R	R Square	Adjusted R Square	Standard Error	Number of Samples	
Ln (N_f)	0.515	0.265	0.081	0.404	16*(2 or 4 repetition)	
Analysis of Varance (ANOVA)						
	df	Sum of Square	Mean Square	F Ratio	Significance F	C.V.
Regression	3	0.705	0.235	1.443	0.279	51.482
Residual	12	1.955	0.163			
Total	15	2.660				
	Coefficients	Standard Error	t Stat	P-value	Lower 95%	Upper 95%
Intercept	78.758	36.526	2.156	0.052	-0.825	158.340
Ln (ε_0)	9.102	6.029	1.510	0.157	-4.035	22.238
VFA	-0.490	3.928	-0.125	0.903	-9.048	8.068
Ln (S_0)	0.024	0.906	0.026	0.980	-1.951	1.998

Table G.13 ANOVA and GLM of log fatigue life for mixture containing cryogenic rubber and RAP L tested at 20ºC (specific strain dependent VFA method)

Dep. Variable	Multiple R	R Square	Adjusted R Square	Standard Error	Number of Samples	
Ln (N_f)	0.857	0.734	0.202	0.376	16*(2 or 4 repetition)	
Analysis of Varance (ANOVA)						
	df	Sum of Square	Mean Square	F Ratio	Significance F	C.V.
Regression	10	1.952	0.195	1.380	0.380	46.434
Residual	5	0.707	0.141			
Total	15	2.660				
	Coefficients	Standard Error	t Stat	P-value	Lower 95%	Upper 95%
Intercept	34.566	59.974	0.576	0.589	-119.601	188.733
R_b	-179.951	172.024	-1.046	0.343	-622.154	262.251
R_p	47.035	37.374	1.259	0.264	-49.038	143.108
$R_{b*}R_p$	-43.393	36.804	-1.179	0.291	-137.999	51.214
R_b^2	510.063	693.745	0.735	0.495	-1273.261	2293.388
R_b^3	-1982.051	2887.692	-0.686	0.523	-9405.087	5440.985
Ln (ε_0)	2.927	8.394	0.349	0.741	-18.650	24.505
VFA	-6.216	17.179	-0.362	0.732	-50.375	37.942
R_b*VFA	213.330	218.434	0.977	0.374	-348.173	774.832
R_p*VFA	-66.247	50.968	-1.300	0.250	-197.263	64.769
Ln (S_0)	0.181	1.241	0.145	0.890	-3.009	3.370

Table G.14 ANOVA and GLM of log fatigue life for mixture containing cryogenic rubber and RAP L tested at 20ºC (traditional air void models)

Dep. Variable	Multiple R	R Square	Adjusted R Square	Standard Error	Number of Samples
Ln (N_f)	0.598	0.357	0.196	0.378	16*(2 or 4 repetition)
Analysis of Varance (ANOVA)					
	df	Sum of Square	Mean Square	F Ratio	Significance F	C.V.
Regression	3	0.950	0.317	2.222	0.138	61.029
Residual	12	1.710	0.143			
Total	15	2.660				
	Coefficients	Standard Error	t Stat	P-value	Lower 95%	Upper 95%
Intercept	47.360	41.594	1.139	0.277	-43.266	137.986
Ln (ε_0)	3.393	7.063	0.480	0.640	-11.997	18.782
V_0	-0.166	0.126	-1.317	0.213	-0.441	0.109
Ln (S_0)	-0.646	0.987	-0.655	0.525	-2.798	1.505

Table G.15 ANOVA and GLM of log fatigue life for mixture containing cryogenic rubber and RAP L tested at 20ºC (specific strain dependent air void method)

Dep. Variable	Multiple R	R Square	Adjusted R Square	Standard Error	Number of Samples
Ln (N_f)	0.853	0.727	0.182	0.381	16*(2 or 4 repetition)
Analysis of Varance (ANOVA)					
	df	Sum of Square	Mean Square	F Ratio	Significance F	C.V.
Regression	10	1.935	0.193	1.334	0.395	46.202
Residual	5	0.725	0.145			
Total	15	2.660				
	Coefficients	Standard Error	t Stat	P-value	Lower 95%	Upper 95%
Intercept	-2.371	66.923	-0.035	0.973	-174.403	169.661
R_b	-25.684	31.598	-0.813	0.453	-106.910	55.541
R_p	7.151	7.266	0.984	0.370	-11.527	25.829
$R_{b*}R_p$	-22.607	31.090	-0.727	0.500	-102.525	57.311
R_b^2	364.481	505.337	0.721	0.503	-934.526	1663.488
R_b^3	-1553.172	2269.034	-0.685	0.524	-7385.901	4279.556
Ln (ε_0)	-1.275	9.986	-0.128	0.903	-26.946	24.396
V_0	0.090	0.418	0.215	0.838	-0.984	1.164
R_b*V_0	1.334	3.028	0.441	0.678	-6.449	9.116
R_p*V_0	-1.431	1.174	-1.219	0.277	-4.450	1.587
Ln (S_0)	0.190	1.454	0.130	0.901	-3.548	3.927

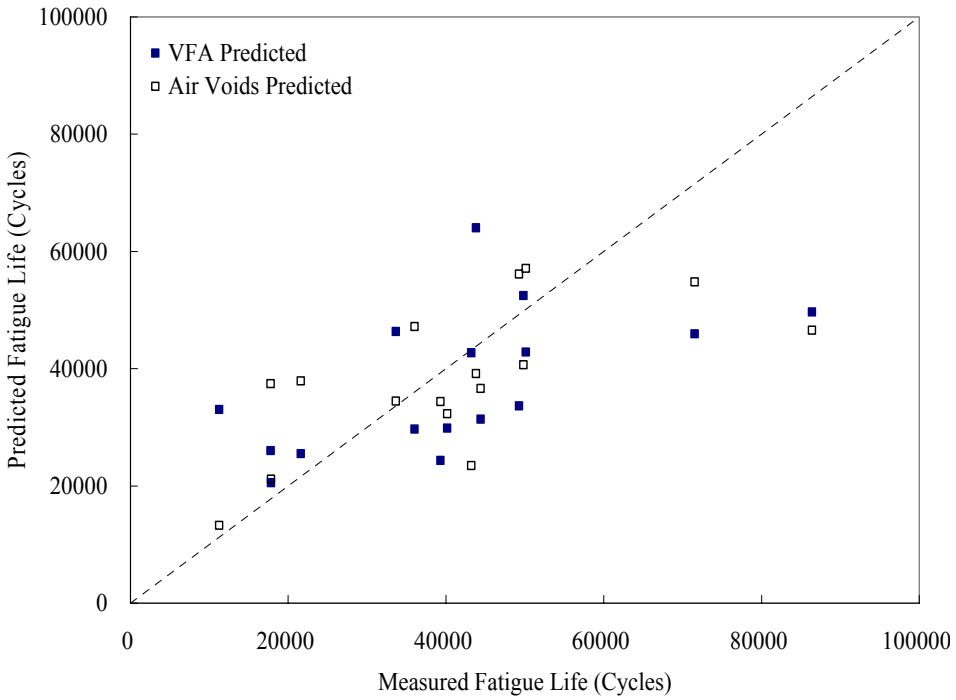

Figure G.1 Comparison of fatigue lives between predicted and measured results using traditional strain dependent method at 20°C (containing ambient rubber and RAP L)

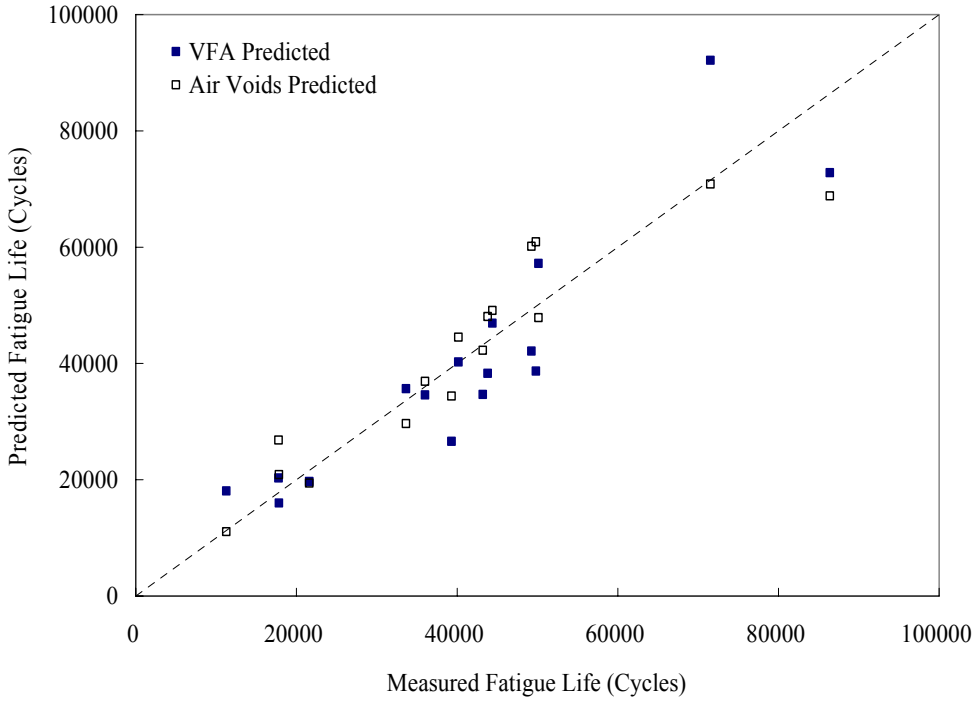

Figure G.2 Comparison of fatigue lives between predicted and measured results using specific strain dependent method at 20°C (containing ambient rubber and RAP L)

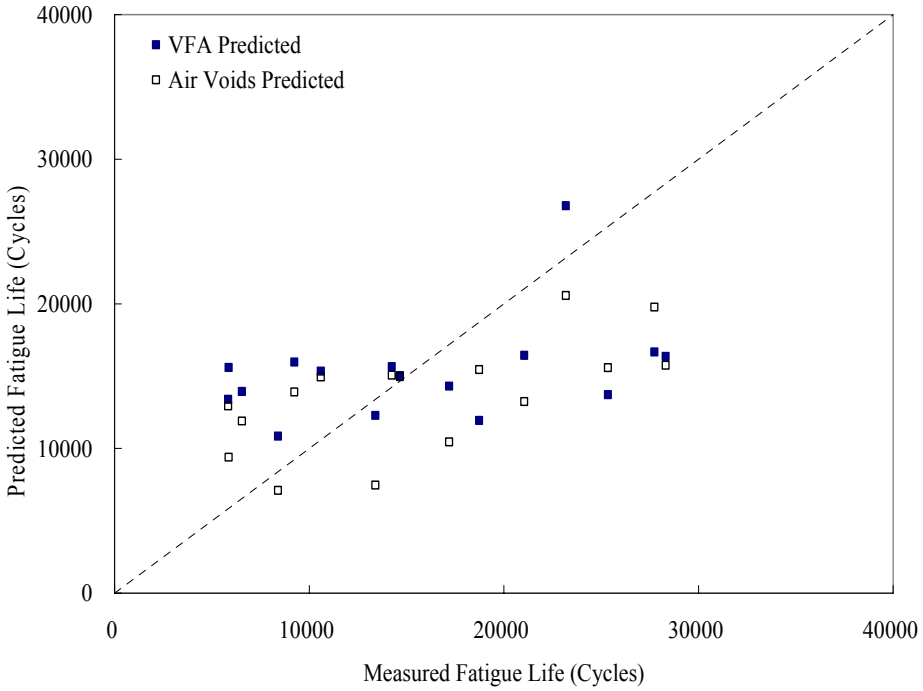

Figure G.3 Comparison of fatigue lives between predicted and measured results using traditional strain dependent method at 5°C (containing cryogenic rubber and RAP L)

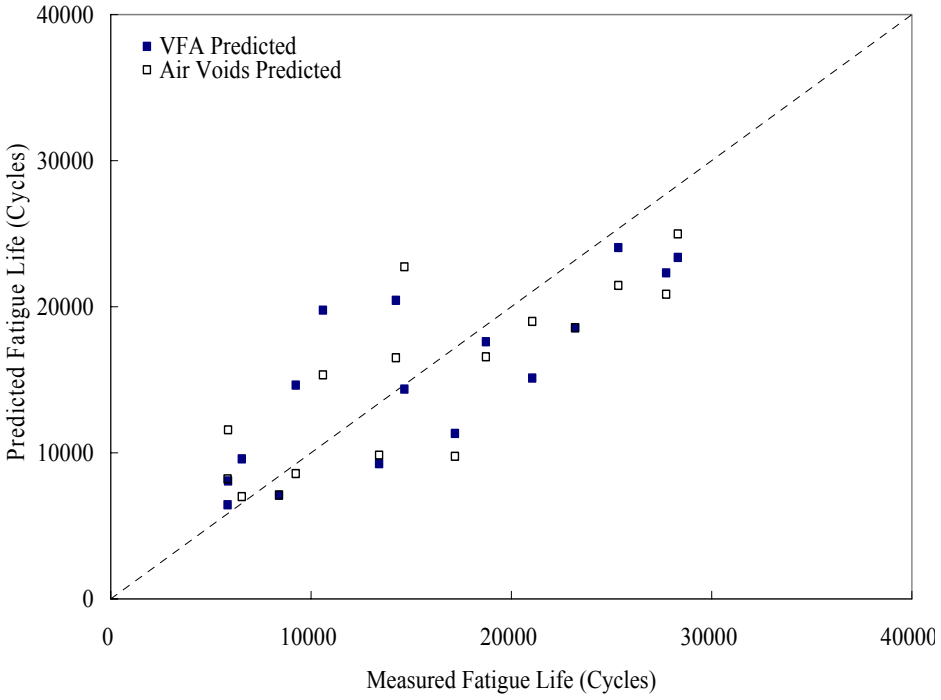

Figure G.4 Comparison of fatigue lives between predicted and measured results using specific strain dependent method at 5°C (containing cryogenic rubber and RAP L)

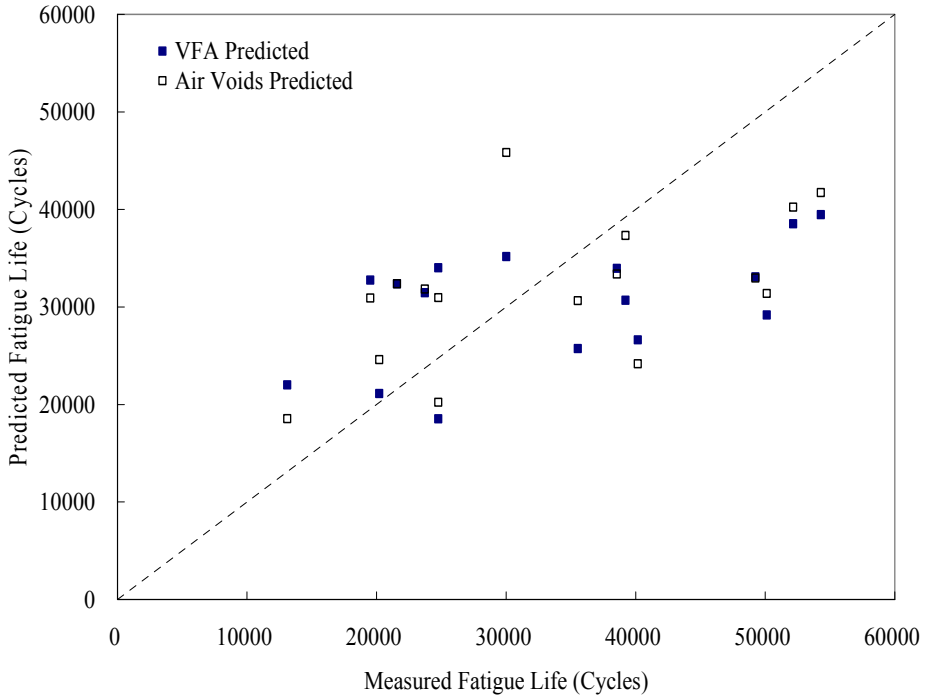

Figure G.5 Comparison of fatigue lives between predicted and measured results using traditional strain dependent method at 20°C (containing cryogenic rubber and RAP L)

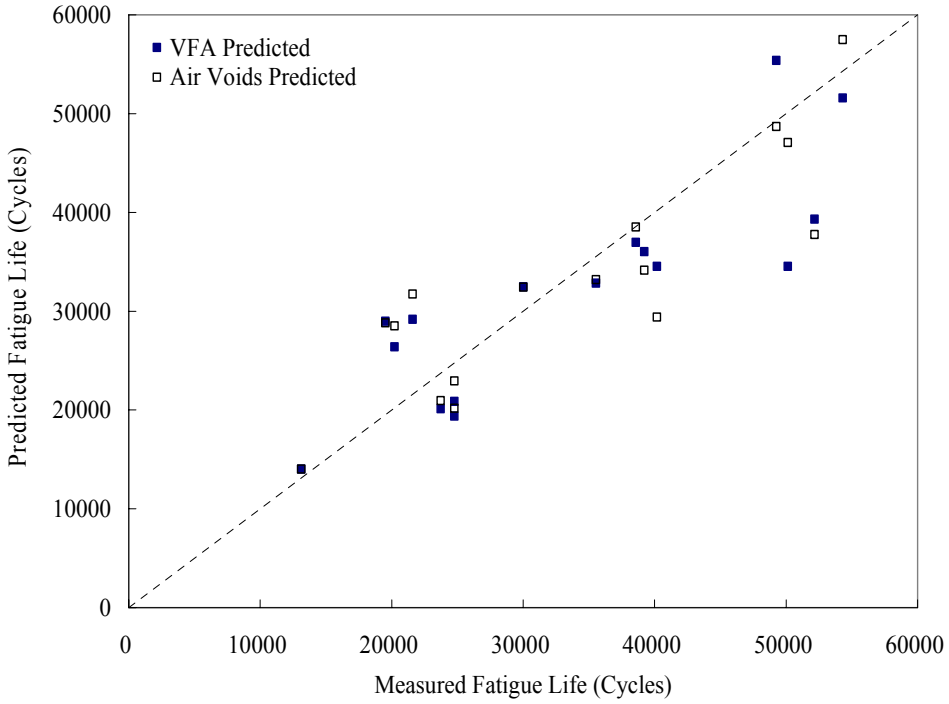

Figure G.6 Comparison of fatigue lives between predicted and measured results using specific strain dependent method at 20°C (containing cryogenic rubber and RAP L)

Table G.16 ANOVA and GLM of log fatigue life for mixture containing ambient rubber and RAP L tested at 5ºC (traditional energy dependent VFA method)

Dep. Variable	Multiple R	R Square	Adjusted R Square	Standard Error	Number of Samples	
Ln (N_f)	0.471	0.222	0.102	0.392	16*(4 repetition)	
Analysis of Varance (ANOVA)						
	df	Sum of Square	Mean Square	F Ratio	Significance F	C.V.
Regression	2	0.569	0.285	1.851	0.196	57.393
Residual	13	1.999	0.154			
Total	15	2.569				
	Coefficients	Standard Error	t Stat	P-value	Lower 95%	Upper 95%
Intercept	-0.313	5.544	-0.057	0.956	-12.291	11.664
VFA	13.819	7.320	1.888	0.082	-1.994	29.632
Ln (w_0)	0.013	0.278	0.047	0.963	-0.588	0.615

Table G.17 ANOVA and GLM of log fatigue life for mixture containing ambient rubber and RAP L tested at 5ºC (specific energy dependent VFA method)

Dep. Variable	Multiple R	R Square	Adjusted R Square	Standard Error	Number of Samples	
Ln (N_f)	0.891	0.794	0.484	0.297	16*(4 repetition)	
Analysis of Varance (ANOVA)						
	df	Sum of Square	Mean Square	F Ratio	Significance F	C.V.
Regression	9	2.039	0.227	2.565	0.132	50.424
Residual	6	0.530	0.088			
Total	15	2.569				
	Coefficients	Standard Error	t Stat	P-value	Lower 95%	Upper 95%
Intercept	-12.103	34.952	-0.346	0.741	-97.628	73.422
R_b	-533.901	211.889	-2.520	0.045	-1052.375	-15.426
R_p	164.648	177.014	0.930	0.388	-268.491	597.787
$R_{b*}R_p$	106.369	57.163	1.861	0.112	-33.504	246.241
R_b^2	374.595	217.368	1.723	0.136	-157.285	906.475
R_b^3	-2039.898	986.201	-2.068	0.084	-4453.046	373.250
VFA	30.095	46.925	0.641	0.545	-84.726	144.916
R_b*VFA	665.870	268.427	2.481	0.048	9.053	1322.688
R_p*VFA	-224.969	239.520	-0.939	0.384	-811.054	361.117
Ln (w_0)	0.021	0.315	0.068	0.948	-0.749	0.792

Table G.18 ANOVA and GLM of log fatigue life for mixture containing ambient rubber and RAP L tested at 5ºC (traditional energy dependent air void method)

Dep. Variable	Multiple R	R Square	Adjusted R Square	Standard Error	Number of Samples	
Ln (N_f)	0.312	0.097	-0.041	0.422	16*(4 repetition)	
Analysis of Varance (ANOVA)						
	df	Sum of Square	Mean Square	F Ratio	Significance F	C.V.
Regression	2	0.250	0.125	0.702	0.513	36.521
Residual	13	2.318	0.178			
Total	15	2.569				
	Coefficients	Standard Error	t Stat	P-value	Lower 95%	Upper 95%
Intercept	10.771	0.610	17.669	0.000	9.454	12.087
V_0	-0.117	0.104	-1.134	0.277	-0.341	0.106
Ln (w_0)	-0.192	0.304	-0.634	0.537	-0.848	0.463

Table G.19 ANOVA and GLM of log fatigue life for mixture containing ambient rubber and RAP L tested at 5ºC (specific energy dependent air void method)

Dep. Variable	Multiple R	R Square	Adjusted R Square	Standard Error	Number of Samples	
Ln (N_f)	0.814	0.663	0.157	0.380	16*(4 repetition)	
Analysis of Varance (ANOVA)						
	df	Sum of Square	Mean Square	F Ratio	Significance F	C.V.
Regression	9	1.703	0.189	1.311	0.383	45.639
Residual	6	0.866	0.144			
Total	15	2.569				
	Coefficients	Standard Error	t Stat	P-value	Lower 95%	Upper 95%
Intercept	10.690	2.432	4.395	0.005	4.739	16.641
R_b	-7.941	24.979	-0.318	0.761	-69.064	53.181
R_p	-4.052	11.472	-0.353	0.736	-32.123	24.018
$R_{b*}R_p$	47.008	24.070	1.953	0.099	-11.889	105.905
R_b^2	365.008	364.356	1.002	0.355	-526.539	1256.555
R_b^3	-1576.814	1577.968	-0.999	0.356	-5437.964	2284.337
V_0	0.018	0.649	0.027	0.979	-1.571	1.606
R_b*V_0	-3.849	3.072	-1.253	0.257	-11.367	3.669
R_p*V_0	0.450	2.495	0.180	0.863	-5.655	6.556
Ln (w_0)	-0.630	0.555	-1.136	0.299	-1.988	0.727

Table G.20 ANOVA and GLM of log fatigue life for mixture containing ambient rubber and RAP L tested at 20ºC (traditional energy dependent VFA method)

Dep. Variable	Multiple R	R Square	Adjusted R Square	Standard Error	Number of Samples	
Ln (N_f)	0.697	0.486	0.407	0.412	16*(4 repetition)	
Analysis of Varance (ANOVA)						
	df	Sum of Square	Mean Square	F Ratio	Significance F	C.V.
Regression	2	2.087	1.044	6.151	0.013	135.623
Residual	13	2.205	0.170			
Total	15	4.293				
	Coefficients	Standard Error	t Stat	P-value	Lower 95%	Upper 95%
Intercept	-7.819	6.212	-1.259	0.230	-21.239	5.601
VFA	21.609	7.926	2.726	0.017	4.485	38.732
Ln (w_0)	2.557	0.862	2.967	0.011	0.695	4.419

Table G.21 ANOVA and GLM of log fatigue life for mixture containing ambient rubber and RAP L tested at 20ºC (specific energy dependent VFA method)

Dep. Variable	Multiple R	R Square	Adjusted R Square	Standard Error	Number of Samples	
Ln (N_f)	0.897	0.805	0.513	0.373	16*(4 repetition)	
Analysis of Varance (ANOVA)						
	df	Sum of Square	Mean Square	F Ratio	Significance F	C.V.
Regression	9	3.456	0.384	2.756	0.115	68.426
Residual	6	0.836	0.139			
Total	15	4.293				
	Coefficients	Standard Error	t Stat	P-value	Lower 95%	Upper 95%
Intercept	-94.262	46.429	-2.030	0.089	-207.869	19.345
R_b	-382.459	260.887	-1.466	0.193	-1020.828	255.910
R_p	500.844	224.395	2.232	0.067	-48.232	1049.920
$R_{b*}R_p$	155.552	78.638	1.978	0.095	-36.867	347.971
R_b^2	403.843	273.702	1.475	0.191	-265.882	1073.568
R_b^3	-1974.415	1259.409	-1.568	0.168	-5056.081	1107.250
VFA	141.750	63.994	2.215	0.069	-14.839	298.339
R_b*VFA	433.204	327.652	1.322	0.234	-368.533	1234.940
R_p*VFA	-680.062	303.800	-2.239	0.066	-1423.435	63.312
Ln (w_0)	0.232	1.588	0.146	0.888	-3.654	4.118

Table G.22 ANOVA and GLM of log fatigue life for mixture containing ambient rubber and RAP L tested at 20ºC (traditional energy dependent air void method)

Dep. Variable	Multiple R	R Square	Adjusted R Square	Standard Error	Number of Samples	
Ln (N_f)	0.648	0.419	0.330	0.438	16*(4 repetition)	
Analysis of Varance (ANOVA)						
	df	Sum of Square	Mean Square	F Ratio	Significance F	C.V.
Regression	2	1.801	0.900	4.696	0.029	120.840
Residual	13	2.492	0.192			
Total	15	4.293				
	Coefficients	Standard Error	t Stat	P-value	Lower 95%	Upper 95%
Intercept	11.633	1.369	8.497	0.000	8.676	14.591
V_0	-0.321	0.143	-2.254	0.042	-0.629	-0.013
Ln (w_0)	1.013	0.935	1.083	0.298	-1.007	3.033

Table G.23 ANOVA and GLM of log fatigue life for mixture containing ambient rubber and RAP L tested at 20ºC (specific energy dependent air void method)

Dep. Variable	Multiple R	R Square	Adjusted R Square	Standard Error	Number of Samples	
Ln (N_f)	0.885	0.783	0.457	0.394	16*(4 repetition)	
Analysis of Varance (ANOVA)						
	df	Sum of Square	Mean Square	F Ratio	Significance F	C.V.
Regression	9	3.361	0.373	2.404	0.149	67.280
Residual	6	0.932	0.155			
Total	15	4.293				
	Coefficients	Standard Error	t Stat	P-value	Lower 95%	Upper 95%
Intercept	6.373	3.190	1.998	0.093	-1.433	14.179
R_b	-4.507	23.077	-0.195	0.852	-60.973	51.960
R_p	9.265	11.925	0.777	0.467	-19.915	38.446
$R_{b*}R_p$	-5.021	17.774	-0.282	0.787	-48.513	38.470
R_b^2	287.657	280.087	1.027	0.344	-397.691	973.004
R_b^3	-1183.049	1208.610	-0.979	0.365	-4140.412	1774.315
V_0	0.414	0.446	0.927	0.390	-0.678	1.505
R_b*V_0	-1.510	2.869	-0.526	0.618	-8.532	5.511
R_p*V_0	-1.983	2.037	-0.973	0.368	-6.966	3.001
Ln (w_0)	2.533	1.417	1.787	0.124	-0.935	6.001

Table G.24 ANOVA and GLM of log fatigue life for mixture containing cryogenic rubber and RAP L tested at 5ºC (traditional energy dependent VFA method)

Dep. Variable	Multiple R	R Square	Adjusted R Square	Standard Error	Number of Samples	
Ln (N_f)	0.202	0.041	-0.107	0.575	16*(4 repetition)	
Analysis of Varance (ANOVA)						
	df	Sum of Square	Mean Square	F Ratio	Significance F	C.V.
Regression	2	0.182	0.091	0.276	0.763	30.900
Residual	13	4.293	0.330			
Total	15	4.475				
	Coefficients	Standard Error	t Stat	P-value	Lower 95%	Upper 95%
Intercept	9.253	3.944	2.346	0.036	0.731	17.774
VFA	-0.192	5.831	-0.033	0.974	-12.789	12.405
Ln (w_0)	0.508	0.724	0.702	0.495	-1.056	2.073

Table G.25 ANOVA and GLM of log fatigue life for mixture containing cryogenic rubber and RAP L tested at 5ºC (specific energy dependent VFA method)

Dep. Variable	Multiple R	R Square	Adjusted R Square	Standard Error	Number of Samples	
Ln (N_f)	0.717	0.515	-0.213	0.602	16*(4 repetition)	
Analysis of Varance (ANOVA)						
	df	Sum of Square	Mean Square	F Ratio	Significance F	C.V.
Regression	9	2.304	0.256	0.707	0.693	54.013
Residual	6	2.171	0.362			
Total	15	4.475				
	Coefficients	Standard Error	t Stat	P-value	Lower 95%	Upper 95%
Intercept	0.612	20.938	0.029	0.978	-50.622	51.846
R_b	284.009	300.068	0.946	0.380	-450.231	1018.250
R_p	-20.606	58.878	-0.350	0.738	-164.675	123.463
$R_{b*}R_p$	48.265	57.949	0.833	0.437	-93.532	190.062
R_b^2	163.872	765.452	0.214	0.838	-1709.123	2036.868
R_b^3	-1104.147	2910.792	-0.379	0.718	-8226.604	6018.310
VFA	12.935	28.972	0.446	0.671	-57.956	83.826
R_b*VFA	-420.703	383.143	-1.098	0.314	-1358.220	516.814
R_p*VFA	26.151	80.467	0.325	0.756	-170.744	223.047
Ln (w_0)	-0.085	0.885	-0.097	0.926	-2.251	2.080

Table G.26 ANOVA and GLM of log fatigue life for mixture containing cryogenic rubber and RAP L tested at 5ºC (traditional energy dependent air void method)

Dep. Variable	Multiple R	R Square	Adjusted R Square	Standard Error	Number of Samples	
Ln (N_f)	0.461	0.213	0.092	0.521	16*(4 repetition)	
Analysis of Varance (ANOVA)						
	df	Sum of Square	Mean Square	F Ratio	Significance F	C.V.
Regression	2	0.952	0.476	1.756	0.211	78.070
Residual	13	3.524	0.271			
Total	15	4.475				
	Coefficients	Standard Error	t Stat	P-value	Lower 95%	Upper 95%
Intercept	10.101	0.772	13.078	0.000	8.433	11.770
V0	-0.180	0.107	-1.685	0.116	-0.412	0.051
Ln (w_0)	0.445	0.610	0.730	0.478	-0.873	1.764

Table G.27 ANOVA and GLM of log fatigue life for mixture containing cryogenic rubber and RAP L tested at 5ºC (specific energy dependent air void method)

Dep. Variable	Multiple R	R Square	Adjusted R Square	Standard Error	Number of Samples	
Ln (N_f)	0.751	0.563	-0.091	0.571	16*(4 repetition)	
Analysis of Varance (ANOVA)						
	df	Sum of Square	Mean Square	F Ratio	Significance F	C.V.
Regression	9	2.522	0.280	0.860	0.597	56.866
Residual	6	1.954	0.326			
Total	15	4.475				
	Coefficients	Standard Error	t Stat	P-value	Lower 95%	Upper 95%
Intercept	15.772	4.027	3.916	0.008	5.918	25.626
R_b	-38.032	31.126	-1.222	0.268	-114.196	38.131
R_p	-1.734	8.653	-0.200	0.848	-22.908	19.439
$R_{b*}R_p$	-52.321	56.254	-0.930	0.388	-189.970	85.328
R_b^2	244.875	418.107	0.586	0.579	-778.196	1267.946
R_b^3	-1370.799	1856.723	-0.738	0.488	-5914.038	3172.441
V_0	-1.463	0.976	-1.498	0.185	-3.852	0.926
R_b*V_0	7.528	7.037	1.070	0.326	-9.692	24.748
R_p*V_0	1.716	1.651	1.039	0.339	-2.325	5.757
Ln (w_0)	-0.221	0.842	-0.262	0.802	-2.280	1.839

Table G.28 ANOVA and GLM of log fatigue life for mixture containing cryogenic rubber and RAP L tested at 20ºC (traditional energy dependent VFA method)

Dep. Variable	Multiple R	R Square	Adjusted R Square	Standard Error	Number of Samples	
Ln (N_f)	0.635	0.403	0.311	0.349	16*(4 repetition)	
Analysis of Varance (ANOVA)						
	df	Sum of Square	Mean Square	F Ratio	Significance F	C.V.
Regression	2	1.072	0.536	4.389	0.035	84.219
Residual	13	1.588	0.122			
Total	15	2.660				
	Coefficients	Standard Error	t Stat	P-value	Lower 95%	Upper 95%
Intercept	10.574	0.650	16.262	0.000	9.169	11.978
VFA	-0.169	0.091	-1.863	0.085	-0.365	0.027
Ln (w_0)	0.859	0.417	2.062	0.060	-0.041	1.759

Table G.29 ANOVA and GLM of log fatigue life for mixture containing cryogenic rubber and RAP L tested at 20ºC (specific energy dependent VFA method)

Dep. Variable	Multiple R	R Square	Adjusted R Square	Standard Error	Number of Samples	
Ln (N_f)	0.853	0.727	0.318	0.348	16*(4 repetition)	
Analysis of Varance (ANOVA)						
	df	Sum of Square	Mean Square	F Ratio	Significance F	C.V.
Regression	9	1.934	0.215	1.776	0.249	48.961
Residual	6	0.726	0.121			
Total	15	2.660				
	Coefficients	Standard Error	t Stat	P-value	Lower 95%	Upper 95%
Intercept	16.834	11.274	1.493	0.186	-10.752	44.420
R_b	-180.699	216.537	-0.834	0.436	-710.545	349.148
R_p	44.740	37.624	1.189	0.279	-47.323	136.803
$R_{b*}R_p$	-39.302	53.280	-0.738	0.489	-169.674	91.070
R_b^2	606.924	429.718	1.412	0.208	-444.560	1658.408
R_b^3	-2381.804	1656.987	-1.437	0.201	-6436.308	1672.700
VFA	-7.936	15.087	-0.526	0.618	-44.854	28.981
R_b*VFA	204.654	295.878	0.692	0.515	-519.335	928.642
R_p*VFA	-63.445	51.451	-1.233	0.264	-189.342	62.452
Ln (w_0)	-0.010	0.954	-0.010	0.992	-2.343	2.323

Table G.30 ANOVA and GLM of log fatigue life for mixture containing cryogenic rubber and RAP L tested at 20ºC (traditional energy dependent air void method)

Dep. Variable	Multiple R	R Square	Adjusted R Square	Standard Error	Number of Samples	
Ln (N_f)	0.520	0.271	0.159	0.386	16*(4 repetition)	
Analysis of Varance (ANOVA)						
	df	Sum of Square	Mean Square	F Ratio	Significance F	C.V.
Regression	2	0.720	0.360	2.414	0.128	65.846
Residual	13	1.940	0.149			
Total	15	2.660				
	Coefficients	Standard Error	t Stat	P-value	Lower 95%	Upper 95%
Intercept	11.331	2.585	4.384	0.001	5.747	16.915
V_0	-2.533	3.646	-0.695	0.499	-10.410	5.343
Ln (w_0)	0.971	0.458	2.121	0.054	-0.018	1.960

Table G.31 ANOVA and GLM of log fatigue life for mixture containing cryogenic rubber and RAP L tested at 20ºC (specific energy dependent air void method)

Dep. Variable	Multiple R	R Square	Adjusted R Square	Standard Error	Number of Samples	
Ln (N_f)	0.853	0.728	0.319	0.348	16*(4 repetition)	
Analysis of Varance (ANOVA)						
	df	Sum of Square	Mean Square	F Ratio	Significance F	C.V.
Regression	9	1.935	0.215	1.781	0.248	48.981
Residual	6	0.725	0.121			
Total	15	2.660				
	Coefficients	Standard Error	t Stat	P-value	Lower 95%	Upper 95%
Intercept	10.215	2.044	4.996	0.002	5.212	15.217
R_b	-20.660	23.021	-0.897	0.404	-76.990	35.670
R_p	6.533	6.890	0.948	0.380	-10.325	23.391
$R_{b*}R_p$	-19.009	26.534	-0.716	0.501	-83.936	45.918
R_b^2	261.512	269.059	0.972	0.369	-396.851	919.875
R_b^3	-1067.697	1183.503	-0.902	0.402	-3963.626	1828.233
V_0	0.076	0.375	0.202	0.846	-0.843	0.995
R_b*V_0	1.211	2.709	0.447	0.670	-5.418	7.840
R_p*V_0	-1.310	1.113	-1.176	0.284	-4.034	1.415
Ln (w_0)	0.178	0.627	0.284	0.786	-1.357	1.713

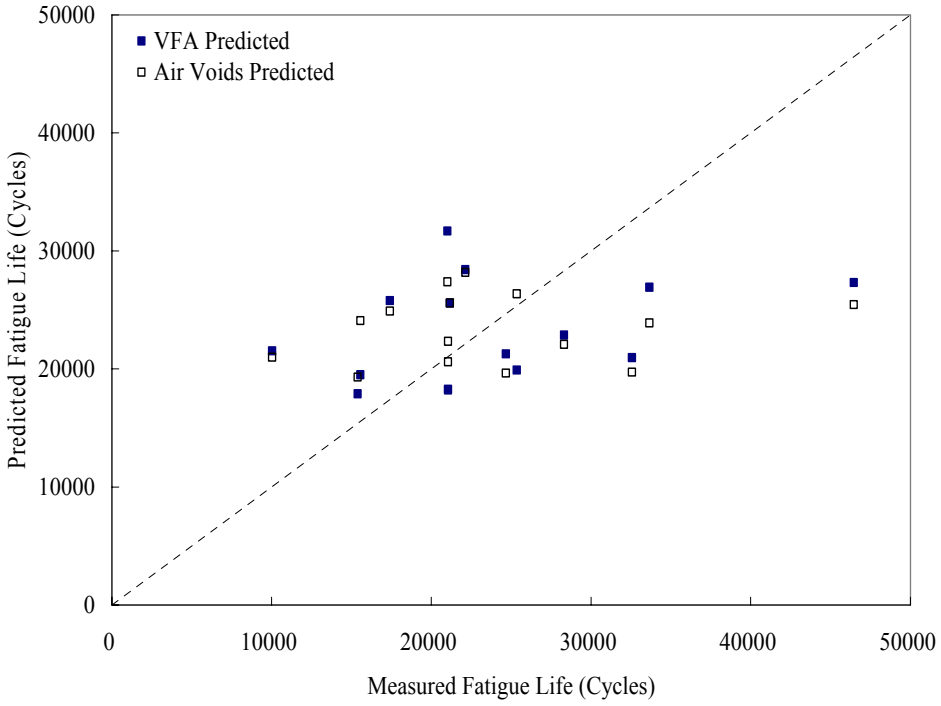

Figure G.7 Comparison of fatigue lives between predicted and measured results using traditional energy dependent method at 5°C (containing ambient rubber and RAP L)

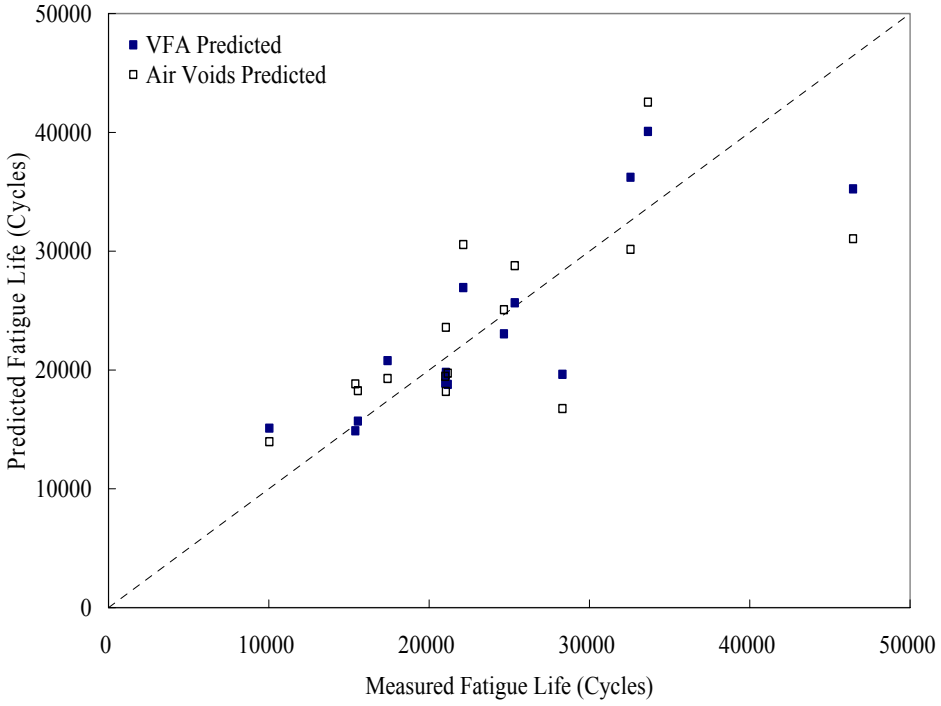

Figure G.8 Comparison of fatigue lives between predicted and measured results using specific energy dependent method at 5°C (containing ambient rubber and RAP L)

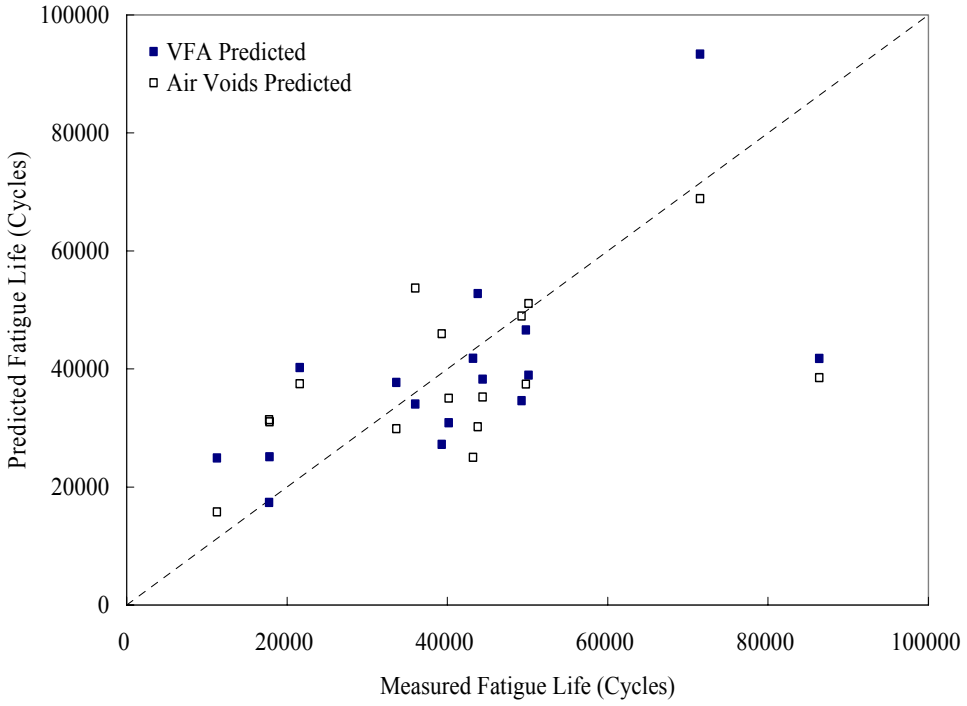

Figure G.9 Comparison of fatigue lives between predicted and measured results using traditional energy dependent method at 20°C (containing ambient rubber and RAP L)

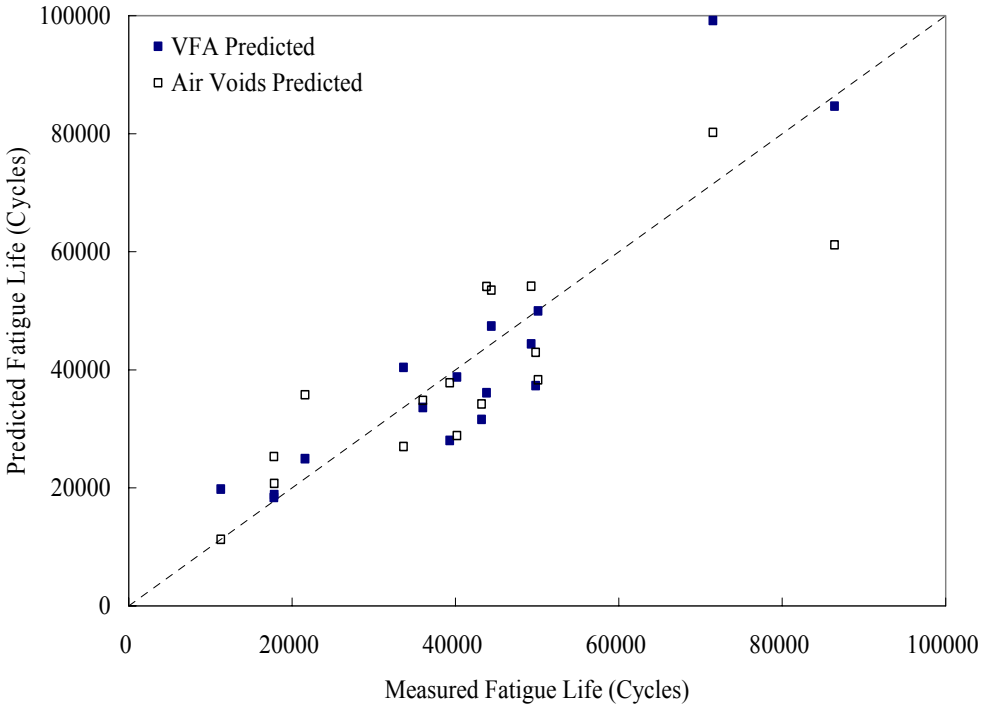

Figure G.10 Comparison of fatigue lives between predicted and measured results using specific energy dependent method at 20°C (containing ambient rubber and RAP L)

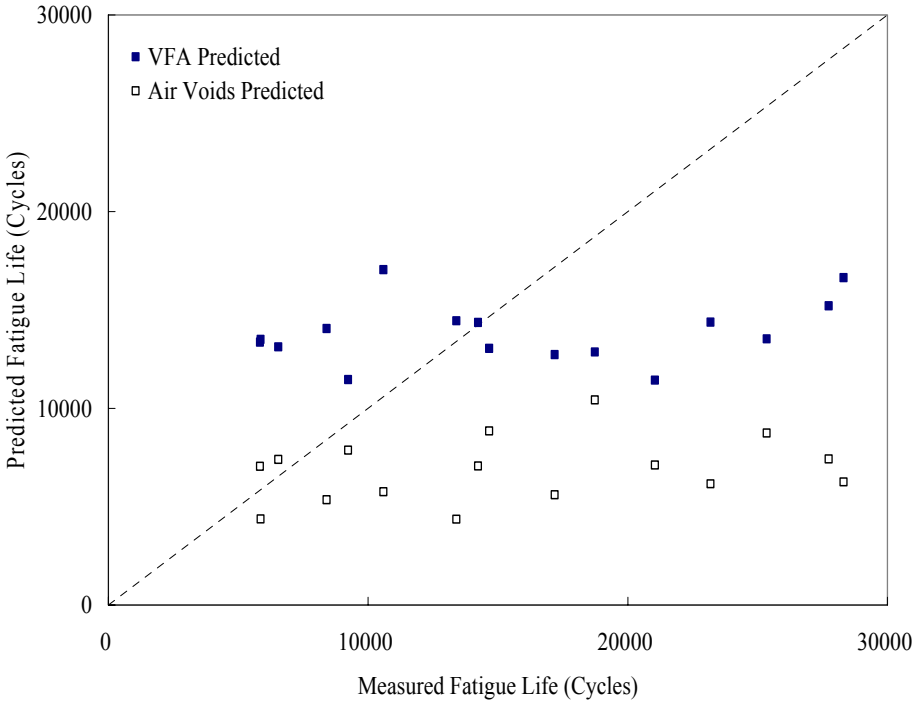

Figure G.11 Comparison of fatigue lives between predicted and measured results using traditional energy dependent method at 5°C (containing cryogenic rubber and RAP L)

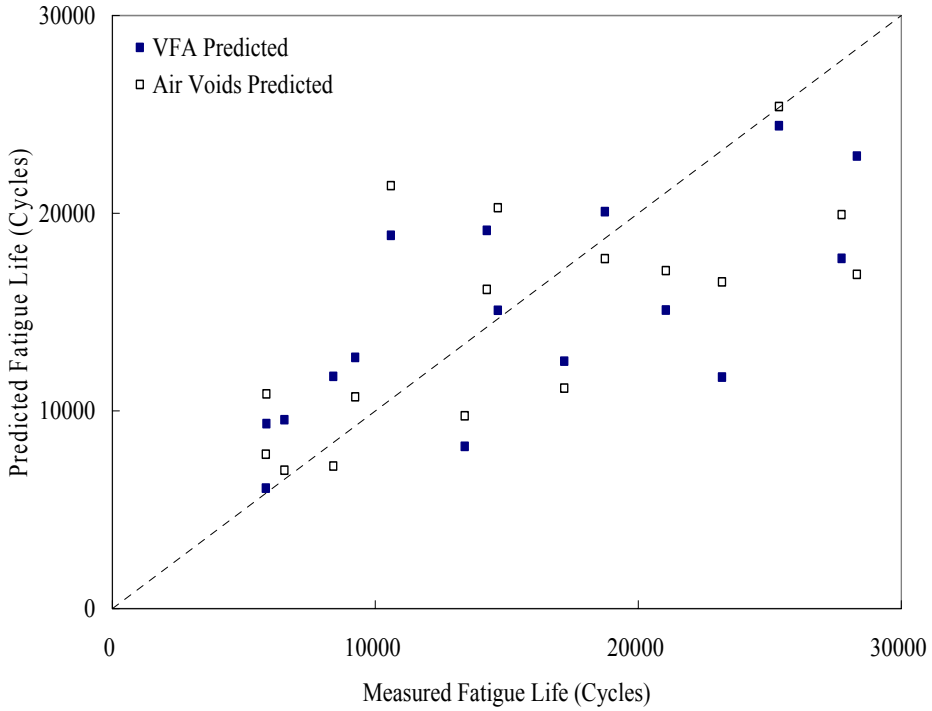

Figure G.12 Comparison of fatigue lives between predicted and measured results using specific energy dependent method at 5°C (containing cryogenic rubber and RAP L)

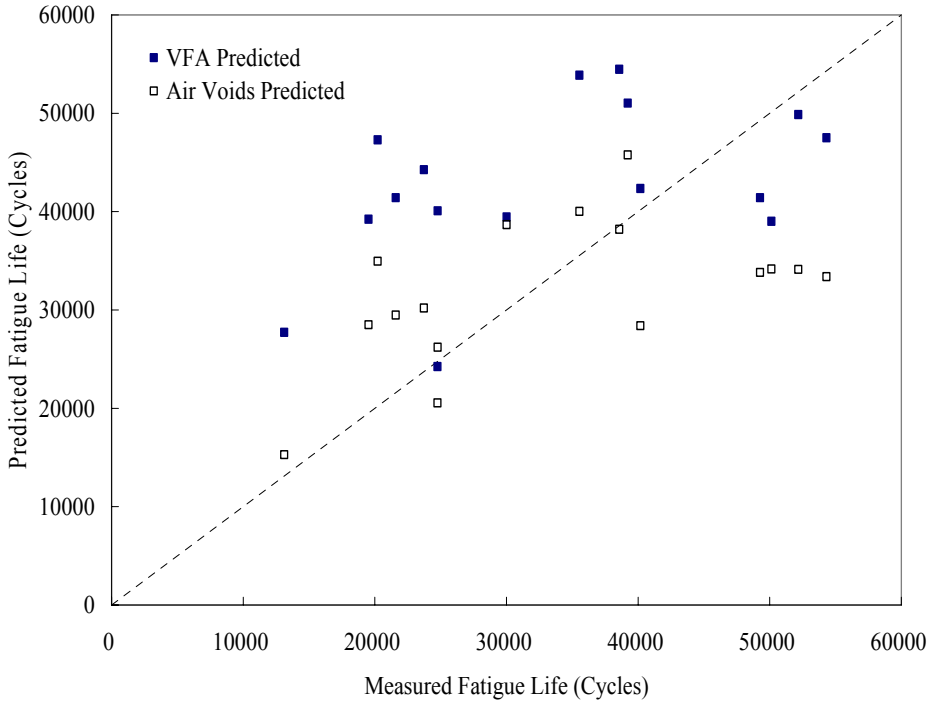

Figure G.13 Comparison of fatigue lives between predicted and measured results using traditional energy dependent method at 20°C (containing cryogenic rubber and RAP L)

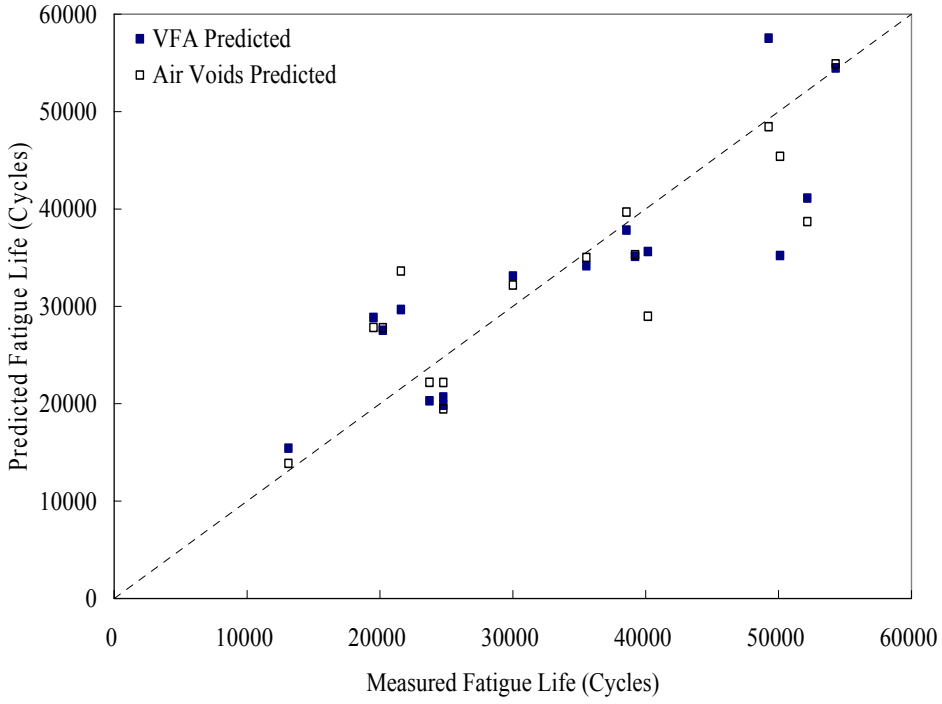

Figure G.14 Comparison of fatigue lives between predicted and measured results using specific energy dependent method at 20°C (containing cryogenic rubber and RAP L)

REFERENCES

Abbas A. R., Papagiannakis A. T., and Masad E. A. (2004) "Linear and Nolinear Viscoelastic Analysis of the Mixcrostructure of Asphalt Concrete," Journal of Materials in Civil Engineering, Vol. 16 pp. 133-139.

Advanced Asphalt Technologies, LLC, (2003) "Quarterly Progress Report to the National Cooperative Highway Research Program on Project NCHRP 9-29: Simple Performance Tester for Superpave Mix Design."

Agrawal, G., Chameau, J.L., and Bourdeau, P.L (1995) "Assessing the Liquefaction Susceptibility at A Site Based on Information from Penetration Testing," Chapter 9, in: Artificial Neural Networks for Civil Engineers – Fundamentals and Applications, ASCE Monograph, New York

Airey G.D, Rahman M. M., and Collop A. C. (2003), "Absorption of Bitumen into Crumb Rubber Using the Basket Drainage Method," The International Journal of Pavement Engineering, Vol. 4(2) pp 105-119.

Amirkhanian S. N. (2003) "Establishment of an Asphalt-Rubber Technology Service (ARTS)," Proceedings of the Asphalt Rubber 2003 Conference, Brasilia, Brazil, pp 577-588.

Anderson D. A., Le Hir Y. M., Marasteanu M. O., Planche J., and Martin D. (2001) "Evaluation of fatigue criteria for asphalt binders," Transportation Research Record 1766, Transportation Research Board, Washington, D.C. pp 48–56.

Anderson D. A., Hir Y. M.L., Marasteanu M. O., Planche J. P., Martin D., and Gauthier G., (2001) "Evaluation of Fatigue Criteria for Asphalt Binders," Transportation Research Record, No. 1766, Transportation Research Board, Washington, D. C.

Antunes M. L., Domingos, P., Eusébio, M., and Sá da Costa, M. (2003) "Studies Concerning the Use of Asphalt Rubber in Portugal," Proceedings of the Asphalt Rubber 2003 Conference, Brasilia, Brazil, pp 195-210.

Asphalt Institute (1982) "Research and Development of the Asphalt Institute's Thickness Design Manual (MS-1)," Ninth Edition, Research Report No. 82-2. Asphalt Institute.

Bahia H.U. and Davis R., (1994) "Effect of crumb rubber modifier (CRM) on performance related properties of asphalt binders," Journal of the Association of Asphalt Paving Technologists Vol. 63 pp 414-449.

Benedetto H. D., Soltani A.A., and Chaverot P., (1996) "Fatigue Damage for Bituminous Mixtures: A Pertinent Approach," Proceedings of Association of Asphalt Paving Technologists, Vol. 65.

Birgisson B., Soranakom C., Napier J. A. L., and Roque R., (2004) "Microstructure and Facture in Asphalt Mixtures Using a Boundary Element Approach," Journal of Materials in Civil Engineering, Vol. 16. pp 116-121.

Button J. W., Little D. N., Kim Y., and Ahmed J. (1987) "Mechanistic Evaluation of Selected Asphalt Additives," Proceedings of Association of Asphalt Paving Technologists, Vol. 56 pp 62-90.

Brunauer S., Emmett P.H., and Teller E., (1938) "Adsorption of Gases in Multimolecular Layers," Journal of the American Chemical Society, Vol. 60.

Chen C.J. (1999) "Risk-Based Liquefaction Potential Evaluation Using Cone Penetration Tests and Shear Wave Velocity Measurements," Ph. D dissertation, Clemson University

Churchill E. V., Amirkhanian S. N., and Burati Jr J. L.(1995). "HP-GPC Characterization of Asphalt Aging and Selected Properties," Journal of Materials in Civil Engineering, Vol. 7 pp 41-49.

Coulter Corporation (1996) "Coulter SA 3100 Series Surface Area and Pore Size Analyzers Product Manual," Coulter Corporation, Miami, FL.

Daniel J. S., and Kim R. Y., (2001) "Laboratory Evaluation of Fatigue Damage and Healing of Asphalt Mixtures," Journal of Materials in Civil Engineering, Vol. 13 p. 434-440.

Demuth, H. and Beale, M. (1998) "Neural Network Toolbox User's Guide, The MATH WORKS, Inc., Natick, Mass

Deacon J. A., Coplantz J. S., Tayebali A. A., and Monismith C. L., (1994) "Temperature Considerations in Asphalt-Aggregate Mixture Analysis and Design," Transportation Research Record 1454, pp 97-112.

Decker Dale S., (1997) "State-of-the Practices for Use of RAP in Hot Mix Asphalt," Proceedings of Association of Asphalt Paving Technologists, Vol. 66.

Federal Highway Administration (1997a) Superpave Mixture Expert Task Group, "Guidelines for the Design of Superpave Mixtures Containing Reclaimed Asphalt Pavement," Washington, D.C.

Federal Highway Administration (1997b) "Pavement Recycling Guidelines for State and Local Governments," Report No. FHWA-SA-98-042, Washington, D.C.

Federal Highway Administration (2002) "User Guidelines for Waste and Byproduct Materials in Pavement Construction," Washington, D.C.

Finn F. N., Saraf C. L., Kulkarni R., Nair K., Smith W., and Abdullah A. (1986) "Development of Pavement Structural Subsystems." NCHRP Report 291. Transportation Research Board, Washington, D.C.

Gardiner M. S., Wagner C., (1999) "Use of Reclaimed Asphalt Pavement in Superpve Hot-Mix Asphalt Applications," Transportation Research Record, No. 1681, Washington, D. C.

Goh, A. T.C. (1994) "Seismic Liquefaction Potential Assessed by Neural Networks," Journal of Geotechnical Engineering, ASCE Vol. 120, pp 1467-1480.

Green E.L. and Tolonen W.J., (1997) "The chemical and physical properties of asphalt-rubber mixtures," Arizona Department of Transport, Report ADOT-RS-14 (162)

Heitzman M., (1992) "Design and construction of asphalt paving materials with crumb rubber modifier," Transportation Research Record 1339, Washington, D.C., pp 1-8.

Hicks R. G., Finn, F. N., Monismith C. L., and Leahy R. B. (1993) "Validation of SHRP binder specification through mix testing," Proceedings of Association of Asphalt Paving Technologists, Vol. 62 pp 565–614.

Hicks R.G., Lundy J.R., Leahy R.B., Hanson D., and Epps J., (1995) "Crumb Rubber Modifier in Asphalt Pavement – Summary of Practice in Arizona, California and Florida," Report Nr. FHWA-SA-95-056-Federal Highway Administration.

Hines M. L., Roche C. De La and Chaverot P.,(1998) "Evaluation of Fatigue Behavior of Hot Mix Asphalt with The LCPC Nantes Test Track and SHRP Testing Tools," Proceedings of Association of Asphalt Paving Technologists, Vol. 67 pp 717-729.

Hossain M., Swartz, S., and Hoque E., (1999) "Fracture and Tensile Characteristics of Asphalt Rubber Concrete," Journal of Materials in Civil Engineering, Vol. 11 pp 287-294.

Jennings P. W. (1980) "High Pressure Liquid Chromatography as a Method of Measuring Asphalt Composition," Report No. FHWA –MT-7930 Montana State University, Bozeman, Montana,

Juang C.H. and Chen C.J. (1999) "CPT-based liquefaction evaluation using artificial neural networks," Journal of Computer-Aided Civil and Infrastructure Engineering Vol. 14 pp. 221-229

Kandhal Prithvi S. (1997). "Recycling of Asphalt Pavement – An Overview," Proceedings of Association of Asphalt Paving Technologists, Vol. 66.

Kearney Edward (1997) "Cold Mix Recycling: State-of-the-Practices," Proceedings of Association of Asphalt Paving Technologists, Vol. 66.

Khattak M. J., and Baladi G. Y., (2001) "Fatigue and Permanent Deformation Models for Polymer-Modified Asphalt Mixtures," Transportation Research Record, No. 1767, Transportation Research Board, Washington, D. C.

Kim K. W., Burati Jr. J. L. , and Park J.-S., (1995) "Methodology for Defining LMS Portion in Asphalt Chromatogram," Journal of Materials in Civil Engineering, Vol. 7 pp 31-40.

Kim J.-I., Kim D. K., Feng M. Q., and Yazdani F., (2004) "Application of Neural Networks for Estimation of Concrete Strength" Journal of Materials in Civil Engineering, Vol. 16. 257-264.

Kim Y. R., Lee H. J., and Little D. N., (1997) ''Fatigue characterization of asphalt concrete using viscoelasticity and continuum damage theory,'' Proceedings of Association of Asphalt Paving Technologists, Vol. 66 pp 520–569.

Kim Y. R., Little D. N., and Lytton R. L. (2003) "Fatigue and Healing Characterization of Asphalt Mixtures," Journal of materials in Civil Engineering, Vol. 15 pp. 75-83.

Kim S., Loh S.W. Zhai, H. and Bahia H., (2001) "Advanced characterization of crumb rubber-modifier asphalts, using protocols developed for complex binder." Transportation Research Record 1767, Washington, D.C., pp 15-24.

Lavin P. (2003) "Asphalt Pavements, A Practical Guide to Design, Production and Maintenance for Engineers and Architects."

Lee H. J. (1996) "Uniaxial constitutive modeling of asphalt concrete using viscoelasticity and continuum damage theory," PhD thesis, North Carolina State Univ., Raleigh, N.C.

Lee H. J., Daniel, J. S., and Kim, Y. R. (2000) "Continuum damage mechanics–based fatigue model of asphalt concrete," Journal of Materials in Civil Engineering, pp 105–112.

Lee G. J., Daniel J. S. and Kim Y. R. (2000) "Continuum Damage Mechnics-Based Fatigue Model of Asphalt Concrete", Journal of materials in Civil Engineering, Vol. 12 p. 105-112.

Little, D.N. (1986) "An Evaluation of Asphalt Additive to Reduce Permanent Deformation and Cracking in Asphalt Pavement: a Brief Synopsis of on-going Research," Proceedings of Association of Asphalt Paving Technologists, Vol. 55, pp 314-320.

Local Road Research Board (1991) "Flexible pavement Distress Manual" St Paul, Minnesota, Minnesota Department of Transportation.

Mathias Leite L. F., Almeida da Silva, P., Edel G., Goretti da Motta L., and Herrmann do Nascimento L. A. (2003). "Asphalt Rubber in Brazil: Pavement Performance and Laboratory Study." Proceedings of the Asphalt Rubber 2003 Conference, Brasilia, Brazil, pp. 229-245.

McDonald C.H. (1966) "A New Patching Material for Pavement Failures," Highway Res. Rec., pp 1-16.

McDaniel R.S., Soleymani H., and Shal A., (2002) "Use of Reclaimed Asphalt Pavement Under Superpave Specifications (Final Report)," North Central Superpave Center, West Lafayette.

Mendenhall W. and Sincich T. (1994) "Statistics for Engineering and the Sciences" 4th edition.

Monismith C. L., Epps J.A., and Finn F. N. (1995) "Improved Asphalt Mix Design," Proceedings of Association of Asphalt Paving Technologists, Vol. 54

Myers R. H., Montgomery D. C., and Vining G. G. (2001) "Generalized Linear Models with Applications in Engineering and the Sciences."

Müller B., and Reinhardt J., (1990) "Neural Network: An Introduction, Springer-Verlag," Berlin, Heidelberg.

National Cooperative Highway Research Program (2001) "Recommended Use of Reclaimed Asphalt Pavement in the Superpave Mix Design Method: Technician's Manual." Transportation Research Board, NCHRP Report 452. Washington, D.C.

Palit S. K., Reddy K.S., and Pandey B.B., (2004) "Laboratory Evaluation of Crumb Rubber Modified Asphalt Mixes," Journal of Materials in Civil Engineering, Vol. 16 pp 45-53.

Pronk A. C. and Hopman (1990) "Energy Dissipation: The Leading Factor of Fatigue," Proceedings, United States Strategic Highway Research Program-Sharing the Benefits. London.

Putman B.J (2005) "Quantification of the effects of crumb rubber in CRM binder" Ph. D, dissertation, Clemson University.

Raad L., Saboundjian S. (1998) "Fatigue Behavior of Rubber Modified Pavements," Transportation Research Record, No. 1338, Washington, D. C. pp 97-107.

Raad L., Saboundjian S., and Minassian G., (2001) "Field Aging Effects on Fatigue of Asphalt Concrete and Asphalt-Rubber Concrete". Transportation Research Record, No. 1767, Transportation Research Board, Washington, D. C.

Read M. J., and Collop A. C., (1997) "Practical Fatigue Characterization of Bituminous Paving Mixtures," Proceedings of Association of Asphalt Paving Technologists, Vol. 66.

Reese R. (1997) "Properties of aged asphalt binder related to asphalt concrete fatigue life," Proceedings of Association of Asphalt Paving Technologists, Vol. 66. pp 604–632.

Roberts F. L., Kandhal P. S., Brown E. R., Lee D. Y. and Kennedy T. W. (1996) "Hot Mix Asphalt Materials, Mixture Design, and Construction," National Center for Asphalt Technology.

Rowe G. M., (1993) "Performance of asphalt mixtures in the trapezoidal fatigue test," Proceedings of Association of Asphalt Paving Technologists, Vol. 62 pp 344–384.

Rubber Manufacturers Association (2003) "U. S. Scrap Tire Markets 2003 Edition," Rubber Manufactures Association 1400K Street, NW, Washington, D.C.

Rumelhart D.E., Hinton G.E., and Williams R.., (1986) "Learning Internal representions by error Propagation," Parallel Distributed Processing: Foundations, Vol. 1 D.E. Rumelhart and J.L. McClelland, eds., MIT Press Combridge, Mass, pp 318-362.

Ruth B. E., Tia M., Jonsson G., Setze J. C. (1997) "Recycling of asphalt mixtures containing crumb rubber," Final report UF Project Nr. 49104504495-12 Florida DOT.

Sebaaly P. E., Bazi G., Weitzel D., Coulson M. A., and Bush D., (2003) "Long Term Performance of Crumb Rubber Mixtures in Nevada," Proceedings of the Asphalt Rubber 2003 Conference, Brasilia, Brazil, pp 111-126.

Shell International (1978) "Shell Pavement Design Manual" London

Shen J. N., Amirkhanian S. N., and Xiao F. P. (2006) "HP-GPC Characterization of Aging of Recycled CRM Binders Containing Rejuvenating Agents," Transportation Research Record, Washington, D.C. No. 1962, pp 21-27.

Smith B. J., and Hesp S. (2000) "Crack pinning in asphalt mastic and concrete: regular fatigue studies," Transportation Research Record 1728, Washington, D.C., pp 75–81.

South Carolina (2000) Department of Transportation Policy for Approval of Coarse Aggregate Sources.

Sondag, M. S., B. A. Chadbourn, and A. Drescher, (2002) "Investigation of Recycled Asphalt Pavement Mixtures," Minnesota Department of Transportation, Final Report 2002-15.

Solaimanian M. and Tahmoressi M., (1996) "Variability Analysis of Hot-Mix Asphalt Concrete Containing High Percentages of Reclaimed Asphalt Pavement," Transportation Research Record 1543, pp 88-96.

Strategic Highway Research Program (1994), "Fatigue Response of Asphalt-Aggregate Mixes," National Research Council, Washington, D. C.

Tarefder F. A., White L., and Zaman M., (2005) "Neural Network Model for Asphalt Concrete Permeability" Journal of Materials in Civil Engineering, Vol. 17. 19-27.

Tayebali A. A (1992) "Re-calibration of Surrogate Fatigue Models Using all Applicable A-003A Fatigue data," Technical memorandum prepared for SHRP Project A-003A. Institute of Transportation Studies, University of California, Berkeley

Tayebali A. A., Tsai B., and Monismith C.L. (1994) "Stiffness of Asphalt Aggregate Mixes," SHRP Report A-388, National Research Council, Washington D.C.

Terrel Ronald L., Epps Jon A., and Scorenson J. B., (1997) "Hot-In-Place Recycling State-of-the-Practices," Proceedings of Association of Asphalt Paving Technologists, Vol. 66.

Thompson J. and Xiao F. P., (2004) "The High Temperature Performance of CRM Binders," ARTS Quarterly, Volume 4, Issue 2.

Treloar L.R.G. (1975) "The Physics of Rubber Elasticity" 3rd Ed., Oxford University Press, Oxford, UK.

Tsoukalas L.H. and Uhrig R.E. (1996), Fuzzy and Neural Approached in Engieering, John Wiley & Sons Inc., pp. 234

Van Dijk W (1975). "Practical Fatigue Characterization of Bituminous mixes," Proceedings of Association of Asphalt Paving Technologists, Vol. 44.

Van Dijk W and Visser W. (1977). "The Energy Approach to Fatigue for Pavement Design," Proceedings of Association of Asphalt Paving Technologists, Vol. 46.

Wang L. B., Wang X., Mohammad L., and Wang Y. P. (2004) "Application of Mixture Theory in the Evaluation of Mechanical Properties of Asphalt Concrete" Journal of Materials in Civil Engineering, Vol. 16 pp 167-174.

Way, G. B. (2003). "The Rubber Pavements Association, Technical Advisory Board Leading the Way in Asphalt Rubber Research," Proceedings of the Asphalt Rubber 2003 Conference, Brasilia, Brazil, pp 17-33.

Williams D. A. (1998). "Microdamage healing in asphalt concretes: relating binder composition and surface energy to healing rate." PhD thesis, Texas A&M Univ., College Station, Texas.

Xiao F. P., Amirkhanian S.N., and Juang H.J., (2007) "Rutting Resistance of the Mixture Containing Rubberized Concrete and Reclaimed Asphalt Pavement," Journal of materials in civil engineering (In Press).

Xiao F. P., Putman B. J., and Amirkhanian S. N., (2006) "Laboratory Investigation of Dimensional Changes of Crumb Rubber Reacting with Asphalt Binder," Proceedings of the Asphalt Rubber 2006 Conference, Palm Springs, USA, pp 693-715.

You A., and Buttlar W. G., (2004) "Discrete Element Modeling to Predict the Modulus of Asphalt Concrete Mixtures" Journal of Material in Civil Engineering, Vol. 16 pp 140-146.

Zhong X. G., Zeng X., and Rose J. G. (2002) "Shear Modulus and Damping Ratio of Rubber-Modified Asphalt Mixes and Unsaturated Subgrade Soils," Journal of Materials in Civil Engineering, Vol. 14 pp 496-502.

Zanzotto L. and Kennepohl G., (1996) "Development of rubber and asphalt binders by depolymerization and devulcaniztion of Scrap Tires in Asphalt," Transportation Research Record 1530, Washington, D.C., pp 51-59.